CRANFIELD UNIVERSITY

HAUWA TALATU ABDULKARIM

MODELLING AND TECHNO-ECONOMIC ANALYSIS OF A SOLAR PV SYSTEM FOR POWER SUPPLY: CASE STUDY OF A RURAL AREA IN NORTH-EASTERN NIGERIA

SCHOOL OF WATER, ENERGY AND ENVIRONMENT
Energy and Power

PhD
Academic Year: 2016 - 2019

Supervisor: Professor Christopher L. Sansom
Associate Supervisor: Dr. Kumar Patchigolla
October 2019

CRANFIELD UNIVERSITY

SCHOOL OF WATER, ENERGY AND ENVIRONMENT
Energy

DOCTOR OF PHILOSOPHY

Academic Year 2016 - 2019

HAUWA TALATU ABDULKARIM

Modelling and Techno-economic Analysis of a Solar PV System for Power Supply: Case Study of a Rural Area in North-Eastern Nigeria

Supervisor: Professor Christopher L. Sansom
Associate Supervisor: Dr Kumar Patchigolla
October 2019

ABSTRACT

Energy which is vital in the economic and social growth of any country is facing increased demand because of technological and industrial developments in the world. Most of the energy supplied globally is being generated from fossil fuels. However, studies have shown that these resources have many negative environmental and health impacts. This gives reason for development of renewable energy sources especially solar photovoltaic system. The investment for large solar PV power plants is capital intensive, therefore, a solar photovoltaic system model (SPVSM) which can be rapidly used for accurate sizing of the system components for optimized solar PV system for power supply becomes imperative. Soiling, which has not received adequate global attention, is a major problem in the operation of solar PV systems. It affects the performance of PV systems; therefore, the study of its impact is crucial especially for location with potential for dust accumulation.

The main aim of this research is to develop a novel, simple and robust decision-making model, Solar-Photovoltaic-System-Model (SPVSM) for an optimised power supply at a competitive cost and to determine the impacts of dust accumulation on the performance of solar PV modules.

The collection and analysis of solar and climatic data is of utmost importance to the development of solar energy conversion system in any location because the knowledge of the availability of solar resource is key to the decision on installation of solar PV systems. For this research, three locations (Maiduguri, Minna and Port Harcourt) were carefully chosen to represent the three radiation regions in Nigeria. This becomes very important because of the scanty availability of solar and climatic data analysis for these regions. Solar irradiance, relative humidity, temperature and sunshine hours data were collected for these locations for a period (2006 to 2016) from the Nigerian Meteorological Agency, Abuja. The data were statistically analysed using Minitab 17 software and Microsoft Excel.

The SPVSM which was developed on a single graphical user interface platform in MATLAB17 is made up of six panels, each handling the sizing of different system components (PV modules, inverters, charge controllers and batteries) as well as energy and economic analysis of the system.

A PV model which generates the I-V and P-V characteristics of the 50W module was developed using Simulink in MATLAB2017. A single diode model was used to produce the ideal equivalent circuit of solar cell, which is a current source in parallel with a single diode. Two sub-systems were developed to handle saturation current and photocurrent. A maximum power point tracking (MPPT) system was developed using thePerturb and Observe algorithm in Simulink. The specification of a 50 W PV module model TDG-PV T050M365 was used for the simulation. The MPPT simulation gave a 50.09 W for solar irradiance of 1000 W/m^2 and 37.9 W/m^2 for irradiance of 800 W/m^2.

A field experiment was carried out in a location in North-eastern Nigeria to assess the impact of dust accumulation on the performance of PV modules. The experiment was conducted for 14 days using a 50W module of model TDG-PV T050M365. The current and voltage output of the module were concurrently measured and logged using Mooshimeter. The temperature, solar irradiance, wind speed and relative humidity were measured and recorded every hour. Dust were collected at different heights (50 cm, 100 cm, 150 cm and 200 cm).The dust so collected were analysed in Cranfield. For dust accumulation to have effect on performance of PV module, there must be adhesion. This led to the laboratory experimentation on the effect of temperature, particle size, humidity, type of sand, and height on the adhesion of sand to glass cover of PV module.

The data analysis shows that the three locations have adequate daily solar irradiance and therefore, have potential for viable development of solar PV systems for power supply with Maiduguri being more viable than Minna and Port Harcourt.

The economic analysis from the SPVSM shows that the Levelized cost of electricity is $0.081/kWh and the net present value (NPV) is positive for Maiduguri, therefore it can be concluded that development of solar PV system in Maiduguri is economically viable. The use of lower peak watt module rating has economic implications on the project total cost and consequently on the overall economics of the system.

Dust accumulation can reduce the performance of solar PV module by more than 50% and the analysis of sand/dust samples from Maiduguri shows varying sizes and shapes of roundness that roll off the panel with less effect on the panel surface erosion; and sharpness that deteriorates the PV module. Also, the chemical analysis further shows that dust from Maiduguri is high in silica (SiO_2) i.e. prevalence of quartz which confirm the zone being desert.

The results of the laboratory experiments show that, some of the factors studied have effect on the amount of sand that sticks to glass. Humidity is the factor with the highest influence. At higher humidity more sand adhere to the glass, this is due to the higher moisture content of the air which aids in dissolving any soluble materials and bind the particles to the surface. Also, desert natural sands adhere more strongly to the glass than artificial quartz-based sands, this is possibly due to the fact that natural sand contains higher amounts of soluble materials.

Keywords:

Dust, energy, humidity, irradiance, performance, temperature

ACKNOWLEDGEMENTS

Foremost, I would like to appreciate Almighty, Allah (Subuhanahu wata'ala) and his Rasuul (S.A.W), first of all for the gift of life then for guard, guide and help all through my life especially for establishing me to complete this research despite all odds.

I am extremely grateful and indebted to Petroleum Technology Development Fund (PTDF), Abuja, Nigeria for the sponsorship and Niger State College of Education, Minna for the study fellowship.

I would like to express my special thanks to my custodians in the United Kingdom, Primary Supervisor, Professor Chris L Sansom and Associate Supervisor, Dr Kumar Patchigolla, who have journeyed with me in this adventure for their guidance to a successful completion of this study. I could not have imagined having better supervisors.

My earnest gratitude to Professor Christopher L Sansom, for a warm reception on the first day I met him on reporting to the University and for his pleasantness, enthusiasm, motivation, and immense knowledge. I admire, the great respect he has for fellow human beings, his tolerance and patience. I am thankful for his excellent and continuous support since inception and all through the period of my research. His kind encouragement, expertise, sincere and valuable guidance helped me all the time of carrying out this research and writing of this thesis. Sir, it is indeed an honour to have you supervise my PhD. My deep appreciation always!

I am very thankful to Dr Peter King and Dr Mounia Karim who were always there for me and I appreciate them both in no small measure for their kind and excellent guides and great contributions to my achievements in this research.

Dr Mounia, special thanks to you for your kind supports, endless help, generous advice, and most especially your friendship.

I would like to express my gratitude to Dr Venkat Sastry, Head of Group, Additional Mathematics and Computing, Shrivenham Campus for the excellent supports he gave me at the time of writing the MATLAB programs for the SPVSM which I developed. Sir, I appreciate your quick responses any time you were contacted and your great inputs in this research.

I acknowledge, with pleasure and owe my special thanks to my progress review team members, the Chair Dr Stephen Hallet, for his constructive criticisms, kind way of appreciating a nice piece of work and useful suggestions especially during the initial, 9 month and the 30th month reviews; My reviewer, Dr Heather Almond, for her thoroughness in reading, asking questions and making inputs, from the first to the last page of any report I submitted to her. Her observations and appreciation of one's efforts was encouraging, her pleasantness and her creating time out of her tight schedule to sit down and give me soothing words of encouragement at the time that I needed it most, is acknowledged gratefully. Thank you very much, dear Dr Heather, for your precious time which you sacrificed to go through my thesis in this challenging period of Covid - 19 and the great inputs you made. I deeply appreciate you.

Worthy of mentions are our administrators especially Sam Skears for her precious time and kind ways of handling students' challenges; the library and IT staff both in the information and service desks, the security staff for always being 'on the go' to help whenever, they were contacted for help. I appreciate you all.

I acknowledge, with pleasure, the help of Dr Sarah Quraish, Dr Alkali Babawuya,

Dr Abutu and a host of others for their help in one way or the other during the period of this research.

I will forever cherish and remember the good times we had and shared with colleagues and friends in and outside the University. I am better knowing you. I acknowledge, with deep pleasure, and gratitude my family and friends way back in Nigeria, for being there always.

To our late loving and adorable parents, of blessed memory, I say big thank you for everything you have done. May Allah, in His infinite mercy and by the honour of His Messenger, Muhammadu Rasulullah (S.A.W) reward your efforts, love, care and concerns for me and the entire Abdulkarim's family, with the highest Jannah ever.

I wish to sincerely, appreciate Sheikh Shariff Abubakar for his continuous support and prayers for me and my family, may God reward him abundantly. Also worthy of mention are Yabagi Alfa (Registrar), Dr Sheikh Buhari Mohammmad, Shehu Mal. Kpataki, all of my Mamas and Sisters of COE, Minna for their deep interests in my progress and constant prayers for my success. I will forever be grateful.

Dr Ugoh Elele (IBBU Lapai) and Shehu Malam Kudu Mokwa, your kindness and prayers are highy appreciated.

To my husband, Professor Abdulkarim Nasir, I do not have enough words to express my heart felt appreciation for your love, care, concern and sacrifices for the family. We thank Allah for having a great husband and father. You and the children are the best thing that ever happened to me in life. I adore you!

To the crew members**,** my love, my joy, my warriors - Al'Amin, Maryam, Aisha, Nasir, Muhammad and Khadijat Abdulkarim, you cannot imagine how deeply indebted I am to you for being my constant source of joy through the struggles and trials of this study. I will forever, remain grateful to Allah for blessing me with humble and reliable children like you. I could not have wish for more!

To the best brother and daughter in-law, Abdullahi and Malama Aisha Tukur and my best confidant, humble and trustworthy sister, Halimat. I will forever, remain grateful for your loyalty to me and the entire family.

I would like to gratefully acknowledge Dr Muhammad Abubakar Isah (McJ) and his family, Dr Ibrahim Umar (Iyan Pandogari) and his Sarauniyan Iya for their kind supports, Officer Kasim Abdullahi (Ministry of interior, Abuja) and family for their friendliness.

Finally, since it is not easy to mention all names, I would also place on record, my sense of gratitude to everyone who, directly or indirectly, have helped me by way of prayers, encouragement and motivation and have guided me to make a fine effort for successful completion of this study. Love you all!

TABLE OF CONTENTS

LIST OF FIGURES

LIST OF TABLES

LIST OF EQUATIONS

LIST OF ABBREVIATIONS

3G	Third Generation
4G	Fourth Generation
a	Diode constant
ABE	Absolute Bias Error
AMBE	Absolute Mean Bias Error
ANOVA	Analysis of Variance
A-Si	Amorphous silicon
BBC	British Broadcasting Corporation
CPV	Concentrated Photovoltaic
C-Si	Crystalline silicon
CSP	Concentrated Solar Power
D	Duty cycle (fraction of a period that a signal is active)
ΔD	Change in duty cycle
delT	Change in temperature
DFIG	Doubly Fed Induction Generator
DNI	Direct Normal Irradiance
DOE	Design of Experiment
DSG	Direct Steam Generation
EDS	Energy Dispersive Spectroscopy
FF	Fill Factor
G	Solar insolation
GFD	Group Frequency Distribution
GHG	Green House Gases
Gn	Nominal solar insolation
GUI	Graphical User Interface
HCPV	High Concentration Photovoltaic
HOMER	Hybrid Optimisation Model for Electric Renewables

HTF	Heat Transfer Fluid
IEA	International Energy Agency
Ign	Nominal current
IQR	Interquartile Range
Iscn	Nominal short-circuit current
K	Boltzmann’s constant
Ki	Current coefficient
KSA	Kingdom of Saudi Arabia
Kv	Voltage coefficient
LCOE	Levelized Cost of Energy
LCPV	Low Concentration PV
LEC	Levelized Electricity Cost
MABE	Mean Absolute Bias Error
MBE	Mean Bias Error
Mc-Si	Monocrystalline Silicon
MPPT	Maximum Power Point Tracking
n	Ideality factor
NASA	National Aeronautics and Space Administration
NOAA	National Oceanic and Atmospheric Administration
NIMET	Nigerian Meteorological Agency
NPV	Net Present Value
Ns	Number of cells connected in series
NTT	Nusa Tenggara Timur
P&O	Perturb and Observe
Pc-Si	Polycrystalline silicon
PGF	Panel Generation Factor
PV	Photovoltaic
PVT	Photovoltaic Thermal Systems

q	Electron charge
RET	Renewable Energy Technologies
RMSE	Root Mean Square Error
Rp	Parallel resistance
Rs	Series resistance
SDGs	Sustainable Development Goals
SEM	Standard Error of Mean
SEM-EDX	Scanning Electron Microscope and Energy Dispersive Xray Spectroscopy
SPVSM	Solar Photovoltaic System Model
STE	Solar Thermal Electricity
Tamb	Ambient temperature
TES	Thermal Energy Storage
Tnom	Standard temperature
ΔV	Change in voltage
Vocn	Nominal open-circuit voltage
Vt	Thermal voltage
WECS	Wind Energy Conversion Systems

1 INTRODUCTION

1.1 Background

The increase in world's population and technological development has undoubtedly led to rapid increase in global energy demand. Energy is an important part of human life and its importance is increasing with technological and industrial developments in the world. The most widely used resource for electrical energy generation are the fossil fuels but studies have shown that these resources have many negative environmental and health impacts (Ayvazoğluyüksel and Filik, 2018). This has led to the growing interest in the use of renewable energy sources such as solar photovoltaic for power supply.

Nigeria has inadequate supply of energy to both urban and rural areas with about 60% of its population in the rural areas having no access to electricity and therefore live below poverty line. The International Energy Agency (IEA) defines energy security as "the uninterrupted availability of energy sources at an affordable price" (IEA, 2019a). Lack of energy security is one of the major causes of poverty in the rural areas of Nigeria as this is associated to the bad economic and social impacts of either lack of adequate energy, or exorbitant prices that are not competitive or are very unstable (IEA, 2019b).

According to the World Energy Outlook 2018, IEA (2018), a little below 1 billion people, for the first time ever, have no access to electricity and from these, about 700 million are in rural settlements in sub-Saharan Africa. These sub-Saharan rural dwellers according to IEA (2018) are projected to remain without access to electricity up till 2040.

The demand for electricity in Nigeria obviously outweighs the supply, this inadequate supply is further bedevilled with frequent outages and consequently low reliability as a result of inadequate power infrastructure, poor grid network and poor maintenance culture. A large percentage of Nigerians rely on petrol or diesel generators for power supply for both domestic and industrial usage.

The Federal Government of Nigeria in 2015 set a target of power generation capacity of 115 GW by 2030 with about 20% being from renewable energy sources. This is laudable but it requires concerted effort to meet this target with both stakeholders from private and public sector synergizing. The most interesting part of the set target is 20% being renewable energy sources – this is about 23 GW. Today, hydropower which is the only renewable energy source used in Nigeria, has an installed capacity of 2040 MW with zero contribution from solar energy. This situation forms part of the justification for this research.

The global concern about the environment has resulted in the drive towards renewable energy sources and consequently this research concerning the harnessing of the available solar energy reaching the Nigerian surface to meet the energy demand of the rural dwellers. The region under study is a high dust accumulation region and it is important to study the effect of dust on the performance of solar PV system. This is to mitigate its impact and suggest frequency of cleaning.

1.2 Global Energy Situation

The development of the globalized economy is accompanied by increasing energy demand. According to the International Energy Agency, the energy consumption of the world economy has drastically increased by around twice during the four decades from 1975 to 2015 (IEA, 2017; Wu *et al.*, 2019). Global energy systems are undergoing rapid transitions that will be responsible for important changes to the energy usage such as fuelling of cars, heating of homes, and powering of industries. These trends will have widespread implications for businesses, governments, and individuals in the coming decades (Mckinsey, 2019).

In 2018, the world energy consumption increased rapidly with natural gas and renewables taking the lead. However, emission of oxides of carbon rose at their highest rate for seven years (Dudley, 2019). According to (IEA, 2019a), the rise

in global electricity demand in 2018 was 4% which is the fastest since 2010 and nearly twice as fast as overall energy demand. The CO_2 emissions increased by 2.5% as a result of increased in generation from coal- and gas-fired power plants.

Figure 1-1 shows the global electricity generation mix in 2018. Fossil fuels (Coal and gas) contribute above 60% of the global electricity generation mix, this confirms the increase in global CO_2 emission and consequently an increase in global rise in temperature. There is the need for increase in the use of renewables for electricity generation globally in order to reduce the carbon footprint and invariably reducing the negative impact of emissions on humans and the environment.

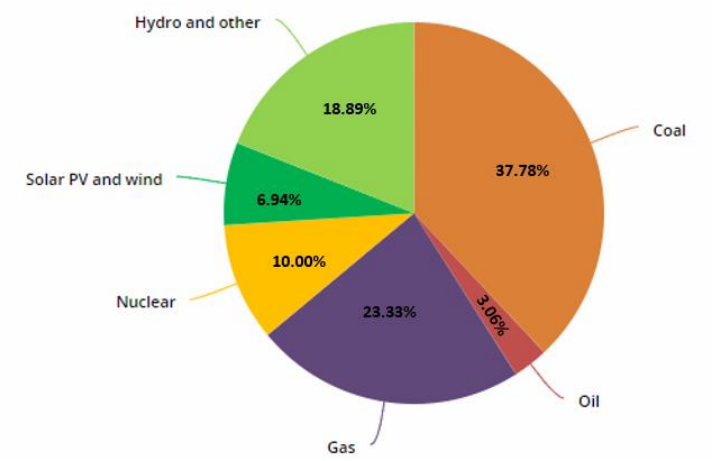

Figure 1-1: Global electricity generation mix (IEA, 2019a)

Figure 1-2 shows the change in primary energy demand globally between 2011 and 2017. There is a sharp rise in the change between 2016 and 2017 of 1.4% difference and this is expected to continue into the near future because of the continuous technological development and population growth (IEA, 2018).

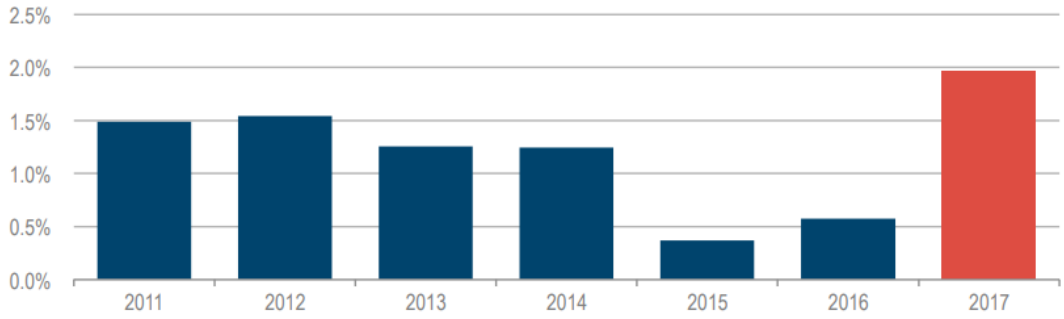

Figure 1-2: Change in global primary energy demand, 2011-17 (IEA, 2018)

1.3 The Global Challenge

The concentration of greenhouse gases in the atmosphere has risen noticeably as a result of industrial revolution of 18th century and gas trapped in polar ice. This is obvious from recordings of remote meteorological stations over some years (Twidell and Weir, 2015).

The rapid changes in climate and environmental challenges which is a great global ecological problem has been adjudged to be as a result of rise in energy demand and consumption resulting from technological progress, increase in global population and advancement in human development (Ferreira *et al.*, 2018). The human need for energy has reached an extraordinary levels as a result of the increased in world population and industrial growth in developing countries (BBC, 2019). Fossil fuels which are extracted from beneath the earth serves as a source of about 50 percent of the world's energy demand. About 135 billion tonnes of crude oil have been extracted from the earth to power cars (Douglah, 2018), fuel power plants and heat homes from 1850s when commercial oil exploration started (BBC, 2019).

British Broadcasting Corporation (BBC) on "The biggest energy challenges facing humanity" stated that it is estimated that about three billion people still cook and heat their homes using wood stoves, coal or dung (BBC, 2019). Developing nations would need more reliable electricity supply as industrialization grows in this region.

1.4 Nigerian Situation- Justification for the Research

Nigeria is country endowed with verse energy resources such as oil, gas, hydro and solar resource. It generates about 12,522 megawatts (MW) of electric power although this varies as hydro-power generates their best during raining season, but most days during dry season only about 4,000 MW is generated which is grossly insufficient to meet the need of the citizens (Bala, 2014). Wide range of tariff is experienced because the distribution companies were privatized. There are currently three hydropower and eleven thermal stations which supplies electricity to the national grid in Nigeria.

The availability of solar energy on the earth depends on the geographical location, time and season. Figure 1-3 shows Nigeria's solar radiation map. The area under study is indicated on the map by Zone I for Maiduguri. Two other areas from which data were collected are also indicated as Zone II for Minna, Zone III for Port Harcourt. The thick circle close to Maiduguri indicates the location of study which is in the North-Eastern Nigeria. Osueke, Uzendu and Ugbonna (2013) studied the variation in solar irradiance in 4 different sites in Nigeria using data acquired from National Aeronautics and Space Administration (NASA) Research and employing SPSS statistical tool and a bar chart. The study concluded among other things that Maiduguri laying at latitude 11.9^{o} and longitude 13.1^{o} seemed to experience highest solar irradiance which ranges from 5.5 – 6.7 kWh/m^2/day, this translates to 229.2 – 279.2 W/m^2.

The utilization of solar energy to economically meet the ever-increasing energy demand of the world relies on two important aspects: the panel generation factor of the site which is a function of solar irradiance availability and the necessary technology to harness it. To be able to assess the performance of solar energy conversion systems in a location, it is imperative to be aware of the level of solar energy availability at the location. It is clear from Figure 1-3 that Nigeria is favoured with the availability of solar energy and North-Eastern Nigeria, which is the area under study, is one of the regions most favoured in terms of solar energy availability.

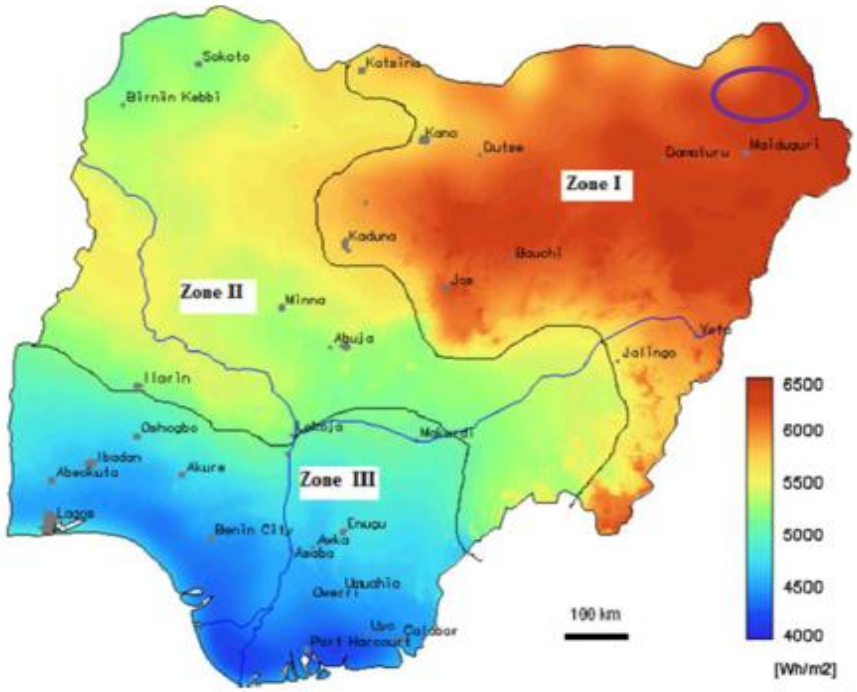

Figure 1-3: Nigeria's Solar Radiation (Giwa *et al.*, 2016)

Figure 1-4 shows a typical village in the North-Eastern Nigeria that is not connected to the National grid and has no form of electricity supply and has high solar irradiance which makes solar PV viable . This is to stress the need to invest in solar PV technology for power supply in Nigeria.

Figure 1-4: A Typical Village in Nigeria (*Azuri to roll out PayGo Solar to 20,000 Nigerian households*, 2016)

Figure 1-6 shows the world installed PV capacity and this shows that the region with abundant solar energy availability (Middle east and Africa) has yet an insignificant contribution. This further buttress the need for development of solar systems for power generation in Africa and particularly in Nigeria – the country with the largest population in Africa.

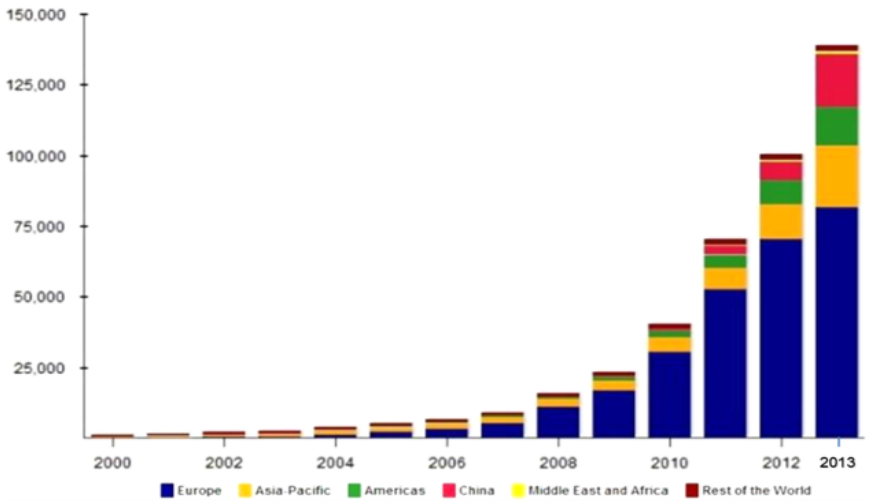

Figure 1-5:World Installed PV capacity in 2013 *(Michael and Goic, 2015)*

Modelling and simulation of solar PV systems prior to installation is of utmost importance as it reveals the behaviour of the system under the varying environmental conditions of the region under study. This describes mathematically the structure of the PV system and its operation and performance (Sangeetha *et al.*, 2015).

Figure 1-7 shows residential electricity use per capita of selected countries. Nigeria with a population of 182 million (Bello, 2017) has the least residential electricity use per capital of 74 kWh/year while United Kingdom with a population of 65.64 million (Park, 2017), about 36% of Nigeria's population, has residential electricity use per capital of 1,985 kWh/year. The electricity use per capital of Nigeria is far less than 844 kWh/year for South Africa whose population is 58.82 million (*South Africa Population Clock (Live)*, 2017) which is about 32% of Nigeria's population. This demonstrates that Nigeria has grossly inadequate power supply.

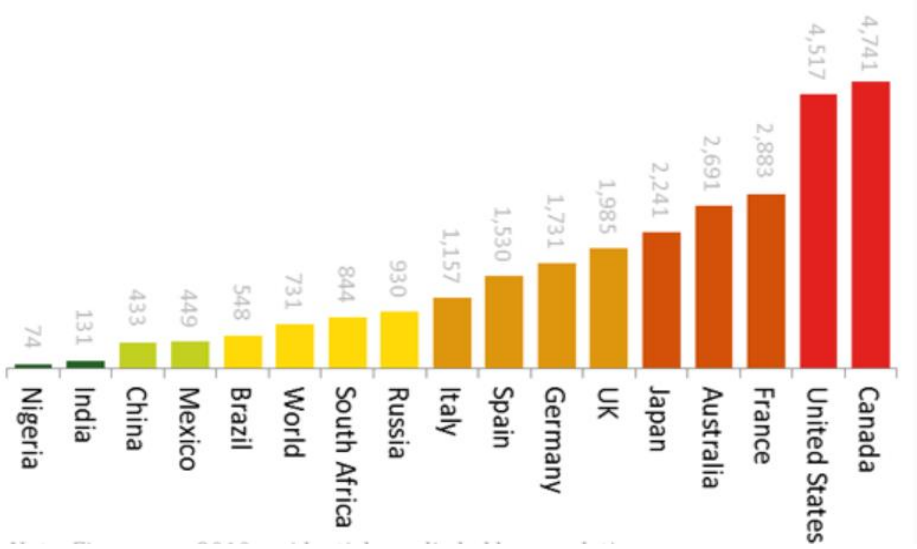

Figure 1-6: Residential Electricity use per Capita of selected Countries (kWh/year) (Wilson, 2012)

1.5 Statement of the problem

Nigeria, a country adjudged to be the largest economy in sub-Saharan Africa, unfortunately has retarded economic and technological growth because of limitations in the power sector. More than 50% of the population have no access to electricity despite the enormous availability of different energy resources such as oil, gas, hydro and solar energy resource. The existing power plants have installed capacity of 12,522 MW and it already has the available power which the power plants are able to produce which is around 4,000 MW, which is grossly insufficient (USAID, 2019). According to World Poverty Clock, 47.7% of Nigerian population lives in extreme poverty. This has a direct link to inadequate power supply. Lack of education, poor health services, and lack of portable water are some of the factors ravaging the most vulnerable, the rural dwellers. Most of these rural people resort to the use of firewood, charcoal, and kerosene to meet their energy needs especially for cooking and lighting. The use of these resources increases deforestation and desert encroachment and also contributes to global warming because of release of oxides of carbon, nitrogen and sulphur. These gaseous emissions apart from environment effect also constitute serious hazard to human health.

There is dearth of information on solar and weather data analysis of the location of study in the Northeastern Nigeria. This is very important for the successful development of solar PV system for power supply. Therefore, the comprehensive data analysis presented in this thesis serves to allow for accurate sizing of the PV system components and contribute to existing literature.

The selected location of study which is rural area of northeastern Nigeria have no access to any form of electricity and they are very far from the national grid which carries insufficient power for distribution. In order to meet the goal set by the Nigerian government of providing electricity to the rural areas, a model which is simple and convenient for local artisan to use for accurately sizing the PV system components, conduct energy and economic analysis is imperative.

The energy demand of the rural area was estimated and planning for future expansion was taking into cognisance. The rural dwellers use kerosene and wood to meet their basic energy needs of lighting and cooking. The location under study is a high dust accumulation region of Nigeria and this has negative impact on the performance of PV panels.

The impact of dust on the performance of PV panels cannot be over emphasized and since the result of studies from other locations around the world cannot be directly applied to this location, the investigation becomes very necessary to assess the impact of continuous dust deposition and suggestion on how to mitigate this impact.

To meet the energy demand of over 50% of Nigerian population who mostly live in the rural areas with sustainability and environmental protection taken into cognisance requires the following conditions to be met:

i. Knowledge of comprehensive energy demand of the area
ii. A constant supply of clean and inexhaustible energy with enough reserves to meet the requirements of peak demand periods.
iii. Adequate solar energy conversion system for power supply
iv. Minimum capital and operating costs
v. High utilization and efficiency of the conversion systems
vi. Energy cost analysis
vii. Knowledge of environmental impact on solar energy conversion system performance

To meet these needs, it is imperative to answer questions such as:

i. What is the energy demand of the area?
ii. What amount of solar irradiance and necessary climatic resource is available for conversion in the region under study?
iii. How many PV modules, batteries, inverters and charge controllers will be required?
iv. What are the minimum capital and operating costs of the conversion system?

v. What is the annual energy obtainable?
vi. What is the Levelized cost of energy (LCOE)?
vii. What is the impact of dust accumulation on the performance of solar PV panels?

All these questions will be addressed in relation to the Techno-Economics of the system in this thesis.

1.6 Aim and Objectives

1.6.1 Aim

The aim of the research is to develop a novel and robust decision-making Solar-PV-System-Model (SPVSM) for an optimised power supply at a competitive cost and to determine the impacts of dust on the performance of solar PV panel.

1.6.2 Objectives

The set objectives necessary to achieve the above stated aim are:

i. To acquire and analyse 11-year solar irradiance, sunshine hours, temperature, and humidity data from 3 radiation zones in Nigeria (Maiduguri in North-Eastern, Minna in North-Central, and Port Harcourt in South-south, Nigeria).
ii. To evaluate the energy demand (watt-hour) of the village under study taking into cognisance the public/common facilities.
iii. To develop a robust decision-making Solar-PV-System-model (SPVSM) using Graphical User Interface (GUI) in MATLAB with appropriate inputs and outputs and taking into cognisance solar irradiance and energy demand. The model will be applicable to all cases of PV sizing, energy, and economic analysis.
iv. To develop a techno-economic module of solar PV system using economic appraisals such as NPV methodology over the expected working life span of the system, this will be directly linked to the SPVSM.

v. To experimentally investigate the effect of certain pertinent parameters on sand adhesion to glass cover of PV module.

vi. To model a solar PV panel and MPPT using Perturb and Observe procedure in MATLAB/Simulink.

vii. To investigate the effect of dust accumulation on the performance of Solar PV panel in the location of study.

2 Literature Review

This chapter presents the review of pertinent literature related to the study. The areas reviewed include renewable energy technologies (RET) with emphasis on solar energy, availability of solar resource in Nigeria and its analysis, the development, processes, modelling and simulation of solar photovoltaic system, hybrid energy systems and a comprehensive review of the impact of dust accumulation on the performance of PV panels. This is meant to establish the needed contribution to knowledge or research gap of this thesis.

2.1 Renewable Energy Technologies

Renewable energy is energy from sources that are virtually inexhaustible, naturally replenishing but limited in the amount of energy available per unit time (Reader, 2020)(EIA, 2019). The major types of renewable energy sources are:

i. Solar
ii. Wind
iii. Hydropower
iv. Biomass
v. Geothermal

2.2 Nigerian Renewable Energy (RE) Potentials

In order to fulfil the requirement of Sustainable Development Goals (SDGs) 7, which states that United Nation member states should “ensure access to affordable, reliable, sustainable and modern energy for all”, it is imperative to evaluate the availability of renewable energy sources such as solar, wind, waves, tides and geothermal (United Nations, 2015; Adedipe, *et al.*, 2018).

Nigeria is endowed with abundant renewable energy sources such solar, hydropower and wind (Mohammed and Mokhtar, 2013). Renewable energy resources are natural, inexhaustible sources of energy whose availability is determined by the biodiversity, climate and geography of a country (Ogbonnaya *et al.*, 2019). Nigeria, by virtue of its location, is endowed with solar energy, wind

energy, biomass, water resources (hydropower) and obviously with a large and energy hungry population (Oghogho *et al.*, 2014). Identifying and quantifying the level of the available RE resources requires scientific approaches such as the measurement of solar irradiation, wind speed, biomass distribution, aquatic characteristics, etc. (Ogbonnaya *et al.*, 2019). Table 2-1 shows the past and future projected electricity generation mix from renewable energy in Nigeria. It can be seen clearly that solar energy has zero contribution up till today.

Table 2-1: Past and future electricity mix in Nigeria from Renewable sources (Aliyu, *et al.,* 2015)

Technology Type	**Capacity (MW) 2003**	**Capacity (MW) 20110**	**Projected Capacity (MW) 2020**	**Projected Capacity (MW) 2030**
Hydro	1920	2030	4740	5748
Biomass	0	0	5	5
Wind	0	0	20	20
Solar PV	0	0	75	425
Solar Thermal	0	0	20	20

Table 2-2 shows Nigeria's RE reserves. It is obvious that Nigeria is endowed with huge renewable energy resources, which can be harnessed to supply a large percentage of the energy requirements especially of rural areas whose connection to the national grid is economically unviable because of the large distance between the rural areas and the national grid.

Table 2-2: Nigeria's RE reserve per capacity (Aliyu, *et al.,* 2013; Aliyu, *et al.,* 2015)

Energy Source	Reserves
Solar energy	3.5 – 7.5 kWh/m^2 -day
Large hydropower	11,235 MW
Small hydropower	3500 MW
Animal waste	61 million tons per year
Crop residue	83 million tons per year
Wind	2-4 m/s at 10 m height
Wave and tidal energy	150,000 TJ/(16.6 x 10^6 toe per year)

2.3 Solar energy potential in Nigeria

Nigeria being geographically located in the equatorial region is one of the greatest assets which favours the country with respect to the availability of solar energy (Bamisile *et al.*, 2017). The country receives abundant solar radiation and sunshine (Ojosu, 1990; Shaaban and Petinrin, 2014). Due to the abundant availability of solar energy resource, it seems to be the most promising of the RE resources in Nigeria (Shaaban and Petinrin, 2014). The distribution of solar energy in Nigeria is such that the Northern region having higher solar irradiance than the coastal region. Nigeria has average solar irradiance of about 19.8 MJ/m^2 per day (229.1 W/m^2) per day with an average sunshine of 6.5 hours per day, which ranges from 9 hours in the far north to 3.5 hours in the far south along the coastal region (GENI, 2014; Shaaban and Petinrin, 2014; Bamisile *et al.*, 2017)

Global Energy Network Institute, GENI (2014) reported that "If solar collectors/modules were used to cover 1% of Nigeria's land area, it would be possible to generate 1850 ×103 GWh of solar electricity per year. This is over 100 times the current grid electricity consumption level in the country".

Nigeria has good radiation sites which is quite favourable to the development of solar energy conversion system but there is little effort in research and government attention. Effective policies need to be wielded to foster solar energy

development in Nigeria. Table 2-3 shows the minimum, maximum and average solar irradiance of some selected cities in Nigeria

Table 2-3: Maximum, minimum and yearly average global solar irradiance (kWh/m^2/day) (Shaaban and Petinrin, 2014)

Stations	Location	Location	Altitude	Max[a]	Min[b]	Monthly
	Lat. °N	Long °E	(m)			Average
Abeokuta	7.25	3.42	150	4.819	3.474	4.258
Abuja	9.27	7.03	305	5.899	4.359	5.337
Akure	7.25	5.08	295	5.172	3.811	4.485
Azare	11.8	10.3	380	6.028	5.022	5.571
Bauchi	10.37	9.8	666.5	6.134	4.886	5.714
Enugu	6.47	7.55	141.5	5.085	3.974	4.539
Ibadan	7.43	3.9	227.23	5.185	3.622	4.616
Jos	9.87	4.97	1285.58	6.536	4.539	5.653
Kaduna	10.6	7.45	645.38	6.107	4.446	5.672
Kano	12.05	8.53	472.14	6.391	5.563	6.003
Katsina	13.02	7.68	517.2	5.855	3.656	4.766
Lagos	6.58	3.33	39.35	5.013	3.771	4.256
Lokoja	7.78	6.74	151.4	5.639	4.68	5.035
Maiduguri	11.85	13.08	383.8	6.754	5.426	6.176
Minna	9.62	6.53	258.64	5.897	4.41	5.427
Nguru	12.9	10.47	342	8.004	6.326	6.966
Obudu	6.63	9.08	305	5.151	3.375	4.224
Owerri	5.48	7.03	120	4.649	3.684	4.146
Port Harcourt	4.85	7.02	19.55	4.576	3.543	4.023
Serti	7.5	11.3	610	4.727	3.972	4.488
Sokoto	13.02	5.25	350.75	6.29	5.221	5.92
Wari	5.52	5.73	6.1	4.237	3.261	3.748
Yola	9.23	12.47	186.05	6.371	4.974	5.774

2.4 Solar Energy and Its Conversion Processes

2.5 Solar Irradiance

Radiant energy from the sun is the primary source of energy to the earth and it is measured as solar irradiance (NASA, 2008). Solar irradiance is the energy per second, which falls on a unit area from the sun in the form of electromagnetic radiation. The amount of radiation depends on the season of the year and the position of the sun in the sky during the day, and the weather (for example, in rainy or cloudy conditions, cloud will limit the amount of radiation reaching a particular spot). Extra-terrestrial irradiance is the solar radiation reaching the earth before encountering the atmosphere and this can be measured using a variety of instruments, a review of which can be found in (Gueymard, 2004). This can also be calculated using the Plank approximation for a black body. Solar irradiance gets either transmitted, scattered, or absorbed as it passes through the Earth's atmosphere with direct irradiance being the radiation reaching the observer directly and "diffuse" when the radiation has undergone scattering.

2.6 Basic Principle of Photovoltaic Process

The photovoltaic principle involves light energy being converted to electrical energy using the photovoltaic effect. This effect takes place in a semiconductor material whose electrical conductivity performance lies between that of an insulator and a conductor. Semiconductor materials exposed to light absorbs some of the photons of light rays, this causes significant numbers of free electrons in the semiconductor crystals. These free electrons from PV effect are extracted to do useful work by the basic unit of the system, which is the solar photovoltaic cell.

Silicon, a semiconductor, and whose atom has four valence electrons is the major material used in the construction of photovoltaic cells. A covalent bond exists in a solid crystal of silicon with each silicon atom sharing its four-valence electron

with the nearest adjacent atom. This leads to the tetrahedral lattice structure of silicon crystals (Panwar, Kaushik and Kothari, 2011).

The incident light intensity of the silicon crystals influences the number of photons absorbed by the crystals. If the strength is adequate, enough photons are absorbed by the crystals and, in effect, these photons excite some of the electrons of the existing covalent bonds and migrate from valence band towards the conduction band, leaving behind a hole. These electrons which move freely are responsible for the generation of electricity in a PV cell.

Figure 2-4 shows the operation of photovoltaic cell. Solar cells are shaped into thin semiconductor wafers specially treated to form an electric field with a positive charge on one side and negative charge on the other (Knier, 2008). In summary, the photovoltaic process involves the liberation of valence electrons by the photon energy from the sun and making the electrons free to move, a movement which constitutes the flow of electrons. Attaching electrical conductors to the positive and negative sides which form an electric circuit and consequently a flow of electron ensues -- that is, electricity. This can then be used to power any electrical load.

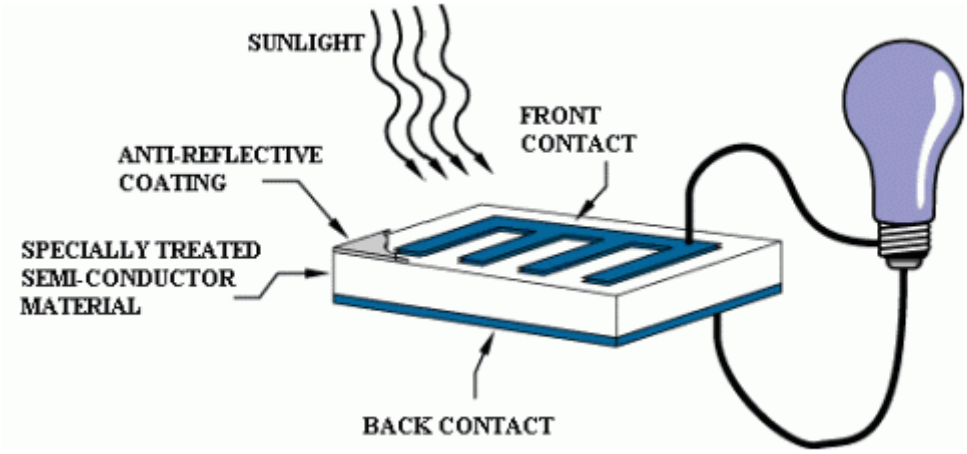

Figure 2-1: : Basic process of PV cell (Knier, 2008)

Figure 2-5 shows the building blocks of a solar array. Several solar cells connected together electrically are called photovoltaic module. Modules are

made to supply electricity at a specified voltage such 12 or 24 volts and the current generated is a function of the amount of solar irradiance striking the module (i.e. the solar irradiance) (Knier, 2008).

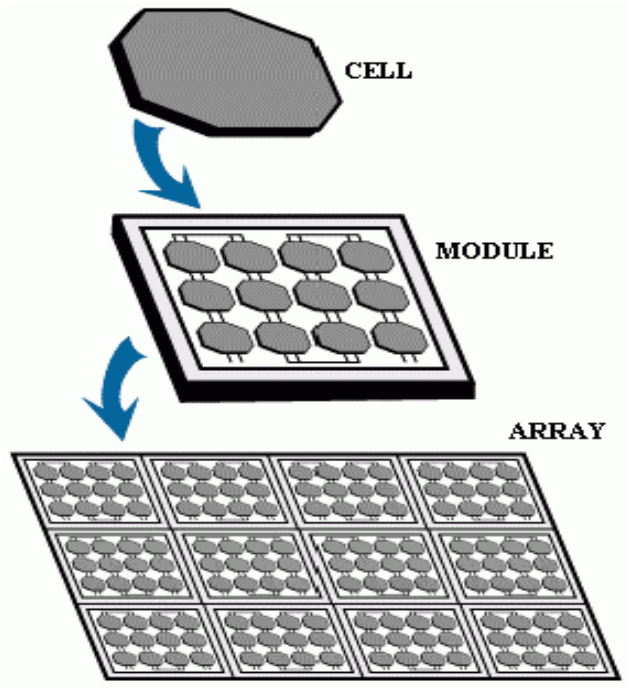

Figure 2-2: Solar Cell, Module and Array (Knier, 2008)

The combination of modules arranged and connected in parallel or series electrically makes up what is called solar array. In general, the amount of electricity produced for a region depends on the size of the solar array, sunshine hours and the average solar irradiance of the region. The solar array produces direct current which are used directly to charge a battery through a charge controller and powering a DC load. The stored DC in the battery is used to power AC loads via an inverter. Figure 2-6 shows the solar PV system.

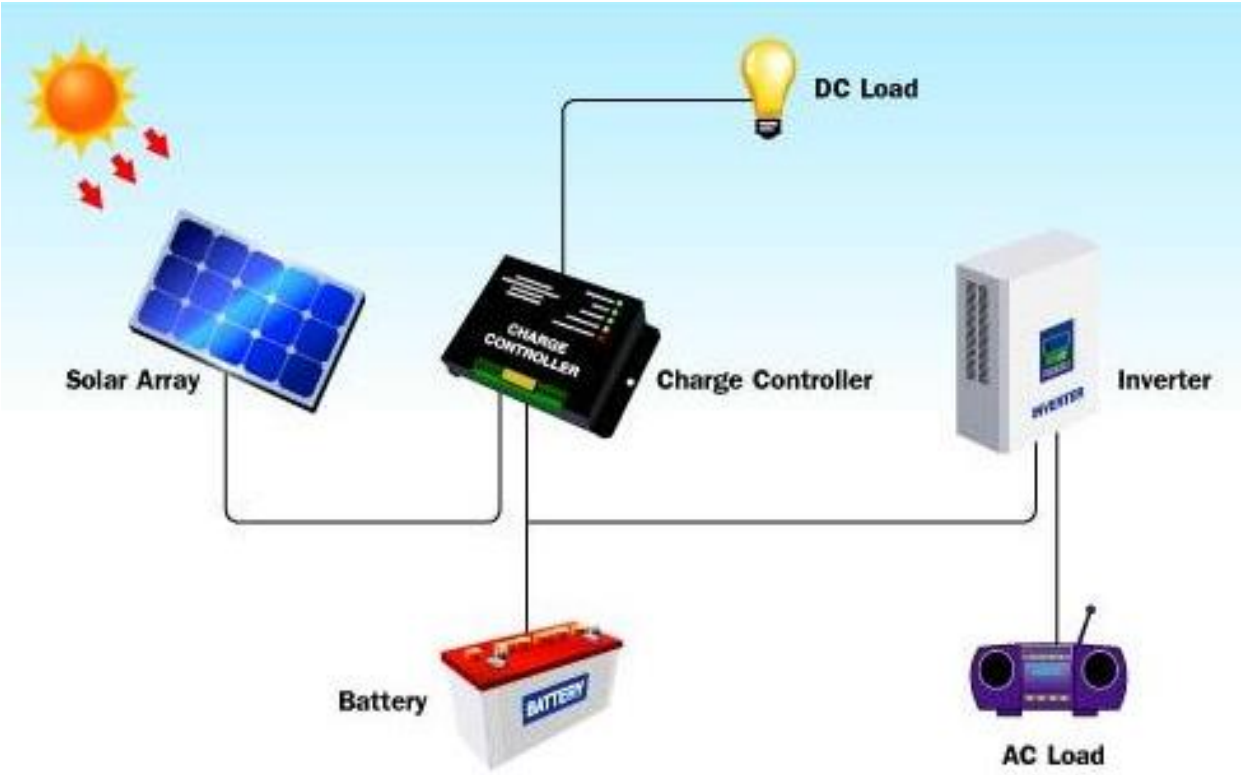

Figure 2-3: Solar PV System (LEONICS, 2017)

2.7 Development of Solar Photovoltaic Technology

Solar photovoltaic and solar thermal technologies offer an environmentally-friendly, clean and inexhaustible energy resource to mankind (Singh, 2013). The research towards the development of cost-effective and safe energy has grown over the past decades. Solar energy technology applications such as solar heating, solar photovoltaic, solar thermal electricity and solar architecture have undergone tremendous development over the years and has had significant impact towards solving the ever increasing global energy demand (International Energy Agency, 2011; Singh, 2013).

The photovoltaic effect was first discovered in 1839 by Becquerel and this effect was observed in Solid Selenium by Adams and Day and subsequently Fritz developed the first PV cell in 1883 with an efficiency of less than 1% (Zweibel and Herch, 1984; Singh, 2013). A new type of photovoltaic cell was developed in 1927 using copper and semiconductor copper oxide, also with a conversion

efficiency of less than 1%. The first silicon photovoltaic cell was developed in 1941 by Ohl with efficiency of 6% and 11% with further researches by Bell laboratories in 1954 (Zweibel and Herch, 1984).

The first 1 W photovoltaic generator was developed for the Vanguard satellite in 1958 and a further increase in power was sought with little or no emphasis on the cost (Zweibel and Herch, 1984; Singh, 2013; Ruuska, Aikala and Weiss, 2014; Michael, Iniyan and Goic, 2015).

The rapid increase in global energy demand, depletion of conventional energy sources and environmental concern have tremendously increased research interest towards investigating the PV technology for large scale energy generation with the application both in stand-alone and grid-connected configuration without storage. Over the past decades, the development of PV technology has been dynamic and has been extensively investigated. The progress in the development of PV technology has been phenomenal with a continuous increase in market (Zweibel and Herch, 1984; Coiante, 1992; Singh, 2013). Although PV technology is still a relatively expensive technology, the costs of solar power are coming down and the market is expanding (Burns and Kang, 2012). The cost has further reduced in recent years with the advances in technology and it is likely to fall further.

Koutroulis *et al.* (2006) developed a methodology for optimally sizing of a hybrid, stand-alone Photovoltaic/ Wind-Generator (PV/WG) system. This was achieved using an optimization tool called a genetic algorithm. Lal and Raturi (2012) investigated the feasibility of a hybrid power system in Fiji and used Hybrid Optimisation Model for Electric Renewables (HOMER) software to simulate and optimise the system, they concluded that a renewable energy-based configuration is feasible and that this would result in the reduction of greenhouse gas.

Friling *et al*.(2009) presented a mathematical modelling of the heat transfer of building integrated photovoltaic modules and Fanni, Virtuani and Chianese

(2011) presented a detailed analysis of fully-integrated flat roof amorphous silicon photovoltaic plants with emphasis on gains and losses.

The development of PV technology has moved from 1st generation to the 4th generation with improvements either in cost effectiveness or efficiency. Bagher, Vahid and Mohsen (2015) studied the types of solar cells and their applications. They discussed the generations of solar cells as first, second and third generation cells. The first-generation cells are commercially the main PV technology which are made of polysilicon and monocrystalline silicon. They are efficient, but expensive. Second generation cells which are commercially significant in small standalone power system are thin film solar cells, that are amorphous silicon which are flexible, some are made from other materials such as CdTe and CIGS cells. They are easier to make and cheaper than the 1st generation but less efficient. The third generation of solar cells are emerging photovoltaics which are of thin-film technologies although not yet commercially available. They combined the features of 1st and 2nd generation (high efficiency as in 1st generation and are likely to be made of other materials other than simple silicon as in the 2nd generation e.g. they are made of perovskite crystals, and feature multiple junctions made from multiple layers of different semiconducting materials). Figure 2-7 shows the three types of solar cells in use today as discussed earlier. Silva (2013) in a keynote address presented his definition for 4th generation (4G) solar cell technology as cells based on "'inorganics-in-organics'" and that they offer higher conversion efficiency than the current 3rd Generation (3G) Solar Cells, while maintaining their low cost base. The 4G solar cells according to Silva (2013), combines the flexibility of polymer films (organic) with the nanostructure (inorganic) within a single layer nanostructures which serves to improve the manipulation of electrical charges and consequently improving the efficiency over the 3rd generation cells (Silva, 2013).

Figure 2-4: Types of Solar Cells

To improve the reliability and efficiency of the solar power plant, hybrid systems have been investigated. The hybrid system which is a combination of two or more energy systems is gaining ground because of its inherent higher efficiency than each of the systems when applied singly (Rajesh, Kulkami and Ananthapadmanabha, 2015). Charfi, Atieh and Chaabene (2016) investigated and analysed the performance of PV/battery storage bank, diesel generator only, and hybrid PV/Diesel Engine/battery bank using a global model and finally compared the cost of the three systems in three different countries. The study concluded that the best method in Kingdom of Saudi Arabia (KSA) is the use of diesel as it is heavily subsidized and the best power supply solution in Tunisia and Jordan is the hybrid PV/DE/Battery storage bank because it will take only nine years to recover the investment. Figure 2-8 shows a hybrid solar PV and Diesel generator power supply system.

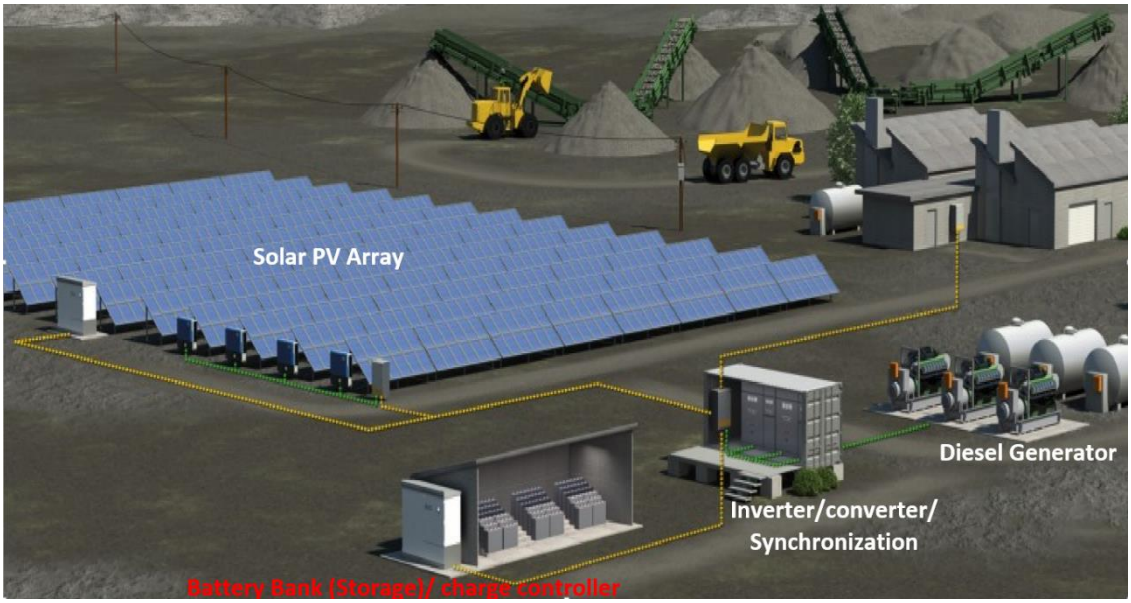

Figure 2-5: Hybrid Solar PV/Diesel Generator System Adopted from (Dumont *et al.*, 2013)

Radwan, Ookawara and Ahmed (2016) used a thermal model to study the influence of operating conditions on the performance of the low concentration photovoltaic (LCPV) thermal system. A microchannel heat sink was used for the cooling of the LCPV and the predicted result shows that the heat sink is very effective with a cell temperature variation of between 33.5 and 35.6^{o}C with concentration ratio of 20.

Salehin, Rahman and Islam (2015) carried out modelling of a PV-Diesel hybrid energy system using HOMER software for energy supply to the Northern part of Bangladesh. An optimum energy system consisting of PV and diesel was designed, even though diesel usage constitutes an environment hazard. The study shows a considerable reduction in the percentage of emission with the hybrid system. The economic analysis shows the net present cost of the system to be $149,112 and the levelized cost of electricity to be $0.461/kWh. It also concluded that although the cost difference between the two systems is just $0.038, the hybrid produces 53.68% lower CO_2 emissions.

Rajesh, Kulkami and Ananthapadmanabha (2015) developed the architecture of a hybrid energy supply system comprising of solar PV and Doubly Fed Induction Generator (DFIG) and simulated the proposed system using MATLAB Simulink,

a boost converter was used to increase the voltage from the solar panel. The output voltage after boosting was 625 V regardless of the variation in solar panel voltage. This is shown in Figure 2-9.

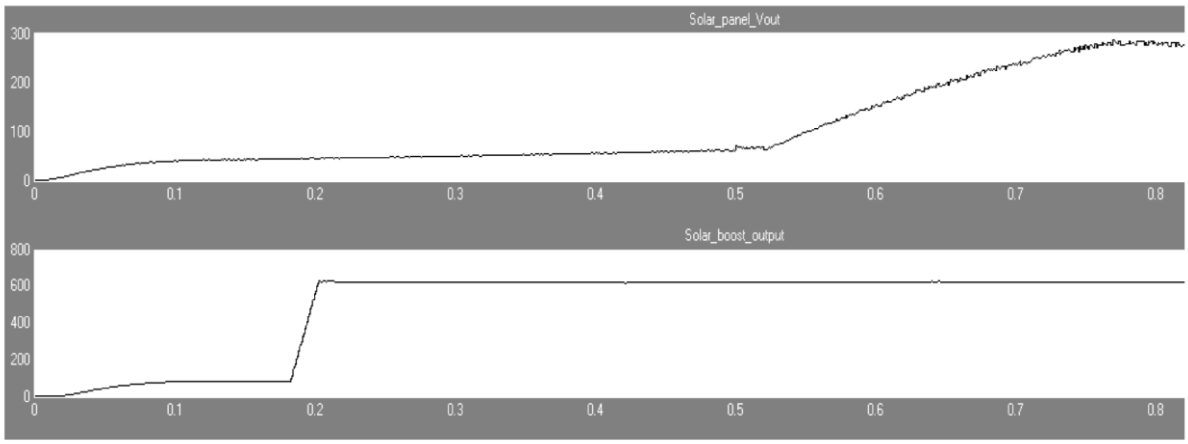

Figure 2-6: Solar Panel Voltage and Boost Voltage (Rajesh, Kulkami and Ananthapadmanabha, 2015)

Photovoltaic power generation has been most useful in remote applications with small power requirements where the cost of running distribution lines was not feasible. As PV power becomes more affordable, the use of photovoltaics for grid-connected applications is increasing. However, the high cost of PV modules and the large area of land that they require continue to be obstacles to using PV power to supplement existing electrical utilities. An interesting approach to both problems is the integration of photovoltaics into buildings.

The growth in the world's population and the move towards global industrialization combines with the rise in concern for the environment, has spurred research into the use of solar energy to meet the increasing energy demand. Beyond the fact that solar PV systems aid economic development, they also eliminate the cost of installing grid systems to isolated rural areas. They also ensure a high level of reliability and a sustainable environment by limiting the emission of CO_2 (Lal and Raturi, 2012).

About 1000,000 TW of energy is released into the solar system from the sun per second (Hunter *et al.*, 2012; Ketlhwaafetse, 2016) and the temperature at the

surface of the sun is approximately 6000 K with solar flux reaching 1353 W/m^2 at a point just outside the earth's atmosphere (Hunter *et al.*, 2012; Ketlhwaafetse, 2016).

The trend of the energy demand in Nigeria for over 25 years was investigated by Ibitoye and Adenikinju (2007) with the assumption that the country develops economically, meets the millennium development goals (MDG) in 2015 and achieves the status of an industrialized nation. The paper concluded that Nigeria require electricity to the tune of 160 GW, as against 6500MW as it was in 2007.

There are a number of studies on concentrated solar power (CSP), however the conversion efficiencies in the range of 7 to 25% are still low and therefore there is the need to significantly reduce the cost (Ju *et al.*, 2017). Commercial CSP plants have their efficiencies within the range of 15 – 20% while for parabolic trough and dish systems are 15% and 25 – 30% respectively, although the dish system has a higher efficiency, the high cost and unreliability of the Stirling engine has made its commercialisation difficult (Graham-Cumming, 2009; Ju *et al.*, 2017)

2.7.1 Development of Solar PV farms in Africa

Africa is attracting global attention in the area solar energy development. This is because of the energy deficiency and increased population, competitive cost and very importantly the abundant availability of high solar irradiance.

South Africa has the largest solar PV farm in Africa with a capacity of 175 MW (Figure 2-10). The entire solar farm facility is spread over a surface of almost 500 hectares and consists of a number of 700,000 solar panels (*The largest Solar Farm in the Southern hemisphere is located in Central South Africa*, 2017). Although it is only 2% of South Africa/s power mix is solar PV power.

Figure 2-7: 175 MW Solar PV Farm in South Africa (*The largest Solar Farm in the Southern hemisphere is located in Central South Africa*, 2017)

Nigeria has no large solar PV farm for huge solar conversion despite having an abundant solar energy potential and about 320 of 365 days of sunshine. This present research will build a model that can be used for the techno-economic analysis including photovoltaic system sizing. This will ultimately reduce the cost of design and economic analysis of the system.

2.8 Solar Resource Assessment for Nigeria

Solar resource information of a location is very crucial to the design and simulation of a solar PV energy supply system. The technical and financial risks associated with solar energy conversion systems for electricity generation can be alleviated through better understanding and knowledge of the available solar resource.

The analysis of monthly and annual values of Global Horizontal Irradiation (GHI) in a given location is the usual approach to quantify and evaluate the solar resource in that location (Zawilska and Brooks, 2011; Moreno-Tejera *et al.*, 2016; Abreu *et al.*, 2018). Zawilska and Brooks (2011); Duffie *et al. (*2013); Abreu *et al. (*2018) recommended the use of past measurements of solar radiation in the

location of interest for designing and prediction of solar energy systems performance. Figure 2-11 shows long time average of global horizontal irradiance (GHI) of Nigeria for 1994-2018.

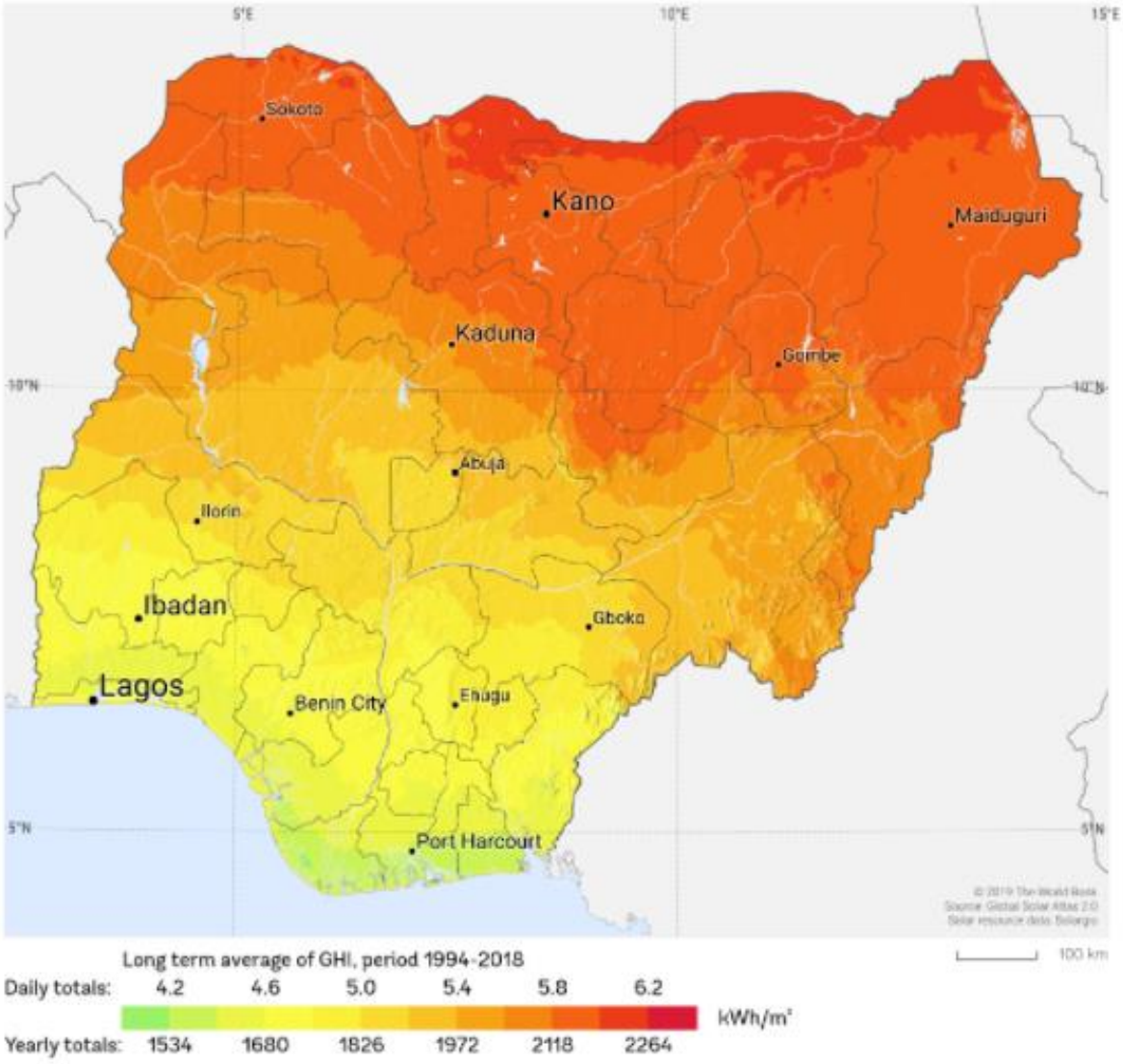

Figure 2-8: Long time average of GHI (1994-2018) for Nigeria (Solarigis, 2020)

From this figure the daily average for the around the location of this study is 6.2 kWh/m^2 which translates to 258.4 W/m^2. This agrees with the calculated daily average from the 11-year (2006-2016) data used in this research which is 266 W/m^2.

Chineke *et al.* (1999) opined that there is paucity of solar radiation data in Nigeria. In 2018, the Director General (DG) of the Nigerian Meteorological Agency (NiMet) said that to effectively cover the entire country which has huge land mass of about 923,768 sq km,, it will need not less than 9,000 weather stations (Sumaina, 2018). Nigeria, according to the DG NiMet, has a target of 200 weather stations by the end of 2018 (Sumaina, 2018). This number of weather stations is grossly inadequate for Nigeria and therefore leads to scanty literature on data analysis in Nigeria.

Because only long time monthly average data are available in some weather stations in Nigeria, Dada and Okogbu (2017) established a procedure for the derivation of daily solar radiation from the monthly averages using Fourier series. The simulated and the measured data were in good agreement.

(Ayoola *et al.*, 2014) collected hourly average net all-wave radiation data spanning three years (2010-2012) at a meteorological station locatated inside the Obafemi Awolowo University campus in Ile-Ife (7.52^{o} N, 4.52^{o} E). From the data set, hourly maxima of the net radiation occurred at 14.00(GMT+1). The values increased considerably from 337.6 ± 146.4 W/m^2 in July which is the peak of the wet season, to 441.7 ± 82.4 W/m^2 in March, the end of dry season.

2.9 Modelling, Simulation and Optimization Software tools

There are several software tools that have been developed for modelling renewable energy system. Some of these have been reviewed here.

2.9.1 System Advisor Model (SAM)

SAM is a computer model that calculates and simulates the performance and financial metrics of renewable energy systems such as photovoltaic, concentrating solar power, solar water heating, wind, geothermal, biomass, and conventional power systems. Its advanced simulation options has the capability for parametric, sensitivity and statistical analyses using Monte Carlo simulation and weather variability studies (Blair *et al.*, 2014). Past versions of SAM over the years do not have the capability for sizing solar photovoltaic system component

until the latest version was released in 2020 with capability to size betteries (NREL, 2020b). Sizing of other components are yet to be included in SAM.

2.9.2 Hybrid Optimisation Model for Electric Renewables (HOMER)

HOMER is a micropower computer optimization model that simplifies the task of designing hybrid renewable micro-grids. It has capability for design of off-grid and grid-connected systems. HOMER finds the least cost combination of components that meet electrical and thermal loads. It simulates thousands of system configurations, optimizes for lifecycle cost, and generates results of sensitivity analyses on most inputs (NREL, 2014). The sensitivity and optimisation analysis algorithms integrated in the software enables the user to evaluate the economic and technical feasibility of many technology options and to account for variations in technology costs and energy resource availability (Onwe, 2017). The latest updated version of HOMER is the HOMER Pro version 3.8.4 (March 2, 2017) (Onwe, 2017). This software uses windows as a computer platform with visual C++ as a programming language. Its features include:

i. “The software can simulate a renewable energy system over an annual cycle.
ii. It can suggest the design of various systems based on economic parameters.
iii. HOMER can generate results and list them per feasibility and sorts them by the net present cost.
iv. HOMER does not allow multi-objective function for minimising the net present cost, it uses only a single objective function in the optimisation process. Also, the software does not rank the results of the hybrid system configurations in terms of levelised energy cost, and this is a potential drawback” (Onwe, 2017).

2.9.3 PVsyst Software

PVsyst is a PC software package for the study, sizing and data analysis of complete PV systems. This software handles grid-connected, stand-alone, pumping and DC-grid (public transportation) PV systems, and includes extensive meteo and PV systems components databases, as well as general solar energy tools. This software is geared to the needs of architects, engineers, researchers. It is also very helpful for educational training. The latest version, PVsyst 7.0, which was released on 25 May 2020 has in its release notes, new features which include economic evaluation such as Levelized Cost of Energy (LCOE), Net Present Value (NPV), multiple loans of multiple types, advanced depreciation configuration economic evaluation now available for Stand-alone and Pumping systems in this latest version.

2.9.4 Solar Photovoltaic System Model (SPVSM)

SPVSM is an acronym for Solar Photovoltaic System Model. It was developed by Hauwa Talatu Abdulkarim (the author of this thesis) for sizing solar PV system components (PV array, battery, inverter and charge controller) and conducting energy and economic analysis of the system. It is a modelling and simulation software developed on a single graphical interface in MATLAB for designing a stand-alone solar PV power supply system which can be applied to villages/households especially in rural settlements which constitute more than 80% of regions without access to electricity in Nigeria. The package has the capability for conducting a sensitivity analysis on the energy and economics of the system considering variation in degradation factor and discount rate. It also gives an economic appraisal such as net present value (NPV) over the expected lifespan of the project. It is built on a single GUI platform but with six executable panels each handling different aspects of component design, energy, and economic analysis. The details of the development of each of the executable panels with some of the controlling equations used are presented in the chapter on methodology. This model does not require extensive software knowledge to

handle and therefore very suitable for the artisans in Nigeria who are generally in charge of solar PV system developments in rural areas.

2.9.5 Maximum Power Point Tracking

Maximum power point tracking (MPPT) controllers play an important role in photovoltaic systems. They maximize the output power of a PV array for a given set of conditions. The maximum power point (MPP) varies with solar insolation because PV systems exhibit nonlinear behaviour, and there is a unique PV panel operating point at which the power output is at a maximum (Babaa, Matthew and Pickert, 2014). Therefore, for maximum output power, which is a consequent of maximum efficiency, the use of a maximum power point tracking (MPPT) algorithm to optimise the delivered PV output power at different operating points to the load is imperative. There are many existing algorithms for the actualisation of maximum power point tracking of PV system and research has been carried out to optimise the various techniques (Sera *et al.*, 2006b; Esram and Chapman, 2007; Faranda and Leva, 2008; Babaa, Matthew and Pickert, 2014).

Tracking the maximum power point (MPP) of a photovoltaic array is crucial to the opyimum operation of a PV system (Femia *et al.*, 2008; Ali *et al.*, 2012; Micheli and Muller, 2017). There are a number of methods with variying advantages.The methods all vary in complexity, number of sensors required, digital or analogue implementation, convergence speed, tracking ability, and cost effectiveness (Babaa, Matthew and Pickert, 2014). A brief review of two most popular of these techniques are presented below.

2.9.6 Perturb and Observe (P & O) Method

P and O method is referred to as a hill climbing method, because it depends on the rise of the curve of power against voltage below the maximum power point, and the fall above that point. It operates by increasing or decreasing the array terminal voltage, or current, at regular intervals and then comparing the PV output power with that of the previous sample point. If the PV array operating voltage changes and power increases (dP/dV PV > 0), the control system

adjusts the PV array operating point in that direction; otherwise the operating point is moved in the opposite direction (Narendiran, 2013). At each perturbation point, the algorithm continues to operate in the same manner (Barakati, Kazerani and Aplevich, 2009; Chen *et al.*, 2010). The main advantage of this approach is the simplicity of the technique. Furthermore, previous knowledge of the PV panel characteristics is not required. In its simplest form, this method generally exhibits good performance provided the solar irradiation does not vary too quickly. At steady state, the operating point oscillates around the MPP voltage and usually fluctuates lightly . Perturb and observe technique is the most commonly used MPPT method due to its ease of implementation.

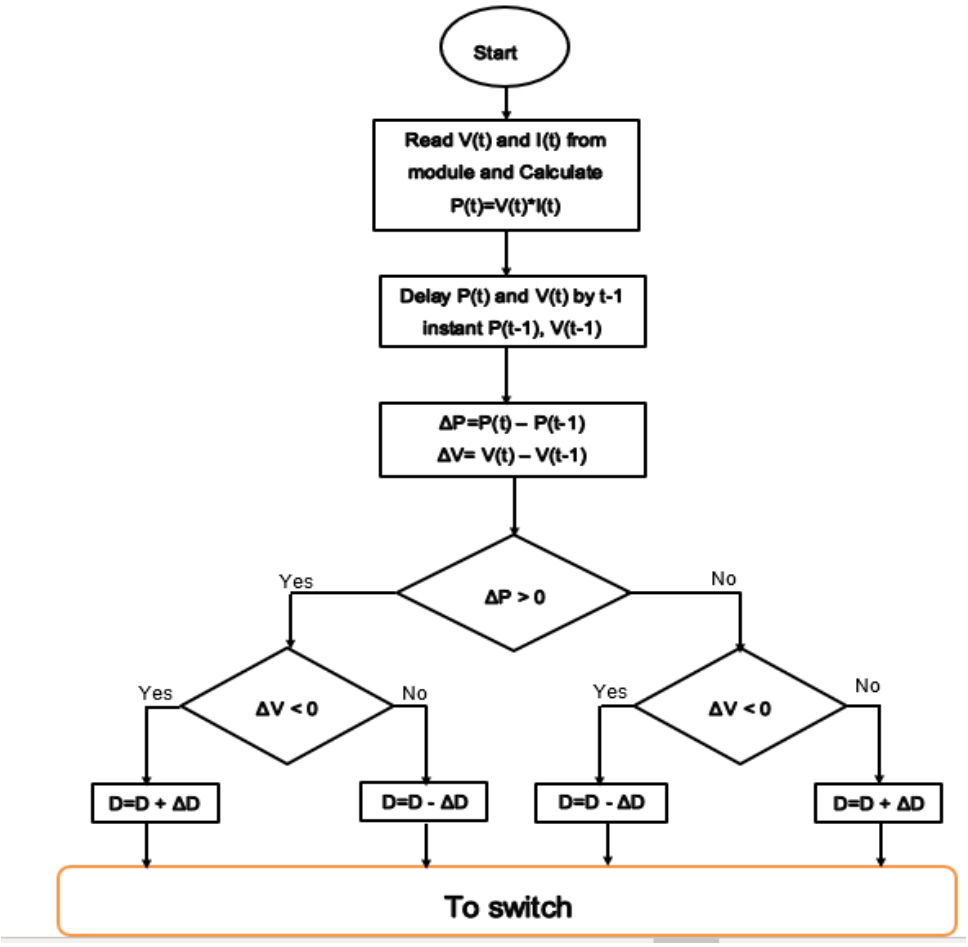

Figure 2-9: Flowchart of Perturb & Observe MPPT Technique

.

2.9.7 Incremental Conductance (IC) Method

The incremental-conductance (INC) [12–18] method is also often applied in PV systems. It tracks the MPP by comparing the instantaneous and incremental conductance of the PV array. The issue of INC method is similar to P&O. The fixed step size is usually adopted, which determines the accuracy and response speed of MPPT.

The incremental conductance (IC) algorithm which is shown in Figure 2-10, seeks to overcome the limitations of the perturbation and observation algorithm by using the incremental conductance of the photovoltaic. This algorithm works by searching for the voltage operating point at which the conductance is equal to the incremental conductance. At this point, the system stops perturbing the operating point. The advantage of this algorithm is that it has the ability to ascertain the relative “distance” to the maximum power point (MPP), therefore it can determine when the MPP has been reached. Also, it is capable of tracking the MPP more precisely in highly variable weather conditions (Dorofte, Borup and Blaabjerg, 2005), and exhibits less oscillatory behaviour around the MPP compared to the P & O method, even when the P & O method is optimized (Salas *et al.*, 2006). Nevertheless, the IC algorithm has the disadvantage that instability can result due to the use of a derivative operation in the algorithm. Also under low levels of insolation, the differentiation process difficult and prone to measurement noise; and results can be unsatisfactory (Liu, Wu and Cheung, 2004)

. In general, the IC tracking approaches use a fixed iteration step size, which is determined by the accuracy and tracking speed requirement. The step size may be increased to improve tracking speed, however, accuracy is decreased. Likewise, reducing the step size improves the accuracy, but sacrifices the speed of convergence of the algorithm (Babaa, Matthew and Pickert, 2014).

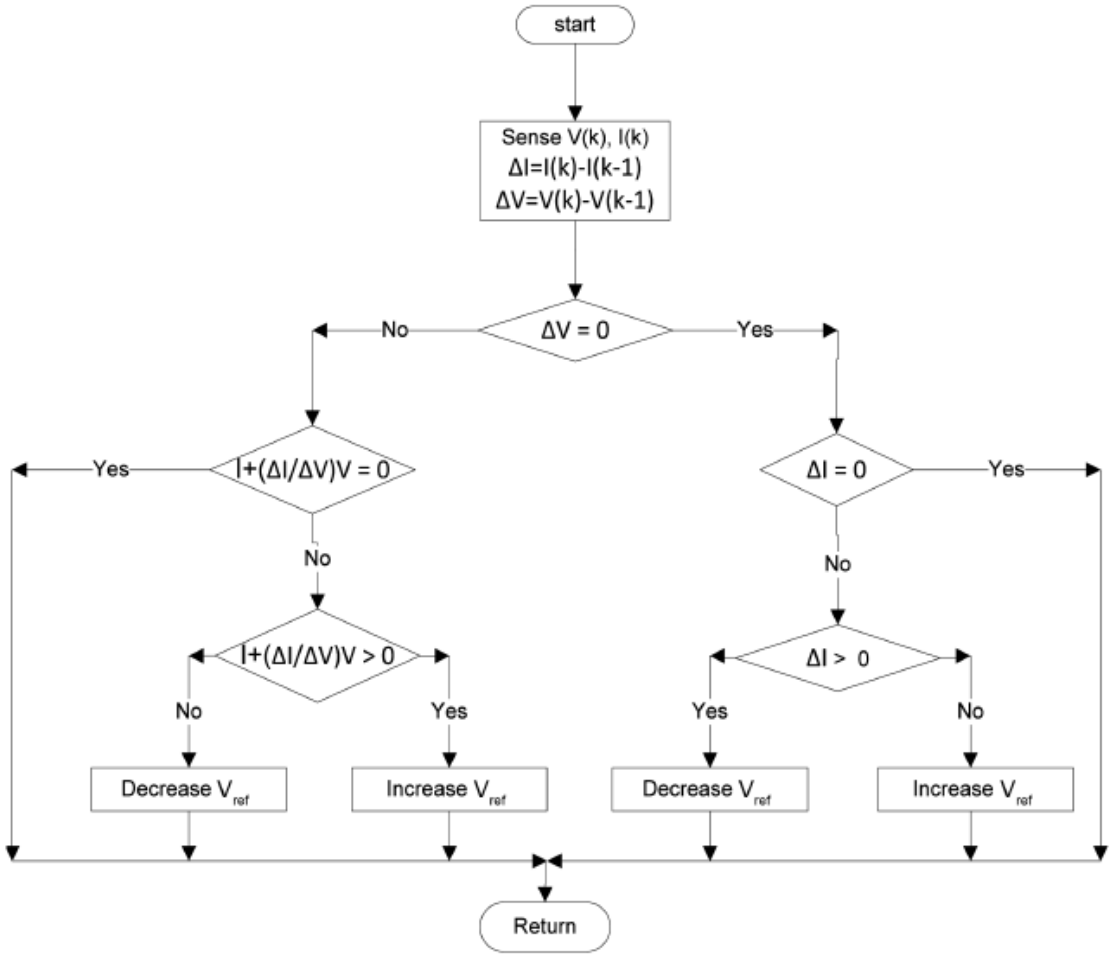

Figure 2-10: Flowchart for Incremental Conductance Algorithm

2.10 Effect of Environmental Condition on the Performance of Solar PV System

Since photovoltaic (PV) panels convert sunlight into electricity and the performance of these panels depends very strongly on the amount of solar irradiance reaching its surface, it then means that any condition which will affect the amount of solar irradiance reaching the panels will affect its performance. One problem is that a build-up of dust over time can significantly reduce the efficiency of the panels, by as much as 30%. De-rating factor is an important factor in the design of solar PV system with power losses due to dust is usually estimated to be 2 - 5% (Tanesab *et al.*, 2017). The reliability of the system to

supply power could be adversely affected if the de-rating factor which takes into cognisance power loss due to dust is underestimated. This could cause serious problems for PV applications especially small-scale projects.

Many researchers have studied the effect of the environmental condition on the performance of solar PV modules. Some of the environmental conditions include ambient temperature, dust, shade, wind speed and rain.

Tanima, Chakraborty and Kaushil (2014) studied the effect of ambient temperature and wind speed on the performance of a PV module. The researchers carried out experimental work using a 37 W monocrystalline solar module with area of 0.3239 sq. meters and the results were subjected to statistical analysis. This revealed that the values of correlation coefficient for ambient temperature and wind speed were 96% and 68% which implies that module performance has high positive linear relationship with ambient temperature and medium linear positive relationship between module performance and wind speed. Ehsan and Abbas (2016) investigated the impact of weather conditions on the performance of the photovoltaic (PV) module with emphasis on temperature and dust settlement. Experiments were performed using two similar 75watt modules each. The module temperature was cooled using water circulation and very fine soil was used to estimate the effect of each of hot weather and dust deposition on the performance of PV respectively. The result of the experiment reveals that the Fill Factor (FF), which is the ratio of the maximum power of the solar panel to the theoretical power and PV efficiency are affected inversely with increased temperature while cooling contributes to increased voltage generation across PV panel by 11.8%. A drop in voltage generation of 3.8% was observed for unclean panels, which is due to natural pollutant deposit on the panel for three months.

2.10.1 Review of Literature on Deposition and Impact of Dust on PV Modules

The performance of solar PV module is greatly affected by dust which is an emerging area of research in photovoltaic energy conversion system. The studies conducted by Menoufi (2017), Figure 2-13, shows that in 26 years (1990 to 2016), only 72 studies were conducted on the impact of dust on the performance of solar PV panels globally.

Figure 2-14 presented Africa to have contributed only 12% which amounts to about 8.64 (approximately 9) studies in 26 years as of 2017. This is grossly inadequate considering that Africa is one of the worst dust accumulation zones in the world, in addition to the fact that there are many initiatives that support renewable energy cooperation between Europe and Africa (Mann, 2012; Menoufi, 2017). This further confirms that there is scanty literature on the effect of dust on the performance of PV panels and therefore, buttresses the need for the study on the effect of dust in Maiduguri, Nigeria. This is a region characterized by intense dust accumulation.

The chosen location for the experimentation of the impact of dust on the performance of solar PV module is Maiduguri in North-eastern Nigeria. This location is the most dust accumulation region in Nigeria because it is a desert area and with highest average solar irradiance in the country.

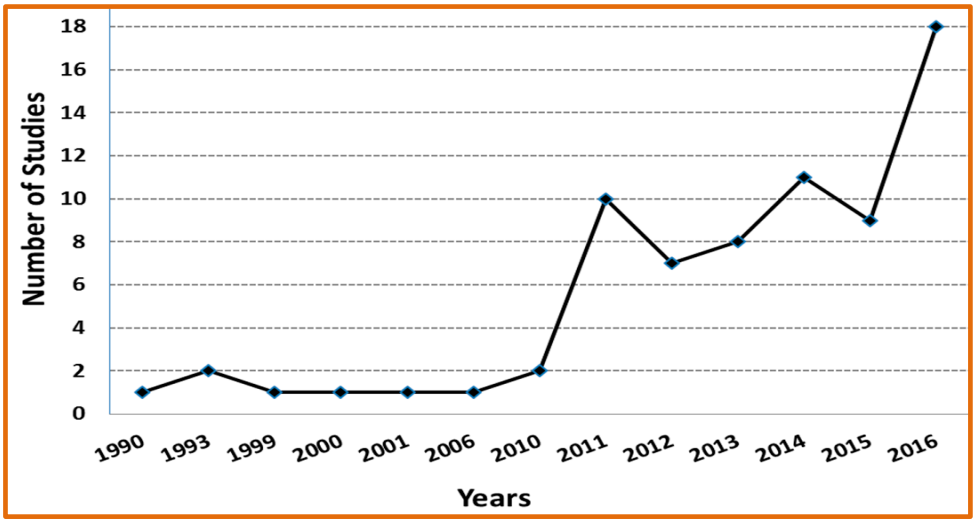

Figure 2-11: Number of studies of the impact of dust accumulation on the performance of PV panels (Menoufi, 2017)

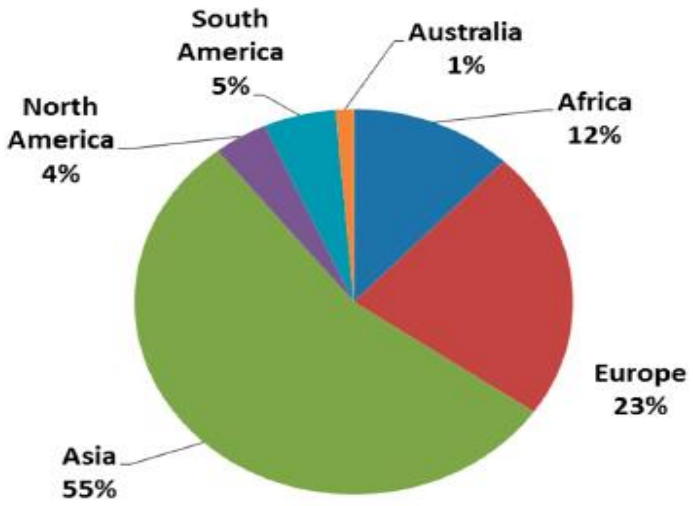

Figure 2-12: Percentage contribution of each continent to the studies of the impact of dust on PV panels (Menoufi *et al.*, 2017)

Solar energy is a renewable energy of choice but the intermittent nature of the solar resource at any location makes solar data analysis imperative and an important prerequisite to accurate sizing of solar PV system components. Nigeria, a country endowed with solar energy and yet having a grossly insufficient energy supply to its citizens for both domestic and industrial purposes, requires a low-

cost solar energy conversion system for the development of local communities. To accurately size solar PV system components, solar radiation data were collected from the Nigerian Meteorological Agency (NIMET) for three radiation regions (Maiduguri in the North-east, Minna in North-central and Port Harcourt in the South of Nigeria) were analysed. The sizing of the solar PV components is somewhat complex because of interdependencies and the variation inherent in solar resource. This makes the development of a Solar PV System Toolkit (SPVST), which can be rapidly used to size/design the components with minimum effort and time, an important tool and innovation. This forms a significant part of this thesis. The toolkit was developed with the capability to accurately size the solar PV modules required for any energy demand at any location because it calculates the Panel Generating Factor (PGF) for any location with the available solar radiation data. Other components such as the battery, inverter and charge controllers can also be accurately sized from the requirement of solar PV model and the desired energy demand. The cost competitiveness of any energy conversion system is a global problem and therefore the model developed also has energy and economic analysis capabilities. This new software model is unique and novel as it connects the design and economic analysis of a photovoltaic energy system on a single graphical user interface (GUI), the first of its kind to the best of my knowledge.

The motivation and justification for this research was drawn from the facts that the world installed PV capacity with the giga-watt contribution from each continent presents Middle East and Africa, a region naturally so endowed with solar energy resource, as having an insignificant contribution to the world installed PV capacity. Ironically, it also has a grossly insufficient energy supply to its citizenry for both domestic and industrial purposes. This buttresses the need for a PV system study which will address the further understanding of the photovoltaic system and encourage increased installation in Africa and particularly in Nigeria. Solar energy has the capacity, if efficiently harnessed, to supply sufficient energy to rural areas in Nigeria which are far from the National grid. Also, the development of solar PV technology is capable of giving improved healthcare

services and economically empowering the rural dwellers. All the above combined with the fact that there is enormous availability of solar energy in Nigeria and the inadequate supply of energy justifies the research which is geared towards increasing the understanding and installation of solar PV. Nigeria has the highest population in Africa and unfortunately among the countries with the lowest electricity consumption per capita in the continent (74 kWh/year). The residential electricity use per capital of Nigeria is very low and this has contributed tremendously to the poverty level of the citizenry (Ibitoye and Adenikinju, 2007). Also, because the region under study is a region where dust is prevalent and apart from the fact that there is scanty literature on effect of dust, the researches have varying results from region to region combine also with the fact that no such study has been carried out in this region, all these necessitated the study of the impact of dust on PV panels in North-eastern, Nigeria.

The impact of sand and dust accumulation on photovoltaic (PV) modules is an emerging area of research in which literature is still scanty especially from regions mostly characterised by dust and also favourable to photovoltaic energy conversion system development (Menoufi, 2017; Menoufi *et al.*, 2017). Some of the available literature in this area have been reviewed in this section.

Sand and dust accumulation on photovoltaic (PV) modules have been shown in both field studies (Al-Hasan and Ghoeneim, 2005; Eliminir *et al.*, 2006) and laboratory experiments (El-Shobokshy and Hussein, 1993; Goosens and Kerschaever, 1999; Jiang, *et al.*, 2011), to cause reduction in module performance because these sand/dust particles prevents sun rays or solar irradiance from getting to the PV cells and consequently, the electrical output of the module is reduced.

The performance of solar PV system is hugely affected by the ability of the glass cover to transmit solar irradiance to the collection surface of the module. Other factor which have effect on module performance include amount of solar irradiance, angle of tilt of the absorbing surface (which will affect the ability of a particle to remain on the surface), and module material properties etc. (Beattie *et al.*, 2012).

The main effect of some of the above factors is the continuous degradation of transmittance of the glass cover which is mostly affected by

dust accumulation. Looking through PV literature, it is obvious that there has been little concern for the problem of dust and therefore limited published works indicating that the problem has not been well investigated (Elminir and Abdel-Moneim, 2006). Salim *et al.,* (1988) conducted experimental research at a solar village near Riyadh in Saudi Arabia. A PV test system was constructed and was used to investigate the impact of long-term dust accumulation on the photovoltaic array electrical output. The PV array was fixed at 24.6^{o} to the horizontal and the monthly energy reduction for the uncleaned array was obtained by comparing its output with an identical array which was cleaned daily. They reported that the reduction in the energy output from the uncleaned array at the end eight months was about 32%. This reduction in energy would have occurred much earlier if the research had taking into consideration time. However, the physical properties of the dust were not studied and the result is somewhat misleading as this reduction would have been attained in a few weeks in a highly polluted site like Saudi Arabia.

Another research conducted by Hassan *et al*. (2005) shows rapid degradation during the first 30 days of exposure. The result shows a reduction in performance of 33.5% after one month and the reduction increased to 65.8% after six months with uncleaned solar panels.

Tanesab *et al.* (2017) investigated the seasonal effect of dust on the degradation of PV modules deployed in two different climate areas, Perth, Western Australia, a temperate climate region and Nusa Tenggara Timur (NTT), Indonesia, a tropical climate region. They reported that the performance of PV module varies from one season to another. In the temperate climate of Perth, the PV modules performance was highest at the onset of summer, was seen to decrease greatly at the end of the season. The performance was seen to increase at the end of autumn and climaxed at the end of winter. Meanwhile, in NTT, PV modules were at their best in early wet season and at the end of the dry season, their output

slightly declined. The research shows that the effect of dust on the performance of all modules in the two sites was higher than the effect of non-dust related factors. Figure 2-12 shows the experimental set-up.

Figure 2-13: A Clean and a Dusty PV Panels (Tanesab *et al.*, 2017)

Garg (1974) conducted a research on the normal transmittance of direct radiation through glass and discovered that the transmittance decreased from 90% to 30% for a horizontal mounting during a period of 30 days. A similar study was conducted by (Sayigh, *et al.*, 1985) in Kuwait. The findings revealed that a 64%, 48%, 38%, 30% and 17% reduction in the transmittance of the glass plates was observed after 38 days of exposure to the environment with tilt angles of 0°, 15°, 30°, 45° and 60°, respectively, thus indicating the effect of tilt angle of the panel on the ability of soiling particles to remain on the surface.

El-Shobokshy and Hussein (1993) conducted laboratory experimental research by polluting PV surfaces with different kinds of dust and assessing the performance of the PV under these conditions in the form of energy output of the cells. The result also shows that the nature of dust (dust material, deposition

density, size distribution) has a huge influence on the performance of PV modules. However, this study was conducted under zero wind speed conditions which is most unlikely in field experiments. This forms a drawback in this research because low winds have a significant effect on the sedimentological structure of dust coatings on flat surfaces (Elminir and Abdel-Moneim, 2006). Another drawback of this research is that no natural desert dust was used in the laboratory experiments.

Adinoyi and Said (2013) studied the effect of dust accumulation on the power output of solar PV modules in the Eastern province of Saudi Arabia. Six modules faced towards the south and tilted at 26^{o} were exposed to outdoor conditions and power outputs of the solar modules were measured and recorded on daily basis using a HT Italia photovoltaic analyzer. The parameters measured during the field experiments were current and voltage readings of the PV modules, ambient temperature, module backside temperature and global radiation on the tilted surface. The research concluded that a single storm can reduce the performance of the PV module by 20% and up to a 50% reduction in output can be observed with unclean PV modules.

Beattie *et al.*, (2012) conducted a simulation of sand accumulation on PV modules under controlled conditions in a laboratory environment. This obviously does not perfectly represent field conditions but could be the basis for the numerical investigation of the fundamental processes leading to a reduction in the incident sunlight levels. This was supported by a laboratory experiment of sand particles accumulated on a glass surface. From their numerical and analytical models, they concluded that the process of accumulation can be described over an order of magnitude by an exponential decay which is the result of particle clustering.

The optical properties of dust, in addition to morphology factors, are dependent on its density. The intensity of light reaching the modules tends to decline as the amount of dust deposited on module's surface increases (Elminir *et al.*, 2006;

Kalogirou, Soteris A., Agathokleous, Rafaela Panayiotou, 2013; Sarver, Al-Qaraghuli and Kazmersk, 2013; Tanesab *et al.*, 2017). The effect of different densities of dust was examined by Appels *et al.* (2013) and they reported that by spraying 20 g/m^2 of white sand onto the surface of a 100 W Sanyo PV module, the transmittance and power output reduced by 4.02% and 4.84% respectively. They also reported from their findings that as the amount of dust increased to 40 and 60 g/m^2, the transmittance decreased as much as 9.18 and 15.03%, while power output dropped by 9.77% and 14.74%.

Ahmed *et al.* (2014) in their study, investigated the effect of the deposition of air borne suspended matter on the surface of PV module. The study employed two identical thin film PV panels, variable load resistance and measuring instrument. The results of the study revealed that with the increase in dust deposition density of up to 0.36 mg/cm^2, this gives rise to a reduction in PV output efficiency of 17.71%.Jiang, Lu and Sun (2011) performed experiments with monocrystalline silicon (mc-Si), polycrystalline silicon (pc-Si) and amorphous silicon (a-Si) and reported that the efficiency of the PV modules decreased by up to 26% as dust deposition increased from 0 to 22 g/m^2 and also that the amount of dust accumulated on a PV module's surface is affected by the inclination angle of the module. The inclination angle of a PV module affects the dust deposition with the deposition decreasing as the inclination angle of a PV module increases (Elminir *et al.*, 2006; Qasem *et al.*, 2014).

Saidan *et al.*, (2016) investigated the impact of dust accumulation on photovoltaic solar modules in Baghdad city in Iraq. In the study, modules were installed with direct exposure to weather conditions and dust accumulation was measured on daily, weekly and monthly basis. This study also investigated size distribution and dust density and it was concluded that dust deposition caused a reduction in short circuit current (I_{sc}) and the output power. The average degradation rate of the modules exposed to dust are 6.2%, 11.8% and 18.74% for one day, one week and one month respectively. This study did not analyse the chemical composition of the dust and the morphology of the dust which is a drawback of the study.

In the work of Gholami *et al.* (2018), a 70-day experiment on the impact of dust deposition on photovoltaic output performance was carried out in Tehran. The study concluded that dust reduces the power output of the panel by 21.47% in 70 days without rain and under 6.0986 g/cm^2 of dust accumulation. This study also has a drawback of not studying the physical and chemical composition of the dust and relating it to the losses.

Gholami *et al.,* (2017) investigated the factors affecting dust accumulation and their effects on the transmission coefficient of glass. A total of 50 pieces of Green soda lime silica window glasses of 100 mm x 100 mm with a thickness of 3 mm were placed in eight geographical directions and at seven distinct angles. The amount of dust accumulated at each stage was measured as being the difference between the initial mass of the clean glass and the glass with dust on it. The dust surface density was calculated weekly and the radiation passing through each sample was measured using a LUTRON SPM-1116SD solar power meter. The ratio of the total radiant flux transmitted by the sample to the incident flux which is the transmission coefficient was calculated for each sample. The study concluded that the tilt angle and the location affect the rate of dust accumulation on glass. This study did not look at the loss of efficiency and properties of the dust.

Guan *et al.* (2017) investigated the effect of dust deposition on the module temperature, the transmittance, and the output power of the PV modules. The study used an array of PV modules with in-situ measurement of module output power, solar irradiance and module temperature. Dust deposition according to this study, apart from reducing the transmittance of the glass, also reduces the temperature of the glass. The study also concluded that within 8 days the relative transmittance of a PV module could decline by 20% due to natural dust accumulation.

The research conducted by Menoufi *et al.* (2017) evaluated the electrical performance of PV panels after exposure to natural dust accumulation in Egypt. They discovered that exposing the panels to natural dust accumulation for three

months caused a significant reduction in performance to about 50%. They also concluded from their studies combined with other literature findings, that it is not quite appropriate to compare the results from different studies because many differences were found between the researches in many aspects, such as the testing methods, parameters, geographic locations of the experiments, and the adopted experimental procedures (Menoufi, 2017).

Salari and Hakkaki-Fard, (2019) numerically investigated the effect of dust deposition density on the performance of photovoltaic PV module and photovoltaic-thermal systems (PVT). The research also investigated the effect of various system parameters on the performance of both clean and dusty PV module and PVT system. The result indicated a reduction in electrical efficiency of 26.36% when dust deposition increased from 0 g/m^2 to $8g/m^2$ for PV system and for PVT, the electrical and thermal efficiencies reduced by 26.42% and 16.11% respectively. The study concluded that increasing solar radiation and temperature, the electrical energy of the PV module reduces. Also, that an increase in dust deposition density reduces the performance of PV and PVT systems. This numerical analysis is somewhat misleading because the increase in solar radiation intensity increases short-circuit current and consequently increasing the PV system performance, which is contrary to the conclusion of the paper.

(Ramli, *et al.,* 2016) in their study, investigated the effect of dust accumulation and weather change on the output power of PV modules in Surabaya, Indonesia. The module was exposed to outside weather conditions and real time measurements of voltage, current, temperature and humidity were made. The study revealed a 10. 8% reduction in power output for a dust accumulation in period of two weeks with a mean relative humidity of 52.24%. A power output reduction of more than 40% was experienced in rainy condition with humidity of 76.32% and a drop, in output power of above 45% in dusty condition and with humidity of 60.45%. The study concluded that dust accumulation and weather conditions significantly reduce the PV power output. The study however

suggested further research be conducted on the effect of dust accumulation on PV output power.

(You *et al.*, 2018) developed a framework to predict the impact of PV dust accumulation on the energy and economic of the system. The study introduced a concept of relative net-present value change to determine the optimal cleaning interval and also includes the study of the effect of relative humidity, tilt angle and precipitation. The framework was used to study the soiling-induced efficiency and economic losses of solar photovoltaic modules in seven cities. The results are significantly different from city to city. An efficiency loss of over 80% was experienced in Doha over a period of 140 days while less than 4% was experienced in Tokyo for the same duration. This further buttress the fact that the effect of dust cannot necessarily be inferred from results of other regions.

Kaldellis and Kapsali (2011) opined that the reduction in the performance of PV modules due to the deposition of dust of varying composition, size and type has not been sufficiently analysed and requires more investigations in different regions. The study investigated the impact of limestone, carbonaceous fly-ash and red soil on the performance of PV panels at the same location and orientation. A significant reduction in energy performance of the panel was experienced. The study revealed a significant reduction in PV energy yield and efficiency due to dust particle deposition which depends on the type of the dust (composition, diameter, etc.) and secondly the mass accumulated.

Micheli and Muller (2017) investigated one hundred and two environmental and meteorological parameters and compared with the performance of 20 soiling stations installed in the USA, in order to determine their ability to predict the soiling losses occurring on PV systems. This outcome of this investigation showed that the annual average of the daily mean particulate matter values recorded by monitoring stations deployed near the PV systems are the best soiling predictors, with coefficients of determination (R_2) as high as 0.82. Other parameters which show some importance in this respect are precipitation pattern and average length of dry periods.

Tanesab *et al.*, (2019) collected dust from Babuin, Indonesia and Perth, Australia and investigated the effect of dust with different morphologies on the performance degradation of various photovoltaic (PV) technologies consisting of polycrystalline silicon (pc-Si), mono-crystalline silicon (mc-Si), and amorphous silicon (a-Si). Their findings shows that that dust from Babuin was dominated by larger size and porous particles so that it passed more light than ones from Perth. This gives more reason on why results of dust experiments from a region cannot be directly applied to another region because of the inherent differences in properties and morphology of the particles. Dust from Perth with angular and diagonal shapes had better optical property than that from Babuin featuring elliptical and spheroid particles.

Hachicha, Al-Sawafta and Said (2019) conducted experiments to investigate the effect of dust on the electrical performance of PV modules under Sharjah, UAE weather conditions. The morphology of the dust sample indicates that dust particles have different shapes and small sizes (1.61 - 38.40 μm), this indicates that the observed particles are not homogenous. The results show about 1.7% drop in PV power per g/m^2 dust accumulation. The tilt angle of the modules also affects dust accumulation. Dust accumulation increases by 37.63%, 14.11% and 10.95% with respect to the tilt angle of 0^o, 25^o and 45^o respectively.

Chanchangi *et al.*, (2020) reviewed the effects of dust accumulation on PV module performance and provided measures to mitigate them. Energy losses from PV due to dust is an issue which cannot be ignored and can be an obstacle to achieving renewable energy targets in Nigeria. They opined that there is a need for conduction of comprehensive research on the effects of dust in all geopolitical regions in Nigeria to acquire data that can be used for designing the PV module system considering the most suitable technique in reducing or preventing the effects of soiling in each specific area.

2.10.2 National Renewable Energy Laboratory's Country and Regional Projects in Africa

In developing African countries and regions, NREL supports initiatives for deploying renewable energy, energy efficiency, sustainable transportation, and advanced grid management technologies and systems. African countries with NREL has renewable energy developmental projects in the following countries of Afica: Algeria, Angola, Cape Verde, Ethiopia, Gabon, Ghana, Kenya, Malawi, Morocco, Sierra Leone, South Africa, Tanzania, Zambia but dust impact is only being studied in Morocco and Egypt (NREL, 2020a). There only three West African countries with NREL presence. NREL provided training on energy efficiency and renewable energy technologies, assessment methods and tools, and policy solutions and on gender and energy issues in Cape Verde while in Ghana, NREL is partnering with the Government of Ghana, the U.S. Agency for International Development, and other energy institutions to plan and achieve an advanced, flexible, reliable, and cost-effective power system. Specific activities include: analysis and modeling support (e.g. load flow, forecasting) of large-scale solar and wind systems, grid code assessments, and capacity building to understand grid impacts of distributed generation deployment. In Sierra Leone NREL and other partners are providing technical support for evaluation and development of standards for efficient lighting.

Some of the publications by NREL on study of dust impact are reviewed here in this section. (Smestad *et al.*, 2020) studied the comparison of naturally accumulated soiling on coupons of PV glass soiled at seven locations worldwide. The spectral hemispherical transmittance was measured. It was found that natural soiling disproportionately impacts the blue and ultraviolet (UV) portions of the spectrum compared to the visible and infrared (IR). The countries are India, Egypt, USA, UK, and Spain. Costaa, Diniza and Kazmerskia (2018) presented list of publication on soiling for both PV and CSP during the 2016 and some parts of 2017. They opined that more researches are ongoing in this area with focus on modelling and simulation and also prediction of the impact of soiling. Micheli and Deceglie (2018) analyzed the correlations between average historical

environmental data and future soiling losses. They found the parameters describing the particulate matter concentrations to be the best predictors of soiling, even when historical data were used to estimate future soiling losses. In particular, PM2.5 was found to be the most consistent predictor, independent of the time period considered, because of the steady distinction in PM2.5 concentrations between high and low soiling sites. Among the rainfall parameters, the maximum length of the dry period returned the best results because of the consistent longer summer dry periods experienced by high soiling.

This study investigated sand adhesion to the glass cover of solar PV panels and examines the effect of temperature, particle size, humidity, sand type and height on sand adhesion to glass.

Modelling and simulation of solar PV and maximum power point tracking (MPPT) system prior to installation is of utmost importance as it reveals the behaviour of the system under varying environmental conditions. The MPPT optimizes the output power from the solar PV module.

2.11 Gaps in Knowledge

Solar and climatic data analysis of the three locations selected for this research is certainly a contribution to the body of knowledge as the Nigerian Government Agency responsible for data collection has opined that there are inadequate data and data analysis and about 9000 weather stations are required as a result of Nigeria's huge land mass instead of the 800 that are currently on ground (Kasim Sumaina, 2018)

From the literature review, it is obvious that there are limited studies on the effect of dust and the fact that it is not quite appropriate to adopt or compare the results from different existing studies encountered because many differences were found between them. Some of these differences include testing methodology adopted, geographical location of experiments, parameters considered for experimentation and experimental design/procedures. The study carried out in Maiduguri, a region

characterized by high dust accumulation and most favourable for the development of solar PV energy conversion system in Nigeria will certainly remain an important contribution to the body of knowledge for a couple of reasons. The first being that it contributes to an emerging area of solar PV studies with renewed vigour to establish a world encyclopaedia of real dust and soiling trends and knowledge. Secondly, these data from this research will serve as a source of important information for stakeholders in solar PV system development such as the installers, system holders and practitioners. The benefits of the output of this research range from assisting in accurate location of site and also schedule of module cleaning to guarantee optimum energy output of the system. This will also guide the operation and maintenance cost for the system. Finally, this research will also gear up collaboration between researchers and developers in the field of PV system as well as soil scientist to address the mitigation of impact of soiling on PV modules.

In addition, the present drive of the Nigerian Government towards the use of solar PV energy conversion system will require a simple software which can be rapidly used for accurate sizing and conducting energy and economic analysis because many stakeholders ranging from engineers, technologist, technicians and craftsmen will be involved as this is going to be a huge investment. The development of a robust and simple solar PV system model (SPVSM) which is a decision-making toolkit for accurately sizing of the solar PV system components for optimum power supply at competitive cost and with the capability to conduct energy and economic analysis on a single graphical user interface platform is certainly novel and a contribution to the body of knowledge as this will serve as a guide to solar PV practitioners.

3 MATERIALS AND METHOD

This chapter discusses the materials and methods adopted in this research to achieve each of the stated objectives. The theoretical, experimental and mathematical instruments applied are extensively discussed and presented.

3.1 Weather data collection and analysis

This section describes the data collection procedure and the statistical analysis methods and tools adopted.

3.1.1 Study Area

The study areas are Maiduguri in the North-east, Minna in North-central and Port Harcourt in the South of Nigeria. These locations were carefully chosen to represent the three radiation zones in Nigeria as depicted in Figure 1-3. Table 3-1 presents the geographical location of the selected sites (Osinowo *et al.*, 2015).

Table 3-1: Details of Study Area (Osinowo *et al.*, 2015)

LOCATION	LATITUDE [deg.]	LONGITUDE [deg.]	ALTITUDE [m]	AVERAGE ANNUAL SUNSHINE HOURS
Maiduguri	11.8° N	13.2° E	320	2877.5
Minna	9.6° N	6.5° E	299	2435.4
Port Harcourt	4.8° N	7.0 E	468	1474.2

3.1.2 Site Analysis

Maiduguri is located along the seasonal Ngadda (Alo) River, the waters of which disappear in the *firki* (“black cotton”) swamps of Lake Chad, northeast of Nigeria. In Maiduguri, the wet season is hot, oppressive, and mostly cloudy and the dry season is sweltering and partly cloudy. Over the course of the year, the temperature typically varies from $14^{o}C$ to 41°*C* and is rarely below 11°*C* or above 43°*C*. The length of the day in Maiduguri does not vary substantially over

the course of the year, staying within 49 minutes of 12 hours throughout. In 2020, the shortest day is December 21, with 11 hours, 26 minutes of daylight; the longest day is June 20, with 12 hours, 49 minutes of daylight.

The site is desert and therefore with very large expance of land some of which are used for farming. The latitude and longitude of the site is 11.8^{o} N and 13.2^{o} N respectively. The average annual sunshine hour and average total daily solar irradiance are 2977.5 hours and 6,384 W/m^2. The site is very far from the national grid and therefore grid-tied is not economical. The people living in this location are predominantly farmers, consequently, would lose some part of the farmland to the development of the solar PV system. The site is a high dust accumulation region and therefore the study of the impact of dust on the performance of PV module is imperative.

3.1.3 Data

The data used in this study are daily average solar irradiance, average monthly ambient temperature, average relative humidity, and average monthly sunshine hours for 11 years (2006-2016). These were collected for the three locations from the Nigeria Meteorological Agency, Abuja, Nigeria.

3.1.4 Data Analysis

The data was analysed using Minitab 17 software and Microsoft Excel. Frequency distribution was explored with correlation of the solar data by making the solar irradiance a dependent variable and individually making ambient temperature, relative humidity, and sunshine hours independent variables. The statistical indicators used for these analyses include R^2 which is the Coefficient of Determination, R (Coefficient of Correlation) and frequency distribution. The descriptive statistics which gives statistical information such as mean, standard error of mean (SEM), standard deviation, quartile, and interquartile range (IQR) of the data were performed, and results obtained using Minitab17. Regression and interaction analysis were performed to generate a model and to also study the interaction between the variables. Boxplots and Normal distributions were

also plotted to analyse the data and 3-sigma, or 3 standard deviation limits were used to set the upper and lower limits for the solar irradiance of the three locations, this is meant to study the distribution of the data. The Root Mean Square Error (RMSE), Absolute Bias Error (ABE) and Absolute Mean Bias Error (AMBE) were also statistical indicators used in this study to relate the calculated and measured data. Existing models were used in the calculation of solar radiation. There are several empirical models which have been developed to predict solar radiation. The most widely used model is the modified Angstrom-type regression equation as presented in equation 3-1.

$$H = H_o\left(a + b\frac{S}{S_{max}}\right) \quad \textbf{(3-1)}$$

H (W/m^2) is the monthly average daily global solar radiation falling on a horizontal surface at a particular location, H_o (W/m^2) the monthly average daily extra-terrestrial radiation, S the monthly average daily number of observed sunshine hours, S_{max} the monthly mean value of day length at a particular location and “a”, “b” the climatologically determined regression constants to be determined as follows (Abdullahi and Singh, 2014):

$$a = -0.10 + 0.235Cos\emptyset\left(\frac{S}{S_{max}}\right) \quad \textbf{(3-2)}$$

Where Ø is the latitude of the location.

$$b = 1.449 - 0.553Cos\emptyset - 0.694\left(\frac{S}{S_{max}}\right) \quad \textbf{(3-3)}$$

The monthly average daily extra-terrestrial radiation, H_o is given by equation 3-4.

$$H_o = \frac{24}{\pi}I_{sc}\left[1 + 0.033cos\left(\frac{360n}{365}\right)\right]\left[cos\emptyset cos\delta sin\omega_s + sin\emptyset sin\delta\left(\frac{2\pi\omega_s}{360}\right)\right] \quad \textbf{(3-4)}$$

The sunset hour angle, ω_s is given as

$$\omega_s = cos^{-1}[-tan\delta tan\emptyset] \quad \textbf{(3-5)}$$

The solar declination, δ, is the angular distance of the sun's rays north (or south) of the equator and it can also be said to be referred as the angle between the line joining the centres of the Sun and the Earth and its projection on the equatorial plane, north declination designated as positive (Osinowo *et al.*, 2015).

The solar declination, δ can obtained from the following expression:

$$\delta = 23.45\ sin\left(\frac{360(n+284)}{365}\right) \quad \textbf{(3-6)}$$

The accuracy of the calculated global radiation is examined using Root Mean Square Error (RMSE), Mean Bias Error (MBE) and Mean Absolute Bias Error (MABE) which are given by equations 3-7 to 3-9 (Ayvazoğluyüksel and Filik, 2018).

$$RMSE = \sqrt{\frac{1}{n}\sum_{i=1}^{n}(c_i - m_i)^2} \quad \textbf{(3-7)}$$

$$MBE = \frac{1}{n}\sum_{i=1}^{n}(c_i - m_i) \quad \textbf{(3-8)}$$

$$MABE = \frac{1}{n}\sum_{i=1}^{n}(|c_i - m_i|) \quad \textbf{(3-9)}$$

where c_i is the i^{th} calculated global radiation data, m_i is the i^{th} measured global radiation data and n is the number of data. The sunshine hours and the daylength S_{max} was used to establish the percentage daily sunshine.

.

3.2 Energy Demand

The energy demand of the village in watt-hour including the demand for common facilities such as schools, Hospital and market was calculated using MATLAB2016a.

The rating of the individual electrical appliances and estimated number of hours of operation per day were used to calculate the energy demand per day of the village which is the basis for designing an appropriate solar PV energy conversion system. The general procedure is depicted in the equation 3-10. For appliances with power ratings of a_1, a_2, a_3, ……a_n in watts with estimated operating hours per day of h_1, h_2, h_3, ….h_n, the energy demand per day can be written as:

$$Energy\ demand\ per\ day\ = \sum_{i=1}^{n} (a_i \times h_i) \quad \textbf{(3-10)}$$

$$Total\ load\ (W)\ = \sum_{i=1}^{n} a_i \quad \textbf{(3-11)}$$

The total load in watts is given by the summation of all the ratings of the individual appliances. This is given by equation 3-11.

Simulink is a graphical extension to MATLAB for modeling and simulation of systems. One of the main advantages of Simulink is the ability to model a nonlinear system, which a transfer function is unable to do. Another advantage of Simulink is the ability to take on initial conditions. The disadvantage of PVsyst to the target technicians and artisans in Nigeria is that high knowledge of simulation is required, and it is also very expensive to acquire for this group of people. The developed model is simple to apply in any situation and requires very little simulation technique.

3.3 Design and Layout of 1 MW solar PV System

3.3.1 Solar PV Modules and Inverter Distribution and Layout

For a 1 MW solar PV system, the number of modules required to make up 1 MW depends on the peak watt of the module selected.

$$Number\ of\ modules\ for\ 1\ MW\ plant = \frac{1000000}{peak\ watt\ of\ module} \quad \textbf{(3-12)}$$

For a 250 W module, the number of modules require is 4000. Appropriate layout of arrays becomes very important for optimized cable length as well as optimized energy production. Figure 3—1 shows the module and inverter layout for a 1 MW power plant.

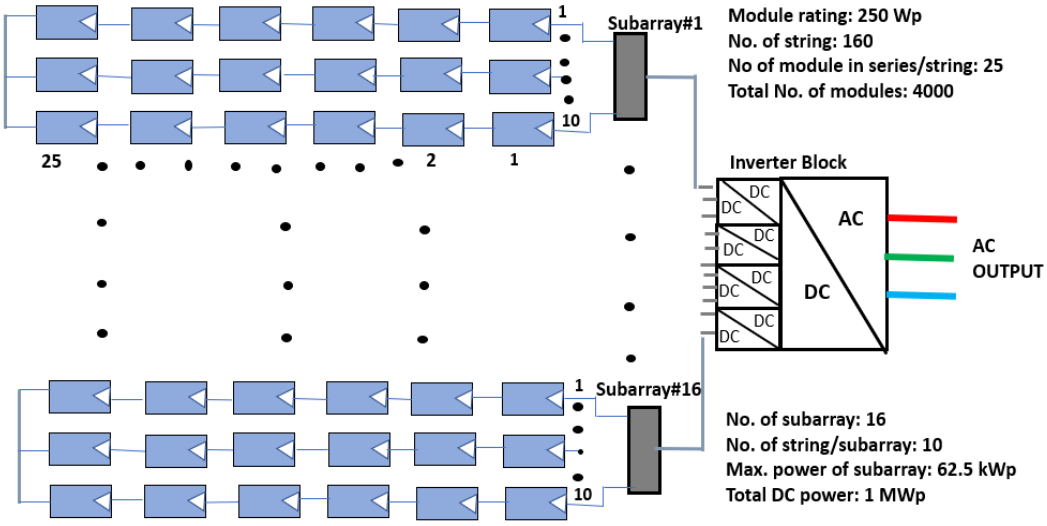

Figure 3-1: Module and inverter layout for 1 MW plant

3.3.2 Earthing and Electrical Protection

The process of transferring the immediate discharge of the electrical energy directly to the earth by the help of the low resistance wire is known as the electrical earthing. The electrical earthing is done by connecting the non-current carrying part of the equipment or neutral of supply system to the ground. A PV

system is defined as a grounded system when one of the DC conductors (either positive or negative) is connected to the grounding system, which in turn is connected to the earth. The NEN1010, a Dutch series of safety provisions for low voltage installations used by installers in the electrotechnical industry, requires that all PV installations should be earthed. The mounting system is seen as a metal construction and thus should be earthed. The solar panels do not need to be earthed as they are double isolated. Earthing provides electrical safety and protect system components against surges that may be caused by lightning discharge.

Mostly, the galvanised iron is used for the earthing. The earthing provides the simple path to the leakage current**.** The shortcircuit current of the equipment passes to the earth which has zero potential. Thus, protects the system and equipment from damage.

The electrical equipment mainly consists of two non-current carrying parts. These parts are neutral of the system or frame of the PV panel. From the earthing of these two non-currents carrying parts of the electrical system earthing can be classified into two types.

- Neutral Earthing
- Equipment Earthing

In neutral earthing, the neutral of the system is directly connected to earth by the help of the GI wire. The neutral earthing is also called the system earthing. Such type of earthing is mostly provided to the system which has star winding. For example, the neutral earthing is provided in the generator, transformer, motor etc. Such type of earthing is provided to the electrical equipment. The non-current carrying part of the equipment like their metallic frame is connected to the earth by the help of the conducting wire. If any fault occurs in the apparatus, the short-circuit current to pass the earth by the help of wire. Thus, protect the system from damage.

The earthing is essential because of the following reasons:

- The earthing protects the personnel from the shortcircuit current.
- The earthing provides the easiest path to the flow of shortcircuit current even after the failure of the insulation.
- The earthing protects the apparatus and personnel from the high voltage surges and lightning discharge.

Earthing can be done by electrically connecting the respective parts in the installation to some system of electrical conductors or electrodes placed near the soil or below the ground level. The earthing mat or electrode under the ground level have flat iron riser through which all the non-current-carrying metallic parts of the equipment are connected. As the installations and demand for PV systems increases, so does the need for effective electrical protection. PV systems, as with all electrical power systems, must have appropriate overcurrent protection for equipment and conductors. Globally there is a push for utilizing higher voltages (trending to 1000Vdc and above) to achieve more efficiency. This will mean an even greater need for circuit protection in the future.

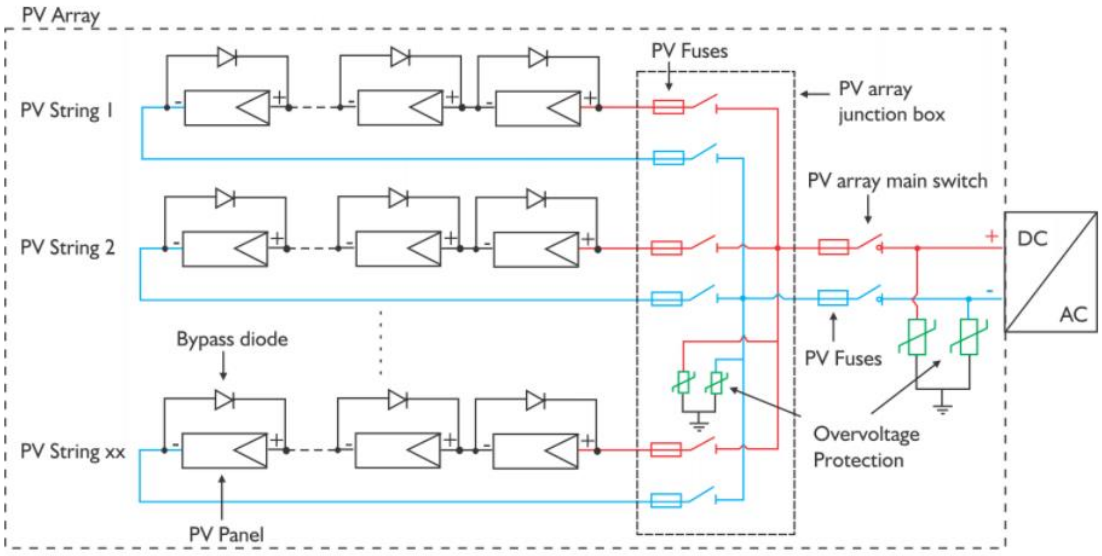

Figure 3-2: PV array showing electrical protection on DC side.

PV systems that have three or more strings connected in parallel need to have each string protected.Systems that have less than three strings will not generate enough fault current to damage the conductors/equipment and therefore do not present a safety hazard as long as the conductor was sized properly based on local code requirements. Where three or more strings are connected in parallel, a fuse on each string will protect the conductors from damage and eliminate any safety hazards. It will also isolate the faulted string so that the rest of the PV system can continue to generate electricity.

Depending on the desired capacity of the Photovoltaic (PV) system, there may be several PV sub-arrays(each subarray consists of multiple strings) connected in parallel to achieve higher currents andsubsequently more power. A fuse link on each sub-array will protect the conductors from current faults and help minimise any safetyhazards. It will also isolate the faulted sub-array so that the rest of the PV system can continue to generateelectricity. If several sub-arrays are subsequently combined, then a further fuse link should beincorporated. This would be termed the array fuse link.

3.3.3 Cable Selection and Voltage Drop

Choosing the right cables sizes in a PV system is important for both performance and safety reasons. If the cables are undersized, there will be a significant voltage drop in the cables resulting in excess power loss. In addition, if the cables are undersized, there is a risk that it may heat up to the point in which a fire may result.

Cables are extensively used in photovoltaic systems and their management can often be critical for effective functioning. Cable management is one of the most important aspects of the safety and longevity of nearly every photovoltaic (PV) system. This is primarily due to the extensive use of exposed cables in the DC PV array. Since the equipment is installed outdoors on rooftops and in open fields, the electrical conductors must be rated for sunlight resistance and be supported and secured properly.

Despite being a critical component, wiring for solar panels is rarely discussed. In home solar power systems, there are four components to connect: the solar panels, the charge controller, the batteries, and the inverter. The charge controller is used to prevent the batteries from overloading; the wires that connect the panel to the charge controlled should be correctly sized to minimize transmission power loss.

Correspondingly, the further away the panels are, the larger the wire gauge should be. The inverter is used to convert the DC power collected by the panels into AC power, which is the most popular form of electricity accepted by appliances. These systems are typically outdoors, so any cable used for this type of application needs to be ultraviolet radiation resistant and suitable for wet locations. For solar tracking panels, the cables used need to be flexible as the panels will be moving along with the sun.

3.4 Development of Solar PV System Model

3.4.1 Description of the Model

SPVSM is an acronym for Solar Photovoltaic System Model. It was developed by Hauwa Talatu Abdulkarim (the author of this thesis) for designing solar PV system components (PV array, battery, inverter, and charge controller) and conducting energy and economic analysis of the system. It is a modelling and simulation software developed on a single graphical interface in MATLAB for designing a stand-alone solar PV power supply system which can be applied to villages/households especially in rural settlements which constitute more than 80% of regions without access to electricity in Nigeria. The package has the capability for conducting a sensitivity analysis on the energy and economics of the system considering variation in degradation factor and discount rate. It also gives an economic appraisal such as net present value (NPV) over the expected lifespan of the project. It is built on a single GUI platform but with six executable panels each handling different aspects of component design, energy and economic analysis. The development of each of the executable panels with some of the controlling equations used are presented in the following sections.

3.4.2 Peak Power Generation

The maximum electric or nominal power of your PV system can be defined as its 'Peak Power' (in Watt Peak). The Peak Power generation of solar panels is only possible under the following Standard Test Conditions:

- a light intensity of 1000 W/m²
- sunlight hitting the positioned solar cells perpendicularly
- a standard airmass (AM) of 1,5. This is a measure for the relative length of the optical path through the atmosphere.
- a temperature of 25°C at the solar cells

In other words, the Peak Power is a specific feature of PV system, regardless of the location where it is tested. Under these standard conditions, the nominal power of solar panels can be compared with each other. A solar panel with a Peak Power of 5 kWp in Spain is for example the same as such a panel in Belgium.

3.4.3 Executable Panel 1 - PV array Sizing

System sizing is the determination of the minimum number of panels and battery sizes required to deliver electrical energy needed under the solar conditions that exist at the system site. This includes sizing of the inverter, cables, wires that will be able to deliver the electrical energy safely.

Accurate sizing of photovoltaic array is one of the most important aspect of solar PV energy conversion system. The first parameter required in sizing solar PV array is the energy requirement, E_D. The peak watt of solar PV panel required for any energy demand depends on the panel generation factor (PGF) of the location. Some of the model equations used for the sizing are given in equation 3-11 to equation 3-14. Figure 3-1 shows the Executable Panel 1. The PGF can be calculated from equation 3-12.

$$PGF = \frac{Solar\ irradiance\ of\ site \times sunshine\ hours}{Standard\ test\ condition\ irradiance} \quad \textbf{(3-13)}$$

For an energy demand E_D, the energy that can be expected from the solar PV array is assumed to be 30% higher than the demand in order to take care of uncertainties in weather conditions as well as losses. Therefore, energy from array, E_{ARRAY} is given by equation 3-13.

$$E_{ARRAY} = E_D \times 1.3 \quad \textbf{(3-14)}$$

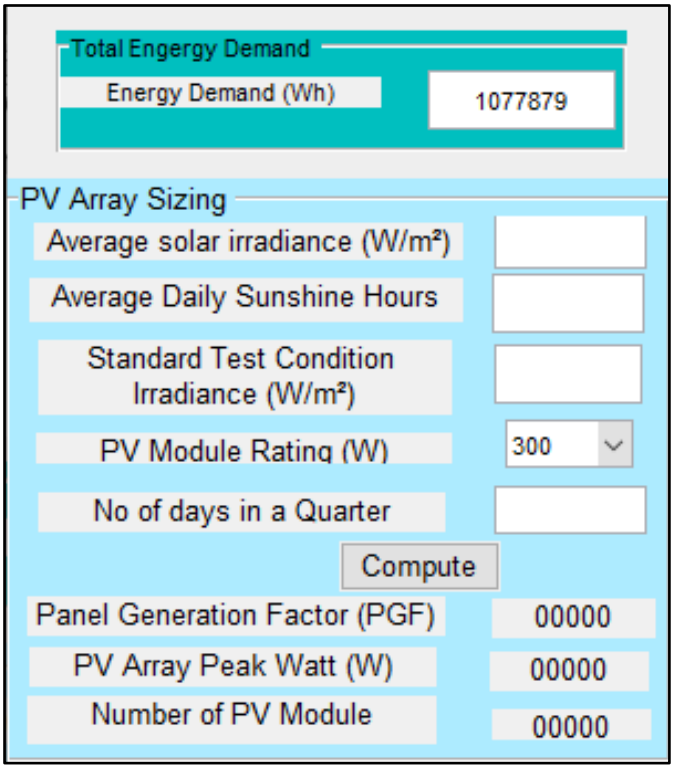

Figure 3-3: Photovoltaic Module Sizing Executable GUI panel

The peak watt W_p, of the solar PV array is given by equation 3-14:

$$W_p = \frac{E_{ARRAY}}{PGF} \quad \textbf{(3-15)}$$

For any module rating M_R, the number of modules M_N which is adequate to meet the energy demand is given by equation 3-15.

$$M_N = \frac{W_p}{M_R} \quad \textbf{(3-16)}$$

3.4.4 Solar Panel Selection

There are lot of things to consider when solar PV system is to be installed, one of which being what kind of solar panels to get. The panel to select depends on a number of factors such as budget, what is available in the market around you, efficiency and possibly aesthetics, that is how good looking and rugged. Most of the solar panels on the market today for residential solar energy systems can fit into three categories: monocrystalline solar panels, polycrystalline solar panels, and thin film solar panels. Each of these types of solar cells causes the solar panels to have different characteristics and distinctive features that make them better suited for certain solar projects. Monocrytalline solar panels which was chosen in this research are the most common for residential solar installations. They have higher efficiencies than other one but also with high cost. The advantages and dsiadvantages are enumerated in Table 3-2.

Table 3-2: Advantages and Disadvantages of different types of solar panels

Type of solar panel	Advantage	Disadvantage
Monocrystalline	• High efficiency/performance • Aesthetics	• Higher costs
Polycrystalline	• Low cost	• Lower efficiency & performance
Thin film	• Portable and flexible • Lightweight • Aesthetics	• Lowest efficiency & performance

3.4.5 Executable Panel 2 - Battery Sizing

Two key parameters that guides the accurate sizing of a battery bank is the energy demand and number of days of autonomy which is the number of days that the battery can supply without being recharged from the PV modules. Figure 3-2 shows the executable GUI panel for battery sizing. It should be noted that the energy demand has been declared in the PV module sizing panel

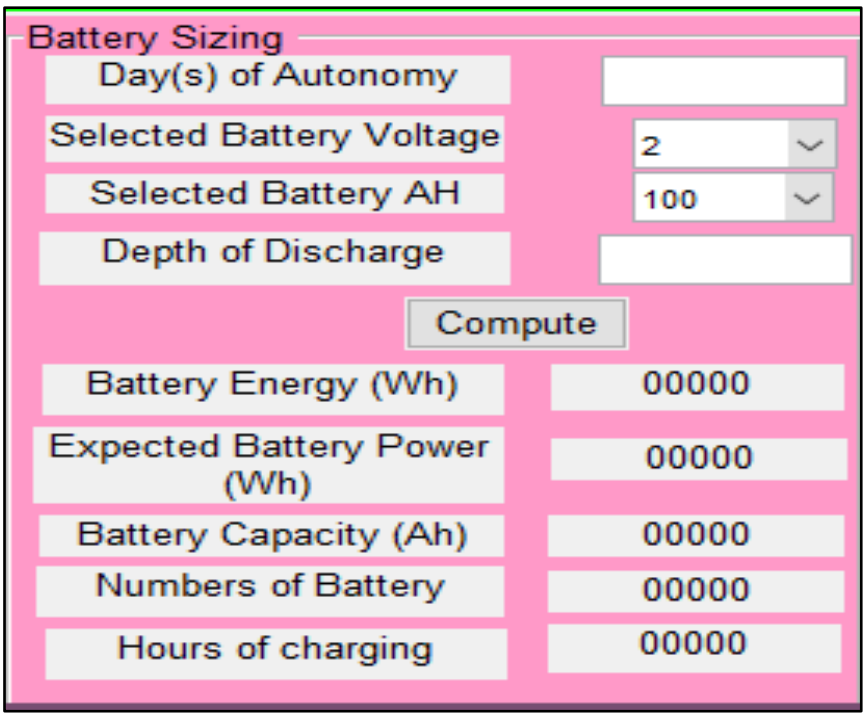

Figure 3-4: Battery Sizing Executable GUI panel

Considering the number of days of autonomy, N_D and the depth of discharge of the battery, (DOD), the battery bank energy (kWh) is given by equation 3-16. Since battery life strongly depends on the level of discharge before it is recharged, the rule of thumb will be adopted in this regard. That is, the battery will discharge only to 50% (depth of discharge DOD=50%).

$$Battery\ bank\ energy\ (kWh) = \frac{E_D \times N_D}{DOD} \quad \textbf{(3-17)}$$

The battery voltages are usually rated 6V, 12V, 24V or 48V. For a selected battery of voltage, V, the battery bank total capacity (Amp.hour) is given by equation 3-17.

$$Battery\ bank\ capacity\ = \frac{E_D \times N_D}{V \times DOD} \quad \textbf{(3-18)}$$

For a selected battery of amp hour, AH, the total number of batteries required to meet the energy demand is given by equation 3-18.

$$Number\ of\ batteries\ = \frac{Battery\ bank\ capacity}{AH} \quad \textbf{(3-19)}$$

3.4.6 Executable Panel 3 - Inverter Sizing

In sizing the inverter for the solar PV system, the power demand for the village will be considered. The inverter size must be large enough to safely handle the wattage demand at any time. Usually the inverter is sized 25-30% (Chandel *et al.*, 2014) higher than total wattage demand (Leonics, 2017). This research will adopt 30% higher than the wattage demand of the village. Figure 3-3 shows the executable GUI panel for inverter sizing.

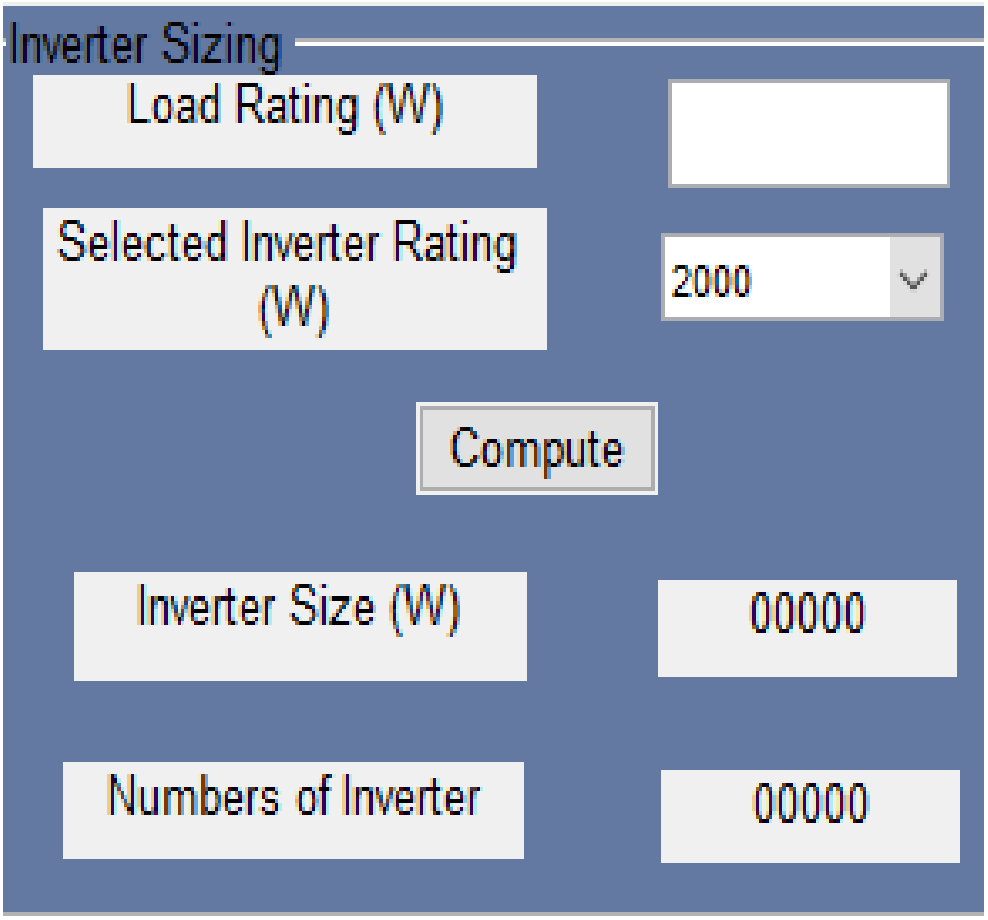

Figure 3-5: Inverter Sizing Executable GUI panel

For a load of wattage W_L, the total wattage of inverter required is given by equation 3-19.

$$Total\ Inverter\ Wattage, W_{T\_INV} = W_L \times 1.3 \quad \textbf{(3-20)}$$

Inverters are sized in wattage that is “continuous” or “surge” watts. Continuous watts is the total power an inverter can support indefinitely while surge watts is the amount of power an inverter can supply for a very short time. For large solar farms W_{INV} will be large such that more than one inverter is required, therefore the number of inverters to meet the required power for a selected inverter wattage of W_{INV} is given by equation 3-20.

$$Number\ of\ inverters, N_{INV} = \frac{W_{T\_INV}}{W_{INV}} \quad \textbf{(3-21)}$$

3.4.7 Executable panel 4 - Charge controller sizing

The charge controller controls the current from the solar panel into the battery bank and prevents, at night-time, over-charging and reverse flow of current employing a transistor to shunt the PV charging circuit. This means that the charging stops when the battery is full and discharging stops if the battery hits an unhealthy level. This unhealthy level depends on battery design, it could be anywhere below 50% discharge or 85% discharge. Not preventing this can reduce battery performance and its lifespan considerably. Figure 3-4 shows the charge controller sizing GUI executable panel.

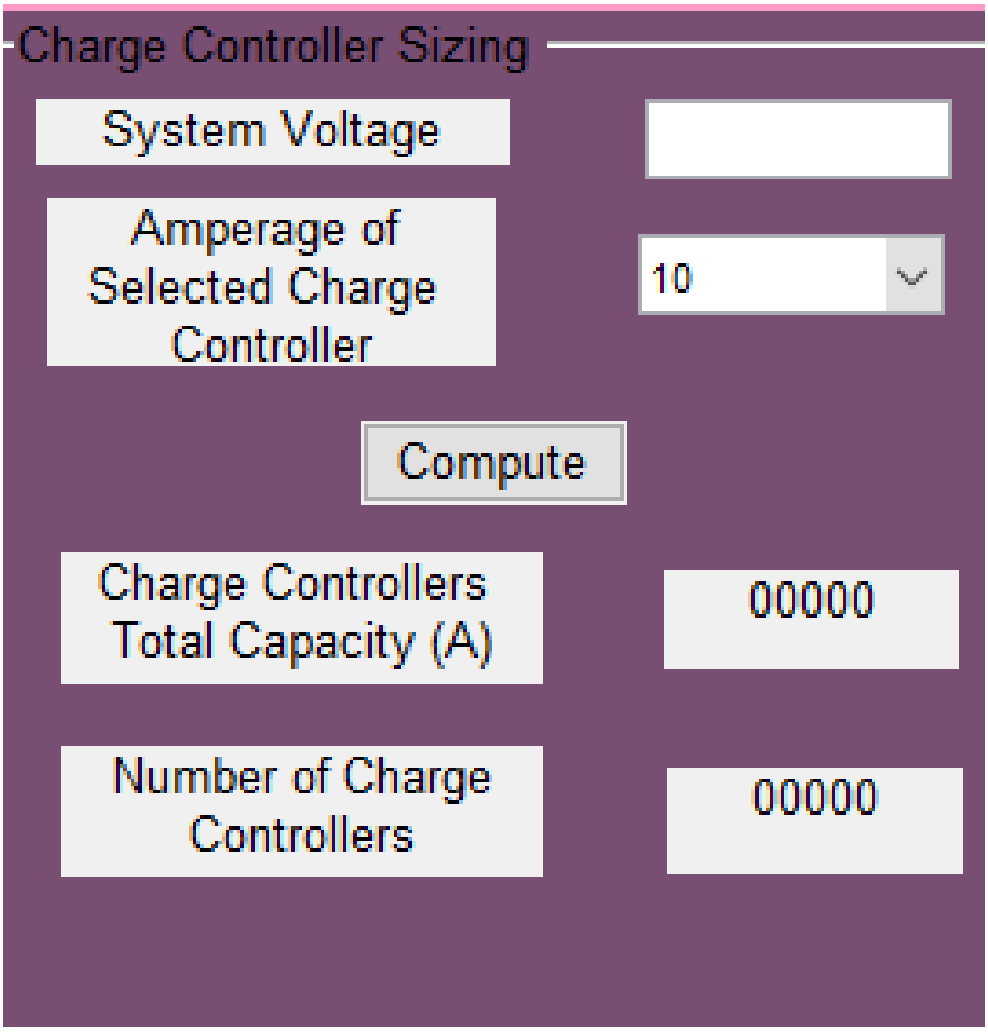

Figure 3-6: Charge controller Sizing Executable GUI panel

The parameters necessary for sizing inverter are the peak watt of the solar array and the system voltage S_v. Charge controllers are rated in amperes. The ratio of the peak watt of the solar array and the system voltage gives the ampere that the charge controller is expected to deal with in controlling the rate of charging and discharging of the battery. 30% is added to the calculated amperage for unexpected current increase due to factors such as light reflection. The total charge controller capacity is given by equation 3-21.

$$Total\ Charge\ controller\ capacity, \qquad T_{CC} = \frac{W_P}{S_V} \tag{3-22}$$

For any chosen charge controller unit with capacity, CC_C, the total number of such charge controllers that are required is given by equation 3-22.

$$Number\ of\ charge\ controllers\ N_{CC} = \frac{T_{CC}}{CC_C} \tag{3-23}$$

3.4.8 Executable panel 5 - Energy analysis

Energy is the power produced or expended over a period. In order to assess the capability of a PV system in supplying the required daily energy for domestic and industrial purposes, it is crucial to determine the total amount of energy that is produced by the system.

The energy from a PV array depends on the peak watt of the array (W_p), conversion efficiency, the daily sunshine hours (SSH) and the average solar irradiance (ASI) of the site. The energy produced by the array per annum can be obtained from equation 3-23, taking into cognisance the derate factor of the array (PV_Derate).

$$E_A = W_P \times \frac{ASI}{STCI} \times SSH \times PV\_Derate * Efficiency * 365 \tag{3-24}$$

Where STCI is standard test condition irradiance which is 1000 W/m^2

In the analysis of the annual energy production over the lifespan of the PV system, attention is paid to the estimated annual degradation of the system which is put at 0.6-5%/year (Kumar *et al.*, 2019), 1.12%/year (Malvoni, De-Giorgi and Congedo, 2017) and a mean degradation of 0.8%/year (Jordan and Kurtz, 2012). In this research, a degradation of 1% was used for the system energy production over the estimated lifespan of 25 years. Quarterly energy production was also evaluated. Figure 3-5 shows the energy analysis GUI executable panel.

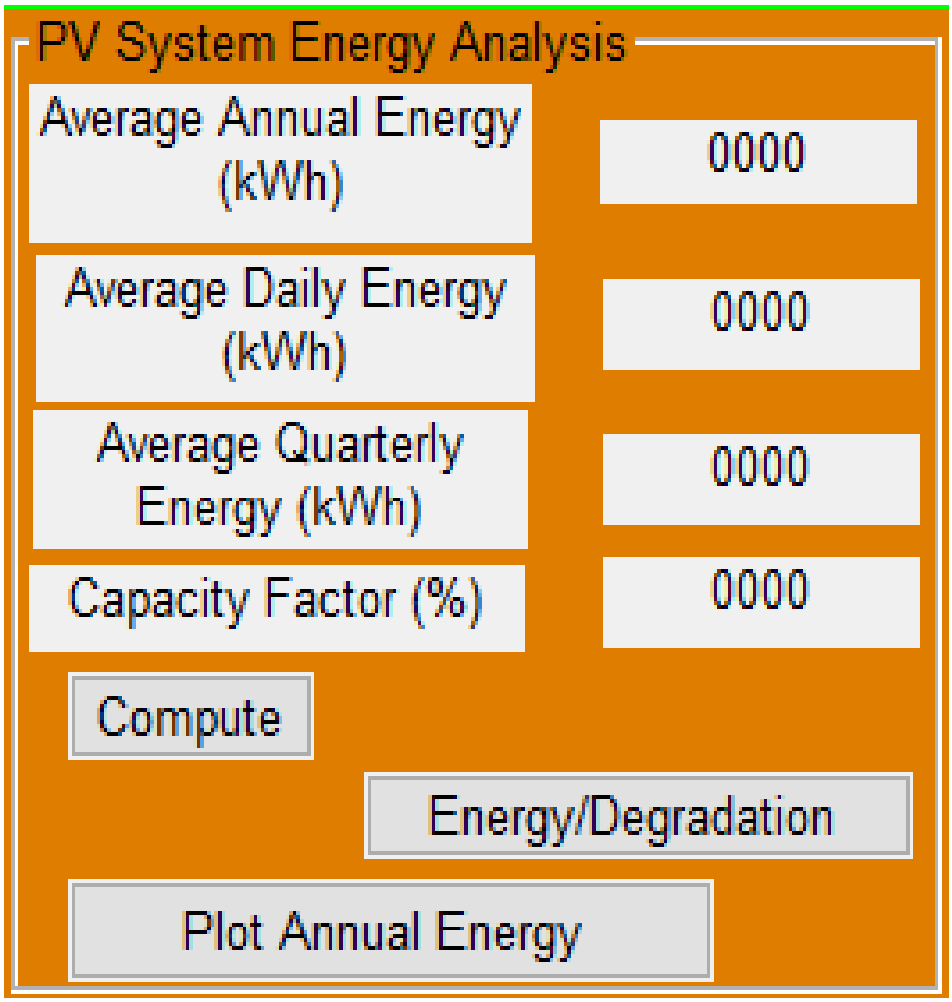

Figure 3-7: Energy Analysis Executable GUI panel

The panel also has the capacity to calculate and plot the annual energy production taking into cognisance of the degradation factor as the years roll by. The annual energy over the lifespan of the system is calculated using equation 3-24. An array of annual degradation and energy generated was created within a

MATLAB loop in the model to be able to generate the plot of energy and degradation over the lifespan of the project.

$$E_A = W_P \times \frac{ASI}{STCI} \times SSH \times DF * Efficiency * 365 * (1 - DEG_A * YR) \quad \textbf{(3-25)}$$

Where DEG_A is annual degradation rate

3.4.9 Capacity Factor

Capacity factor is the frequency of operating a power plant for a certain period of time. It is presented as a percentage and determined as the ratio of electricity generated from the unit to the average electricity output over one year. This is an important parameter as it demonstrates how the power of a unit is completely used.

Capacity factors for renewable sources are less compared with nuclear, coal or natural gas plant. This may be due to variability of wind and solar resource, maintenance issues, weather conditions and fuel cost.

$$Capacity\ Factor = \frac{Actual\ energy\ generated\ over\ a\ period\ of\ 1\ year}{Energy\ generated\ over\ 1\ year\ for\ 24/7\ operation} \quad \textbf{(3-26)}$$

3.4.10 Executable panel 6 - Economic Analysis

Large solar photovoltaic farms are projects known to require huge capital investment and therefore an economic appraisal technique to assess the profitability or otherwise of the project is imperative. Over the last few decades, there have been concerted effort in searching for an accurate project evaluation methods due to investors' worries about the profitability of project (Akalu, 2003). There are many forms of project assessment in literature used by organizations in taking decision with huge capital investment (Sillignakis, 2003). The choice of

the evaluation methodology depends not only on the investment cost, but also on the planned project life and company type (Akalu, 2003).

The economics of the system was developed bearing in mind the market price of components and some economic assumptions. The economic appraisal methodology employed to assess this proposed project in this thesis is the NPV approach. This gives the present worth of the project by calculating the cash flow and discounting it over the expected life span of the project. The key objective of economic appraisal of a project is to ascertain the profitability of the project when the calculated Net Present Value (NPV) is positive. The NPV approach demonstrate the values of cash earned now to cash earned in the future. The discount of cash flow represents the risk of earning less today to earning more in the future.

To conduct the economic analysis of the system, assumptions on some economic parameters were taken to serve as a basis for the appraisal. The assumptions are given in equations 3-26 to 3-29.

$$Discount\ rate\ = 5\% \quad \textbf{(3-27)}$$

$$Electricity\ tariff\ = \$0.12 \quad \textbf{(3-28)}$$

$$Equity\ = 30\% \times TPC \quad \textbf{(3-29)}$$

$$Loan\ = 70\% \times TPC \quad \textbf{(3-30)}$$

Where TPC is total project cost. The discount factor, D_F can be obtained from equation 3-30, where r represents the discount rate.

$$D_F\ = \frac{1}{(1+r)^{YR}} \quad \textbf{(3-31)}$$

The capital cost can be calculated using equation 3-31.

$$C_C\ = PV_C + INV_C + CC_C + B_C + A_C \quad \textbf{(3-32)}$$

Where PV_c, INV_c, CC_c, B_c, A_c represent costs associated with the PV array, inverters, charge controllers, and the land respectively.

Figure 3-6 shows the economic analysis GUI executable panel with capability for sensitivity analysis.

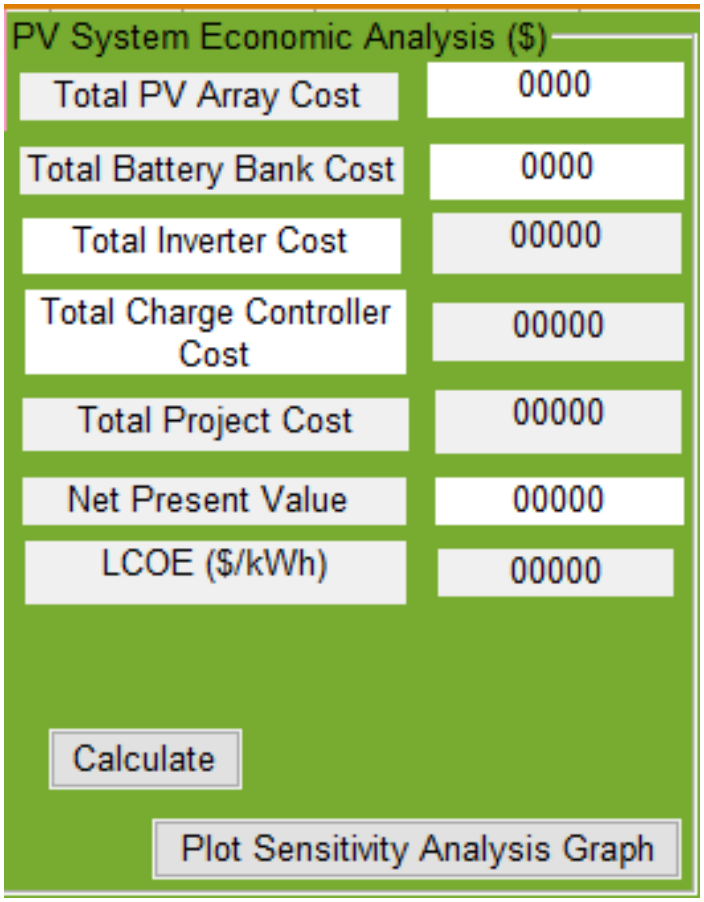

Figure 3-8: Economic Analysis Executable GUI panel

The NPV of the system over its lifespan, N years can be calculated using equation 3-32.

$$NPV = \sum_{i=4}^{N} \frac{Revenue\ stream}{(1+r)^i} - \sum_{i=4}^{N} \frac{capital + O\&M}{(1+r)^i} \quad \textbf{(3-33)}$$

The levelized cost of electricity (LCOE) is the ratio of net present value of the total cost of building and operating the solar PV energy conversion system to the

total electricity generation over its lifetime. It is a measure of a power source that allows comparison of different methods of electricity generation on a consistent basis and this can be obtained from equation 3-33.

$$LCOE = \frac{\sum_{i=1}^{n} \frac{(C_C + OM_C)_i}{(1+r)^i}}{\sum_{i}^{n} \frac{E_i}{(1+r)^i}} \quad \textbf{(3-34)}$$

The sensitivity entails the study of the effect of discount rate on NPV over the lifespan of the project.

3.5 Modelling and Simulation of Photovoltaic Panel

Modelling refers to a mathematical or logical analysis of a system, as a basis for simulation of physical or empirical processes that occur within the system. This is usually based on developing an algorithmic representation that mimics the real-life behavioural characteristics of the system. This section describes the procedure for modelling the photovoltaic module using MATLAB/SIMULINK.

3.5.1 Description of solar cell equivalent circuit

The ideal equivalent circuit of solar cell is a current source in parallel with a single diode. Figure 3-7 shows the equivalent circuit of a photovoltaic cells which is the representation of an ideal solar cell with single-diode (Abdulkadir, Samosir and Yatim, 2012; Ramos-Hernanz *et al.*, 2012; Hayrettin, 2013; Kane and Verma, 2013). In order to plot the electrical characteristics of a solar cell, it can be represented by an electric circuit with a current source, I_g and single diode, D connected in parallel and two resistive loads R_{sh} representing the shunt resistance which is usually very large and a series resistance, R_s which is small. I_D is the internal diode current, I_{sh} is current through shunt resistor, V is the output voltage and I_{PV} is the current from the photovoltaic cell. Im is the difference between I_g and I_D as expressed in equation 3-35. I_{PV} is PV output current.

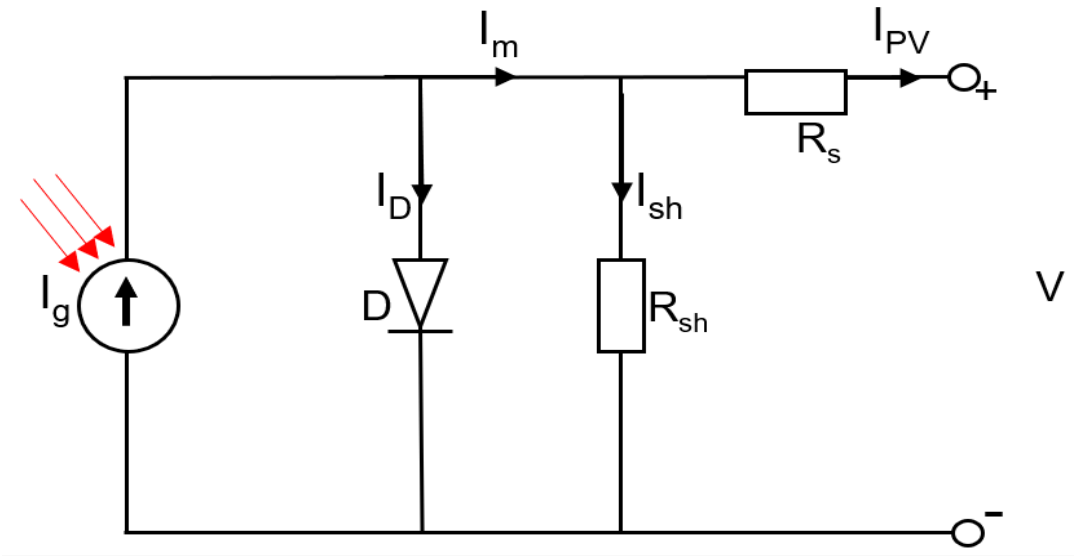

Figure 3-9: Equivalent circuit of a solar cell

The power output of a single cell is very small and cannot be enough for any application, therefore, to increase the power output, solar cells are connected in series and parallel configuration to form solar modules and modules connected in series and parallel to form an array.

3.5.2 Modelling of solar PV module

Applying Kirchhoff's Law to the equivalent solar cell circuit of Figure 3-7 yields equation 3-34 for the output current of the cell. From Figure 3-7, I_m can be written as shown in equation 3-35.

$$I_{PV} = I_g - I_D - I_{sh} \quad \textbf{(3-35)}$$

$$I_m = I_g - I_D \quad \textbf{(3-36)}$$

The current generated from a photovoltaic array is directly proportional to the solar irradiance. This is governed by equation 3-36; where I_g is a function of solar irradiance, G, I_D is the internal diode current.

$$I_g = \left(I_{gn} + K_i \Delta T\right) \frac{G}{G_n} \quad \textbf{(3-37)}$$

Where K_i is the current coefficient.

Diode current, I_D is proportional to the saturation current, I_o and it is given by equation 3-37.

$$I_D = I_o\left[exp\left(\frac{V + I_{pv}R_s}{aV_t}\right) - 1\right] \quad \textbf{(3-38)}$$

Where a is ideality factor and V_t, the thermal voltage of diode is given by equation 3-38.

$$V_t = \frac{N_s K T_{amb}}{q} \quad \textbf{(3-39)}$$

Where N_s is the number of cells in series, K is Boltzmann constant (1.381×10^{-23} J/K), q is electron charge (1.602×10^{-19} C) and T_{amb} is the ambient temperature in ^oC.

The reverse saturation current, Io which is that part of the reverse current in a semiconductor diode caused by diffusion of minority carriers from the neutral regions to the depletion region can be expressed as in equation 3-39.

$$I_o = \frac{I_{scn} + K_i\Delta T}{exp\left[\left(\frac{V_{ocn} + K_v\Delta T}{aV_t}\right)\right]} \quad \textbf{(3-40)}$$

Where I_{scn}, V_{ocn}, and K_v are the nominal short-circuit current, nominal open-circuit voltage and voltage coefficient, respectively.

From the circuit of Figure 3-7, the voltage across the diode, V_d can be written as equation 3-40.

$$V_d = V_{pv} + I_{pv}R_s \quad \textbf{(3-41)}$$

3.5.3 Determination of parameters and simulation of PV module

The following sections describes the determination of pertinent parameter in PV modelling as well as the simulation of photovoltaic module.

3.5.4 Determination of photocurrent I_g

Since the shunt resistance is very large, it implies that the current through it, Ish is negligible and therefore from Figure 3-7, the PV output current at Standard Test Condition Irradiance (STCI) is given by equation 3-41.

$$I_{pv} = I_{gn} - I_{on}\left[exp\left(\frac{V + I_{pv}R_s}{aV_t}\right) - 1\right] \quad \textbf{(3-42)}$$

When the PV cell is short circuited, the current in equation 3-40 becomes the short circuit current at reference point. Therefore, equation 3-41 can be written as;

$$I_{scn} = I_{gn} - I_{on}\left[exp\left(\frac{0}{aV_t}\right) - 1\right] \quad \textbf{(3-43)}$$

Equation 3-42 signifies that the I_{gn} is approximately equal to I_{scn} which is known from the data sheet of the solar PV module.

$$I_{scn} \approx I_{gn} \quad \textbf{(3-44)}$$

Equation 3-43 shows that the photocurrent is dependent on irradiance and temperature. Therefore photocurrent can be calculated from equation 3-44.

$$I_g = \left(I_{gn} + K_i\Delta T\right)\frac{G}{G_n} \quad \textbf{(3-45)}$$

3.5.5 Matlab/Simulink model of PV module

Figure 3-8 shows the Matlab/Simulink model of PV module developed using mathematical equations of PV module stated in the preceding section.

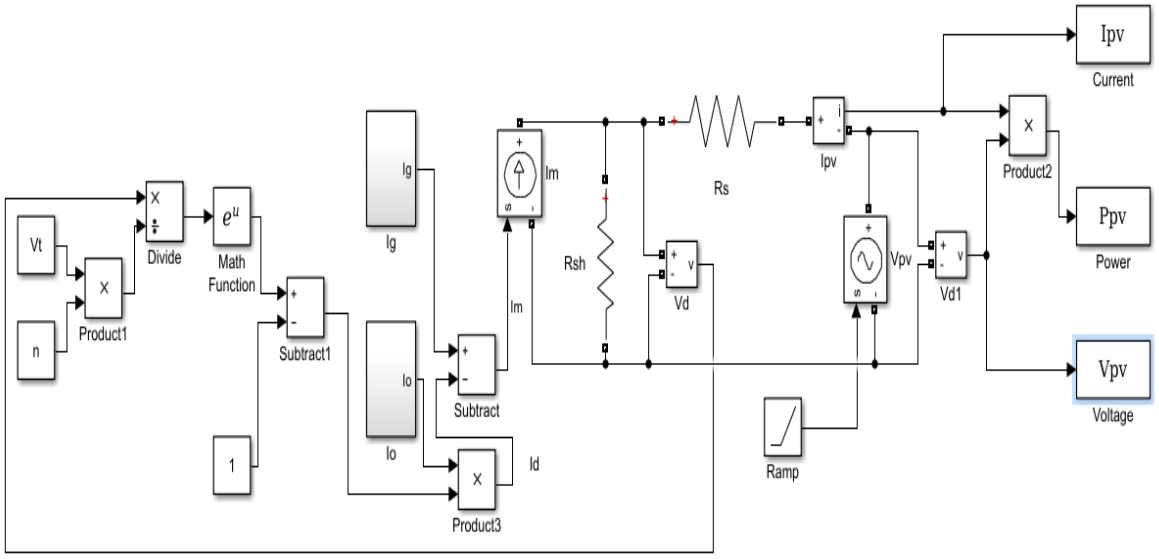

Figure 3-10: Matlab/Simulink model of PV module

Figures 3-9 and 3-10 show the implementation of the two subsystems in the main Matlab/Simulink model in Figure 3-8 representing I_g and I_o.

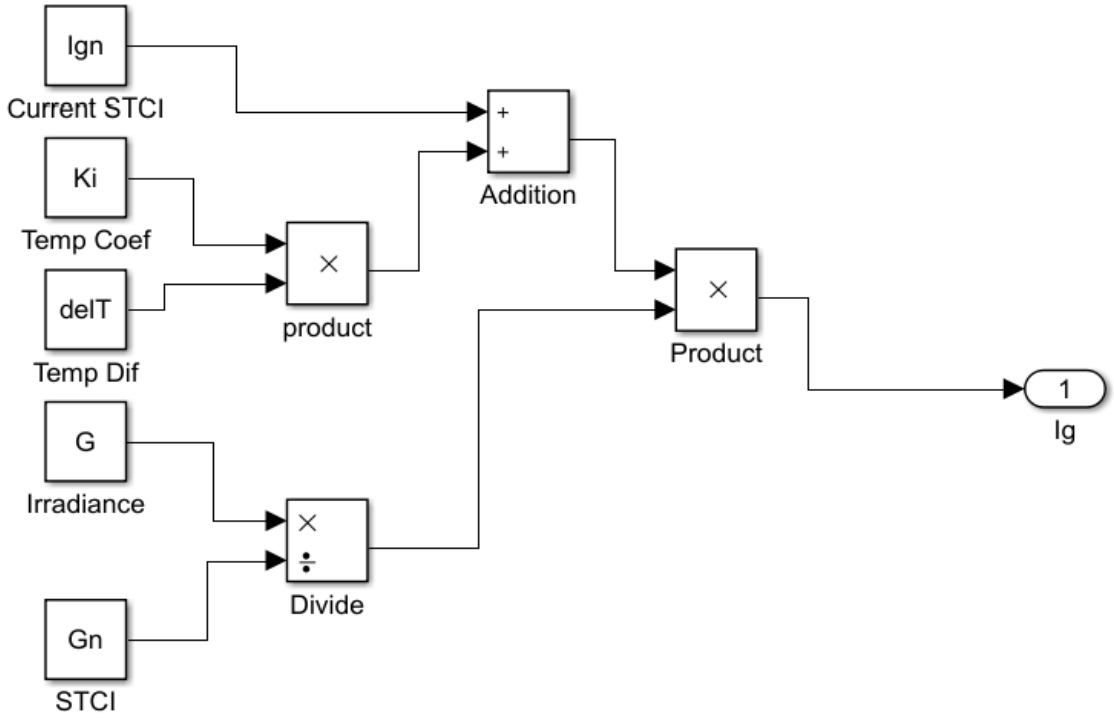

Figure 3-11: Implementation of I_g

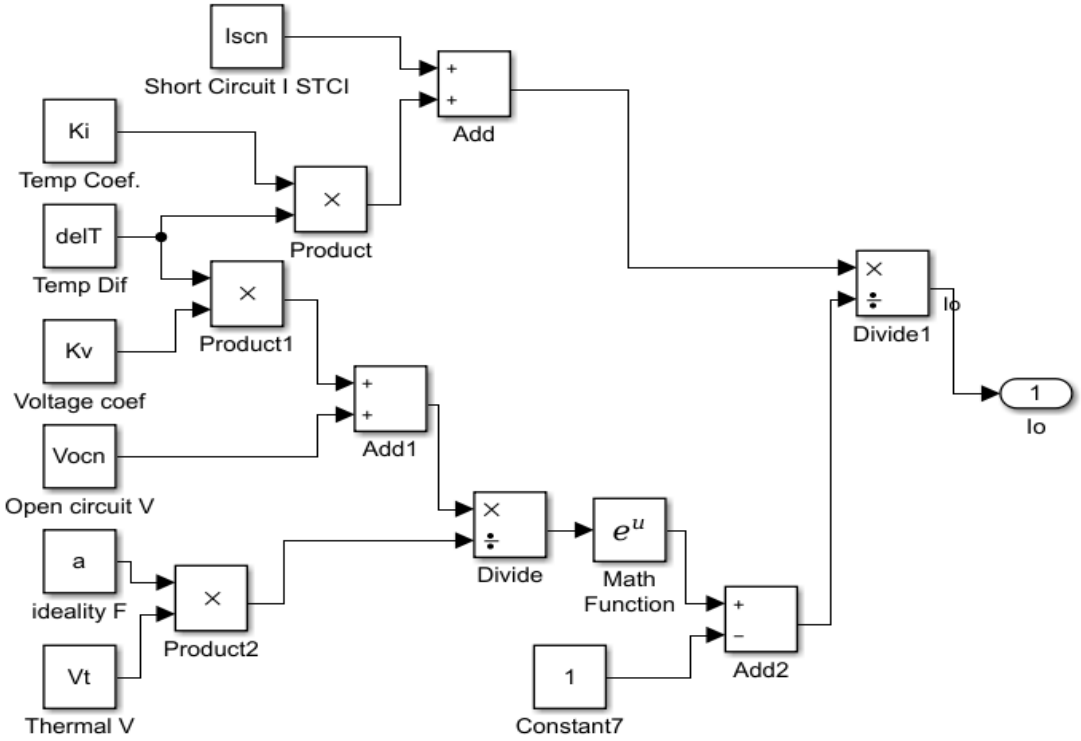

Figure 3-12: Implementation of I_o

TDG-PV model T050M365 was used for the simulation and experiments were performed to validate the simulation results as well as the I-V and P-V characteristics. The I-V characteristics of a solar module provides the key indications of its performance and can help identify defects and issues with manufacturing process and determine cell efficiency. The key specification of TDG-PV model T050M365 are given in Table 3-2

Table 3-3: Key specifications of 50 W module -TDG-PV T050M365

S/N	PARAMETERS	SYMBOL	VALUE
1	Rated maximum power	P_{max}	50W
2	Voltage at maximum power	V_{mp}	18.75V
3	Current at maximum power	I_{mp}	2.690A
4	Open-circuit voltage	V_{oc}	22.83V
5	Short-circuit current	I_{sc}	2.940A
6	Operating temperature	T_c	-40^{o}C to +85^{o}C
7	Cell Technology	Mono-Si	
8	Weight	W_c	4.0 kg
9	Dimension		554X636X30 mm

The result obtained from the simulation was validated experimentally.

Figure 3-11 shows the experimental set-up used to validate the modelling and simulation of the solar PV module. The 50W module was connected in a circuit with a potentiometer (range, 0.5mΩ – 5kΩ) and electrical measuring instrument. The potentiometer was used to vary the resistance in the circuit from very low resistance i.e. near zero to large value to very small value indicating the I_{sc} and V_{oc} respectively. If the resistance is very small, by ohm's law (I being inversely proportional to resistance, I α $\frac{1}{R}$, the current will be high i.e. I_{sc}, also from V=IR, when R is very large, the value of I will be minute and the resulting voltage will be large i.e. V_{oc} In between these two-extreme resistances, were other resistances to obtain the current and voltage at each setting which was used for the I-V and P-V characteristics from experimental results. The results are presented in the next chapter.

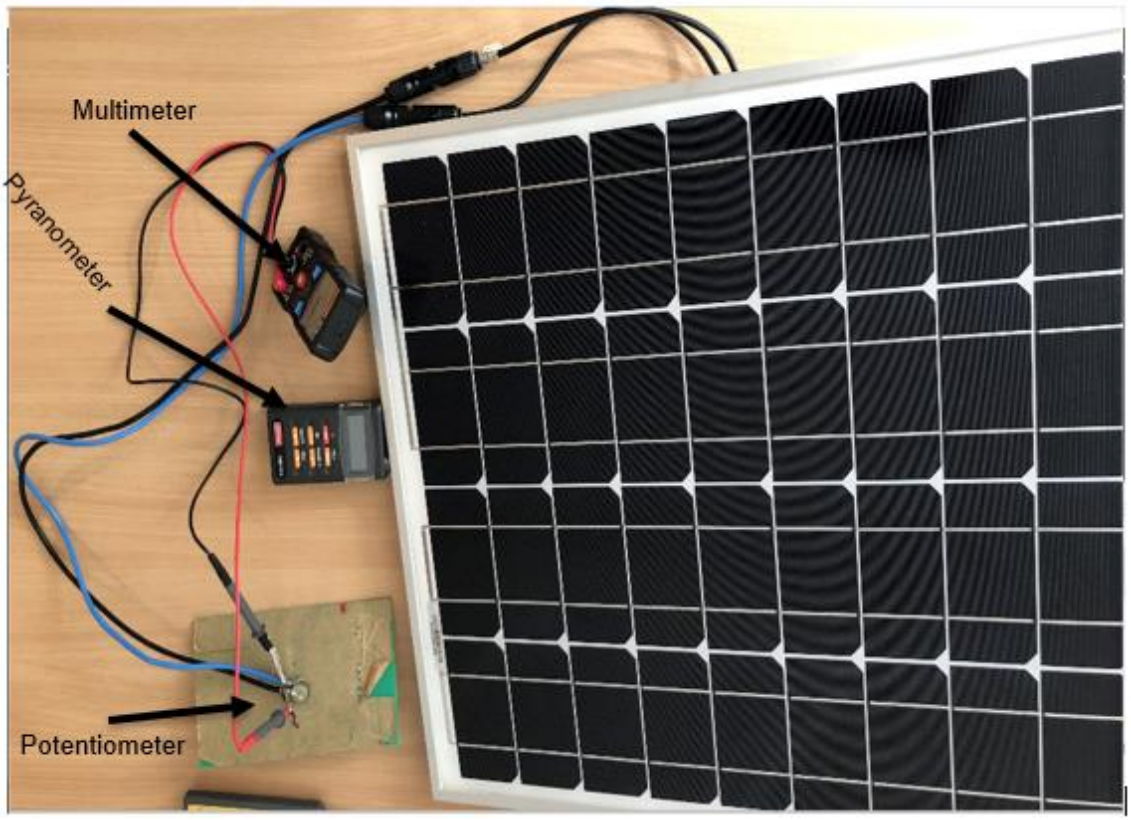

Figure 3-13: Experimental Set-up for validating Simulink model of 50 W Module

3.5.6 Fill Factor

Short-circuit current (I_{SC}) and open-circuit voltage (V_{OC}) are the maximum attainable current and voltage from a solar module. The power from the solar module at this ideal operating point is zero. This is because the voltage corresponding to short circuit current is zero and the current corresponding to the open circuit voltage is zero and consequently their product which produces power becomes zero. The fill factor (FF) is a parameter which in conjunction with I_{sc} and V_{OC} determines the maximum power from a solar cell. It can be defined as the ratio of the maximum power that can be obtained from the solar cell to the product of $I_{SC}\ and\ V_{OC}$. This shows the maximum power that can be obtained from a solar module and it is as given in equation 3-45

$$FF = \frac{P_{MP}}{V_{OC} \times I_{SC}} \quad \textbf{(3-46)}$$

Therefore

$$FF = \frac{V_{MP} \times I_{MP}}{V_{OC} \times I_{SC}} \quad \textbf{(3-47)}$$

As can be seen in Figure 3-12, fill factor is a measure of the "squareness" of the solar cell characteristics and it is also the ratio of the area of the larger rectangle to the smaller rectangle which will fit in the IV curve. The FF is illustrated below (Honsberg and Bowden, 2019).

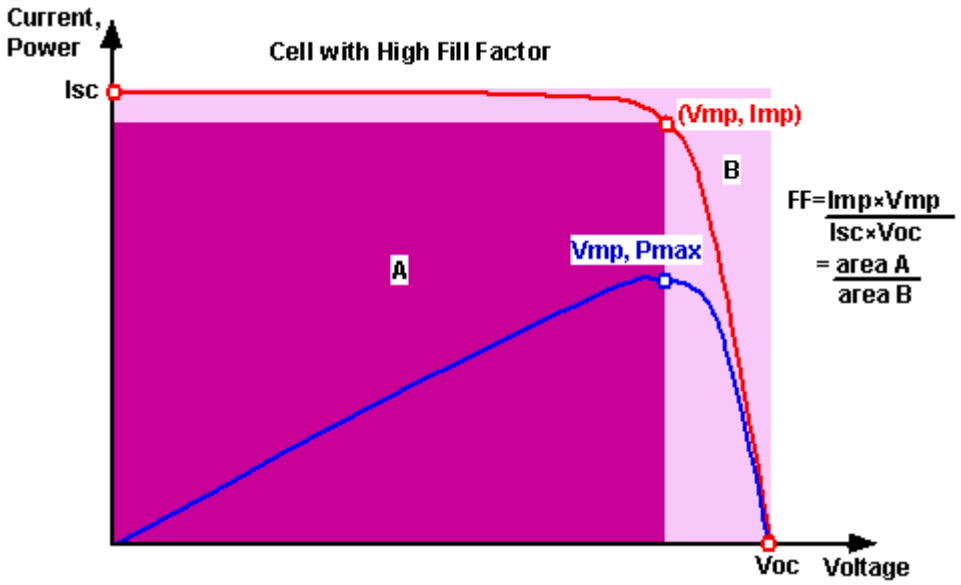

Figure 3-14: Sketch of I-V and P-V Characteristics (Honsberg and Bowden, 2019)

3.6 Development of Matlab/Simulink model for Maximum Power Point Tracking

The power output of a PV system depends basically on environmental factors such as solar irradiance and temperature. These factors are not constant through the day, therefore, for effective PV performance, a maximum power point tracking (MPPT) system is imperative. Perturb and Observe (P&O) MPPT algorithm is a widely used algorithm when compared to Incremental conductance method because it is a lot cheaper, quickly responds to very small changes in temperature and irradiance levels which means that it is inefficient at tracking large shifts in temperature and irradiance level and its oscillation is around the exact MPP. It has a simple control structure and only PV current (I_{pv}) and voltage (V_{pv}) are required for tracking maximum power output of the system. These parameters say k_{th} are measured each time where the time (k-1) corresponds to the previous time (t -1), where k is the real cycle calculated values (Subudhi and Pradhan, 2013; Hahm *et al.*, 2015). The algorithm relates measured voltages, current and power at different times and they are compared to previous measurements in time. The actual power value and previous power value are compared to track the actual maximum power.

If the actual power $P_{pv}(k)$ has increased, the voltage of the PV array V_{pv} is adjusted in the same direction; otherwise, if actual power $P_{pv}(k)$ has decreased, it is perturbed in the opposite direction as in the previous cycle (Sera *et al.*, 2006a; Hahm *et al.*, 2015). To achieve continuously the MPP, this process is repeated periodically when the MPP is reached. The perturbation steps could lead to power loss, but the algorithm responds to rapid or sudden changes in operating conditions. The method oscillates around the optimal value. The process leads to power loss that increases with perturbation step size.

Figure 3-13 shows the developed MATLAB/Simulink model of perturb and observe MPPT model. TDG-PV model T050M365 with specification as given in Table 3-2 was used for the simulation. The simulation was done at standard test conditions ($25^{o}C$, 1000 W/m^2) as well as varying the irradiance and temperature. The results gave an insight into the effects of these environmental parameters on the PV maximum power point (MPP).

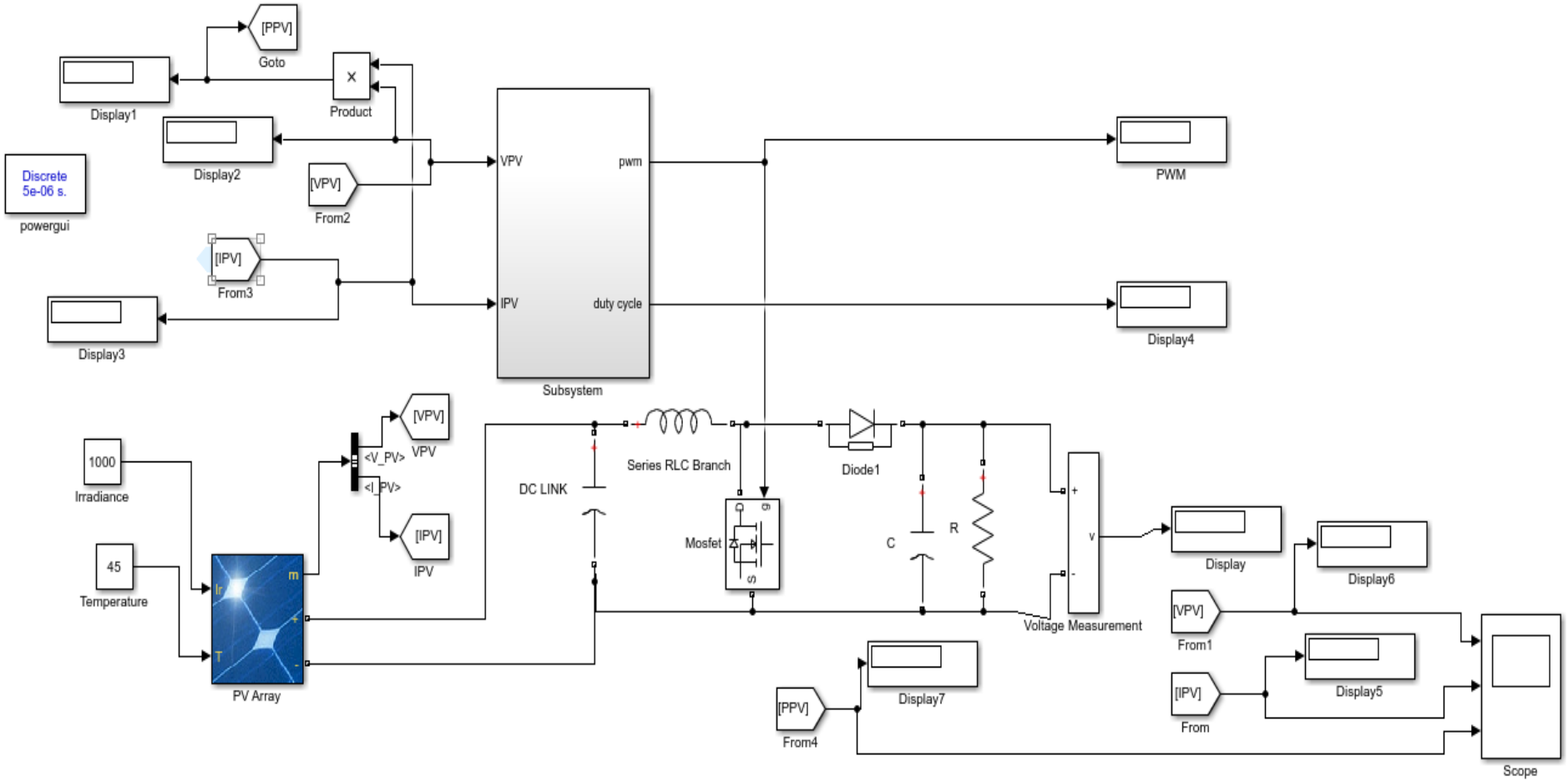

Figure 3-15: Matlab/Simulink model of P&O MPPT System

3.7 Experimental investigation of impact of dust on PV module

Maiduguri in the North-eastern Nigeria is the most dust accumulating region in the country and the most suitable region for the development of solar energy conversion systems has large rural communities without access to electricity. This makes the development of solar energy conversion system in this region very important and the study of the impact of dust imperative to guide the maintenance and cleaning of the modules for optimum power supply. The experiment to investigate the impact of dust on the performance of PV modules was conducted in Maiduguri, North-eastern Nigeria during the dustiest period.

The following are the list of the instruments used to conduct this field experiment:

i. Anemometer CR2032
ii. Pyranometer ISM 410
iii. Digital Multimeter DT9205A
iv. Thermo anemometer DT-618B
v. Hanmer s1 Digital Multimeter 2 serial no. 902016355
vi. Mooshi meter DMM-BLE-2x01A
vii. Pentype digital thermo hygrometer DTH10. 1109142
viii. Thermometer CHY506
ix. Data logging Solar power meter ISM410

A 50 W monocrystalline solar PV module (TDG-PV Model T050M365), the data of which is presented in Table 3-2 was used for the experiment. The experimental was set-up as shown in Figure 3-12. The current and voltage were measured at an interval of 10 minutes using Mooshimeter, an instrument that can measure current and voltage concurrently and log them. The Mooshimeter was set to log the readings every 10 minutes for 14 days during the day.

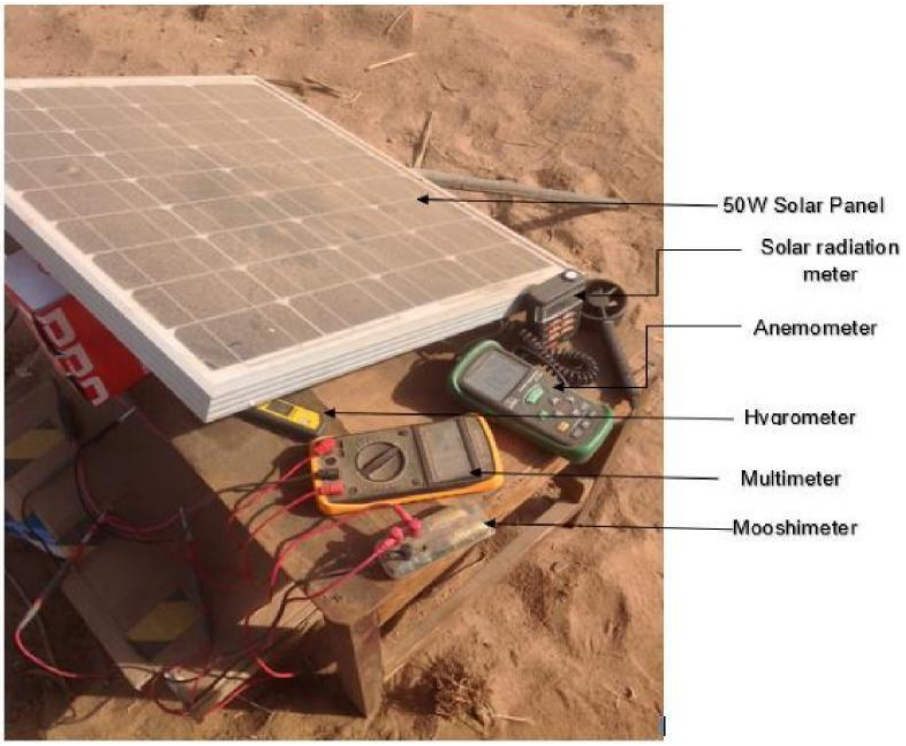

Figure 3-16: Experimental Set-up for effect of dust on PV performance

The ambient temperature, relative humidity, solar irradiance, and wind speed were recorded every hour. The experiment was conducted from 06:00 to 18:00 daily for 14 days. Figure 3-14 shows the experimental set-up for the study of impact of dust on the performance of PV module.

3.7.1 Dust collection and analysis

The accurate quantification of power decline over time that the solar panels experience is referred to as degradation. This is important to predict power delivery correctly. And the ability to predict power supply accurately over time is crucial for development and growth of photovoltaic industry. In order to assess the potential degradation of the Photovoltaic modules, it is important to have full knowledge of how the deterioration by sand occurs. It is from high wind speed (above 10 m/s) that causes sand/dust transportation that leads to potential deterioration.

In this study, we intend to determine the properties of the sand/dust that could reach the module surfaces. This is why, during the Maiduguri field experiments

on the impact of dust, dusts were collected at different heights. Four wooden poles with fixed collector plates were individually planted at different positions and the heights of 0.5 m, 1.0 m, 1.5 m and 2.0 m for dust collection for 14 days before transferring the sand into different labelled bottles which were brought to Cranfield University for analysis. . Figure 3-15 shows the wooden poles and the plastic plates used for dust collection.

Figure 3-17: Wooden poles and plastic plates for dust collection

.

In addition, and for comparison, sand was collected from the ground level as well as from the module surface. Dust was collected at different heights in order to compare and note the possible kind of particles that could reach the panels' surfaces since collection at different heights will have different results of the characterization (i.e. one would expect larger particles to collect at lower heights and for smaller/lighter particles to be airborne at greater heights). The dust collected at different heights from Maiduguri were brought to Cranfield University for analysis.

3.7.2 Characterization technique

After collecting the sand from the site, a set of analyses were carried out at Cranfield University laboratories in order to determine the main characteristics of the sand/dust particles present in the site.

Three phases of analysis were conducted in this part:

I. High precision digital weight balance was used to determine the initial mass of sand collected from each height; the objective is to see the weight of particles collected according to the height.

II. Another analysis that was carried out before the phase separation is particle size distribution to determine whether size influences the height to which a particle will be carried.

III. The mass of the samples was weighted by high precision digital weigh balance. The particle size distribution of the aggregate collected were analysed using Mastersizer3000. Humid separation of fraction of sand/soil was carried out, this separates sand part from soil part of the samples collected from the field. Soil particles have sizes from 0.002 to 0.05 mm in diameter while sand ranges from 0.05 to 2.0 mm. The chemical compositions of the samples were determined using X-ray diffraction.

The analysis conducted are particle size distribution, soil sand fraction, sand particle shape and nature and chemical analysis of the sample. Details are presented in the next section.

3.7.3 Particle size distribution

Samples of sand were properly mixed with the aid of a spatula and small quantity was taken and poured into the wet sample dispersion unit (i.e a unique dip-in centrifugal pump and stirrer that achieves full and rapid dispersion in a standard laboratory beaker) of the Mastersizer 3000 for analysis. The distribution was made into seven groups viz; 0 - 50 µm, 50 - 100 µm, 100 - 150 µm, 150 - 250 µm, 250 - 500 µm, 500 – 1000 µm and >1000 µm.

The Mastersizer 3000 uses principles of static light scattering (SLS) or the technique of laser diffraction to measure the particle size and particle size distribution of materials. It does so by measuring the scattering of light intensity as a laser beam passes through a dispersed particulate sample. Mie theory is used to calculate the size of particles in a sample. The basic principle is that small particles will scatter light at large angles and large particles will scatter light at small angles (Malvern-Panalytical, 2020)

3.7.4 Sand and soil separation

After weighing each of the samples from the four different heights of collection, sand and soil separation was carried out using phase separation method. This entails putting samples in a clean bottle and pouring distilled water to allow dirt to float and was removed. This was done a couple of times until it became clean of dirt. A fresh distilled water was then poured into the bottle containing the sample and shaken lightly to allow very fine soil particle to float in the water. The suspension mixture was poured out of the bottle leaving sand particles settled below the bottle. The bottles were then labelled with their contents as either sand or soil. This procedure was repeated for all the individual samples collected from the four different heights. The bottles were placed in an oven set to 150^{o}C to dry the sand and soil. The dried samples were then taken to analyse the characteristics of the collected particles (i.e. size, morphology and minerology) using scanning electron microscope and Energy Dispersive X-Ray Spectroscopy (SEM-EDX).

3.8 Investigation of sand adhesion to solar glass collector surfaces

The efficiency of PV modules has improved over the years as a result of research into material development but there is the need to study the environmental effect on PV performance. Soiling of PV panels is a major challenge which adversely affects the efficiency of the panels in energy conversion by factors such as soil, bird droppings, snow and debris. The experiment designed here is to investigate the sticking of soils to the glass of solar panels.

3.8.1 Materials

The materials used to conduct this experiment are:

i. Plastic box or sheets to be glued together into a box and sample holder
ii. Glass – to represent the surface of a PV panel (1089mm^2)
iii. Sand sizes range (75 – 212 microns)
iv. 4 types of sand (Sand 1- Libya 4, sand 2 – Erg Chebbi desert, sand 3 – MIL SPEC (Quartz Silica), Sand 4 – Esqua DOR)
v. Pentype digital thermo hygrometer DTH10. 1109142 for humidity monitoring
vi. Thermometer CHY506 for temperature measurement
vii. Sieves(Aperture of 75-212 microns)
viii. Humidifier and Heater (Hair dryer)
ix. High Precision Portable Digital Electronic Balance Weight
x. Spectrophotometer
xi. Tubes height range(0.5m-2m) and Paper funnel

The experimental set-up is shown in Figure 3-16. This comprises of a glass stand, and holder, a humidifier, tubes and measuring instruments.

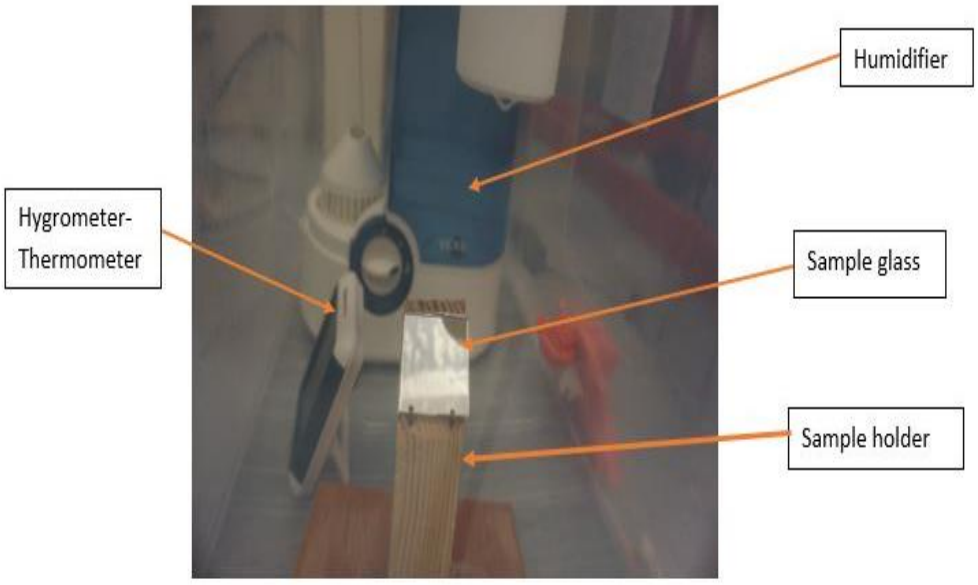

Figure 3-18: Experimental Set up (A)

Figure 3-19: Experimental set-up showing the plain plastic enclosure

Transparent plastic with opening on top for tube insertion as seen in Figure 3-17 serves an enclosure for the experiment. Some of the other parts/equipment of the set up are:

- -A funnel by means of which the sand was poured on to the sample glass via the tube
- -Inside the transparent glass was a humidifier for generating the desired humidity,
- A hygrometer – thermometer for measuring the humidity and temperature respectively.
- -Sample glasses were weighed using a high precision digital weight measuring balance and the masses noted
- Four types of sand were sieved using sieves of apertures ranging from 75->212 µm

3.8.2 Methods

The methods adopted include design of the experiment (DOE) using a software called Design-Expert, version 11 to design the required experiment employing Taguchi method. The DOE is explained in the next section of this thesis. The detail description of the experimentation is also presented.

3.8.3 Design of Experiment

The experiment considered the effect of the following five factors on the performance of glass cover of PV module and the ability of particle to adhere to it.

i. Temperature (^{0}C)
ii. Size (µm)
iii. Humidity (%)
iv. Sand type
v. Height

The levels to be considered for above 5 factors is 4. Table 3-3 shows the factors and respective levels

Table 3-4: Factors and Levels for the experiment in Taguchi design

	FACTORS	**LEVELS**			
		Level 1	**Level 2**	**Level 3**	**Level 4**
A	Temperature (^{o}C)	20	27	33	40
B	Size (µm)	0-75	75-125	125-212	212+
C	Humidity (%)	30	50	70	90
D	Type of sand	Sand 1	Sand 2	Sand 3	Sand 4
E	Impact speed Height (m)	IS 1 2	IS 2 1.5	IS 3 1.0	IS 4 0.5

Design Expert – a software for Design of Experiment (DOE) was used with 16 array Taguchi method to get the combination of the experimental runs as presented below. Figure 3-18 shows the output of Design Expert.

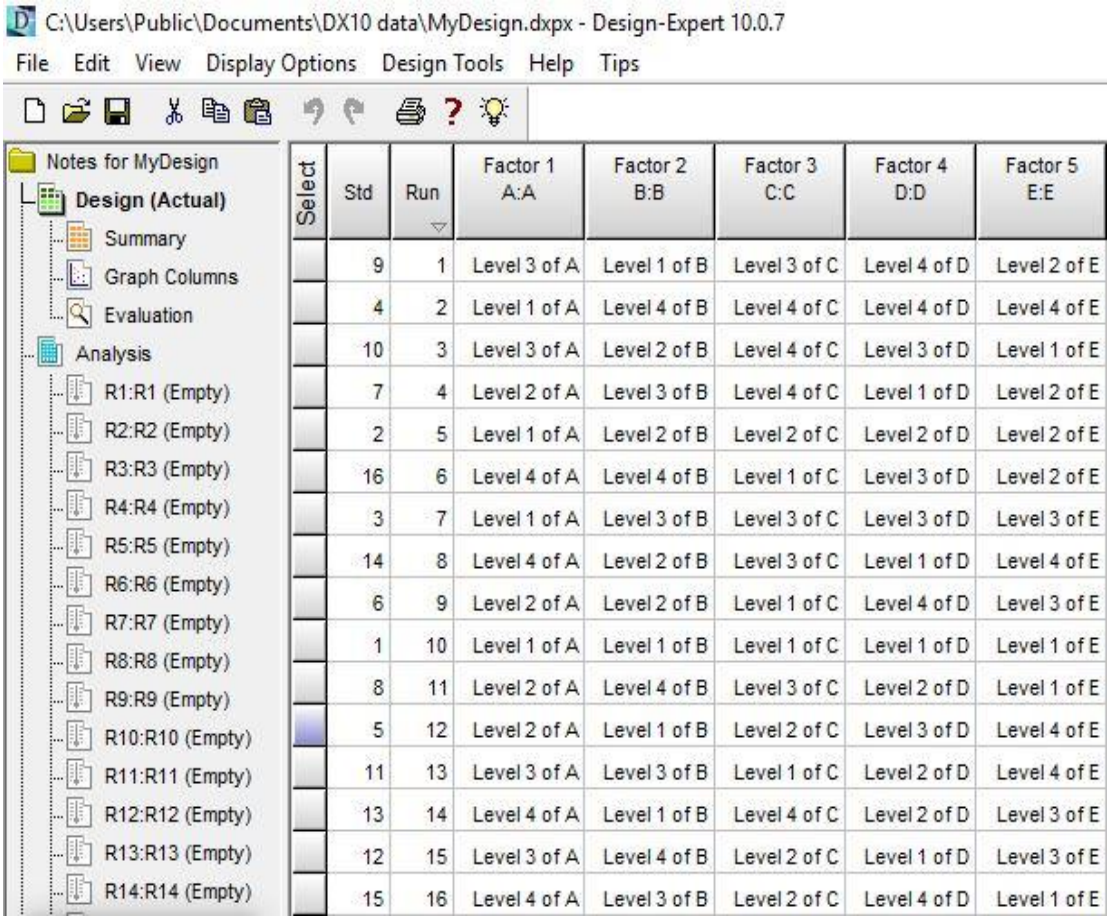

Select	Std	Run	Factor 1 A:A	Factor 2 B:B	Factor 3 C:C	Factor 4 D:D	Factor 5 E:E
	9	1	Level 3 of A	Level 1 of B	Level 3 of C	Level 4 of D	Level 2 of E
	4	2	Level 1 of A	Level 4 of B	Level 4 of C	Level 4 of D	Level 4 of E
	10	3	Level 3 of A	Level 2 of B	Level 4 of C	Level 3 of D	Level 1 of E
	7	4	Level 2 of A	Level 3 of B	Level 4 of C	Level 1 of D	Level 2 of E
	2	5	Level 1 of A	Level 2 of B	Level 2 of C	Level 2 of D	Level 2 of E
	16	6	Level 4 of A	Level 4 of B	Level 1 of C	Level 3 of D	Level 2 of E
	3	7	Level 1 of A	Level 3 of B	Level 3 of C	Level 3 of D	Level 3 of E
	14	8	Level 4 of A	Level 2 of B	Level 3 of C	Level 1 of D	Level 4 of E
	6	9	Level 2 of A	Level 2 of B	Level 1 of C	Level 4 of D	Level 3 of E
	1	10	Level 1 of A	Level 1 of B	Level 1 of C	Level 1 of D	Level 1 of E
	8	11	Level 2 of A	Level 4 of B	Level 3 of C	Level 2 of D	Level 1 of E
	5	12	Level 2 of A	Level 1 of B	Level 2 of C	Level 3 of D	Level 4 of E
	11	13	Level 3 of A	Level 3 of B	Level 1 of C	Level 2 of D	Level 4 of E
	13	14	Level 4 of A	Level 1 of B	Level 4 of C	Level 2 of D	Level 3 of E
	12	15	Level 3 of A	Level 4 of B	Level 2 of C	Level 1 of D	Level 3 of E
	15	16	Level 4 of A	Level 3 of B	Level 2 of C	Level 4 of D	Level 1 of E

Figure 3-20: Array of Experimental Runs from Design Expert

The different sand types were coded as shown in Table 3-4

Table 3-5: Sand sample types

CODE	NAME OF SAND
Sand 1	Libya 4
Sand 2	Erg Chebbi desert
Sand 3	MIL SPEC MIL-E-5007C
Sand 4	Esqua DOR O

Table 3-6: Real Values for each of the Factors used in the Experiments

Runs	Temperature (°C)	Size (µm)	Humidity (%)	Sand Type	Height (m)
1	33	0-75	70	Sand 4	1.5
2	20	212+	90	Sand 4	1.5
3	33	75-125	90	Sand 3	2
4	27	125-212	90	Sand 1	1.5
5	20	75-125	50	Sand 2	1.5
6	40	212+	30	Sand 3	1.5
7	20	75-125	70	Sand 3	0.5
8	40	75-125	70	Sand 1	0.5
9	27	75-125	30	Sand 4	1.0
10	20	75	30	Sand 1	2.0
11	27	212+	70	Sand 2	2.0
12	27	75	50	Sand 3	0.5
13	33	125-212	30	Sand 2	0.5
14	40	75	90	Sand 2	1.0
15	33	212+	50	Sand 1	1.0
16	40	125-212	50	Sand 4	2.0

3.8.4 Experimental procedure

After setting up the experiment as discussed in section 3.6.4 and coding the four different types of sands as shown in Table 3-4, the following procedure was adopted to conduct the experiment.

2 g of each of the sand samples was carefully measured using a high precision weighing balance for each of the 16 experimental runs. 16 glass samples were cleaned and weighed. The weight of each was recorded. A different piece of glass was used for each experimental run. The total number of experiments performed were 16 and the design is as presented in Table 3-5.

At a desired temperature and humidity, the sand was poured onto the glasss placed on the sample holder inside the plastic box via the funnel and tube. Then the panel was turned upside down to pour the sand off. The sample glass with the remaining sand that got stuck to the glass was weighed and the mass noted.

The air heater was used to increase the temperature inside the box and the humidifier to increase humidity or decrease temperature as required. The humidity and temperature were carefully set with the humidifier and electric air-heater respectively. The humidifier was switched on to increase the humidity when there is the need and air heater is switched on to raise temperature when there is the need. These procedures were repeated during each of the sixteen experimental runs to set the required humidity and temperature which were carefully measured using a hygrometer (having both temperature and humidity sensor and meter). Four tubes of length (0.5, 1, 1.5 and 2 meters) and a funnel were used to correctly direct each 2 g of sand to impact on the glass. Separate glass was used for each of the experiments. The mass of each of the glasses was measured after the sand impact (glass + sand that stuck to glass after impact). This procedure was repeated for the 16 experimental runs and the measurements were carefully recorded.

In addition to measuring the mass of sand remaining or stuck to the glass, microscopy was also performed at a number of locations on each sample to

examine the particles stuck on the surface. Specular reflectance was attempted before and after using an Abengoa Condor at 650 mm, again at different locations on the samples Sansom *et al.* (2017).

4 Results and Discussion

This chapter presents the results for each of the objectives enumerated in chapter one with detailed discussion. To remind the reader, these are:

i. To acquire and analyse 11-year weather data from 3 radiation zones in Nigeria and to evaluate the energy demand of the village under study.
ii. To develop a robust Solar PV system Model using graphical user interface (GUI) in MATLAB with appropriate inputs and outputs and model PV module and maximum power point tracking (MPPT)
iii. To experimentally investigate the impact of dust on the performance of Solar photovoltaic module in Nigeria and study the effect of certain pertinent parameters on sand adhesion to glass cover of PV module.

Also presented are the aims and the tools used in each case.

4.1 Solar and climatic data analysis

The need to collect and analyse solar and climatic data from the three radiation regions in Nigeria is important for two reasons. Firstly, the data analysed will form the basis for the development of solar energy conversion systems in these regions. Secondly, it will contribute to knowledge base of solar and climatic data analysis of these regions which is very scanty now.

Measured data were used in order to establish the uncertainties of the data using Root Mean Square Error (RMSE), Absolute Bias Error (ABE) and Absolute Mean Error (AME). These analyses can only be carried out by combining measured and estimated data in some established models. Future data cannot be said to be measured but estimated using various models. It is therefore, recommended to use measured data for the development of solar PV energy conversion system.

4.1.1 Descriptive statistics

The data collected from the Nigerian Meteorological Agency as stated earlier were analysed using Minitab 17 software. Tables 4-1, 4-2, 4-3 and 4-4 shows the descriptive statistics for solar irradiance, temperature, humidity and sunshine hours respectively for the three locations for a period of 11 years (2006 - 2016).

From Table 4-1, the mean irradiance for Maiduguri is 265.6 W/m^2 which is 10.9% and 21.8% higher than that of Minna and Port Harcourt, respectively. The standard error of mean is 0.798, 0.633 and 0.596 for Maiduguri, Minna and Port Harcourt, respectively. These values indicate that the individual sample means do not vary widely from the true population mean. This implies that it is more 95% confidence with all the three locations. Although Maiduguri has the highest maximum temperature of 41.95^{o}C as can be seen in Table 4-2, its average temperature is lower than that of Minna. This is because Maiduguri although with highest temperature, its minimum temperature is the lowest of the three locations. The high temperature is associated with high irradiance in Maiduguri.

From Table 4-3, the mean relative humidity for Port Harcourt is 79.09% which about 58.5% higher than the mean relative humidity for Maiduguri. This is an indication that Maiduguri is a desert area with low relative humidity almost all year round. The harmattan season in Maiduguri is usually cold and dry.

Table 4-1: Descriptive Statistics of Solar Irradiance (W/m^2) for 2006-2016

CITIES	N	MEAN	SEM	σ	Sum	Min	Q1	Median	Q3	Max	IQR	Skewness
MAIDUGURI	4018	265.60	0.798	50.61	1067177.94	77.52	225.62	271.89	310.08	376.03	84.46	-0.46
MINNA	4018	236.55	0.633	40.13	950463.93	67.11	205.95	238.34	269.58	337.84	63.63	-0.29
PORT HARCOURT	4018	207.64	0.596	37.78	834310.55	41.65	182.81	211.73	234.87	329.75	52.06	-0.48

Table 4-2: Descriptive Statistics of Temperature (^oC) for 2006-2016

CITIES	N	MEAN	SEM	Σ	Sum	Min	Q1	Median	Q3	Max	IQR	Skewness
MAIDUGURI	4018	27.56	0.099	6.28	110726.89	12.03	23.32	27.81	31.99	41.95	84.46	-0.19
MINNA	4018	28.24	0.064	4.03	113480.86	19.00	25.19	28.10	30.99	37.97	63.63	0.16
PORT HARCOURT	4018	27.32	0.048	3.05	109787.39	21.00	24.80	27.18	29.59	34.73	52.06	0.17

Table 4-3: Descriptive Statistics of Relative Humidity (%) for 2006-2016

CITIES	N	MEAN	SEM	σ	Sum	Min	Q1	Median	Q3	Max	IQR	Skewness
MAIDUGURI	4018	32.85	0.264	16.72	131997.79	10.06	20.30	27.43	42.09	79.95	21.79	0.99
MINNA	4018	49.50	0.325	20.63	198889.59	11.02	30.37	50.18	68.34	86.05	37.97	-0.04
PORT HARCOURT	4018	79.09	0.122	7.75	317766.94	51.68	74.70	80.38	85.25	90.43	10.49	-0.98

Table 4-4: Descriptive Statistics of Sunshine Hours (hour) for 2006-2016

CITIES	N	MEAN	SEM	Σ	Sum	Min	Q1	Median	Q3	Max	IQR	Skewness
MAIDUGURI	4018	7.89	0.23	0.79	31702.02	10.06	20.30	27.43	42.09	79.95	21.79	0.06
MINNA	4018	6.68	0.36	1.25	26840.24	11.02	30.37	50.18	68.34	86.05	37.97	-1.20
PORT HARCOURT	4018	3.57	0.31	1.07	14344.26	51.68	74.70	80.38	85.25	90.43	10.49	-0.83

Table 4-4 shows Maiduguri having highest average sunshine hour of 7.89 hours with Port Harcourt having lowest average of 3.57 hours. This clearly shows more prevalence and hence a better prospect for the use of solar energy conversion system in Maiduguri than Port Harcourt.

4.1.2 Analysis using normal distribution curve

Figures 4-1, 4-2 and 4-3 shows the normal distribution chart of the irradiances for the three locations under study. Three sigma or 3 standard deviation limits was used to set the upper and lower limits for the solar irradiance for the three locations as depicted in the normal distribution curves in Figures 4-1, 4-2 and 4-3. The majority of the data points fall into these limits except for 0.348%, 0.398% and 0.449% which fall outside the limits for Maiduguri, Minna and Port Harcourt respectively. The percentages for Maiduguri and Minna occur below the lower limit and none above the upper limit but the percentage for Port Harcourt combines data above the upper limit and those below the lower limit.

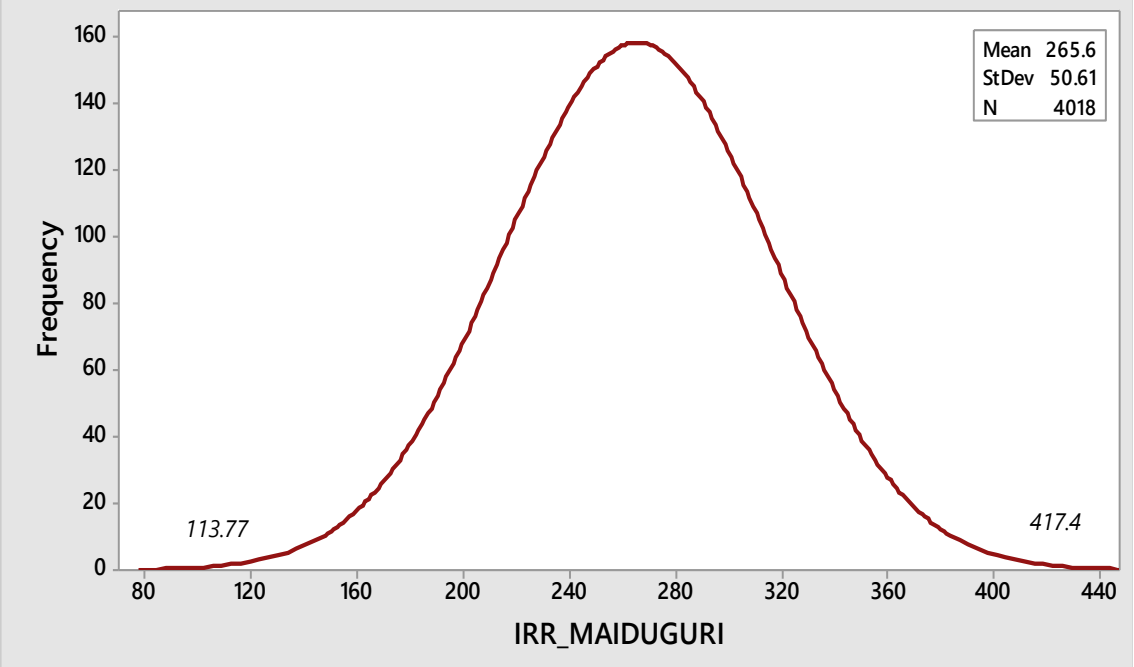

Figure 4-1: Normal distribution curve for Irradiance for Maiduguri (W/sq-m)

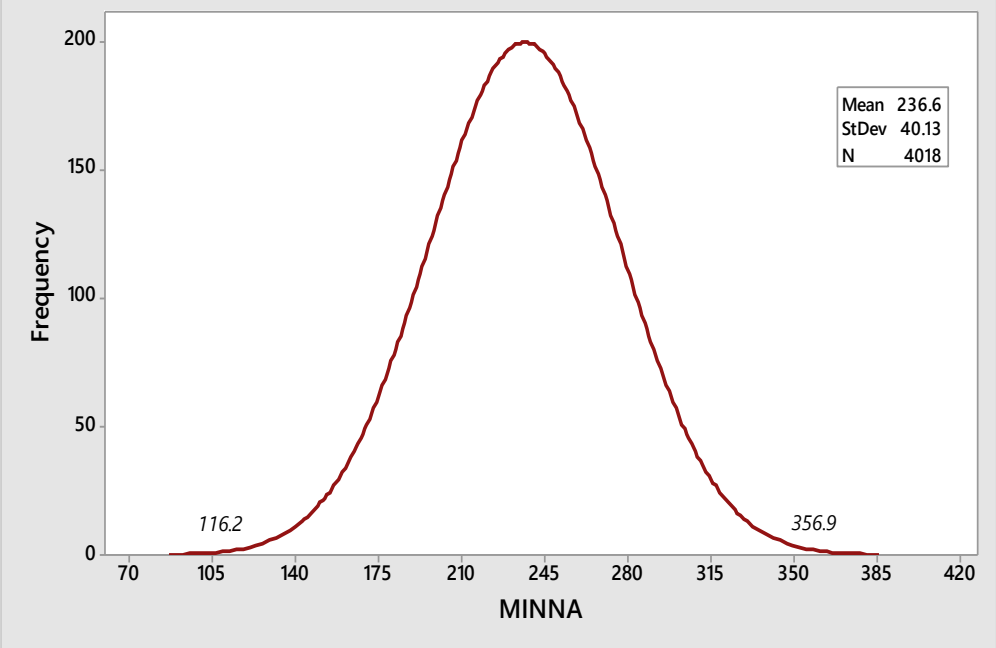

Figure 4-2: Normal distribution curve for Irradiance for Minna (W/sq-m)

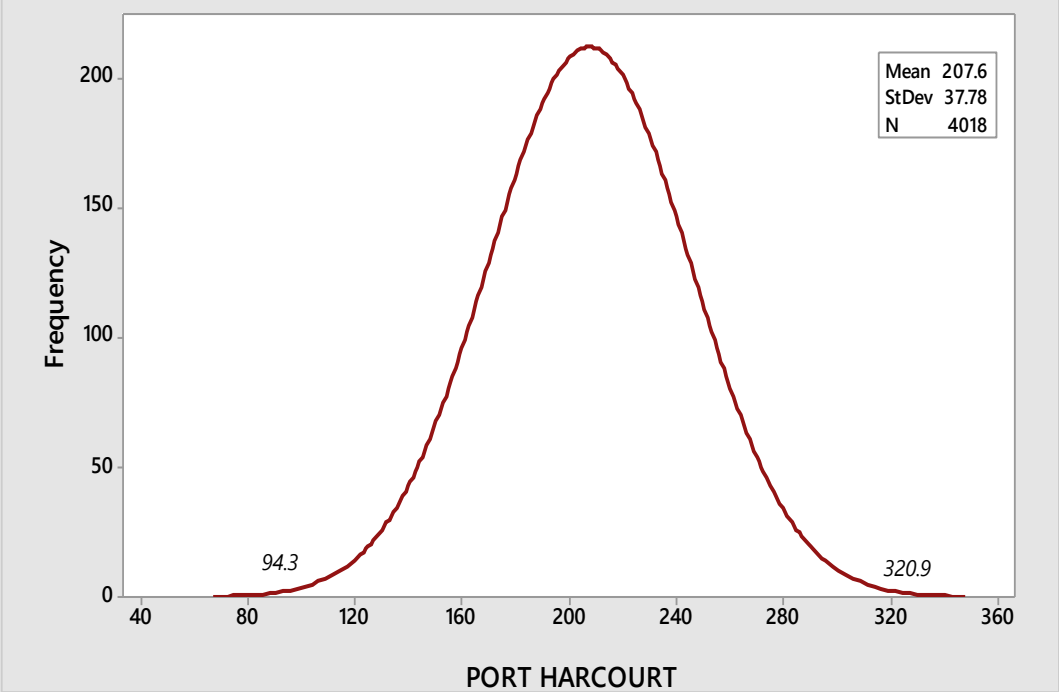

Figure 4-3: Normal distribution curve for Irradiance for Port Harcourt (W/sq-m)

4.1.3 Data analysis using Boxplot

The boxplot shows the visual representation of the five-number summary of the 11-year solar irradiance data. These are

i. Minimum
ii. First Quartile
iii. Median (Second Quartile)
iv. Third Quartile
v. Maximum

Boxplot shows the values of outliers in a data set. It could show whether a data set is tightly grouped and also the skewness of data and whether it is symmetrical or not.

Figure 4-4 shows the boxplot of solar irradiance for the three locations with the above five points indicated. The values are as indicated on the boxplot. The interquartile range (IQR) for the Maiduguri, Minna and Port Harcourt are 84.46, 63.63 and 52.06 respectively. The IQR box contains 50% of the total data. From the boxplot, 75% of the data for Maiduguri has a solar irradiance of 225.6 W/m^2 and above, while 75% of the data for Port Harcourt has a solar irradiance of 182.1 W/m^2. The asterisks in the boxplot depict the outliers in the data. Outliers are data that are significantly different from the data set of a sample. Maiduguri and Minna have outliers only below the lower limit while Port Harcourt has outliers both below the lower limit and above the upper limits.

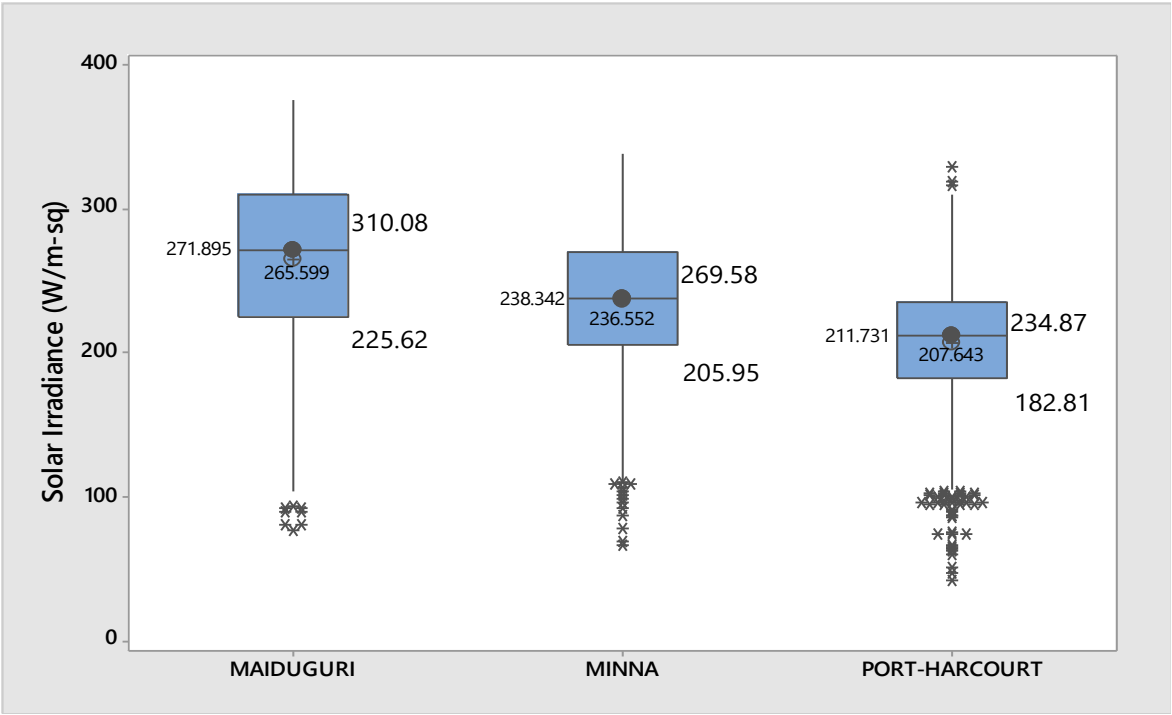

*outliers

Figure 4-4: Boxplot for solar irradiance (W/m^2)

4.1.4 Analysis of Variance (ANOVA)

Table 4-5 to 4-7 shows the results of the ANOVA for the climatic data for Maiduguri in the North-eastern Nigeria.

Table 4-5: Analysis of Variance for Maiduguri Data

Source	DF	Adj SS	Adj MS	F-Value	P-Value
Regression	3	19634.9	6545.0	18.57	0.001
Average Ambient Temperature	1	889.3	889.3	2.52	0.151
Average Relative Humidity	1	9921.0	9921.0	28.16	0.001
Average Sunshine Hours	1	263.6	263.6	0.75	0.412
Error	8	2818.9	352.4		
Total	11	22453.9			

Table 4-6: Model Summary for Maiduguri data

S	R^2	R^2 (adj)	R^2 (pred)
18.77	87.45	82.74	75.29

Table 4-7: Coefficients for Maiduguri data

Term	Coef	SE Coef	T-Value	P-Value	VIF
Constant	387	111	3.49	0.008	
Average Amb. Temp.	-2.98	1.88	-1.59	0.151	1.30
Average Rel. Humidity	-1.915	0.354	-5.40	0.001	1.90
Average Sunshine Hours	9.10	8.75	1.04	0.329	1.56

Equation 4-1 is the Regression model for analysis.

$$AVG\ Irradiance = 387 - 2.98\ AVG\ AMB\ TEMP - 1.915\ AVG\ REL\ Humidity + 9.10\ AVG\ SUNSHINE\ HOURS \quad \textbf{(4-1)}$$

The hypotheses for the F-test of the overall significance are as follows:

- **Null hypothesis (H_o)**: The model with no independent variable (intercept-only model) fits the data equally as the above regression model (equation 4-1).
- **Alternative hypothesis (H_a)**: The fitted Regression model (equation 4-1) fits the data better than the intercept-only model.

The result of the Analysis of Variance (ANOVA) gives the overall assessment of the fitted model. It shows that the sum of squares of Regression (19,634.9) is greater than that of the error (SS error = 2,818.9). The F-value for regression is 18.57, which is high. The P value for the F-test of overall significance test (0.001) is less than the significance level of 0.05, the null-hypothesis is therefore rejected, and it can be concluded that the above regression model provides a better fit than the intercept-only model. A P-value of 0.001 indicates that the model is statistically significant, and it fits the data well.

The **Model Summary** agrees with the Analysis of variance table. Table 4-6 which provides the summary shows that the fitted regression model explains about 87.45% (R^2 = 87.45%) of the total variability in the data, leaving only 12.55% (100-87.45) for error. This agrees perfectly with the result of the Analysis of Variance presented in Table 4-5, indicating that the fitted regression model fits the data well.

Table 4-7 presents the **Coefficients** of the model and it the statistics for the coefficients in the fitted model. From Table 4-7, it is observed that the variable (Average Ambient Temp.) does not contribute significantly to the fitness of the model, as it has a p-value of 0.151, which is greater than 0.05 levels of significance. The variable (Average Relative Humidity) is highly significant, with a P-Value of 0.001, which is less than 0.05. This indicates that the variable contributes significantly to the goodness–of-fit of the fitted model equation 4-1. The last variable (Average Sunshine Hours) has a p-value of 0.329, which is very high and above 0.05 level of significance. This indicates that the variable does not have significant impact on the response variable, that is, it is not significant and therefore has no significant impact on the goodness-of-fit of the fitted model.

Table 4-8 to 4-10 shows the results of the ANOVA for the climatic data for Minna North-central Nigeria.

Table 4-8: Analysis of Variance for Minna Data

Source	DF	Adj SS	Adj MS	F-Value	P-Value
Regression	3	10109.6	3369.85	25.54	0.000
Average Ambient Temperature	1	2.4	2.44	0.02	0.895
Average Relative Humidity	1	1289.5	1289.5	9.77	0.014
Average Sunshine Hours	1	322.16	322.16	2.44	0.157
Error	8	1055.6	131.95		
Total	11	11165.1			

The result of the Analysis of Variance presented in Table 4-8 is the overall assessment of the fitted model, Regression equation 4-2. The result shows that the sum of squares of Regression (10109.6) is greater than the sum of squares of error (SS error = 1055.6). The F-value for regression is 25.54, which is high, with a p-value of 0.000 which less than 0.05 level of confidence. This indicates that the regression model is highly significant. It fits the data well.

Table 4-9: Model Summary for Minna data

S	R^2 (%)	R^2 (adj) %	R^2 (pred) %
11.48	90.55	87.00	82.39

Table 4-9 shows the model summary for Minna climatic data and this result agrees with the results of the Analysis of Variance presented in Table 4-8. In

these results, the predictors explain 90.55% of the variation in the response, leaving only 9.45% for error. This indicates that the model fit the data well. S indicates that the standard deviation between the data points and the fitted values is approximately 11.48. The adjusted R^2 is 87.00%, which is a decrease of 3.55%. The high predicted R^2 value (82.39%) indicates that the model has high predictive ability and shows that it can predict new observations as well as fitting the sample data. Thus, the model could be used to generalize beyond the sample data.

Table 4-10: Coefficients for Minna data

Term	Coef	SE Coef	T-Value	P-Value	VIF
Constant	252	102	2.47	0.039	
Average Ambient Temp.	0.38	2.79	0.14	0.895	6.51
Average Relative Humidity	-1.091	0.349	-3.13	0.014	4.78
Average Sunshine Hours	6.42	4.11	1.56	0.157	2.18

Regression Equation

$$AVG\ Irradiance = 252 + 0.38\ AVG\_TEMP\_MINNA - 1.091\ AVG\_HUMIDITY\_MINNA + 6.42\ AVG\_SUNSHINE\_MINNA \quad \textbf{(4-2)}$$

The hypotheses for the F-test of the overall significance are as follows:

- **Null hypothesis (H_o)**: The model with no independent variable (intercept-only model) fits the data equally as the above regression model (Equation 4-2).
- **Alternative hypothesis (H_a)**: The fitted Regression model (equation 4-2) fits the data better than the intercept-only model.

Table 4-10 (coefficients table) gives the statistics for the coefficients in the fitted model (equation 4-2). From this table, it is observed that the variable (Average Ambient Temp) do not contribute significantly to the fitness of the model, as it has a p-value of 0.895, which is greater than 0.05 levels of significance.

The variable (Average Relative Humidity) is highly significant, with a p-value of 0.014, which is less than 0.05. This indicates that the variable contributes significantly to the goodness-of-fit of the fitted regression model (equation 4-2).

The last variable (Average Sunshine Hours) has a p-value of 0.157, which is higher than 0.05 level of significance. This indicates that the variable does not have significant impact on the response variable, that is, it is does not contribute significantly to the goodness-of-fit of the model.

4.1.5 Data Analysis using Interaction Plot

Figure 4-5 presents the interaction plot for average irradiance. In any data analysis where there are more than one independent variable, it is important to analyse the interaction between the independent variables. This is necessary to see if the interaction between the independent variable can affect the result of the response or dependent variable. From the interaction plot of Figure 4-5, there is interaction between the independent variables (Average Ambient Temperature x Average Relative Humidity x Average Sun shine Hour, and Average Temperature x Average Sun shine hour).

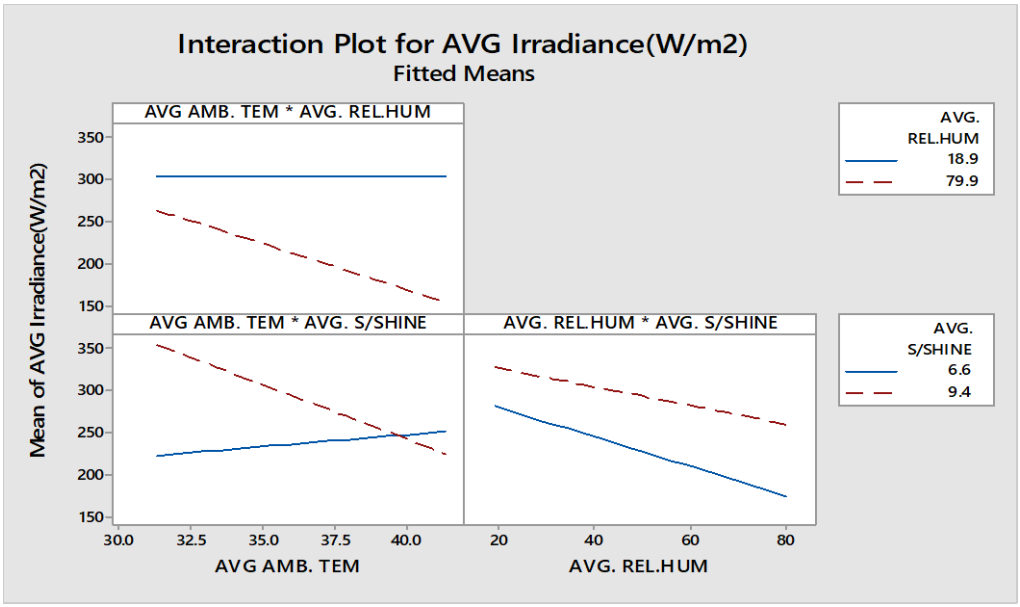

Figure 4-5: Interaction Plot for average Solar Irradiance

The effect of the interaction was subjected to Analysis of Variance (ANOVA) in order to determine whether the interaction is statistically significant or not. The result of the ANOVA is presented in Table 4-11.

Table 4-11: Result of ANOVA for effect of Interaction

Source	DF	Adj SS	Adj MS	F-Value	P-Value
Regression	6	20738.6	3456.43	10.08	0.0110
Average Ambient Temperature	1	400.5	400.5	1.17	0.329
Average Relative Humidity	1	67.9	67.9	0.20	0.675
Average Sunshine Hours	1	306.9	306.9	0.89	0.388
Average Ambient Temperature* Average Relative Humidity	1	520.8	520.8	1.52	0.273
Average Ambient Temperature* Average Sunshine Hours	1	370.5	370.5	1.08	0.346
Average Relative Humidity* Average Sunshine Hours	1	19.6	19.6	0.06	0.820
Error	5	1715.3	343.05		
Total	11	22453.9			

❖ **Regression Equation**

$$AVG\ Irradiance \quad \textbf{(4-3)}$$
$$= -1481 + 48.1\ AVG\_AMB.\_TEMP$$
$$+ 3.26\ AVG\_HUMIDITY + 213\ AVG\_SUNSHINE\_HOURS$$
$$- 0.182\ \text{AVG AMB. TEMP\_} * \text{AVG. REL. HUMIDITY}$$
$$- 5.64\ \text{AVG AMB. TEMP} * \text{AVG. SUNSHINE\_HOURS}$$
$$+ 0.228\ \text{AVG. REL. HUMIDITY} * \text{AVG. SUNSHINE\_HOURS}$$

Model Summary

S	R^2 (%)	R^2 (adj) %
18.52	92.36	83.19

The result of the Analysis of Variance gives the overall assessment of the fitted model for the interaction. It shows that the sum of squares of Regression (20,738.6) is greater than that of the error (SS error = 1,715.3).

The F-value for regression is 10.08, which is high. The P value for the F-test of overall significance test is 0.011 which is less than the significance level of 0.05, the null-hypothesis is therefore rejected, and it can be concluded that the above regression model (equation 4-3) provides a better fit than the intercept-only model. A P-value of 0.011 indicates that the interaction model is highly significant, and it fits the data well.

The **Model Summary** agrees with the result of the Analysis of variance. From this summary table, the fitted regression model explains about 92.36% (R^2 = 92.36%) of the total variability in the data, leaving only 7.64% for error. This agrees perfectly with the result of the Analysis of Variance (Table 4-11), indicating that the fitted regression model fits the data well.

Table 4-11 also show that although there is interaction between the independent variable as seen in the Intraction plot of Figure 4-5 but the interactions are not statistically significant in all cases as the P-value of the interactions are all higher than the 0.05 level of significance.

4.1.6 Frequency distribution of data

The group frequency distribution (GFD) histogram of the solar irradiance for the three cities are presented in Figure 4-6 to Figure 4-8. The data for the global daily solar irradiance for the three locations was correlated using relative humidity and ambient temperature as independent variables. Figure 4-6 to Figure 4-8 shows that solar irradiance of more than 200 W/m^2 occurs about 80.1% and 61.1% in Minna and Port Harcourt, respectively. A solar irradiance of more than 210 W/m^2 occurs about 84.3% in Maiduguri. The daily average solar irradiance was found to be 266 W/m^2, 237 W/m^2 and 208 W/m^2 for Maiduguri, Minna, and Port Harcourt respectively. This is in agreement with the submission of Adejumo, Suleiman and Okagbue, (2017). The highest frequency occurs at solar irradiance of 311-330 W/m^2, 261-280 W/m^2 and 221-240 W/m^2 for Maiduguri, Minna, and Port Harcourt, respectively.

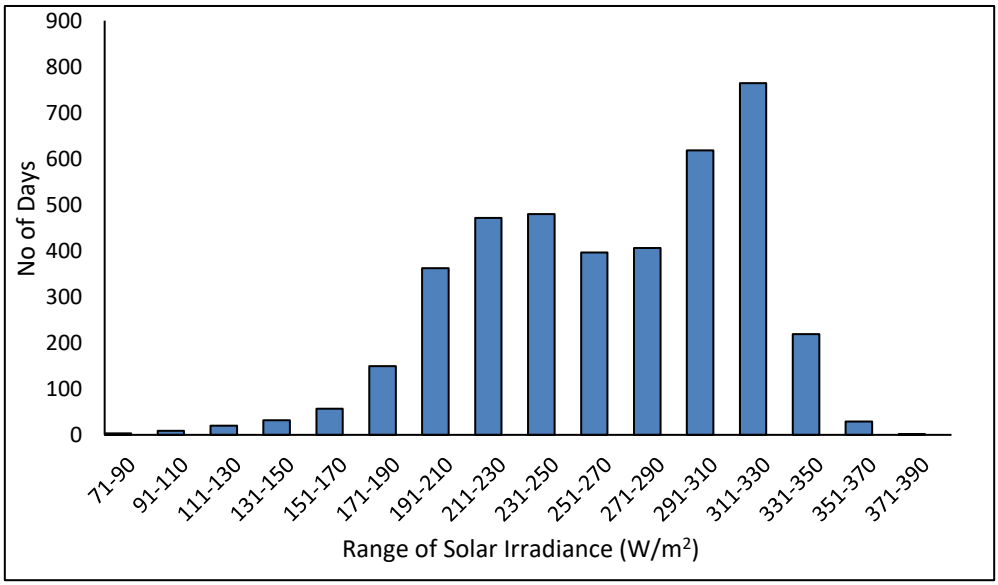

Figure 4-6: Grouped Frequency Distribution Histogram of Solar Irradiance for Maiduguri (2006-2016)

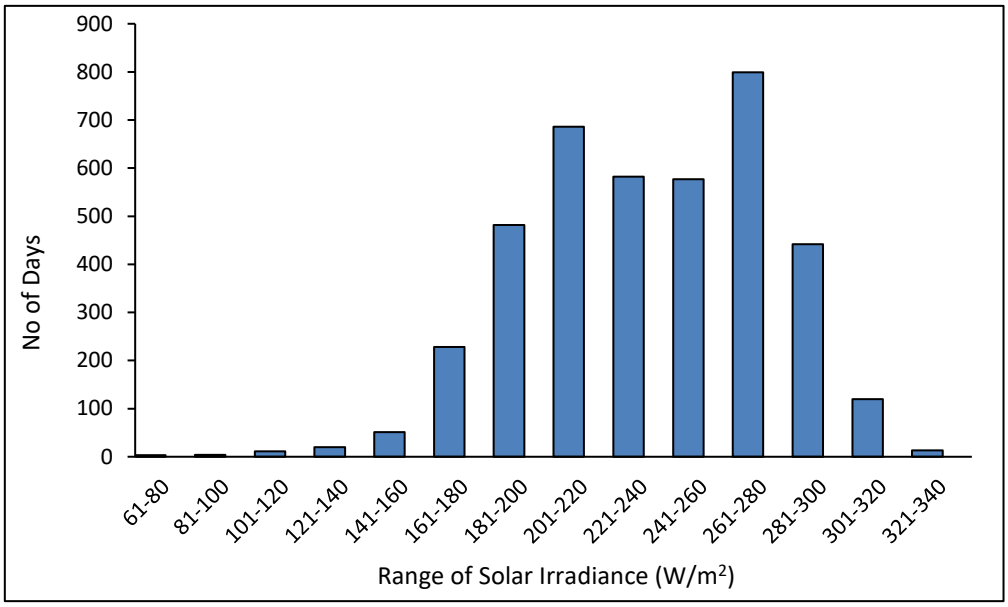

Figure 4-7: Grouped Frequency Distribution Histogram of Solar Irradiance in Minna (2006-2016)

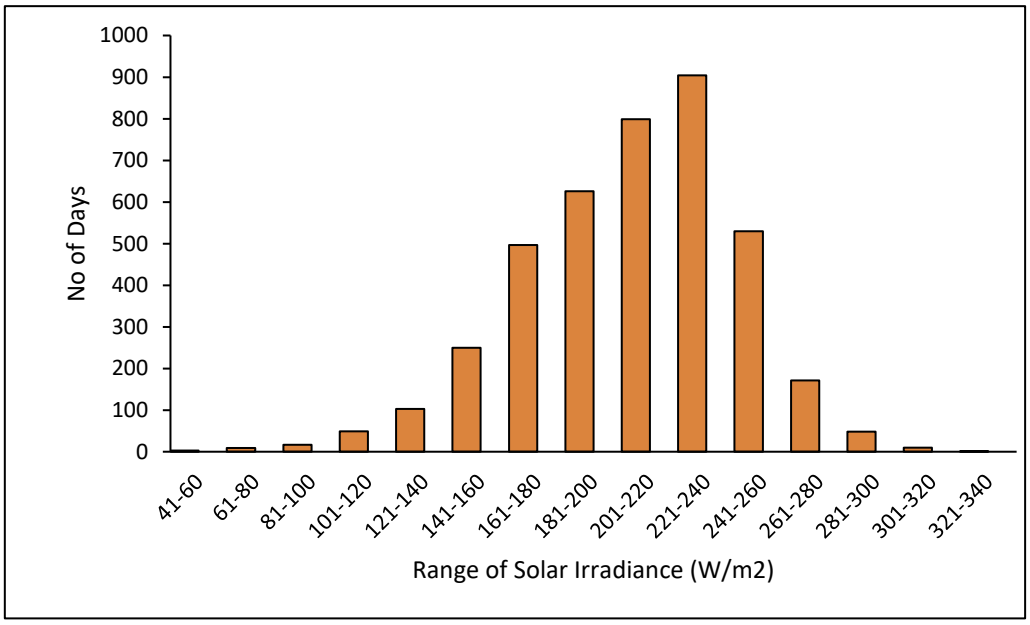

Figure 4-8: Grouped Frequency Distribution Histogram of Solar irradiance for Port Harcourt (2006-2016)

4.1.7 Regression Analysis

Figure 4-9 to Figure 4-14 shows the scatter plot and fitted regression line for the relationship between solar irradiance as the dependent variable with temperature and relative humidity as the independent variables for the three locations. Figure 4-9 shows that the Pearson's correlation coefficient between solar irradiance and ambient temperature is 0.2518 for 11-year Maiduguri climatic data. The correlation is positive but very low. This may be attributed to the fact that Maiduguri experiences the highest and the lowest temperature as a result of dry cold wind during harmattan and dry hot wind in summer.

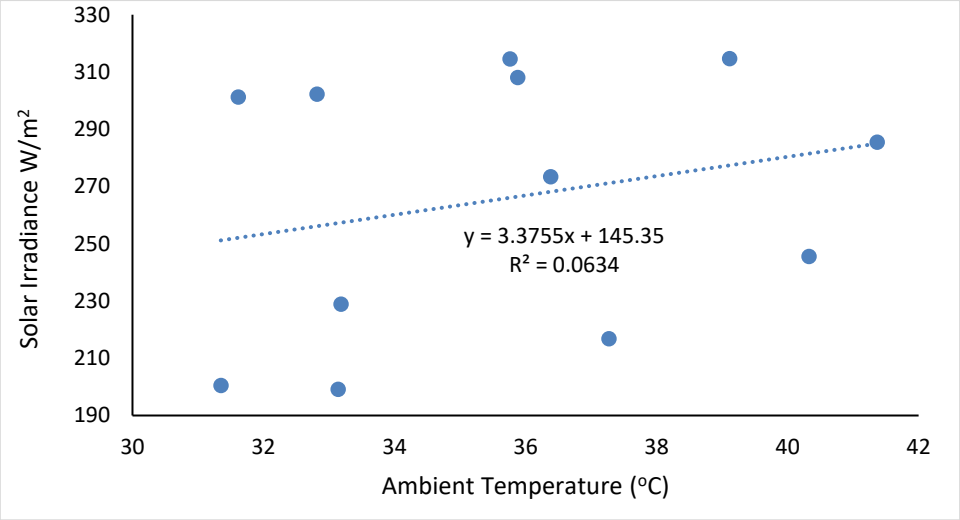

Figure 4-9: Fitted Regression Line of Ambient Temperature and Solar Irradiance for Maiduguri (2006-2016)

Figure 4-10 shows that the correlation coefficient between solar irradiance and relative humidity for Maiduguri during the period under study is -0.9062. The correlation is negative but very high, implying that at high humidity the solar irradiance will be low. This is because at high humidity, the air is dense and so causes reflection and blockage of the sunshine and thereby reducing the amount of solar radiation available at any location.

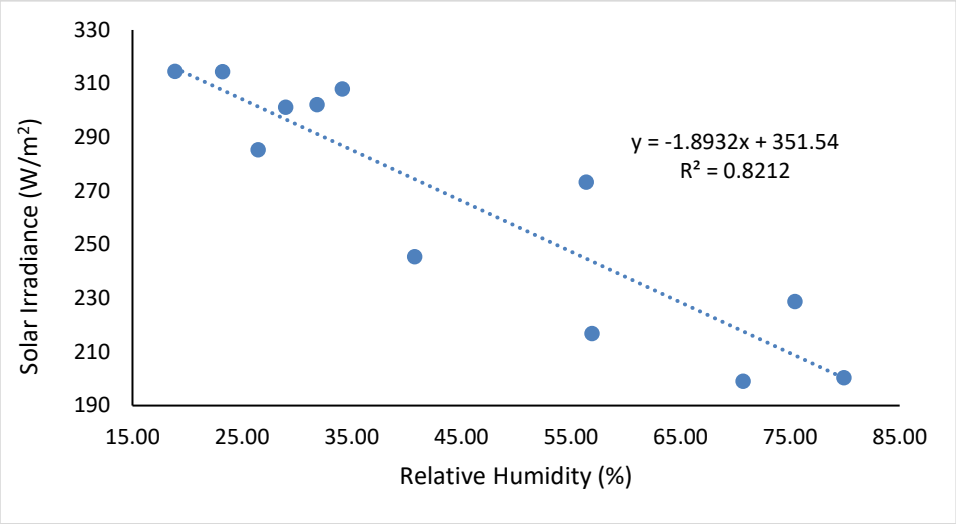

Figure 4-10: Fitted Regression Line of Relative Humidity and Solar Irradiance for Maiduguri (2006-2016)

Figure 4-11 shows the fitted regression line for solar irradiance versus ambient temperature for Minna during the period under study. The Pearson's correlation coefficient relating the two variables is 0.8802. This is a highly positive correlation which indicates how close the data are to the line of best-fit and that the higher the temperature the higher is the solar irradiance.

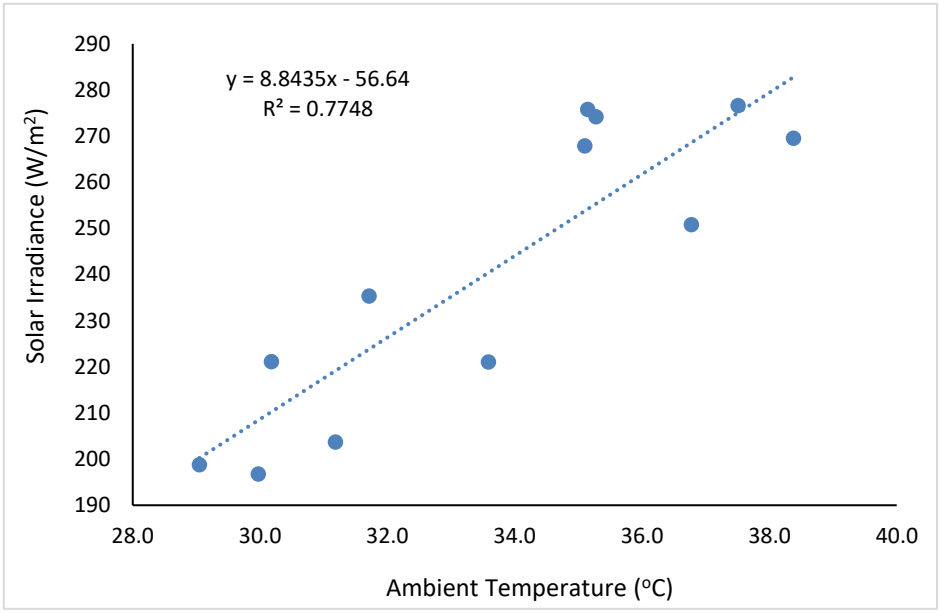

Figure 4-11: Fitted Regression Line of Ambient Temperature and Solar Irradiance for Minna (2006-2016)

Figure 4-12 shows that the correlation coefficient between solar irradiance and relative humidity for Minna during the period under study is -0.9281. The correlation is negative but very high, implying that at high humidity the solar irradiance will be low. This is because at high humidity, the air is dense and so causes reflection and blockage of the sunshine and thereby reducing the amount of solar radiation available at any location.

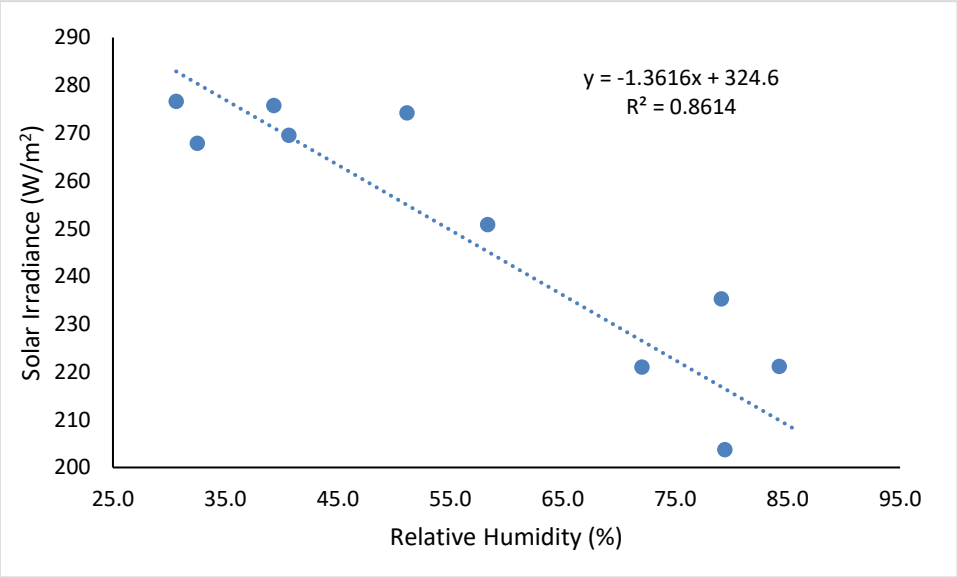

Figure 4-12: Fitted Regression Line of Relative Humidity and Solar Irradiance for Minna (2006-2016)

Figure 4-13 shows the fitted regression line for solar irradiance versus ambient temperature for Port Harcourt during the period under study.

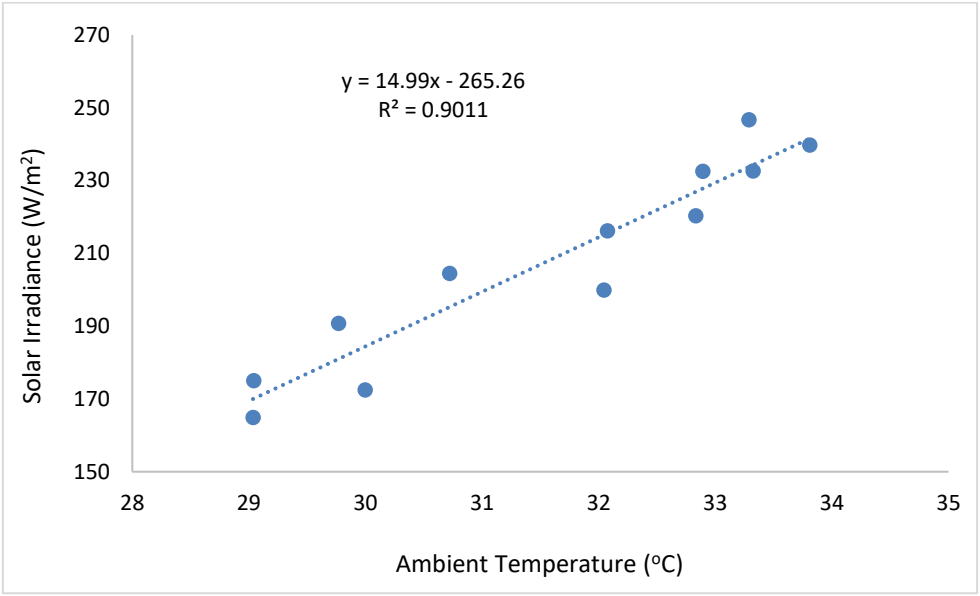

Figure 4-13: Fitted Regression Line of Ambient Temperature and Solar Irradiance for Port Harcourt (2006-2016)

The Pearson's correlation coefficient relating the two variables is 0.9492. This is a positive correlation and high value close to the maximum 1. This implies that the data describing the relationship between the two variables are close to the line of best-fit and the positive correlation implies as the independent variable (temperature) increase the dependent variable (solar irradiance) increases.

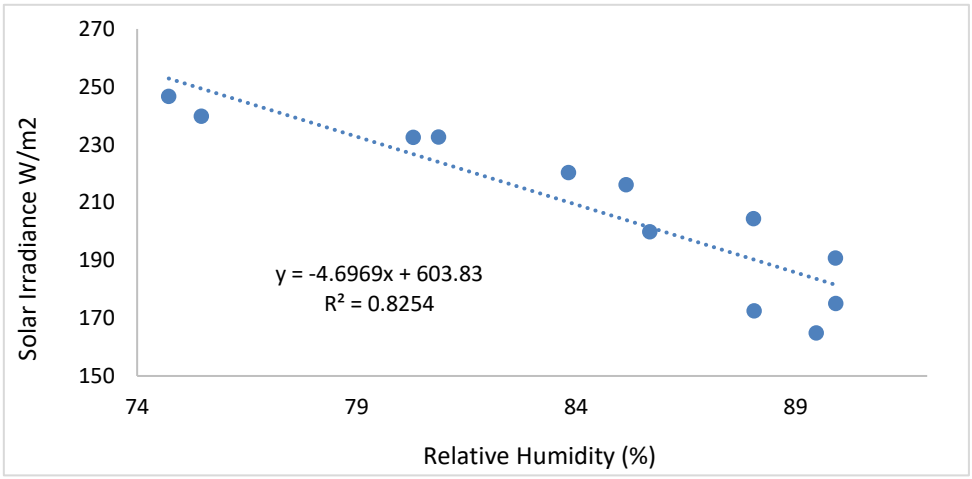

Figure 4-14: Fitted Regression Line of Relative Humidity and Solar Irradiance for Port Harcourt (2006-2016)

The Pearson's correlation coefficient describing the relationship between solar irradiance as the dependent variable and temperature and relative humidity as the independent variables are 0.252 and -0.906; 0.880 and -0.928; 0.949 and -0.909 for Maiduguri, Minna and Port Harcourt respectively. The relationship between solar irradiance and ambient temperature in the three location shows a positive linear relationship with the result for Maiduguri coming out weak. The relationship between solar irradiance and relative humidity in the three location shows a negative linear relationship with the result for the three locations showing strong compliance with the linearity between the two parameters.

Table 4-12 shows some statistical indicators, Sunshine hours and day length used for further analysis of the data. The percentage sunshine per day is highest in the month of November with 68.6% and the least occurred in the month of August with 32.9%. This result shows that there exists more cloudy sky in the month of August than any other month in the year. This usually is the peak of rainfall in any one year. The variation in errors calculated is least in July and highest in the month of November.

Table 4-12: Some statistical indicators

Months	S	S_{max}	S/S_{max}	RMSE	MBE	MAE
JAN	6.9	11.6	0.595	15.3	-13.3	14.1
FEB	7.6	11.8	0.643	9.9	-7.4	7.9
MAR	6.7	12.1	0.558	17.0	14.5	14.7
APR	7.6	12.3	0.616	19.4	17.1	17.9
MAY	7.5	12.6	0.596	18.4	16.2	15.8
JUN	6.6	12.7	0.525	18.7	16.1	15.9
JUL	4.7	12.6	0.375	9.4	3.2	7.4
AUG	4.1	12.4	0.329	13.6	8.3	10.2
SEP	5.5	12.2	0.456	11.4	-3.3	8.3
OCT	7.5	11.9	0.628	18.8	-10.6	13.3
NOV	8.0	11.7	0.686	21.9	-14.9	18.0
DEC	7.4	11.6	0.641	11.2	1.0	8.5

In summary, the analysis and discussion presented shows that the data for the selected locations are well correlated and that the three locations studied have good solar irradiance and climatic data which favours the development and deployment of solar photovoltaic energy conversion system. The analysis of the data shows Maiduguri being most favourable as a result of having highest solar irradiance and lowest relative humidity all year round.

4.2 Energy demand

Table 4-14 shows the breakdown of the calculated energy requirements of a model village taking into cognisance common facilities in the village and based on the appliance ratings of Table 4-13.

Table 4-13: Rating of appliances (DaftLogic, 2019)

APPLIANCES	POWER (W)
Streetlight bulbs	60
Fan	50
All other bulbs	15
Refrigerator	100
Laptop computer	45
Air-conditioner	746

Table 4-13 shows the output of calculations of energy demand using MATLAB17.

Table 4-14: Energy requirements

SECTION	ENERGY REQUIRED (kWh/day)
200 Houses	800.000
1 Hospital	38.855
1 Primary School	69.188
1 Secondary School	69.428
1 Market	78.600
1 Police Office	11.808
1 Garage	10.000
TOTAL	**1,077.879**

The total energy requirement is 1.077879 MWh per day. This forms the basis for the development of the Solar PV model and simulation in GUI interface in order to compute the solar system components needed to meet this requirement.

4.3 Solar Photovoltaic System Model

Most solar photovoltaic systems which are above 500kW are usually grid-tied but the villages in North-eastern Nigeria being considered in this study are very far from the National grid. In some instances, more than 100 km apart. This distance combined with the frequent power outages makes PV grid-tied system economically and technically unviable for this region. Most software does not handle large solar farms as standalone which is one unique thing about SPVSM.

4.3.1 PV array sizing

Considering the energy demand of 1,077.879 kWh/day and all the other inputs such as irradiance and sunshine hours as it relates to Maiduguri, Figure 4-15 shows the output of panel 1. It displays the values of the PGF, Total peak watt of the PV array and the number of 300 W module required to meet the demand. The total peak watt is 667659 W and the number of 300 W modules required is 2226.

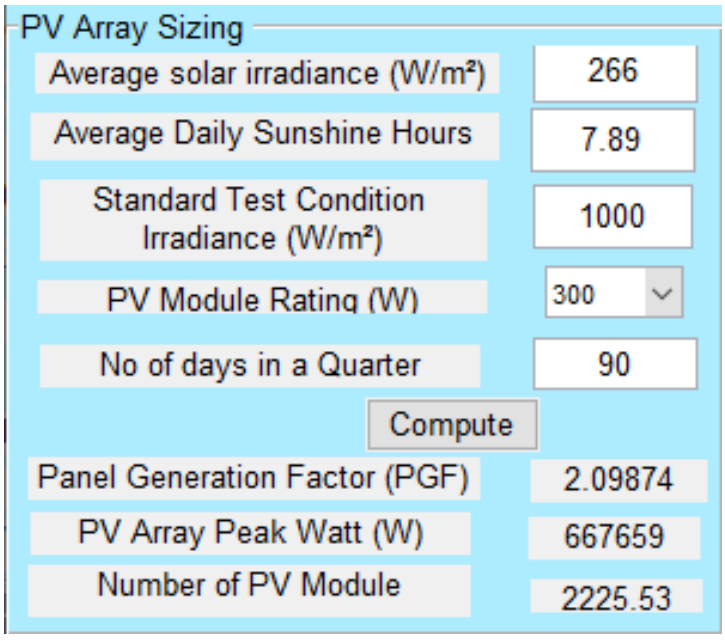

Figure 4-15: PV Array sizing panel output

4.3.2 Battery sizing

To meet the energy needs of the village during days of autonomy which are days that the battery bank should be able to supply the required energy and not discharging the battery completely, an adequate battery bank must be made available. Figure 4-16 shows the output of battery sizing panel. From the panel output, 599 6V 1200 ah batteries would be enough for the village in off-grid condition and it will require about 6.5 hours to fully charge the battery bank from a 50% depth of discharge. The number of batteries required will change when another rating of battery is selected.

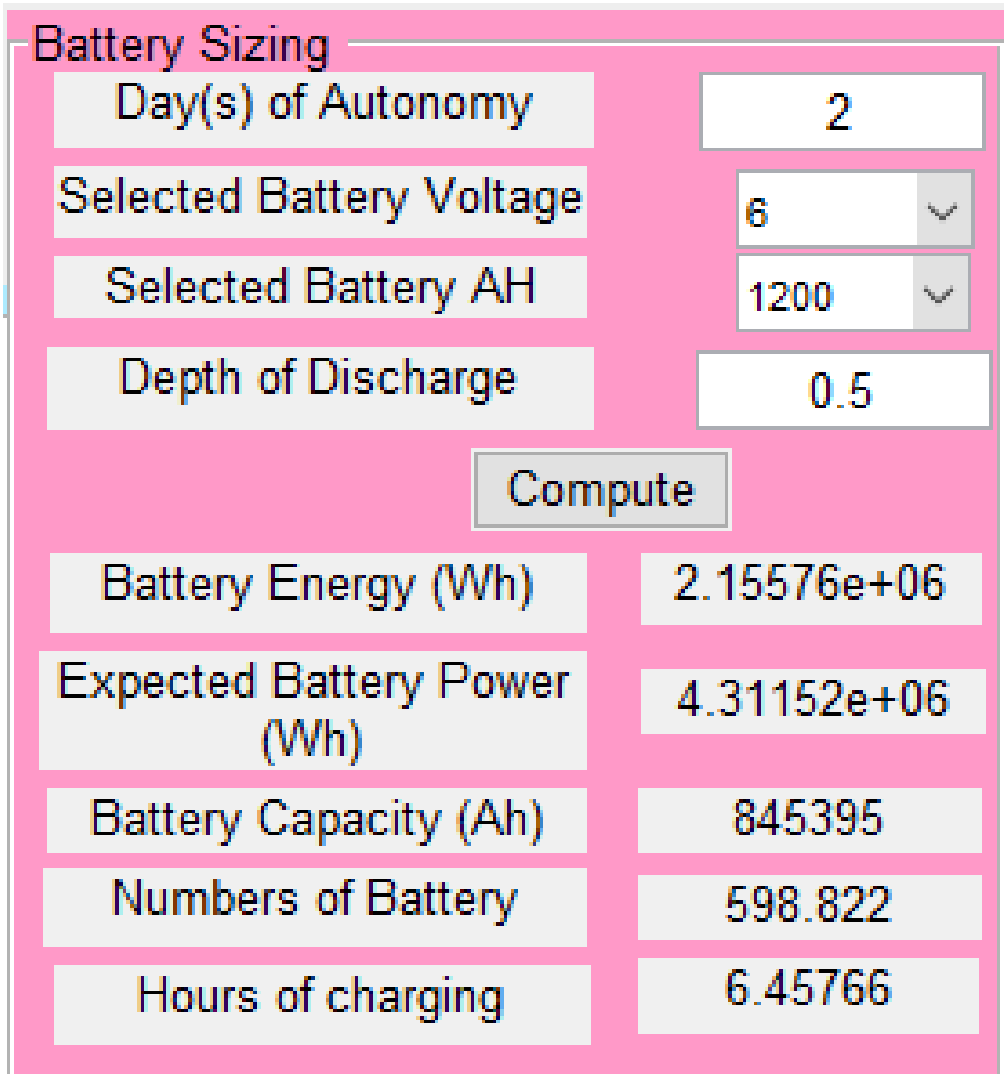

Figure 4-16: Battery sizing panel output

4.3.3 Inverter sizing

Inverters are rated in wattage and the sizing depends basically on the load. The inverter must be sized to have capacity to sufficiently supply adequate power to run the load. Figure 4-17 shows the output of the inverter sizing panel. For the selected inverter size of 8kW, 21 inverters are required to adequately supply the calculated load of about 127.5 kW.

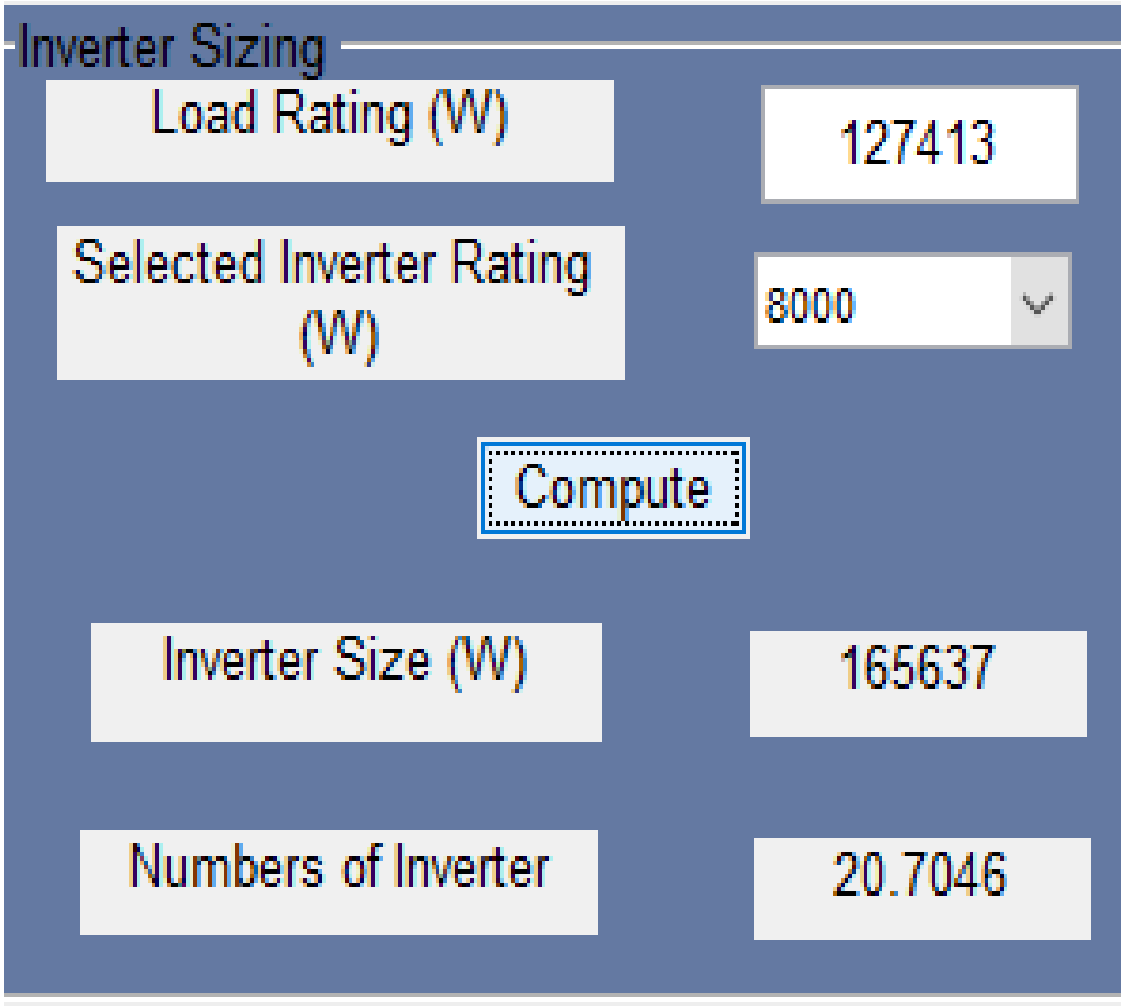

Figure 4-17: Inverter sizing panel output

4.3.4 Charge controller sizing

Charge controllers are rated in amperage in order to be able to control the flow of current for the charging of batteries and also to prevent undue discharging.

Figure 4-18 shows the charge controller panel output. 227 80 ampere selected charge controllers are required for the present battery system.

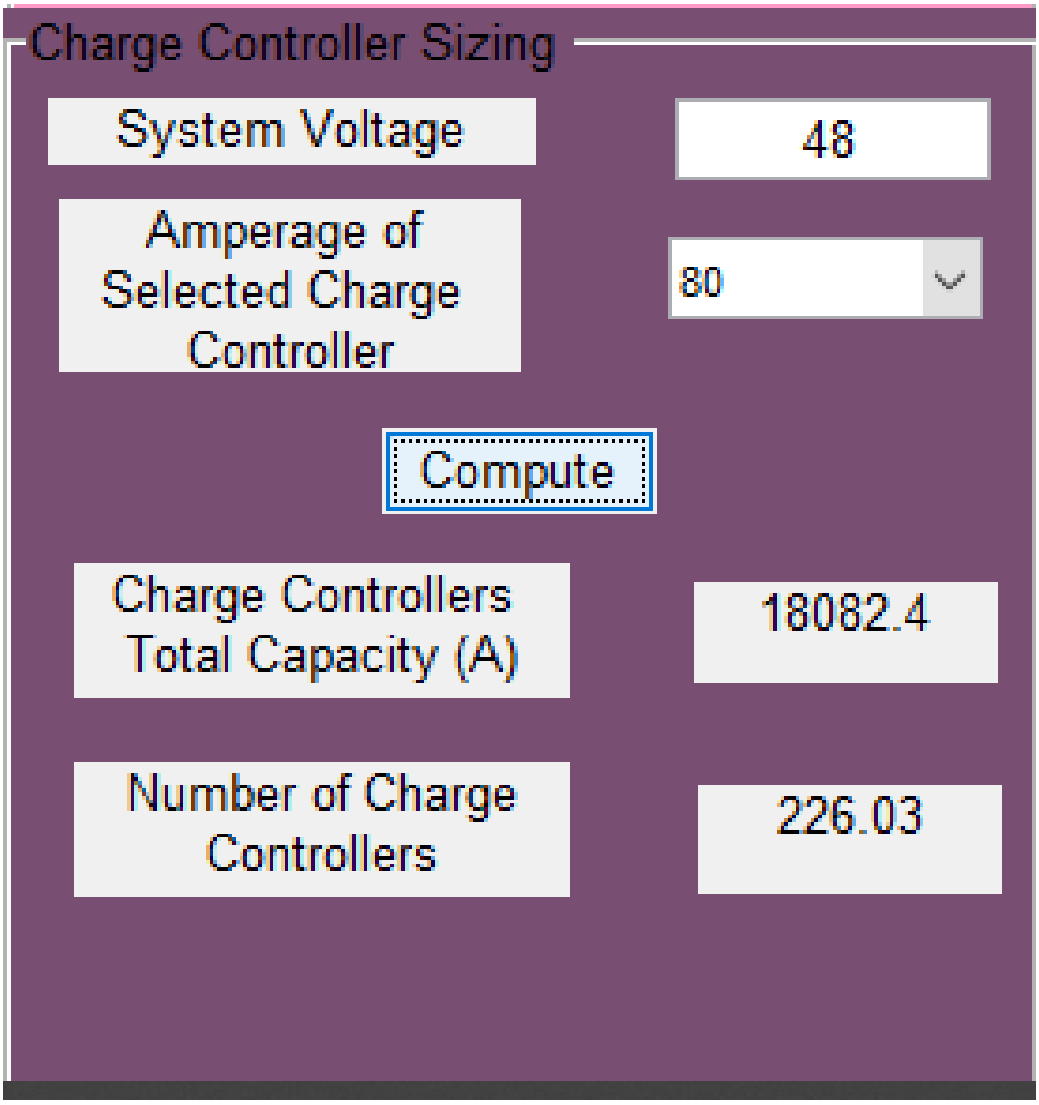

Figure 4-18: Charge controller sizing panel output

4.3.5 Energy analysis

The energy produced by a solar PV array is a measure of the environmental conditions such as solar irradiance and temperature, and the efficiency of conversion of the array. Figure 4-19 shows the output of the energy analysis panel. The panel shows the average annual, daily and quarterly energy generated by the PV array. The panel also has the capability to present graphical representation of the annual energy generated over the lifespan of the plant

taking into account the degradation effect. The average annual energy generated by a 667.7 kW power plant is 409,163 kWh.

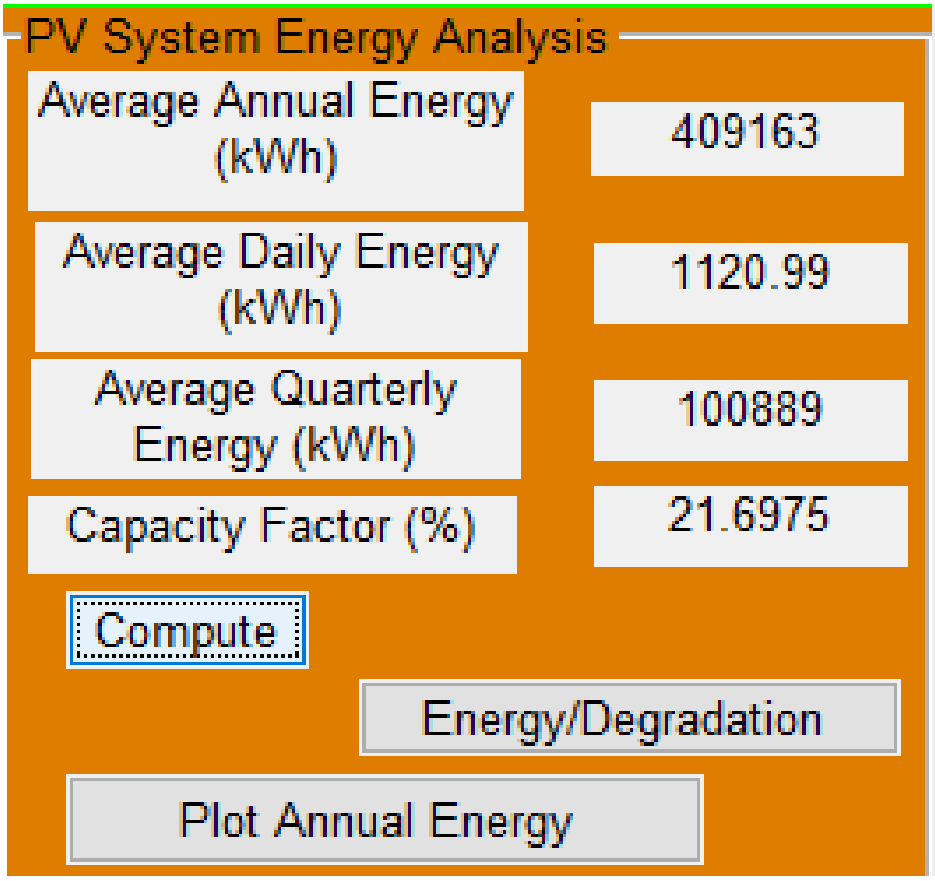

Figure 4-19: Energy analysis panel output

Figure 4-20 shows the annual energy generated over the lifespan of the plant at varying degradation rates. In the model, a degradation of 1% per annum was assumed, this is in tune with available PV system degradation rates found in literature. Zweibel, James and Vasilis, (2008), Branker, *et. al.* (2011) *and* Campbell (2008) stated that annual degradation rate for solar panel is between 0.5% to 1%. There are two phases, the construction/installation phase and the operation phase. During the construction phase as can be seen in Figure 4-20, the energy generated is zero obviously. The highest energy output was obtained during the first year of operation as there is least degradation. The energy generated during the fifth year of operation is 402,800 kWh for a degradation of 0.5% and 392,500 kWh for a degradation rate of 1%, this is about a 2.5% drop in

energy generated. For the purpose of analysis, PV energy generated was simulated with varying degradation rates. The energy generated during the 25th year of operation for a degradation rate of 1% is 3.099x10^{5} kWh which is 16.6% higher than energy generated for a degradation rate of 1.5% during the same year.

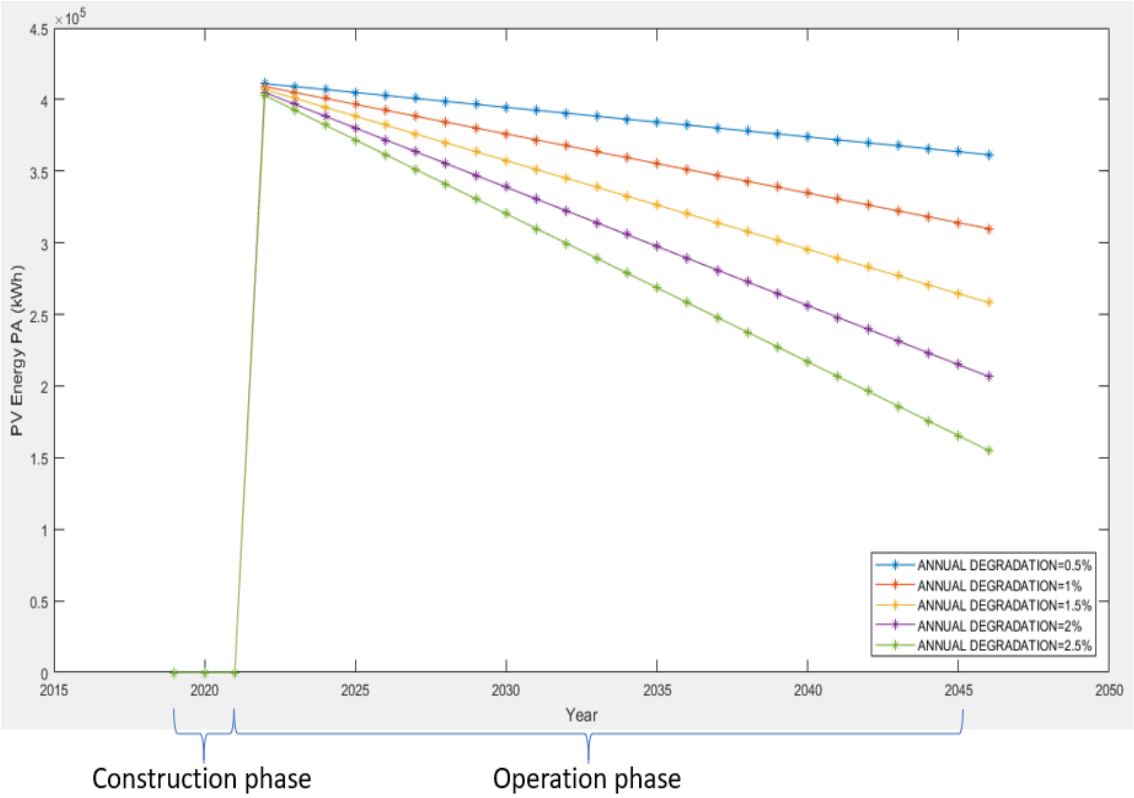

Figure 4-20: Annual energy over lifespan of project at varying degradation rate

4.3.6 Economic analysis

The economic analysis panel gives the economic implication of a PV project and assesses the profitability or otherwise of the project using a NPV economic appraisal technique. Figure 4-21 shows the cost implications for the designed solar PV system to supply about 1,077.9 kWh of energy per day to a village in the North-eastern Nigeria. In carrying out cost calculations, the current cost of components in the markets were considered. The total costs of all major components are presented in Figure 4-21. The net present value of the plant for

estimated lifespan of 25 years is $876.9 million. The levelized cost of energy as shown in Figure 4-21 is $0.0812/kWh. This is in line with the 2019 report of International Renewable Energy Agency. IRENA (2019) stated that solar PV projects commissioned in 2018 had a global-weighted-average LCOE of $0.085/kWh. This LCOE according to IRENA (2019) is around 13% lower than the equivalent figure for 2017 and that the value has fallen by 77% between 2010 and 2018.

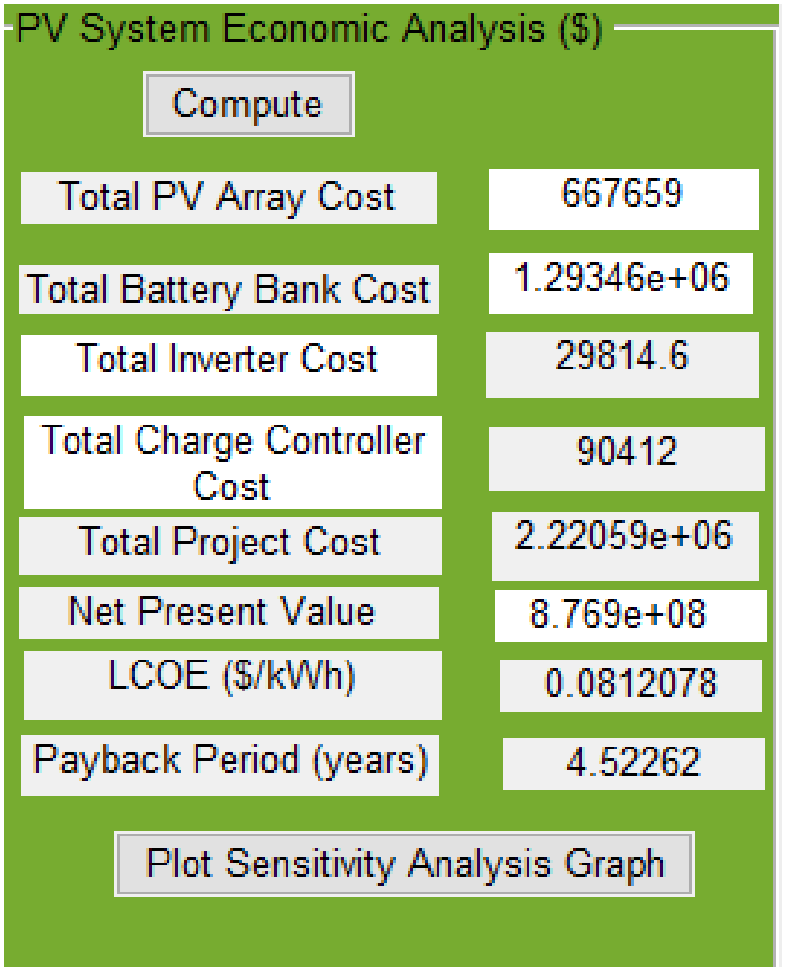

Figure 4-21: Economic analysis panel output

Figure 4-22 shows the graph of annual present value against the year operation with the sensitivity analysis based on varying discount rates. The sensitivity analysis shows that the annual present value of the system increases from the year of commission to the 17th year of operation and then a decline sets in for discount rate of 5% while decline begins at year 7 of operation for discount rate

of 10% (Figure 4-22). During the 1st year of operation, the NPV for a discount rate of 5% is $1.048 million while $0.7285 million for 15% discount factor which gives a 30.5% reduction in NPV. It can be noted there is a downward trend of the annual present value during the construction/installation years, this is because during these years, the cash inflow is obviously zero and therefore the present value which a discounted difference cash inflow and outflow over the lifespan of the plant is negative.

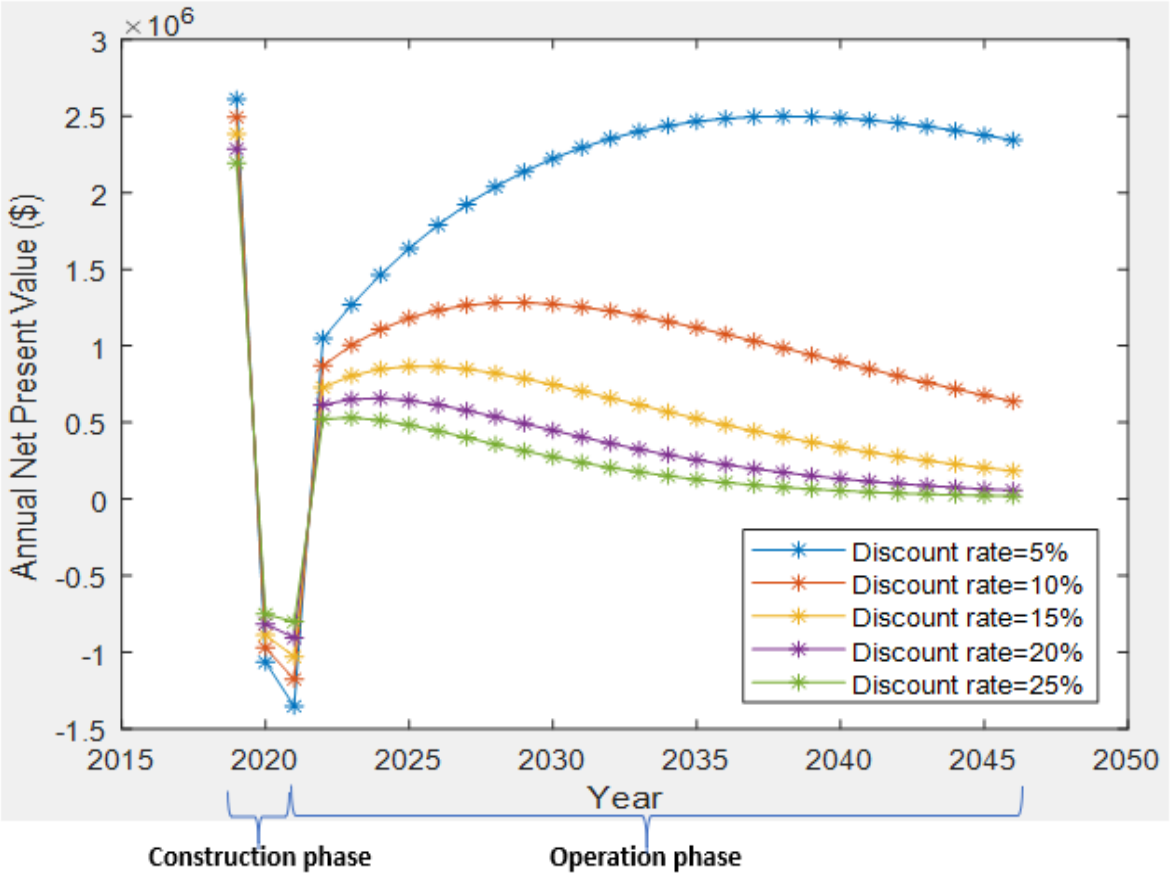

Figure 4-22: Annual present value over years of operation

Figure 4-23 shows the discount factor over the years of operation. At low discount rate the discount factor is high. For a discount rate of 5% during the first year the discount factor is 0.9524 while for discount rate of 15% for the same year is 0.8696. This amounts to about 8.6% drop in discount factor.

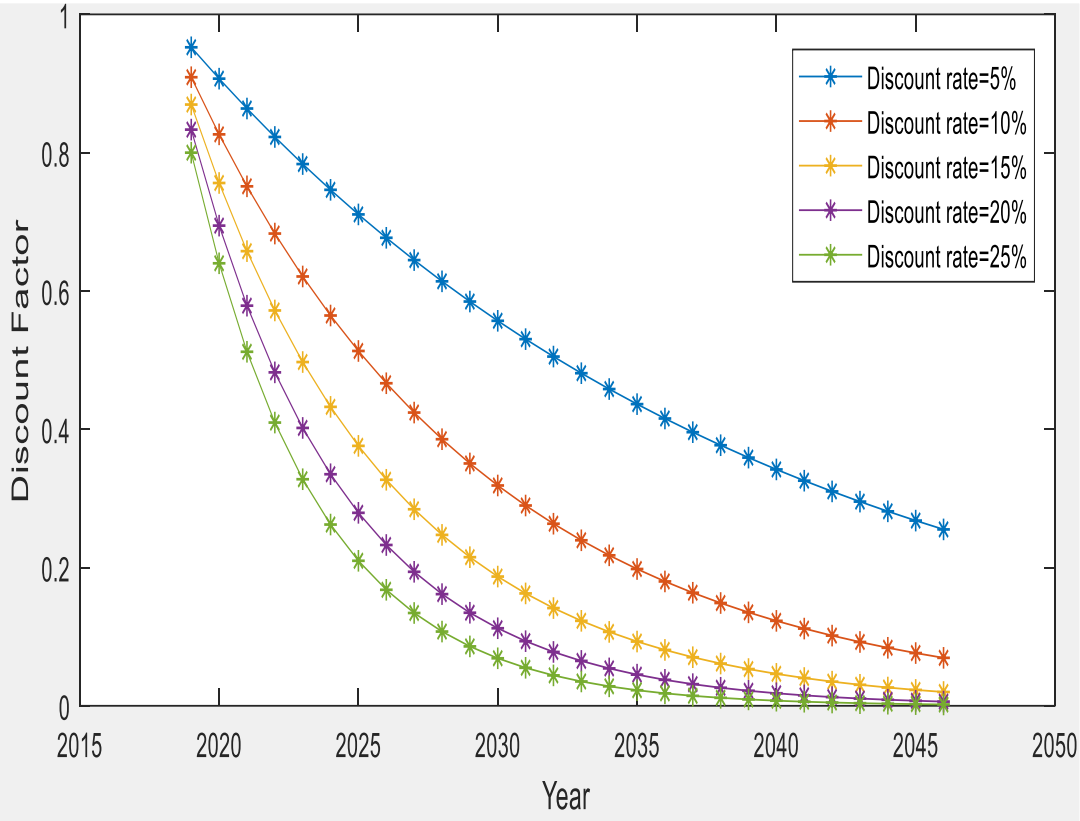

Figure 4-23: Discount factor over years of operation

Figure 4-24 shows the entire SPVSM as the individual panels handling specific parts of the model are systematically linked. This is because of the interdependencies in solar PV system components sizing.

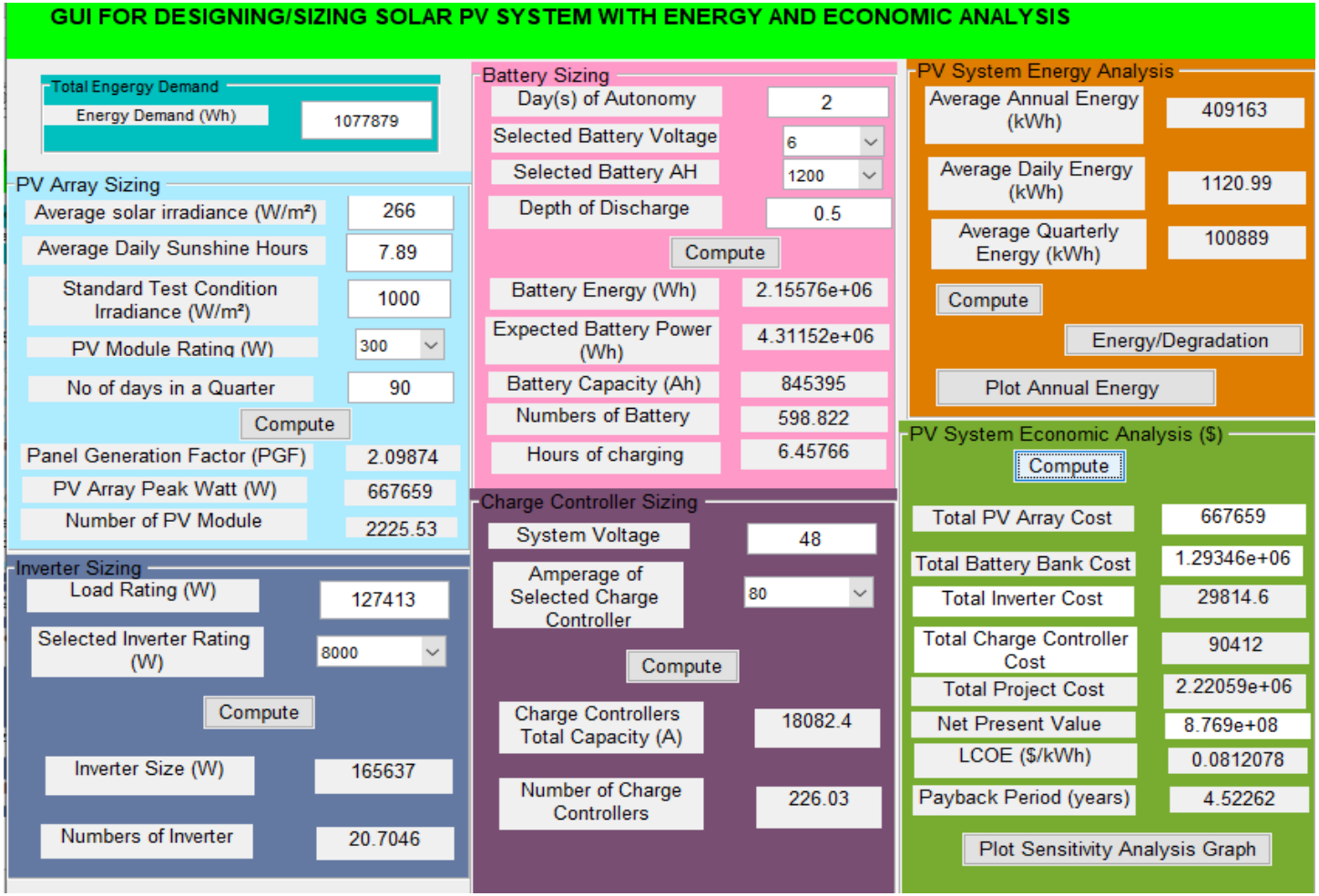

Figure 4-24: Solar PV system model

4.3.7 Financial cost benefit analysis

For the purpose of financial analysis, simulation was carried at minimum, maximum and average irradiances with panels of different peak watts. The effects of this on various parameters of cost are presented in Figure 4-25 to Figure 4-28.

Figure 4-25 shows the variation in total project cost with solar irradiance and for different solar panels. At the minimum irradiance of 78 W/m^2, the total project cost when 50W panels is used is $4.812440 million which is about 12.3 % higher than when 300 W panel is used. As the irradiance increases, the difference in total project cost diminishes. At the maximum irradiance of 376 W/m^2 the total project cost for the usage of 50 W panels is $2.099900 million which is just 5.8% high than for the use of 300 W panels.

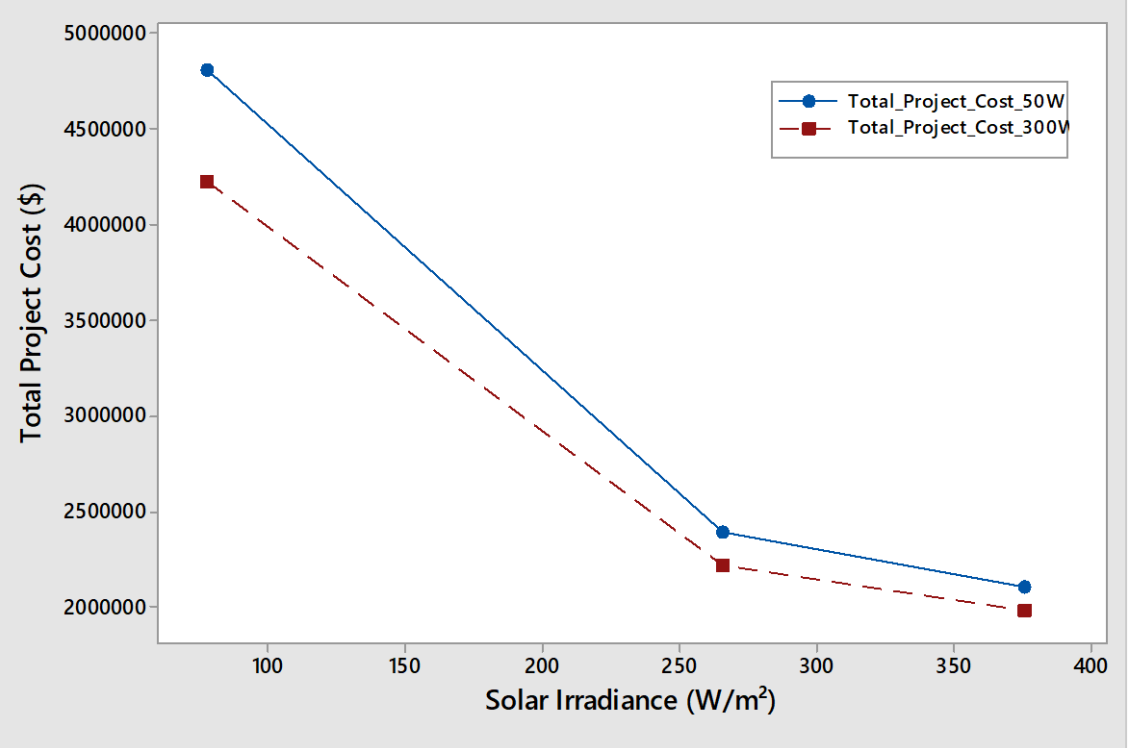

Figure 4-25: Total project cost versus solar irradiance

Figure 4-26 shows the variation in the number of modules against solar irradiance for different module wattages. At an average solar irradiance of 266 W/m^2, the total number of modules required is 2226 when 300 W modules are used, while the required number is 13354 when the use of 50 W module is employed. This constitutes a huge percentage difference of about 83.3%. This is obviously responsible for the cost variations.

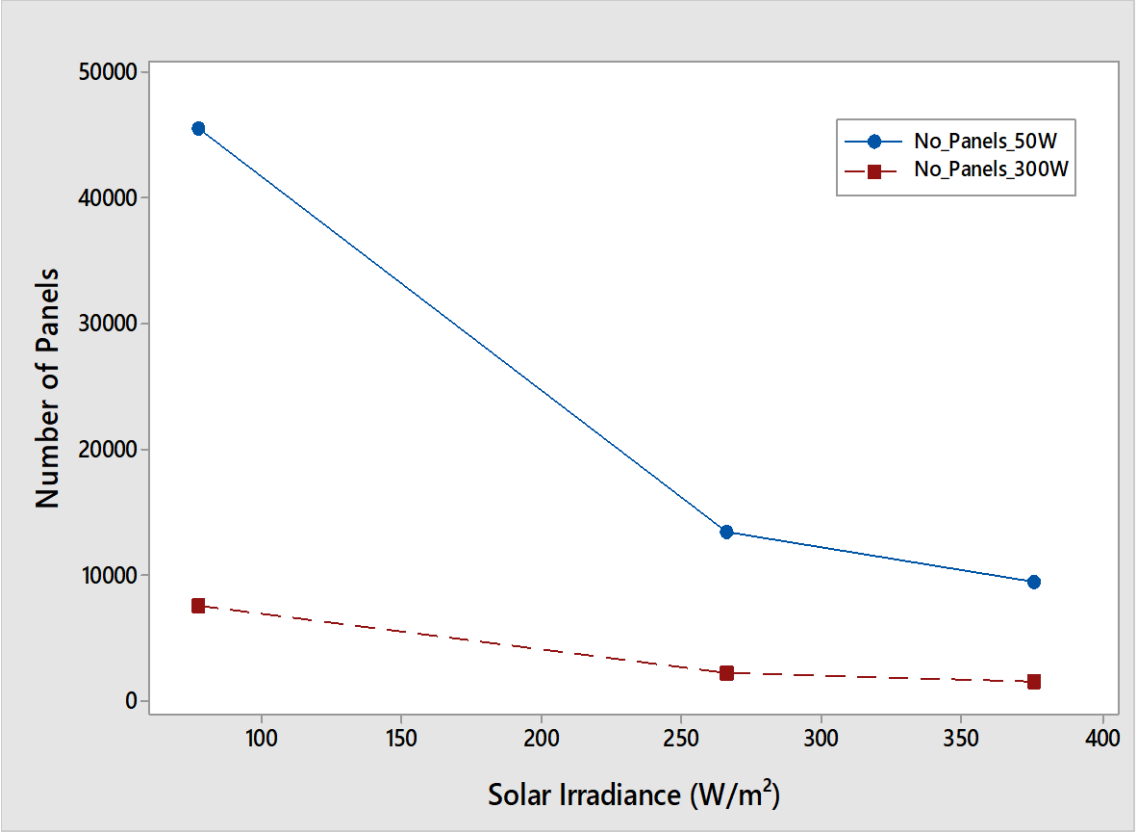

Figure 4-26: Number of modules versus solar irradiance

Figure 4-27 shows the effect of varying solar irradiance and different module wattage on the levelized cost of electricity. For average solar irradiance of 266 W/m^2, the LCOE is 0.081 $/kWh for the use of 300 W modules and 0.088 $/kWh for the use of 50W modules. This is about 7.9% increase in LCOE. A difference of about 6.5% exist between the usage of the two modules (50W and 300W) for maximum solar irradiance of 376 w/m^2.

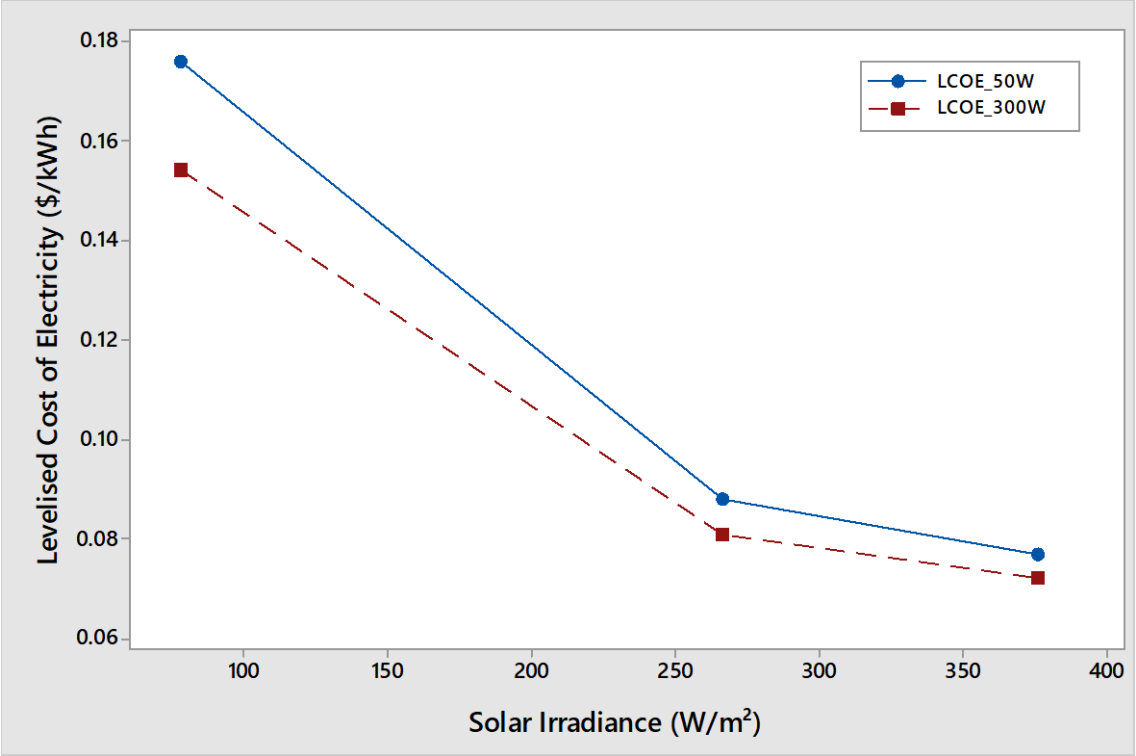

Figure 4-27: Levelized cost of electricity

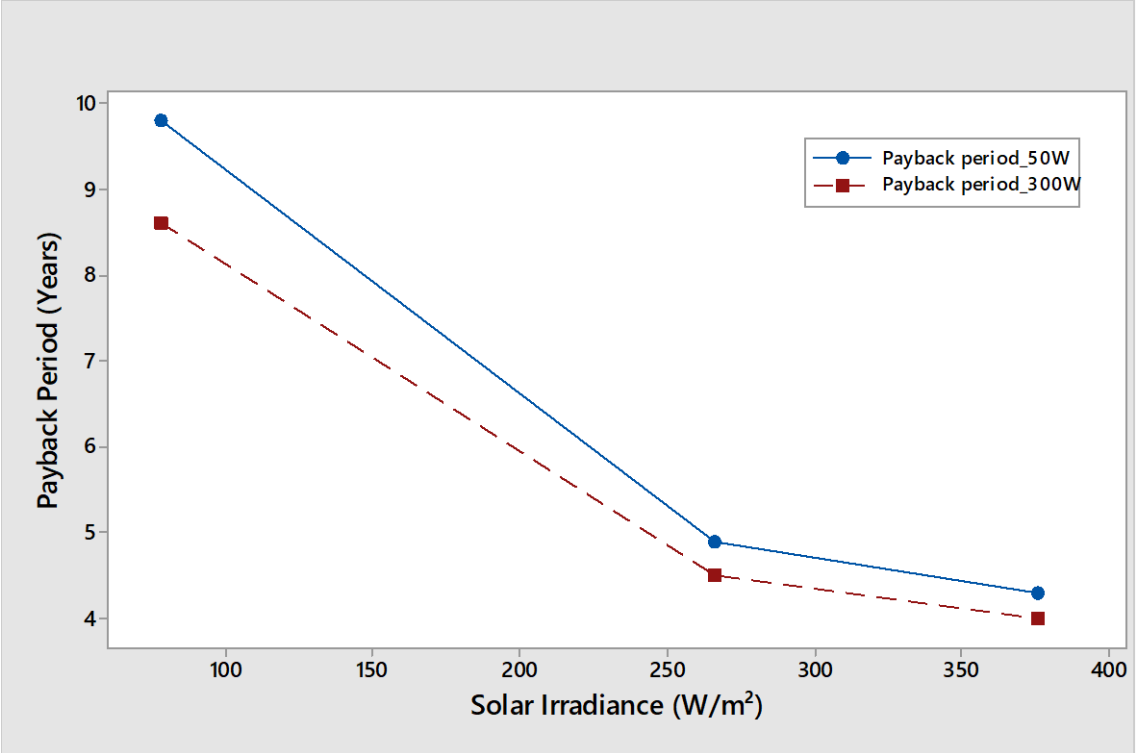

Figure 4-28: Payback period against solar irradiance

Figure 4-28 shows the payback period of the solar PV system against irradiance for the two different modules. At the minimum irradiance, the payback period for the usage of 50 W module is 9.8 years while for the same irradiance the payback period when 300 W modules are used is 8.6 years. Payback period for solar PV system is affected by the amount of solar energy available in the location, cost of the system and how the project is financed.

Figure 4-29 shows a sub-model which was developed to conduct energy analysis for a 50 W panel during different seasons in Nigeria and United Kingdom (UK). The energy generated by a 50 W panel with respect to minimum, maximum and average irradiances for each of the seasons is plotted in Figure 4-30 to Figure 4-33 for Nigeria and UK, respectively.

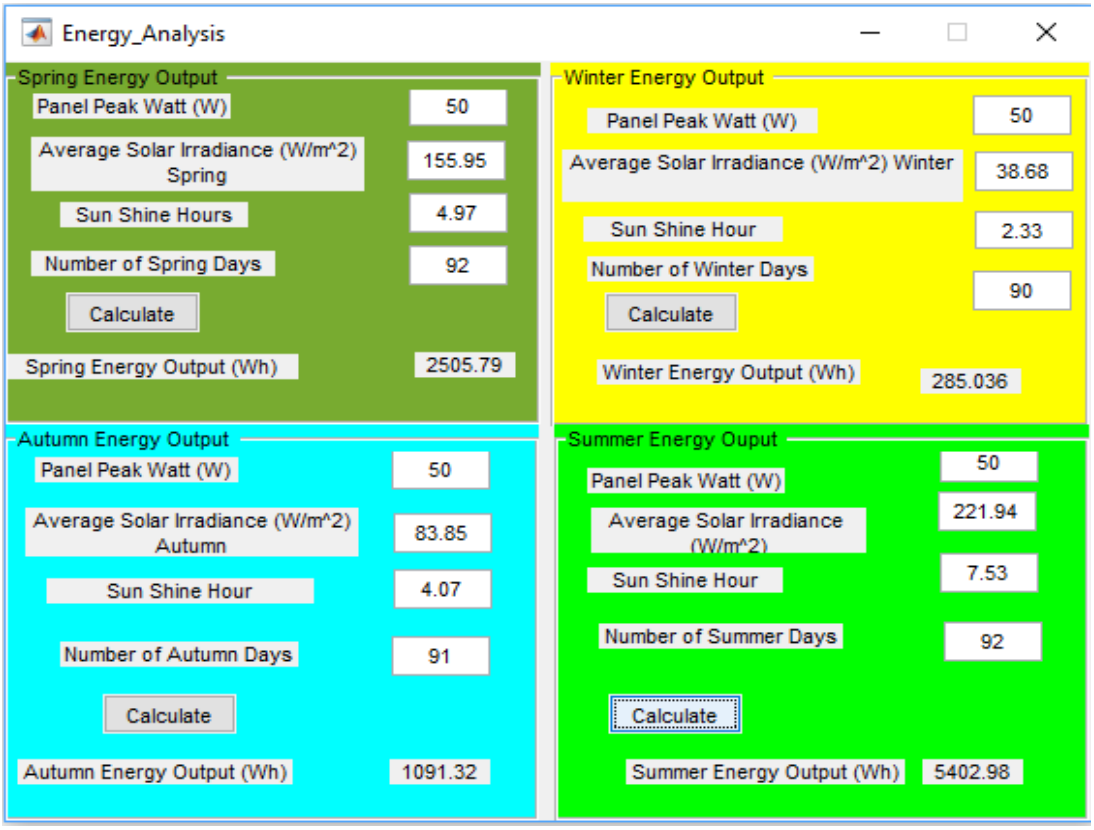

Figure 4-29: PV Energy Analysis sub-model

Figure 4-30 shows the energy output of a 50 W panel during the two distinct seasons (Wet and Dry) in Nigeria. The amount of energy a solar panel can generate depends on the solar irradiance and sunshine hour available during the period and on the number of days in the season. The energy generated during the wet season for minimum, average and maximum irradiance is higher than for the corresponding energy generated during the dry season even though there are generally higher solar irradiance and sunshine hours during the dry seasons. This is because the number of days of wet season is 214 and for dry season is 151 days. For a fair comparison of the two seasons, the energy generated per day of each of the seasons are presented in Figure 4-31.

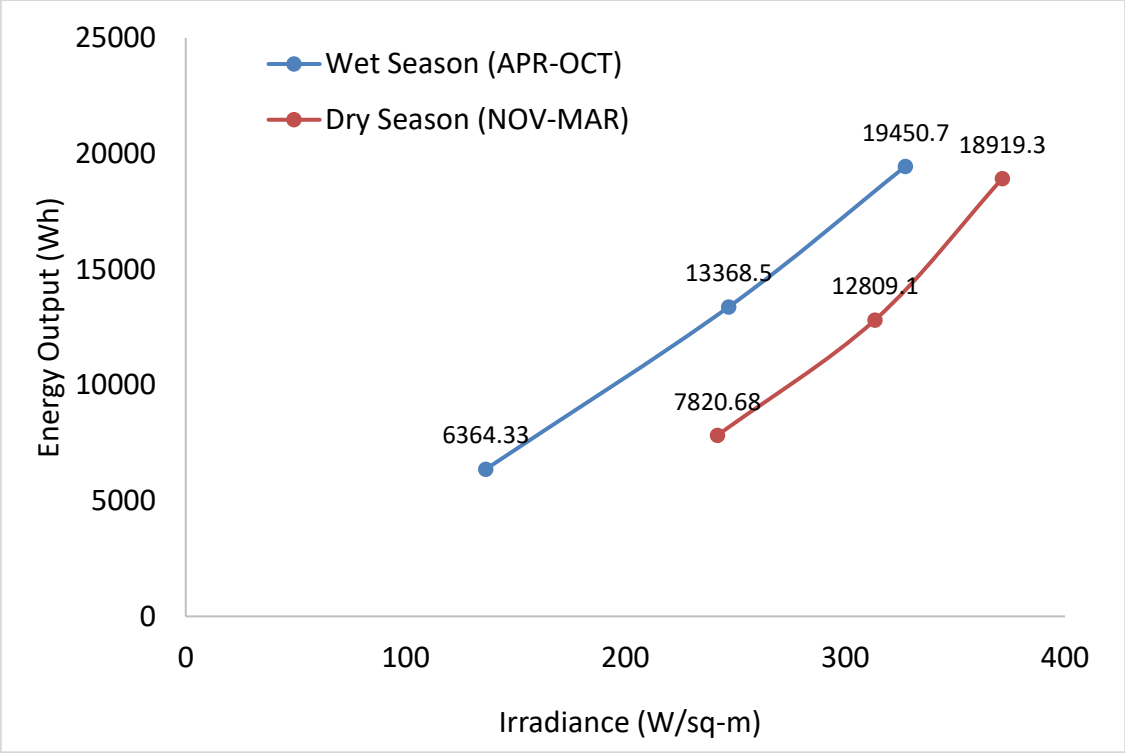

Figure 4-30: Energy Output of a 50 W Panel vs Solar Irradiance for the two Seasons in Nigeria

Figure 4-31 shows that for minimum irradiance for the two seasons, the energy generated per day in the dry season is about 46.2% higher than daily generation

in the wet season. This shows higher prevalence of solar irradiance and sunshine hours during the dry season.

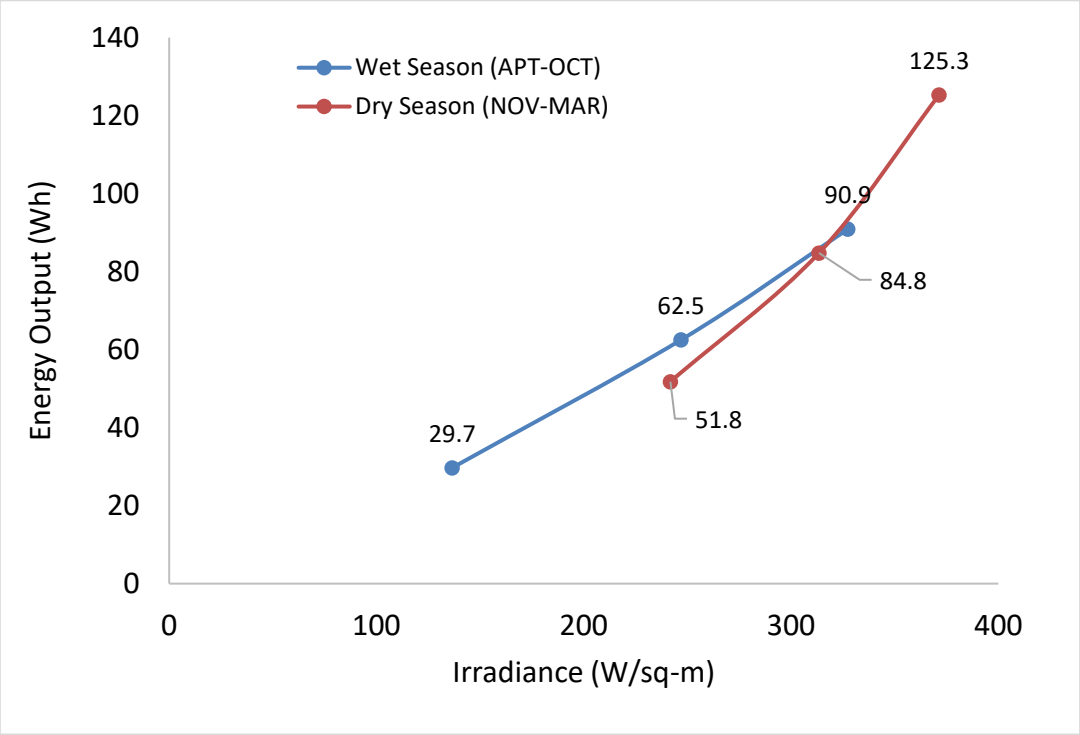

Figure 4-31: Energy Output per Day of a 50 W Panel vs Solar Irradiance for the two Seasons in Nigeria

Figure 4-32 and Figure 4-33 shows the energy output of a 50 W panel during the seasons in UK and on daily basis, respectively. For minimum irradiance, the energy output during summer is 613.9 Wh which is about 93.8% higher than the energy output for winter. The difference in daily averages between spring and autumn for minimum irradiance is about 83.3%, with spring being higher.

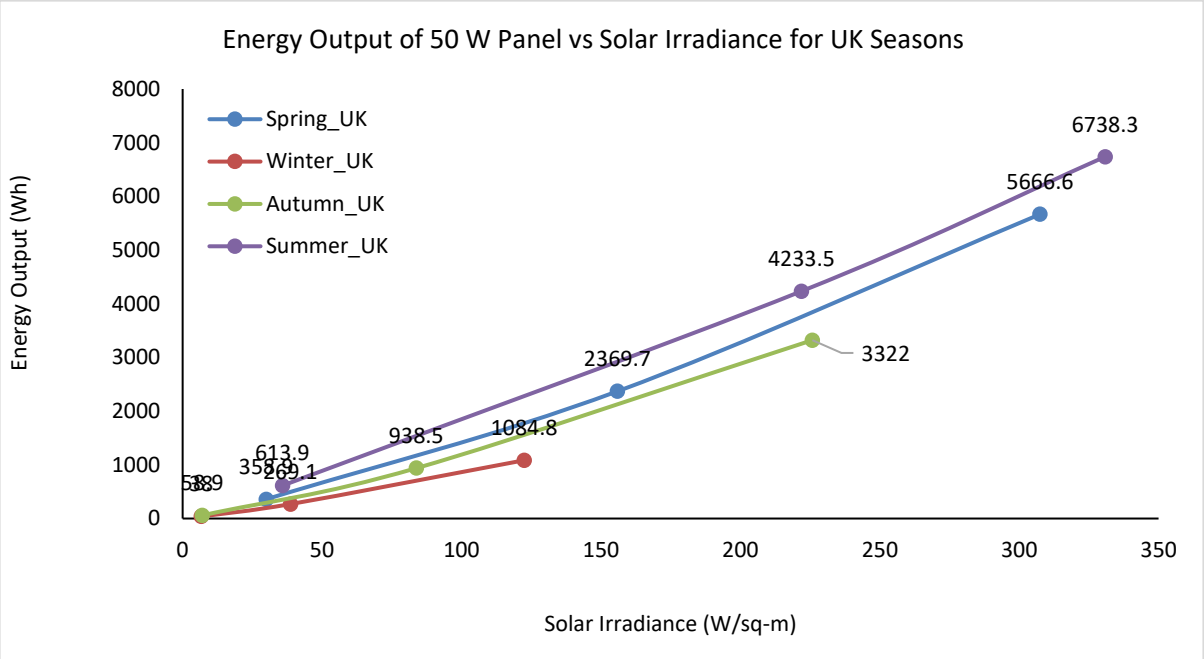

Figure 4-32: Energy Output of 50 W Panel vs Solar Irradiance for UK Seasons

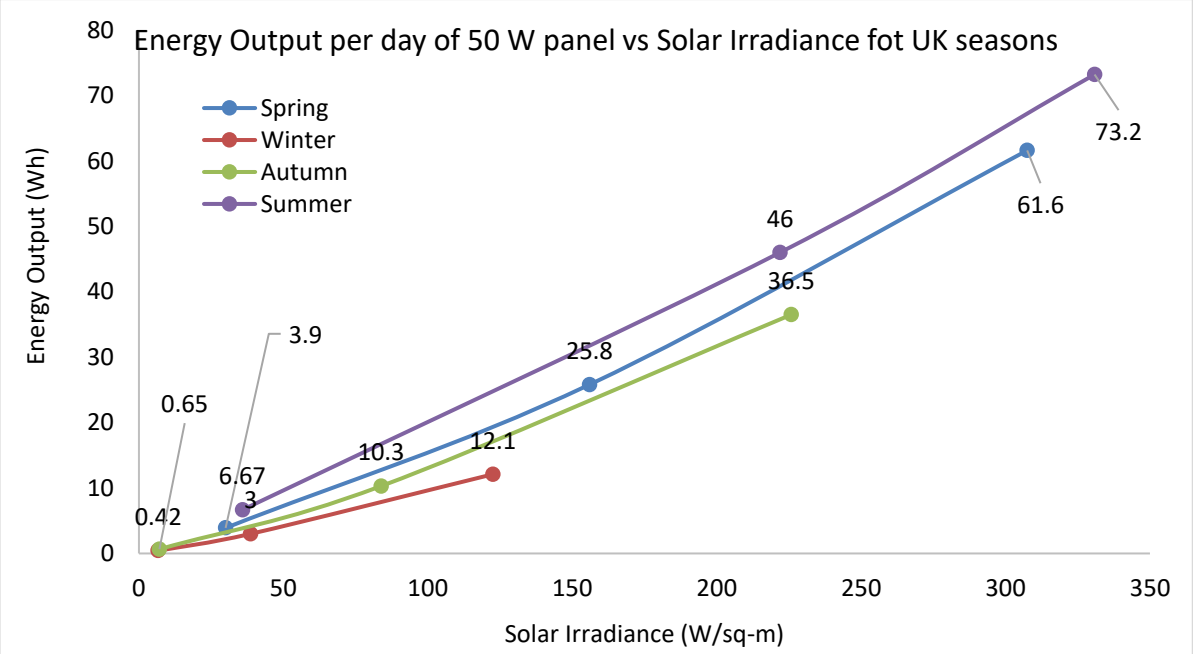

Figure 4-33: Energy Output per day of 50 W panel vs Solar Irradiance for UK seasons

4.4 Simulation and validation of I-V and P-V Characteristics

The results of simulation to obtain the I-V and P-V characteristics of a 50 W solar module at different irradiances is here presented in Figures 4-34 to 4-37.

Figure 4-34 shows the simulation and experimental results of I-V characteristic at 1000 W/m^2 irradiance. The simulation result shows that the maximum power point occurs at current of 2.67 A and voltage of 18.73 V which yields a maximum power output of 50.0 W. The experimentation to validate this simulation model gives the maximum power point to occur at the current of 2.62 A and voltage of 18.69 V which yields a maximum power of 48.96 W. The experimental and simulation are in good agreement as also presented by (Banu, Beniuga and Istrate, 2013; Aysha *et al.*, 2015; Boukili *et al.*, 2018).

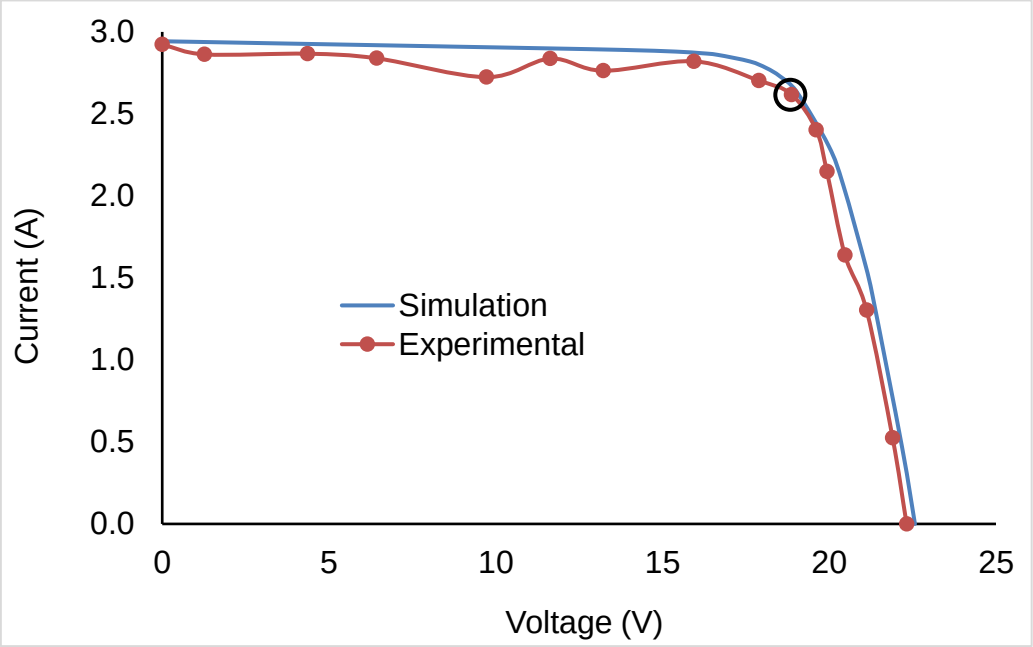

Figure 4-34: I-V Characteristics for a 50 W module at 1000 W/m^2 irradiance

This is about 2.08 % difference between the simulation and experimental results with the simulation result being higher. This difference is expected because in the simulation, the irradiance is set to 1000 W/m^2 and does not change throughout the simulation but during the experimentation, even though it was done within the

shortest possible time, the irradiance could not be set at 1000 W/m^2 as it is nature controlled.

Figure 4-35 shows the simulation and experimental results of P-V characteristic at 1000 W/m^2 irradiance. The maximum power is at the knee of the graph. This obviously is the same as described earlier with the I-V characteristic.

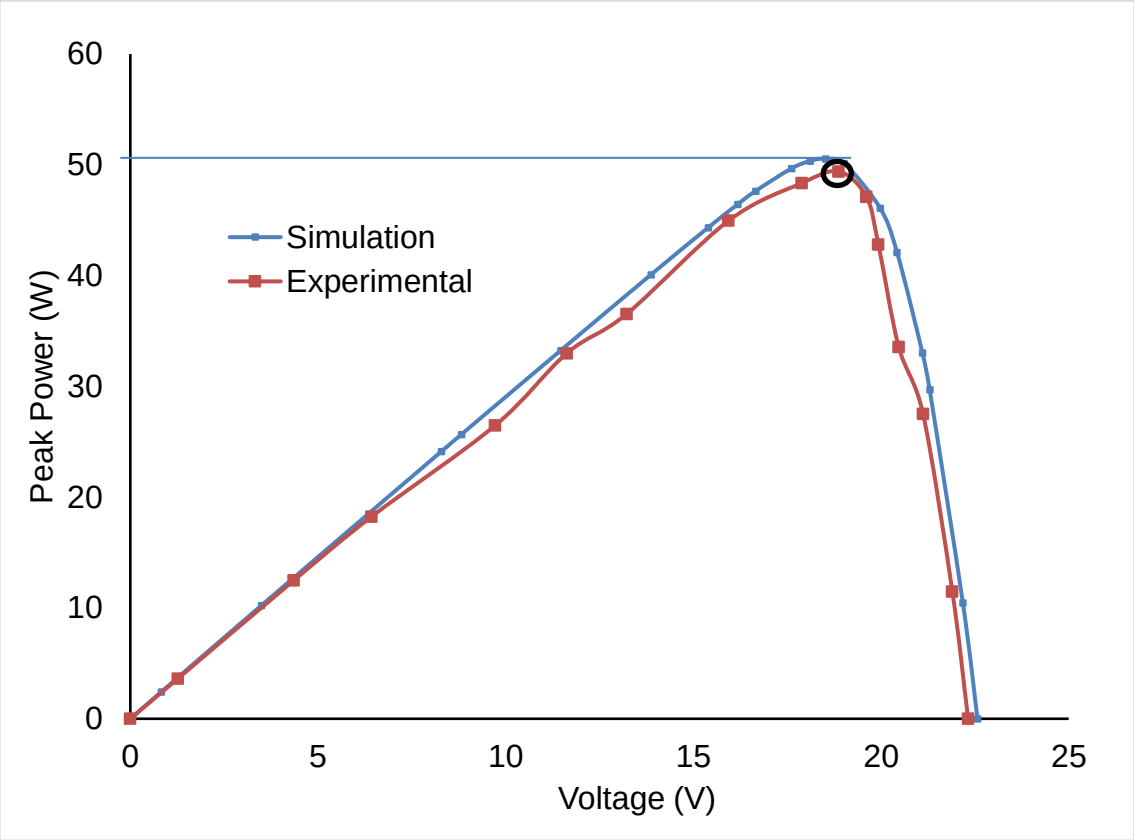

Figure 4-35: P-V Characteristics for a 50 W module at 1000 W/m^2 irradiance

Figure 4-36 shows the simulation and experimental results of I-V characteristic at 700 W/m^2 irradiance. The simulation result shows that the maximum power point occurs at current of 2.03 A and voltage of 16.94 V which yields a maximum power output of 34.4 W. The experimentation to validate this simulation model gives the maximum power point to occur at the current of 2.02 A and voltage of 17.22 V which yields a maximum power of 34.7 W. It can be noted in Figure 4-31 that the experimentation results have higher currents than the simulation results at some points, this is because during the experiment the solar irradiance was above 700

w/m^2 and therefore the solar module yielded more current than the set irradiance. The agrees with the findings of Aysha *et al.* (2015) The maximum power point obtained from the experiment is about 1.26% higher than the power obtained from simulation.

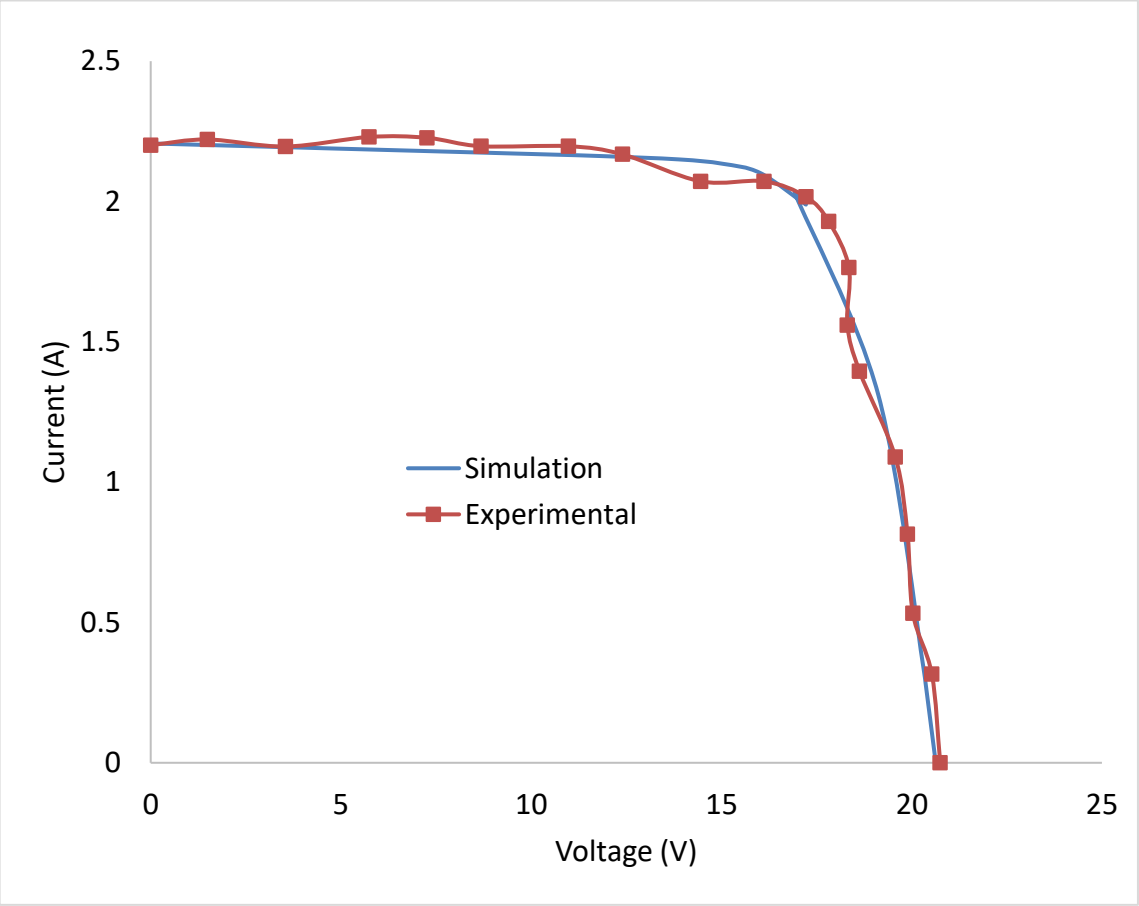

Figure 4-36: I-V Characteristics for a 50 W module at 700 W/m^2 irradiance

Figure 4-37 shows the simulation and experimental results of P-V characteristic at 700 W/m^2 irradiance. The maximum power is at the knee of the graph. The maximum power output for the simulation and experimental results are 34.2 W and 34.7 W, respectively. This has validated the simulation models.

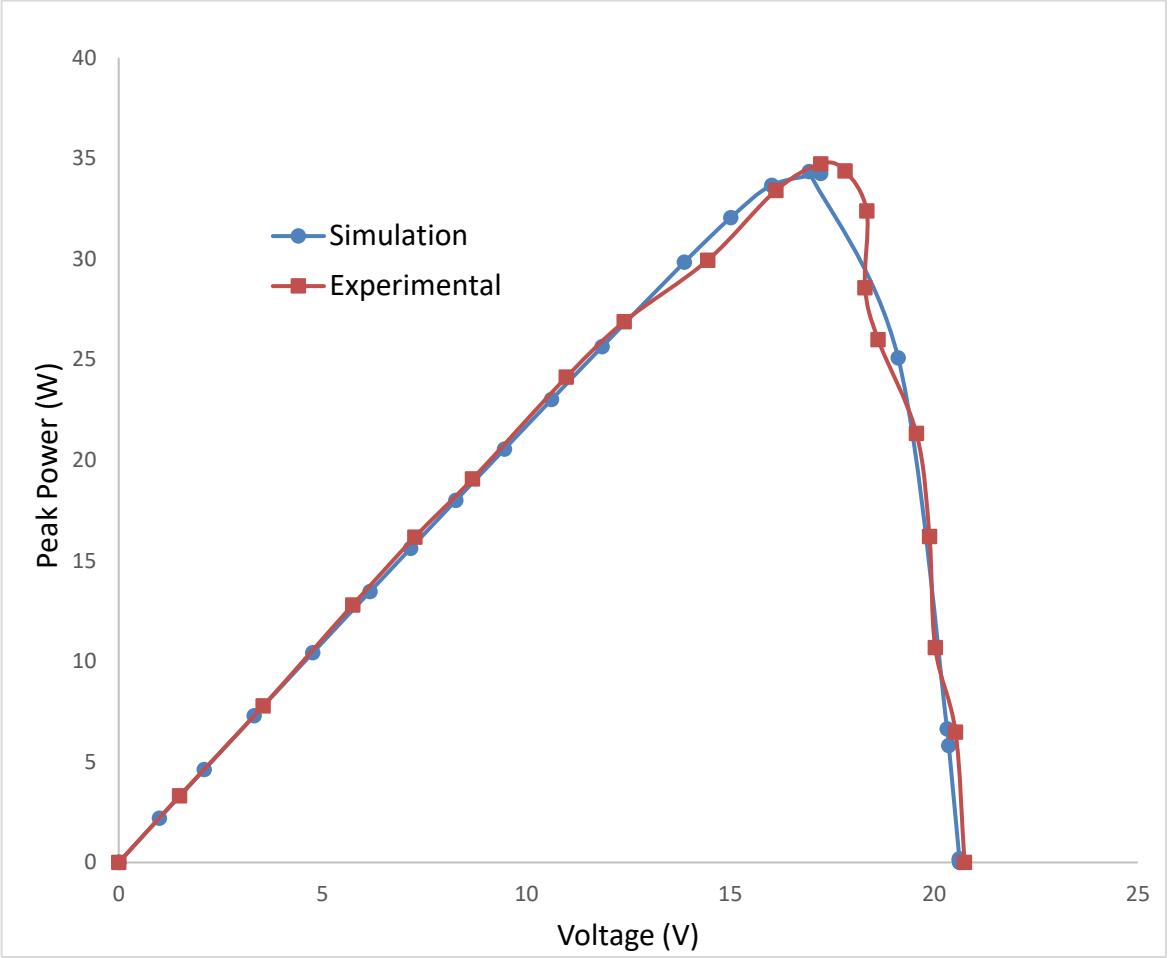

Figure 4-37: P-V Characteristics for a 50 W module at 700 W/m^2 irradiance

Figure 4-38 and Figure 4-39 shows the I-V and P-V characteristics for a 50 W module at irradiances of 800 W/m^2, 500 W/m^2 and 200 W/m^2. After validating the Simulink model, different simulations were carried out to study the effect of varying irradiance on the performance of solar photovoltaic module. As the irradiance increases the output current increases and this consequently yields increased power. This is agreement with the findings of Nasrin, Hassanuzzaman and Rahim, (2017), who concluded that increase irradiance increases the output of solar PV panels and also Musanga, Ligavo Margdaline *et al.* (2018). This is because as the irradiance falling on the module increases, more charges are generated, and the band gap energy reduces thereby forcing the electrons to jump into the conduction band which invariably constitutes an increase in current flow.

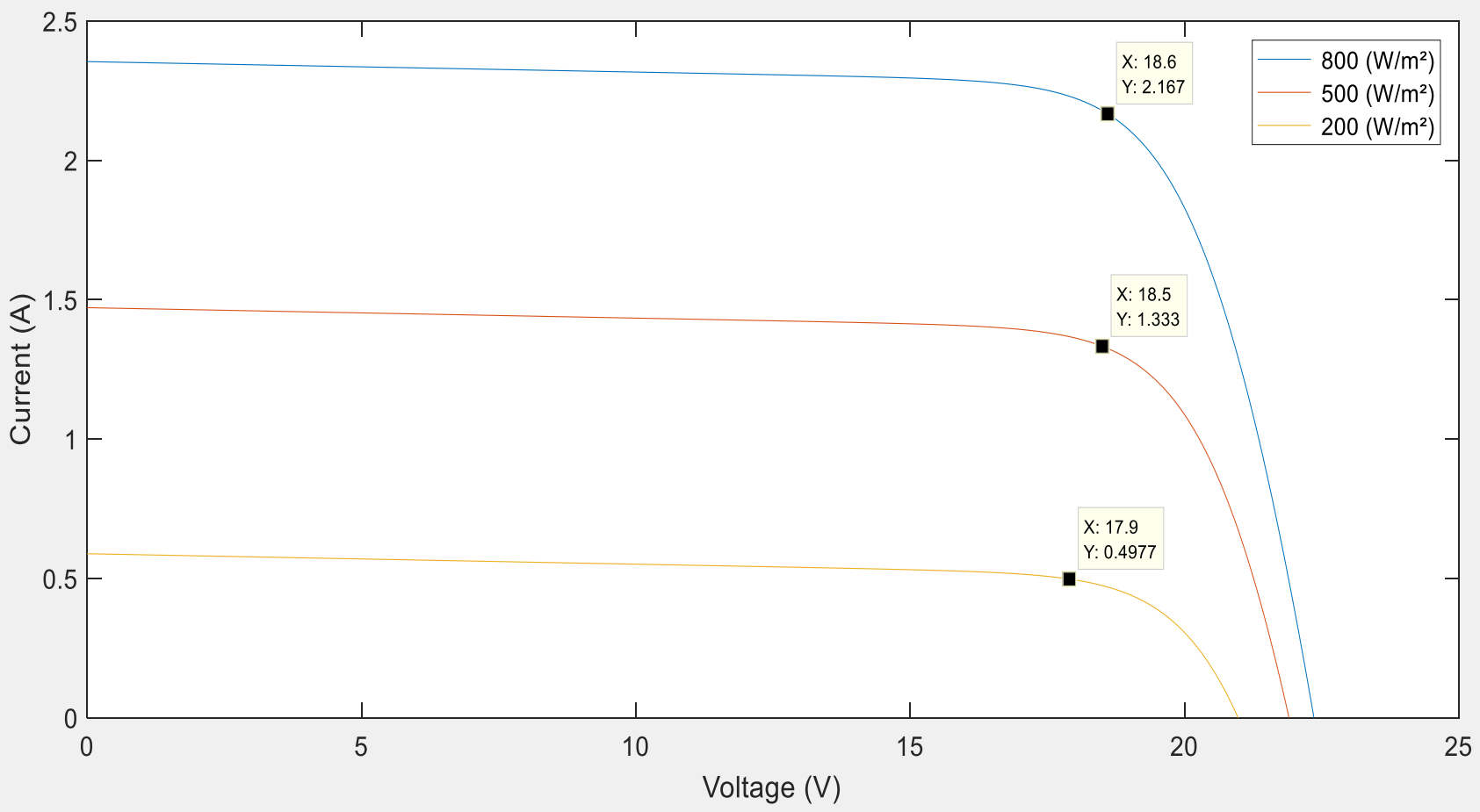

Figure 4-38: I-V Characteristics of a 50 W module with varying irradiance

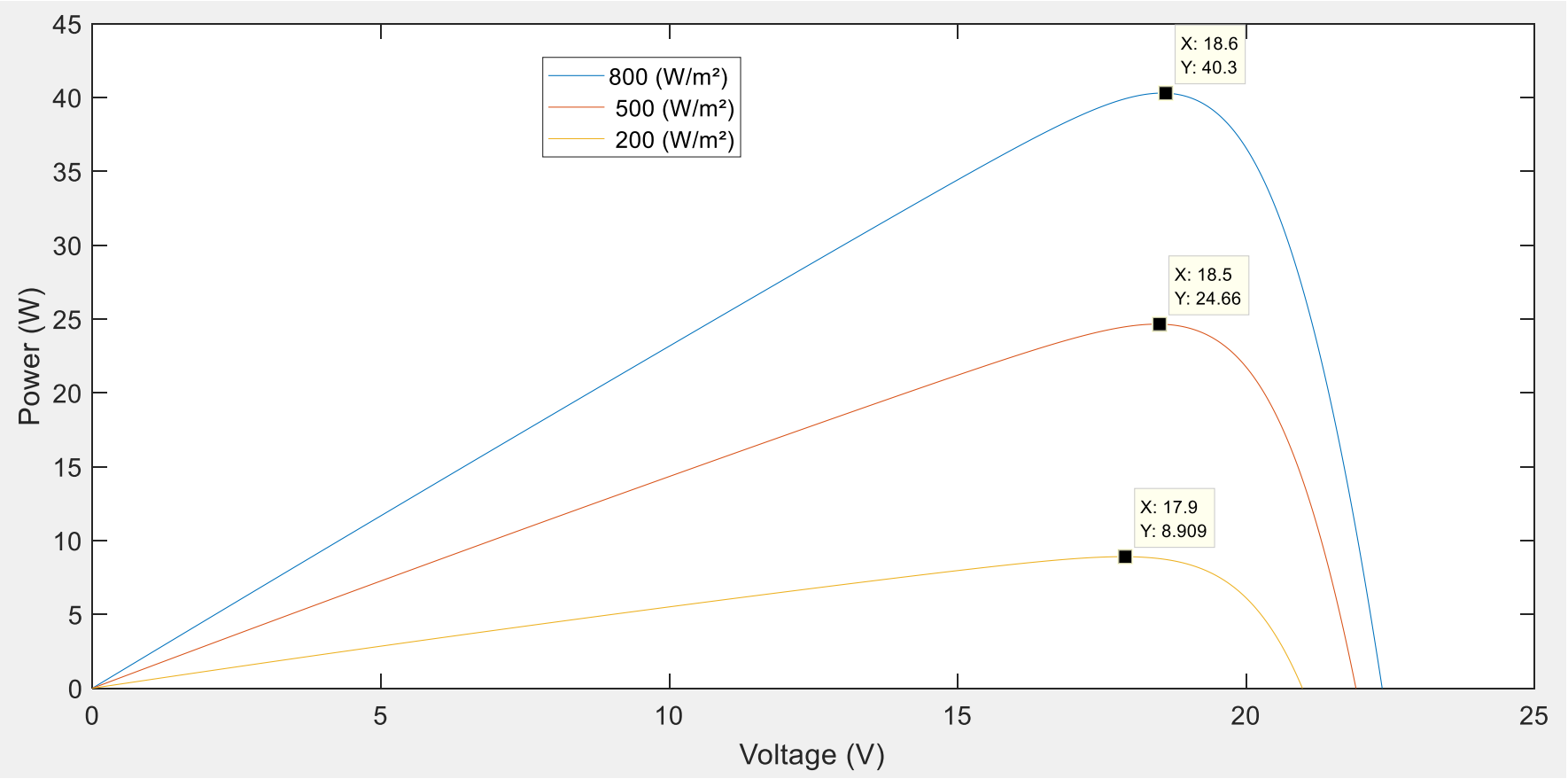

Figure 4-39: P-V Characteristics of a 50 W module with varying irradiance

4.5 Effect of Temperature on PV Performance

Like all other semiconductor devices, solar cells are sensitive to temperature. Increases in temperature reduce the band gap of a semiconductor, thereby affecting most of the semiconductor material parameters. The decrease in the band gap of a semiconductor with increasing temperature can be viewed as increasing the energy of the electrons in the material. Lower energy is therefore needed to break the bond. In the bond model of a semiconductor band gap, reduction in the bond energy also reduces the band gap. Therefore, increasing the temperature reduces the band gap.

In a solar cell, the parameter most affected by an increase in temperature is the open-circuit voltage and consequently maximum power output. This is in agreement with the findings of Musanga, *et al.,* (2018). The impact of increasing temperature is shown in the Figures 4-40 and 4-41. There is

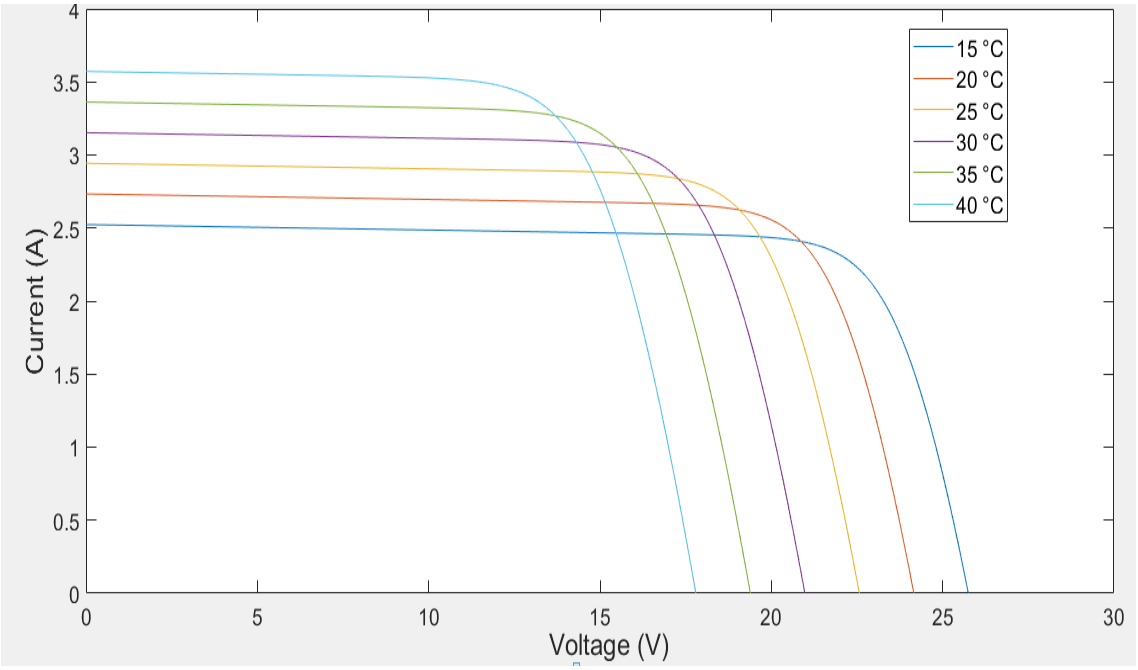

Figure 4-40: I-V Characteristics with varying temperatures

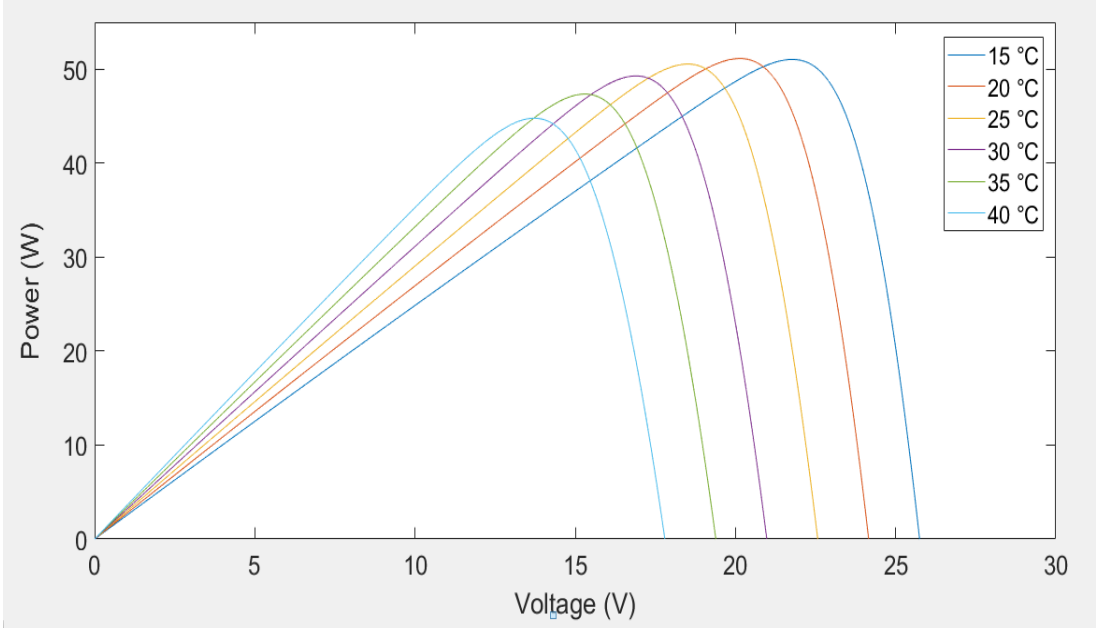

Figure 4-41: .P-V Characteristics with varying temperatures

4.6 Fill factor

The solar module that was used for all the experimentation has its key specification presented in Table 3-2 in Chapter Three. The 50 W module is model TDG-PV-T050M365. The parameters required to calculate the fill factor can be obtained from the Table. The fill factor is thus calculated as

$$Fill\ factor, FF\ = \frac{18.75 \times 2.690}{22.83 \times 2.940} \times 100 \quad \textbf{(4-4)}$$

$$Fill\ factor, FF\ = 75.15\% \quad \textbf{(4-5)}$$

The FF for this module is 75.15% and it falls between the range of FF for solar PV module which is

Table 4-15: Key specifications of TDG-PV T050M365

S/N	PARAMETERS	SYMBOL	VALUE
1	Rated maximum power	P_{max}	50W
2	Voltage at maximum power	V_{mp}	18.75V
3	Current at maximum power	I_{mp}	2.690A
4	Open-circuit voltage	V_{oc}	22.83V
5	Short-circuit current	I_{sc}	2.940A
6	Operating temperature	T_c	-40^{o}C to +85^{o}C
7	Cell Technology	Mono-Si	
8	Weight	W_c	4.0 kg
9	Dimension		554X636X30 mm

4.7 Maximum power point tracking

A photovoltaic module converter's duty cycle is generated through P&O algorithm in the embedded system function block (Figure 3-14 – Chapter 3). The simulation results of output power of the photovoltaic module for different solar irradiances (1000 W/m^2 and 800 W/m^2) and at constant temperature (T= 25^{o}C) are shown in Figure 4-40 and Figure 4-41. The output power reduced from 50.09 W for solar irradiance of 1000 W/m^2 to 37.9 W/m^2 for irradiance of 800 W/m^2.

From the various simulation results for different solar irradiance at constant cell temperature, it is clear that output power of the PV module increases with increasing solar irradiance Nasrin, *et al.* (2017) Musanga, *et al.,* (2018). The results of the output power of the PV module for simulation with different temperatures and at a constant solar irradiance of 1000 W/m^2 are presented in Table 4-15. The results show a slight reduction in the PV max power output with an increase in temperature from 25^{o}C which is the designed point temperature. Below 25^{o}C an increase in max output power is seen.

Table 4-16: PV Module MPP at different temperatures

S/No.	Temperature (ºC)	PV Max. Power Output (W)
1	20	50.98
2	25	50.12
3	30	49.12
4	35	48.06
5	40	46.74

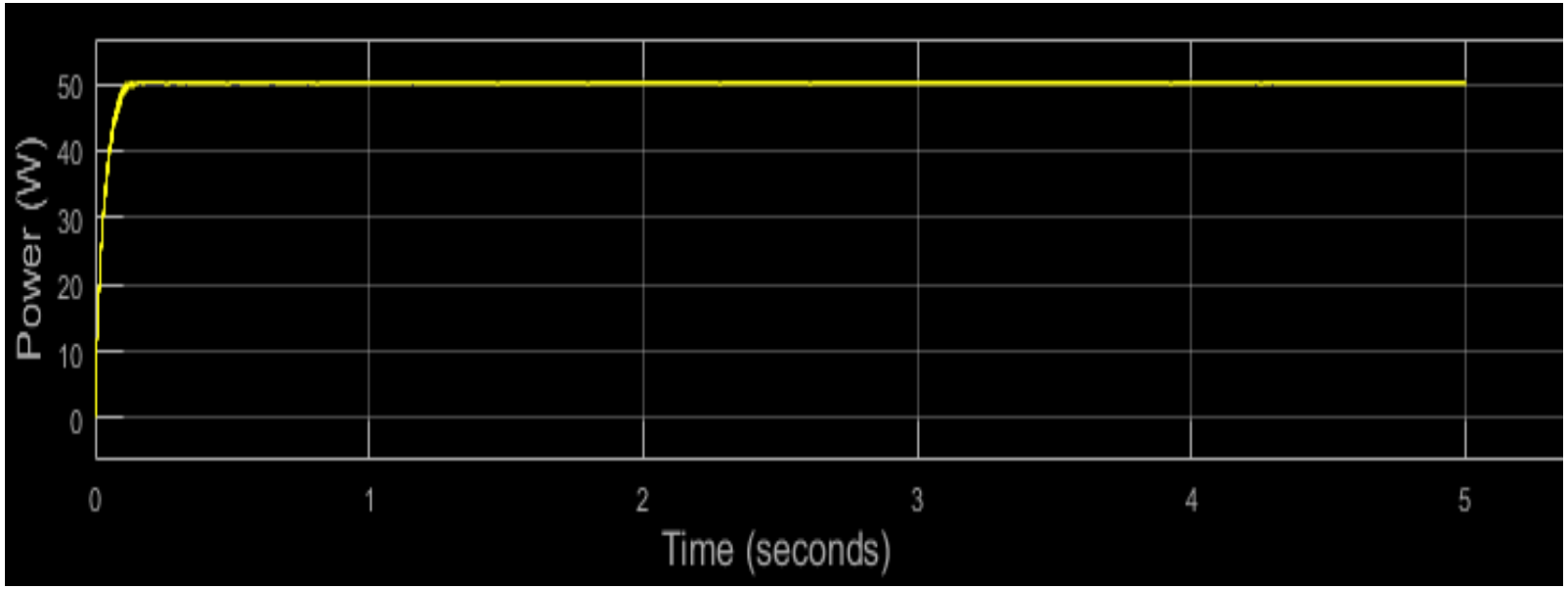

Figure 4-42: Maximum power at 1000 W/m^2 for a 50 W module

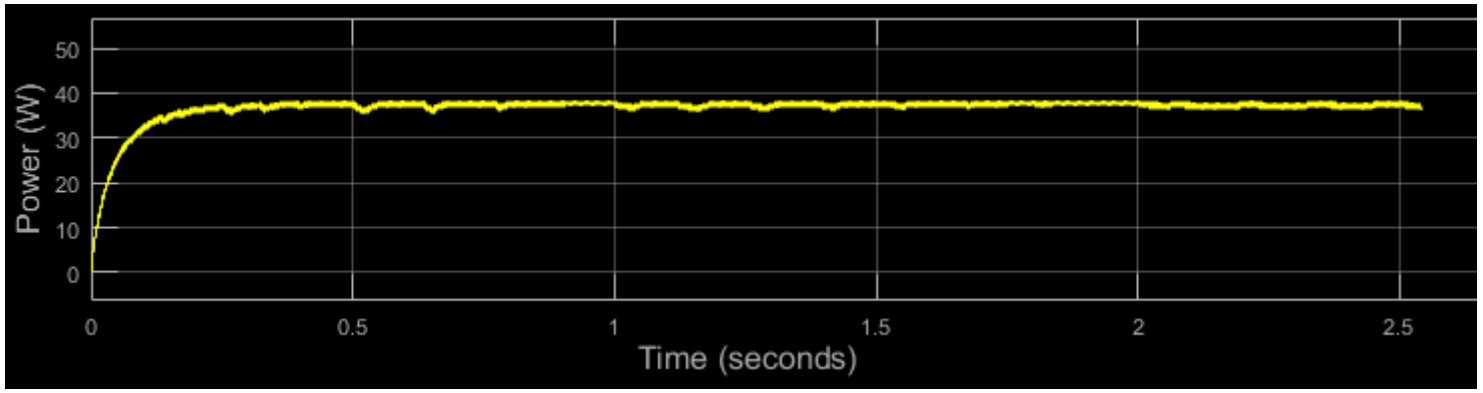

Figure 4-43: Maximum power at 800 W/m^2 for a 50 W module

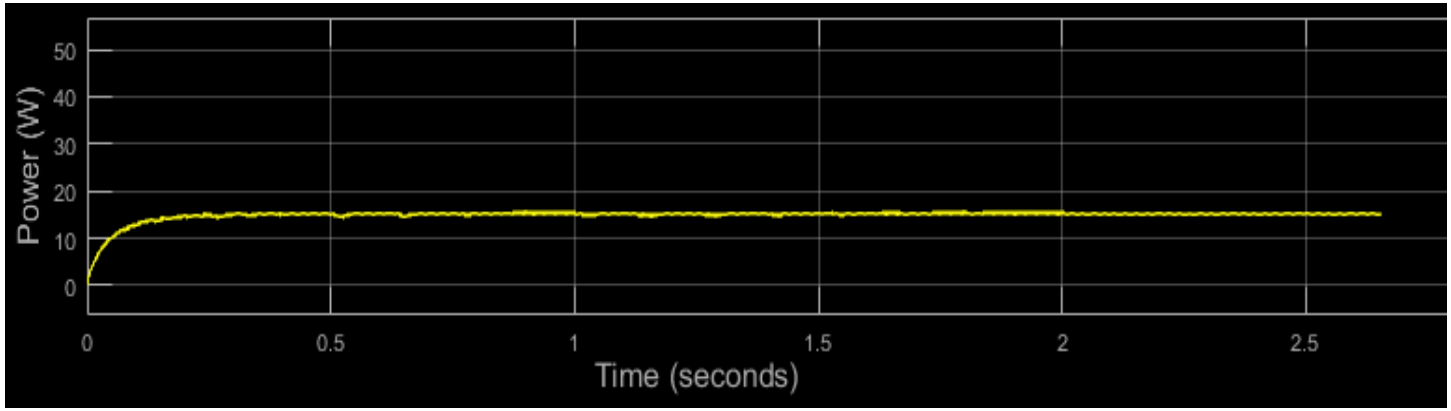

Figure 4-44: Maximum power at 500 W/m2 for a 50 W module

4.8 Results from Fieldwork on Impact of dust on PV Performance

Figure 4-43 shows the time series plot of peak power output of the 50 W module for the 14 days of the experiment. Because the output power depends on the irradiance at any time, the time series plot shows a rise in power from the morning hours and reaching a maximum during the afternoon of each day. The effect of dust accumulation over the 14 days of the field work can be seen in the reduction in power output by the day as shown in Figure 4-43. Day 1 recorded the maximum power output of about 50 W at 14:00 hours and day 14 recorded the lowest power output of about 20.5 W. There was over 50% drop in power output during the period of the field work. This agrees with over 50% reduction in power as a result of dust accumulation on PV modules in Egypt presented by (Menoufi *et al.* (2017).

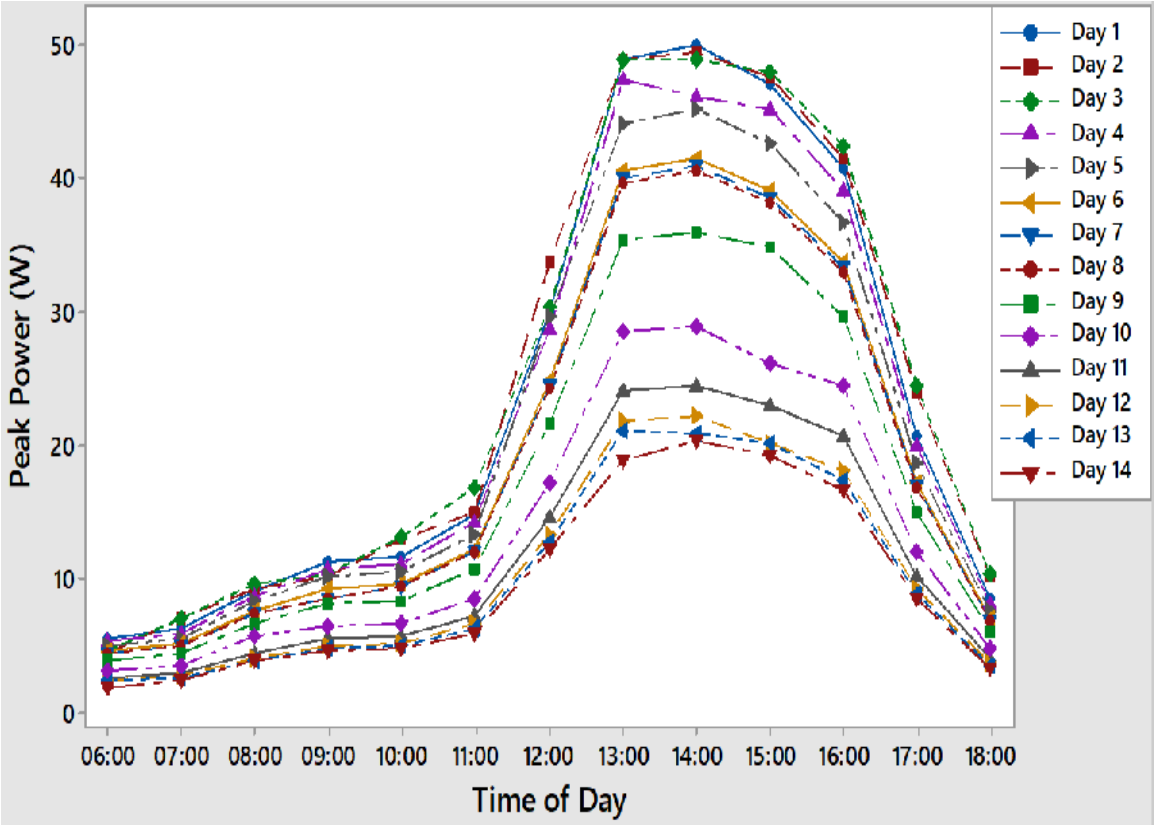

Figure 4-45: Time series plot of Peak Power for 14 Days

The reduction in the efficiency, as a result of a drop in performance owing to dust accumulation, was studied over the 14 days of the field work. Figure 4-44 shows the time series plot of peak power and efficiency during the 14 days. The highest efficiency of 17.1% was obtained on the first day and the least efficiency of 7.2% was obtained on the last day amounting to a 57.6% drop in efficiency. This drop in performance was as a result of the continuous deposition of dust on the solar module without cleaning for 14 days which is the basis for the study. This implies that during the peak dust period in Maiduguri, there is a high loss in performance in just two weeks. It is therefore necessary to clean solar modules at least once in every week to be able to maintain a reasonable reduction in efficiency. Sand dust obstructs illumination as it accumulates on the PV surface by scattering, absorbing and reflecting the incident light.

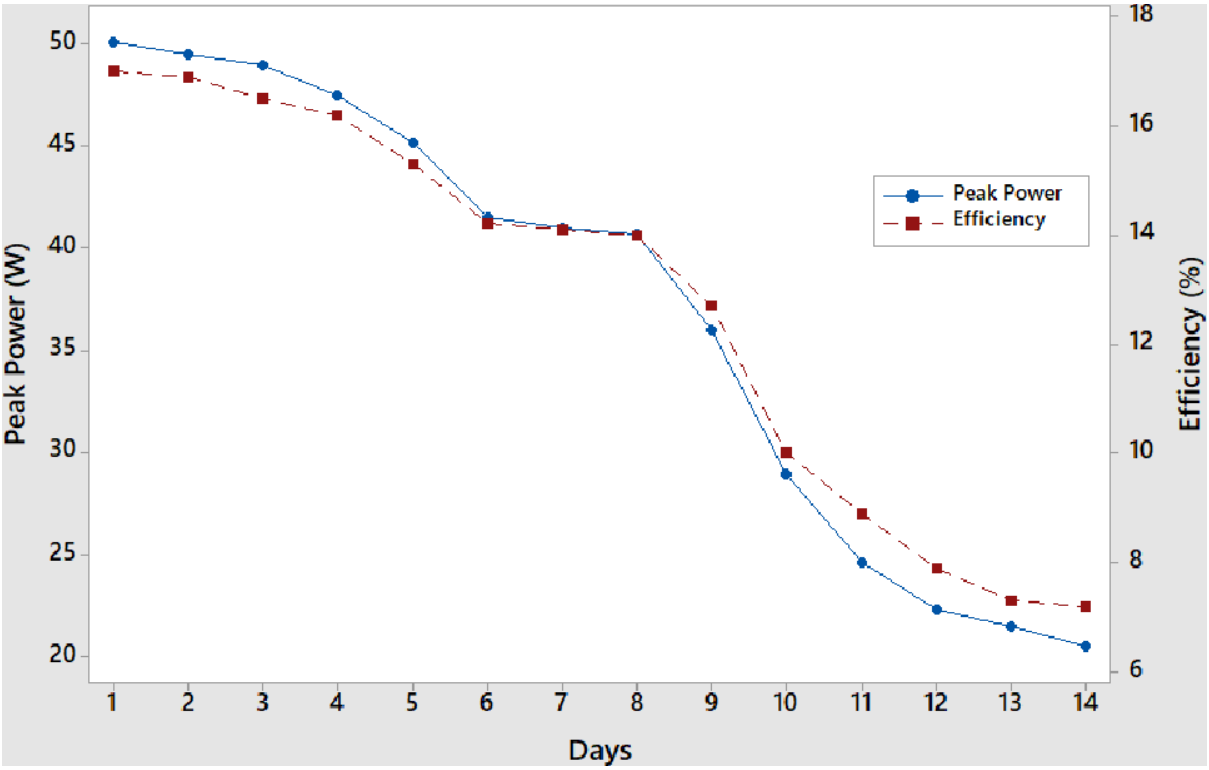

Figure 4-46: Peak Power and Panel Efficiency against Days

Figure 4-45 to Figure 4-48 shows the fitted regression line plots of peak power vs relative humidity for days 1, 5, 8 and 13 of the field experiments.

The fitted regression line indicates that a negative correlation exists between the two quantities. The coefficient of determination, R^2 shows that the regression line fits the relationship to about 71.2%, 78.3%, 79.1% and 72.4% for days 1, 5, 8 and 13 respectively. This can be attributed to the fact that high humidity causes reflection of solar irradiance in air thereby reducing the amount of irradiance reaching the panel and consequently reducing the performance. This agrees with the findings of Amajama and Oku (2016) who concluded that relative humidity has a negative correlation with voltage, current and consequently on power output of solar panel.

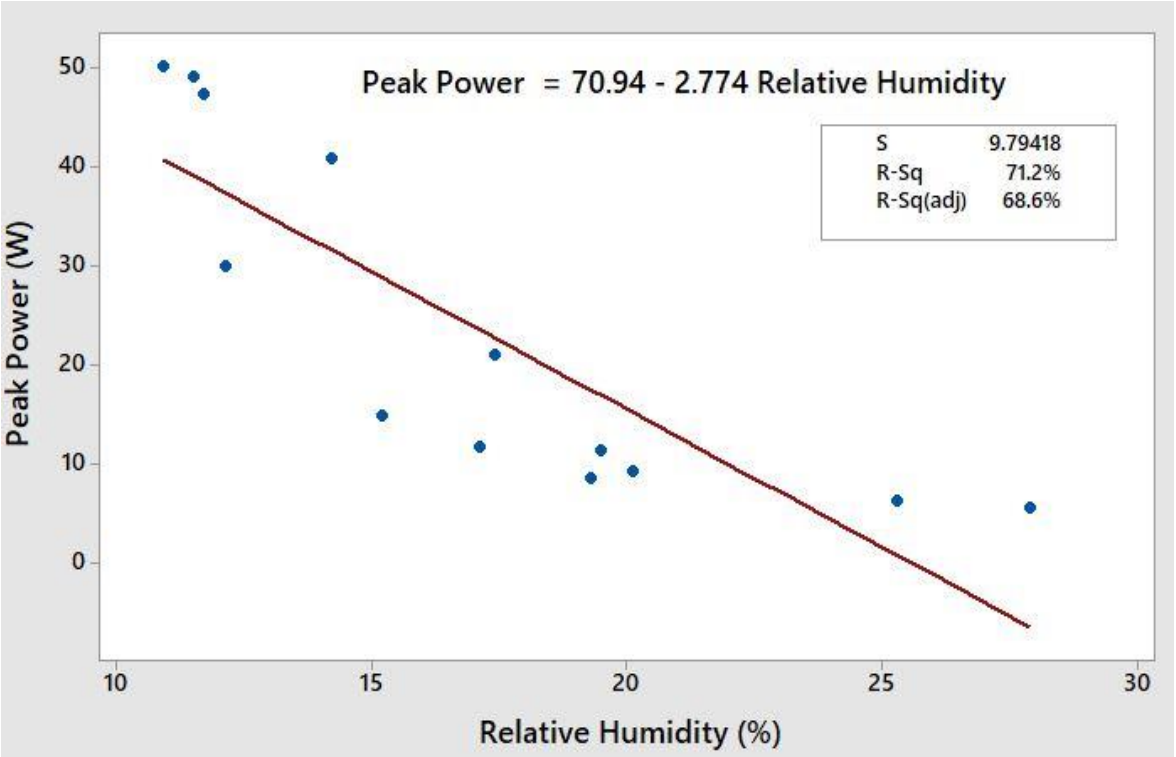

Figure 4-47: Fitted regression line plot for Peak power versus Relative Humidity (Day 1)

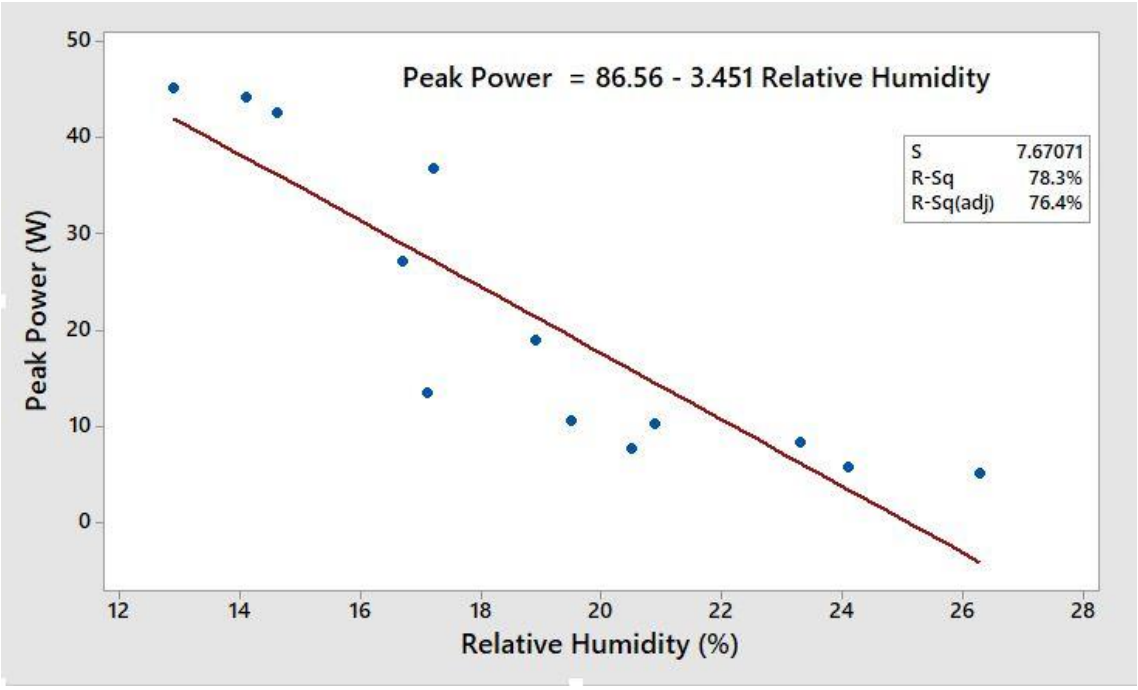

Figure 4-48: Fitted regression line plot for Peak power versus Relative Humidity (Day 5)

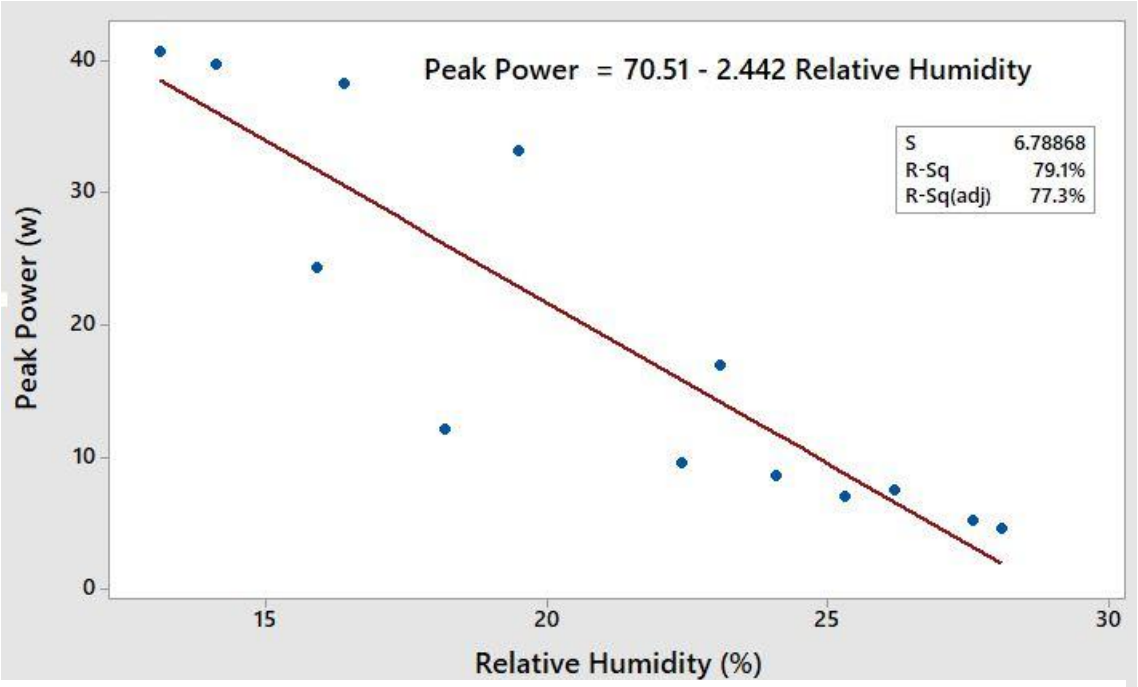

Figure 4-49: Fitted regression line plot for Peak power versus Relative Humidity (Day 8)

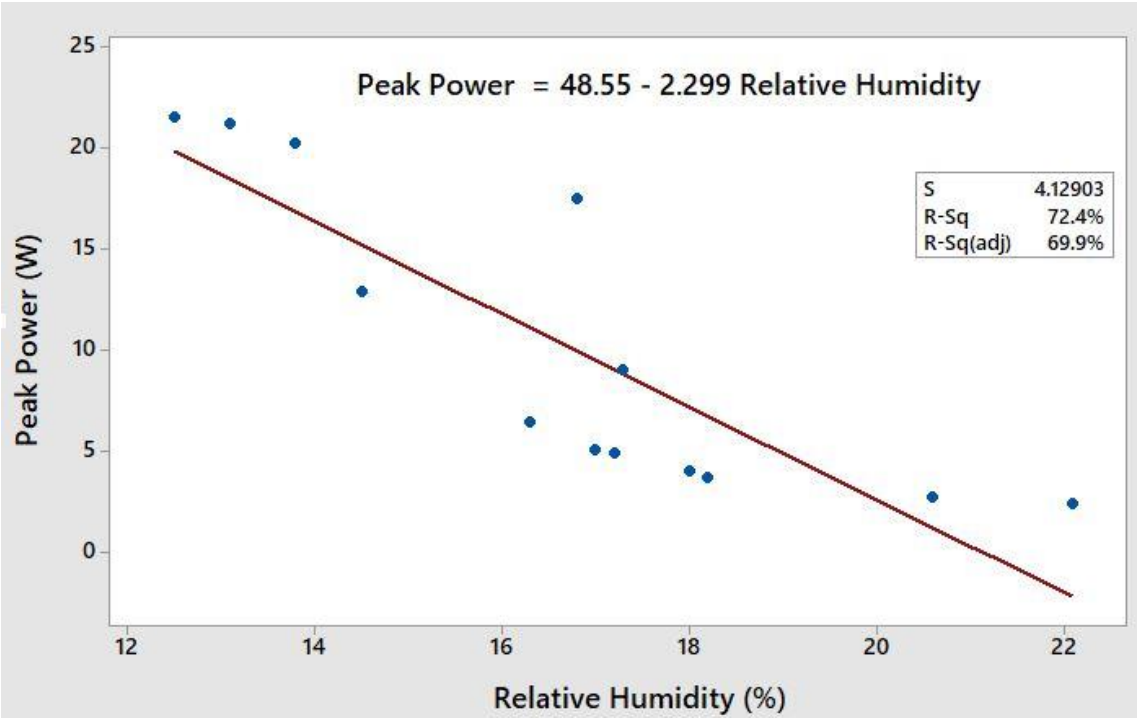

Figure 4-50: Fitted regression line plot for Peak power versus Relative Humidity (Day 13)

Figure 4-49 to Figure 4-52 shows the fitted regression line plots of the relationship between peak power output of the 50 W solar PV module and solar irradiance. The regression line shows a positive correlation with coefficient of determination, R^2 being 97.5% 96.8%, 99.4% and 93.4% for days 1, 5, 8 and 13 respectively. This indicates that an increase in solar irradiance directly translates to an increase in power output of solar photovoltaic modules. This is supported by a number of papers in the literatures (Salim, Huraib and Eugenio, 2013; Chikate and Sadawarte, 2015; Karafil, Ozbay and Kesler, 2016; Nasiri *et al.*, 2019)

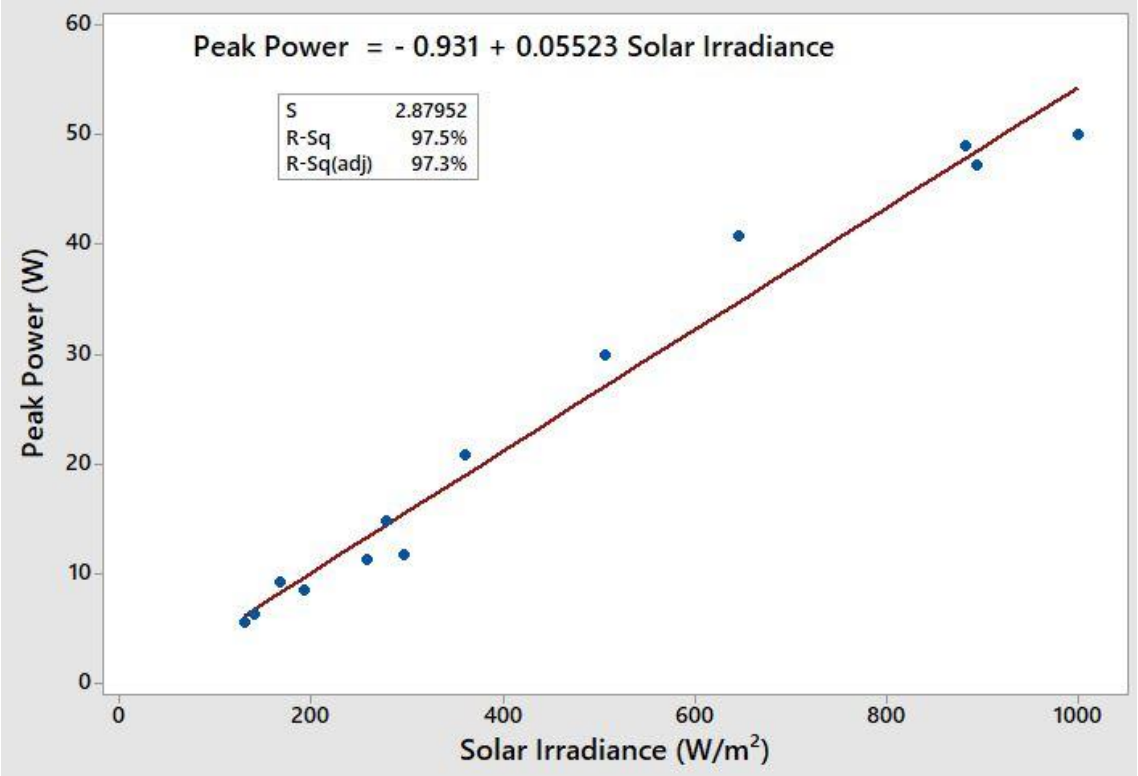

Figure 4-51: Fitted regression line plot for Peak power versus Solar Irradiance (Day 1)

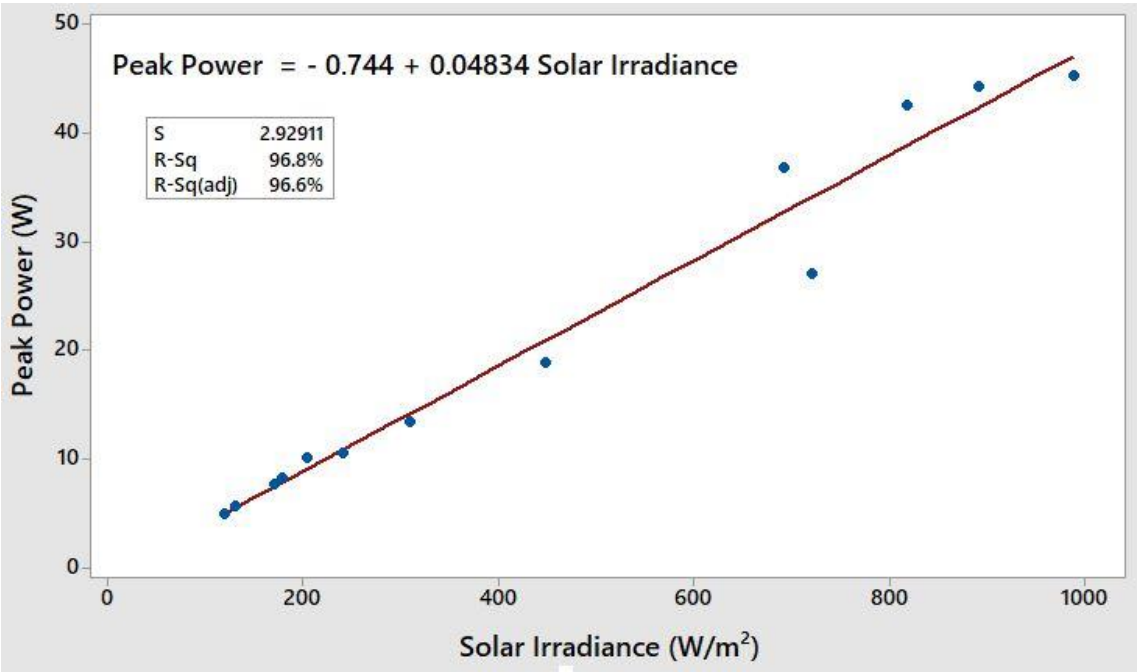

Figure 4-52: Fitted regression plots of Peak power versus Irradiance (Day 8)

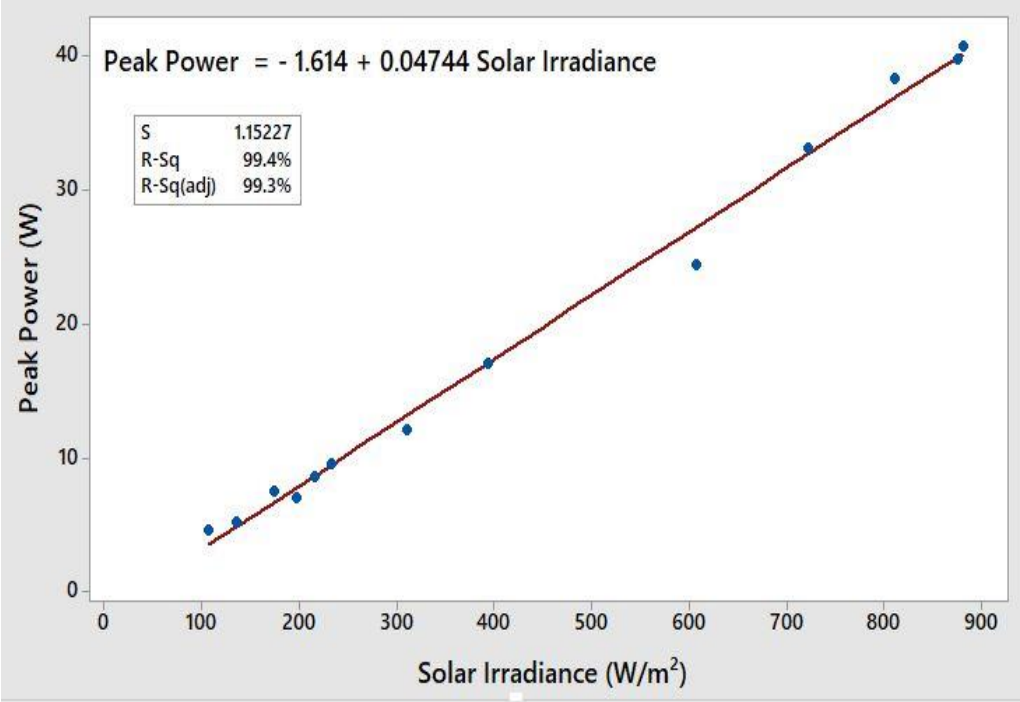

Figure 4-53: Fitted regression plots of Peak power versus Irradiance (Day 13)

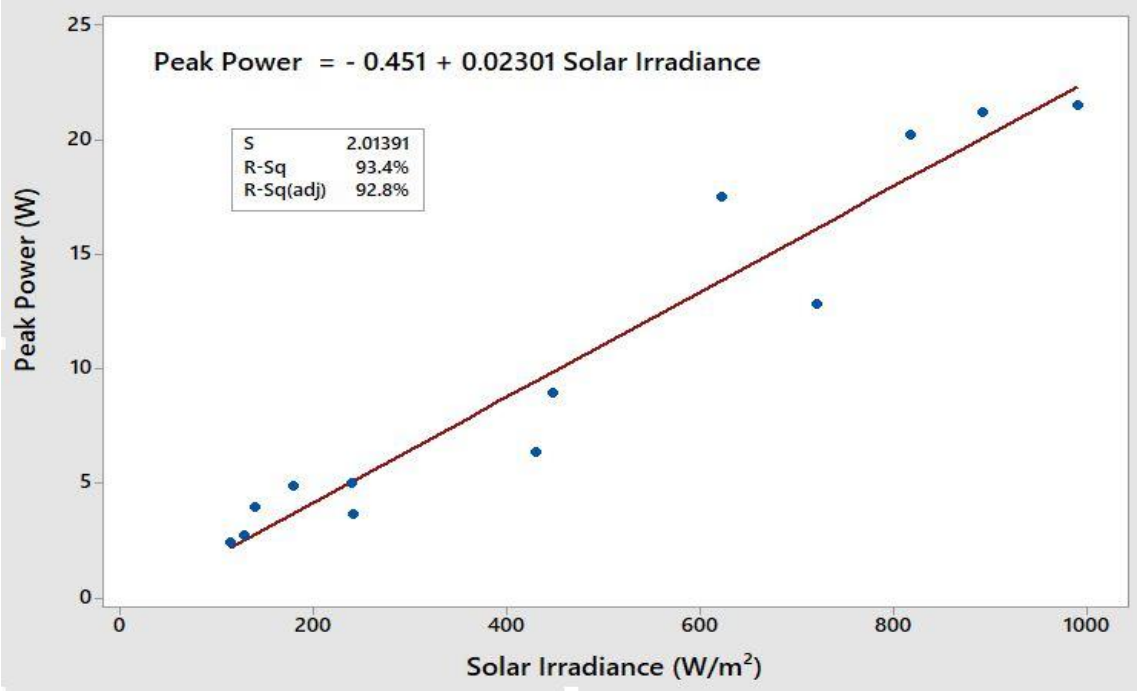

Figure 4-54: Fitted regression plots of Peak power versus Irradiance (Day 13)

Figure 4-53 to Figure 4-56 show the Time series plot of peak power and relative humidity for four selected days of the 14 days of the experiment (days 1,2, 7 and 14). In the four cases, the relative humidity is usually higher in the morning and declines towards afternoon as the temperature begins to increase. This shows a negative correlation between relative humidity and Peak Power with the highest peak power occurring during the lowest humidity which naturally corresponds to highest temperature. This is supported by (Mekhilef *et al.*, 2012; Kazem, Chainchan and Kazem, 2014; Panjwani, Narejo and Panjwani, 2014; Ettah *et al.*, 2015; Amajama and Oku, 2016).

Figure 4-53 shows the results for Day 1 of the experiment with the module very clean. The maximum power of 50.15 W was obtained at the minimum relative humidity of 10.90%. this occurred in the afternoon. The minimum power for Day 1 of 5.61 W was obtained during the experiment at a maximum relative humidity of 32.1% which occurred at the start of the experiment in the morning hour. This agrees with the findings of Amajama and Oku (2016)

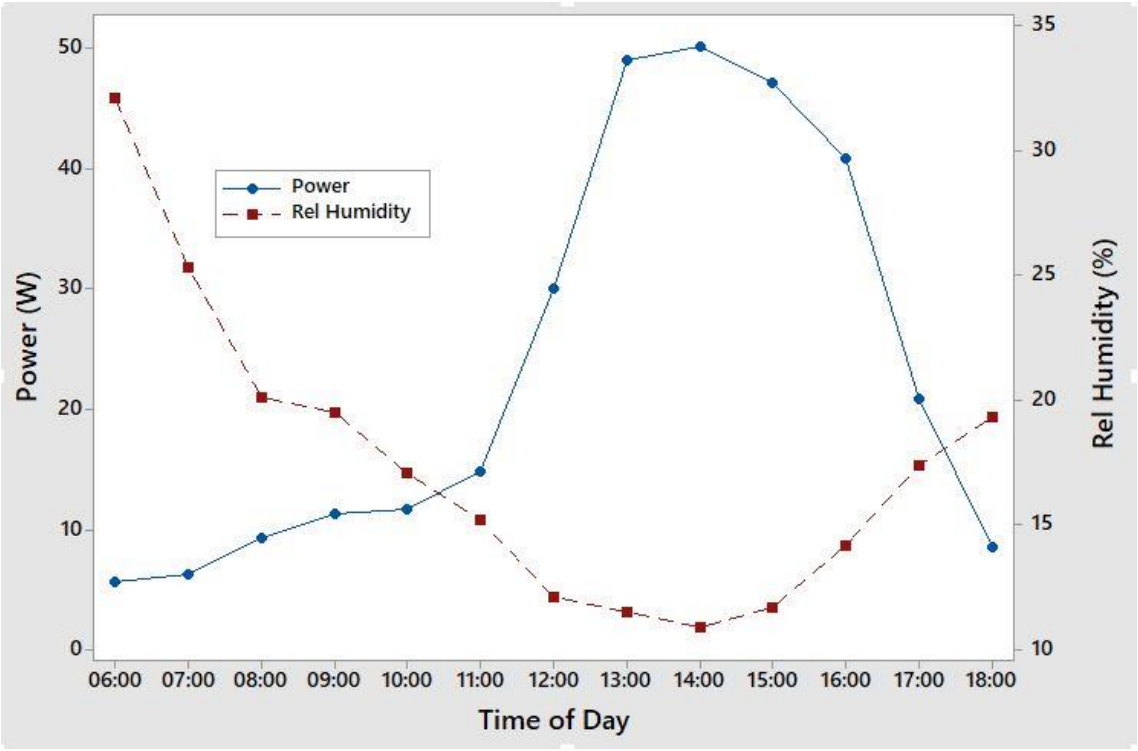

Figure 4-55: Time series plot of Power and Relative Humidity (Day 1)

Figure 4-54 shows the time series plots for power and relative humidity results for Day 2 of the experiment with the module beginning to be dusty. This can be seen in the slight reduction in the maximum power output of the module. The maximum power of 49.55 W occurred at the lowest relative humidity of 10.10%. The lowest output power of 4.59 W occurred at the highest relative humidity of 22.47%.

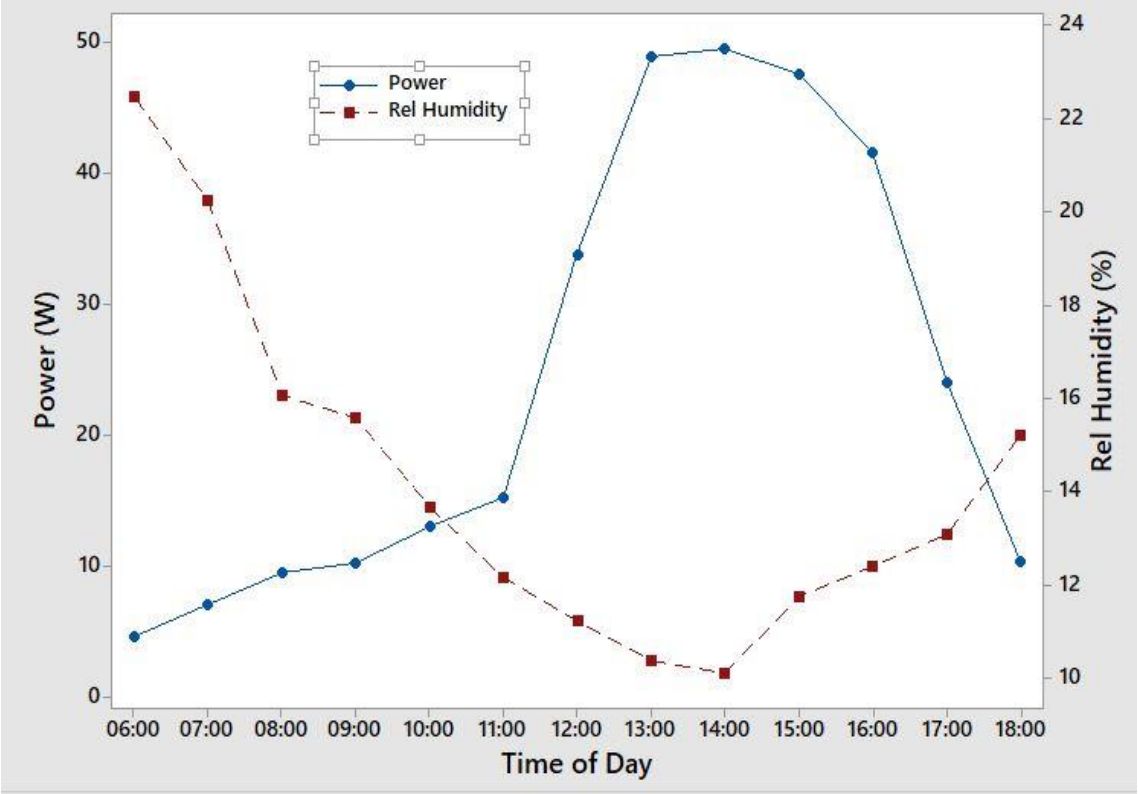

Figure 4-56: Time series plot of Power and Relative Humidity (Day 2)

Figure 4-55 shows the time series plots for power and relative humidity results for Day 7 of the experiment with the module being dustier. This can be seen in the reduction in the maximum power output of the module. The maximum power of 40.67 W occurred at the lowest relative humidity of 13.10%. The lowest output power of 4.55 W occurred at the highest relative humidity of 28.10%.

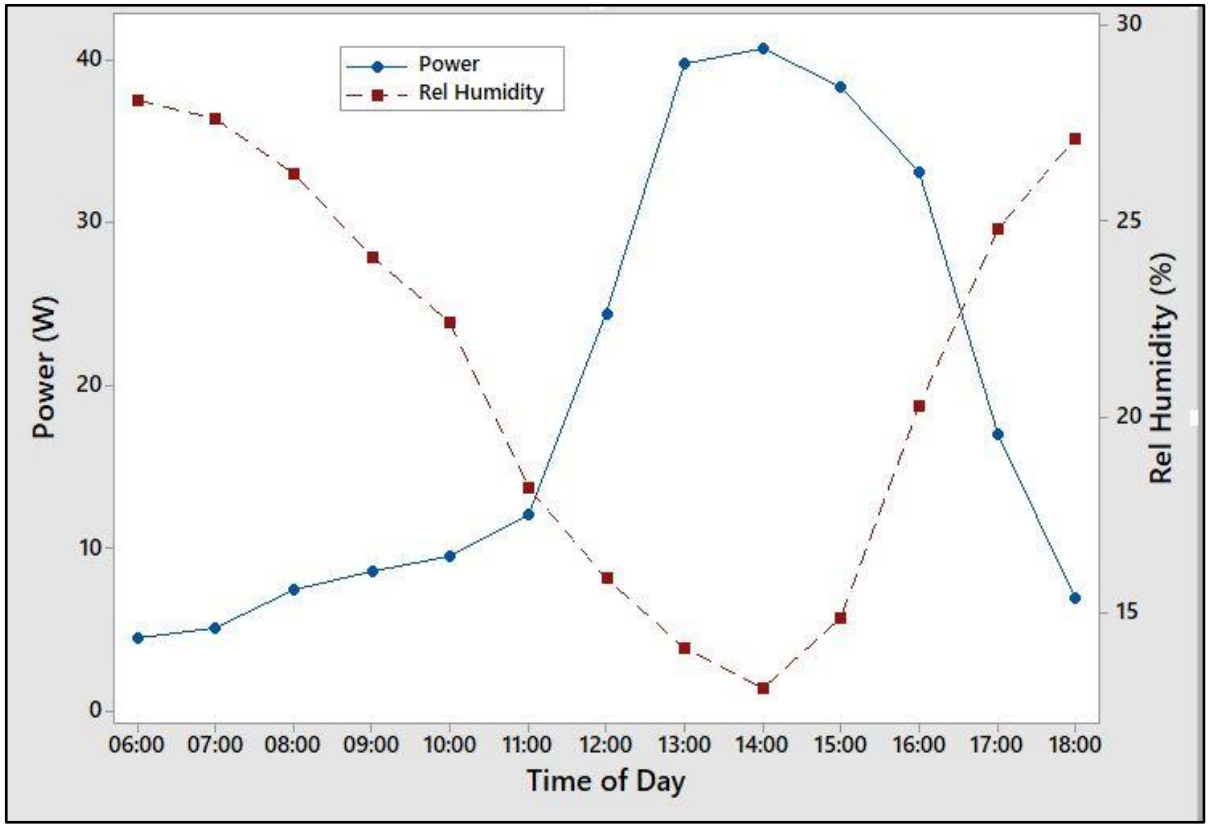

Figure 4-57: Time series plot of Power and Relative Humidity (Day 7)

Figure 4-56 shows the time series plots for power and relative humidity results for Day 14 of the experiment with the module heavily dusty. This can be seen in the major reduction in the maximum power output of the module. The maximum power of 20.52 W occurred at the lowest relative humidity of 9.00%. The lowest output power of 1.87 W occurred at the highest relative humidity of 19.5%.

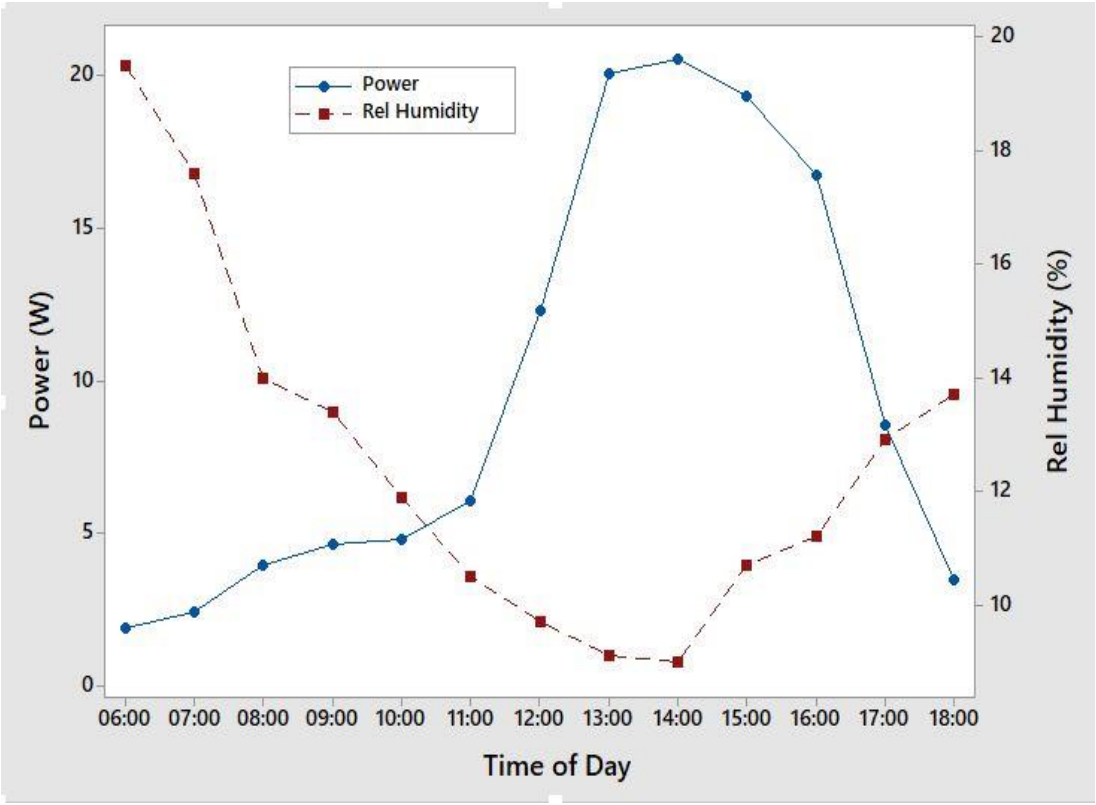

Figure 4-58: Time series plot of Power and Relative Humidity (Day 14)

Figure 4-57 to Figure 4-60 show the trend of peak power and ambient temperature. This shows that as the temperature increases, the peak power increases which is a result of increase in irradiance. Although beyond 25^{o}C the impact of temperature on performance is negative for every degree rise in temperature beyond 25^{o}C. The highest peak power corresponds to the highest ambient temperature and vice versa. This is in agreement with the conclusion of Amajama and Oku (2016).

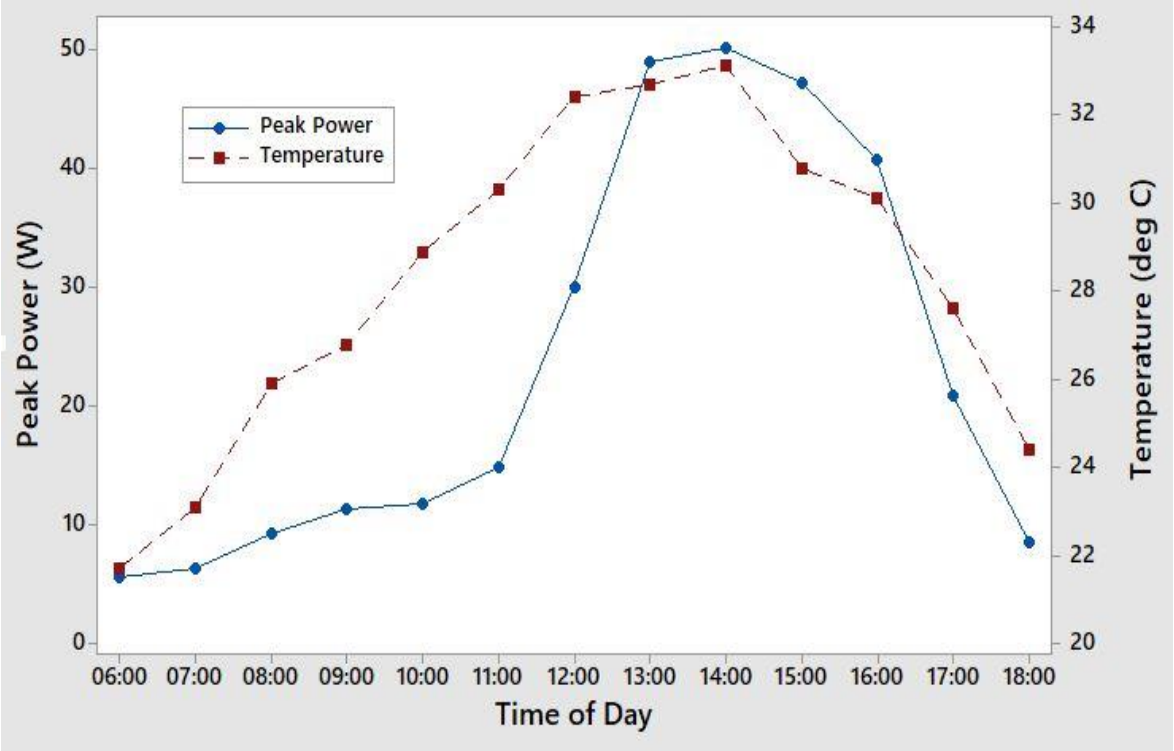

Figure 4-59: Time series plot of Power and Temperature (Day 1)

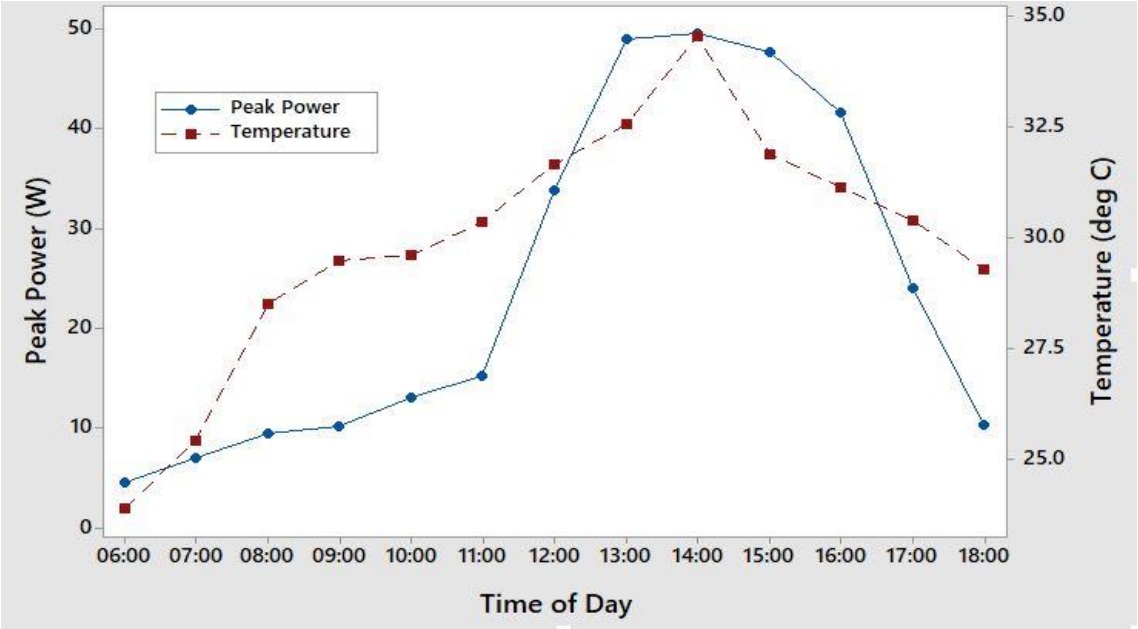

Figure 4-60: Time series plot of Power and Temperature (Day 2)

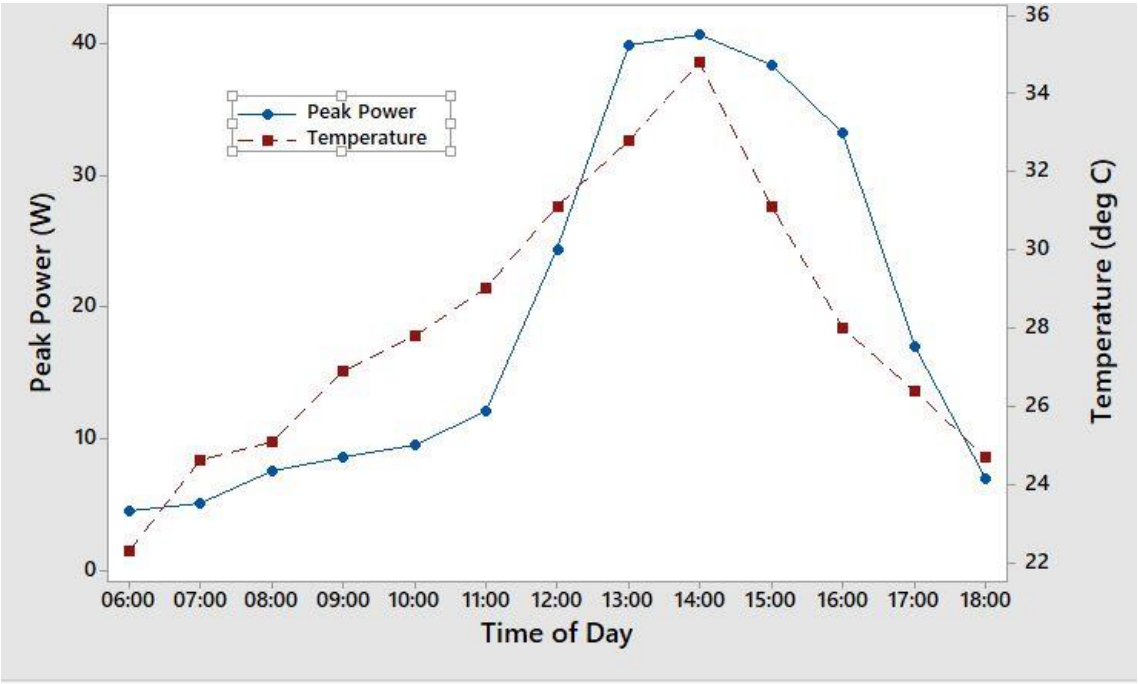

Figure 4-61: Time series plot of Power and Temperature (Day 8)

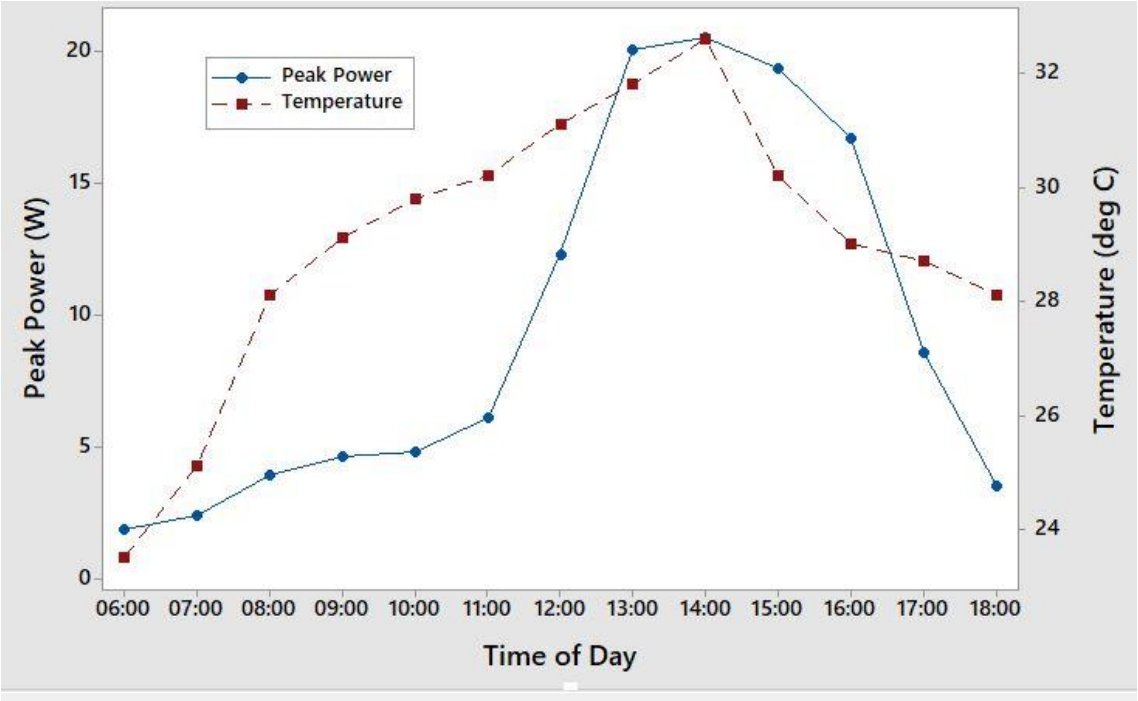

Figure 4-62: Time series plot of Power and Temperature (Day 14)

4.8.1 Maiduguri Sand Analysis

Figure 4-61 shows the particle sizes from each height of collection, panel and ground. The 0.5 m height contains larger particle size up to 1600 µm range. This is expected at lower heights. The highest height of 2.0 m contains the tiniest particle sizes and no larger particle beyond 516 µm. This is because finer particles tend to be blown higher than heavier ones.

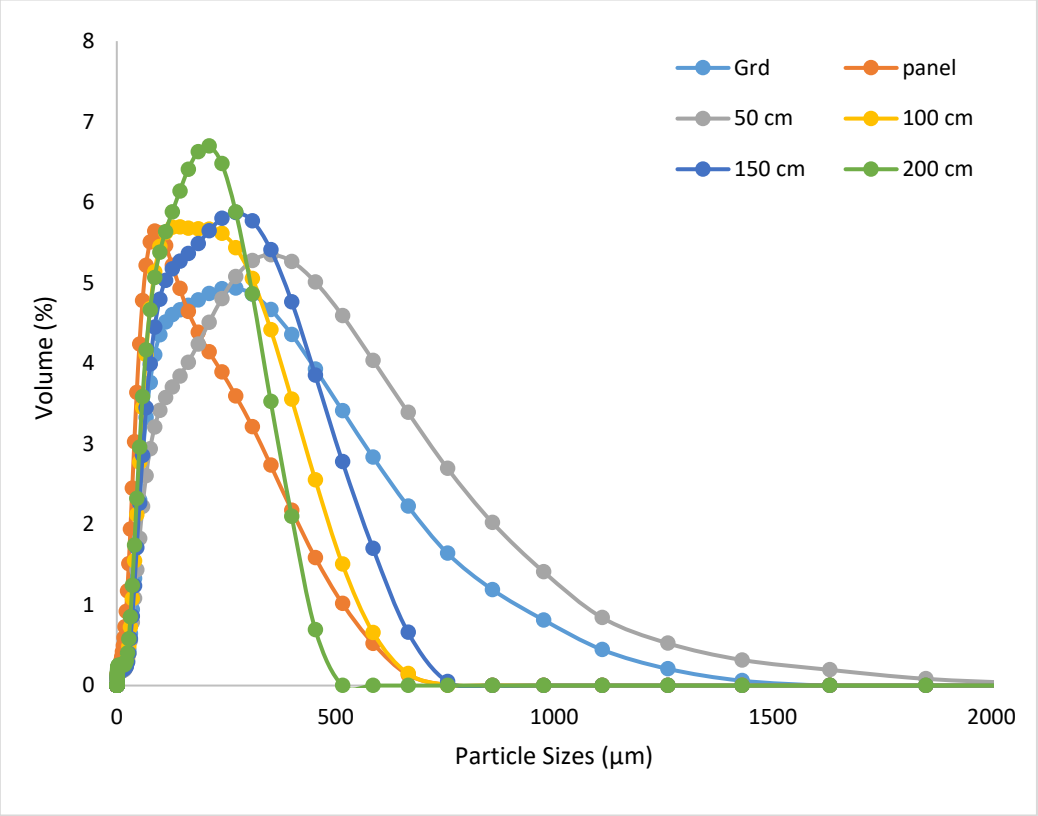

Figure 4-63: Percentage Volume vs Particle size

Figure 4-62 shows the masses of sand collected at different heights. The mass of sand collected at height 50 cm is 19.2 g while the one collected at the height of 200 cm which is the lowest is 14.6 g. The mass collected for height 150 cm which is higher may be attributed to sudden and brief gust in the direction of the 150 cm collector plater.

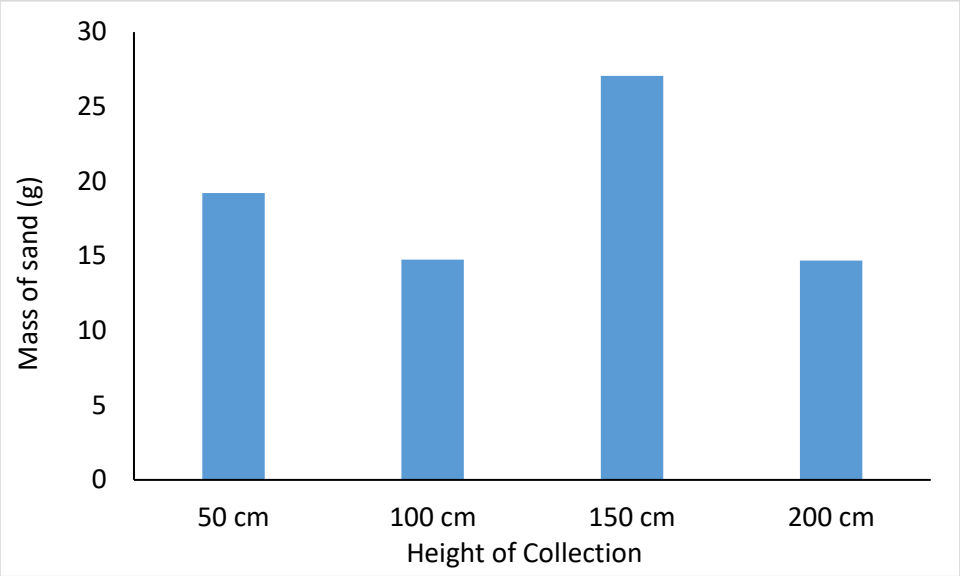

Figure 4-64: Mass of sand at different Heights

Figure 4-63 shows the particle size range for each of the different height collections. The range of 0-50 µm presents 200 cm height having the highest percentage and higher particle size range presents 50 cm height having highest percentage. This is quite logical because larger particle size range are usually heavier and would naturally drop out at lower heights.

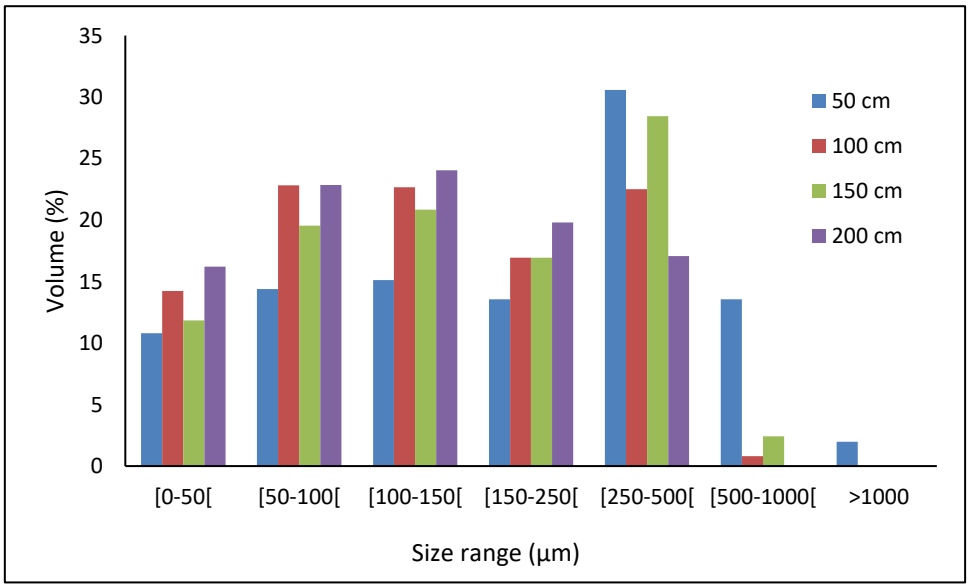

Figure 4-65: Percentage volume vs Particle size range

Figure 4-64 shows the picture of Maiduguri sand collected at a height of 0.5 meter from the ground. The picture shows that the shape of the sand is quite irregular (more ovoid tan round) but with rounded edges as if they have been tumbled in the wind for a while i.e. the edges are smoothed out. The sizes varied from 50 to bigger than 500 microns. Figures 4-65 to Figure 4-68 shows Scanning Electron Microscopy (SEM)- Energy Dispersive Spectroscopy (EDS) for different spectra of sand particles from height of 0.5 meter. The chemical composition for each of the spectra is presented in Table 4-16 and the statistical analysis is shown in Table 4-17. The chemical composition shows high content of O_2 and Si which indicates that the sample is quartz. This confirms the site which is the desert part of Nigeria with intense sandy soil.

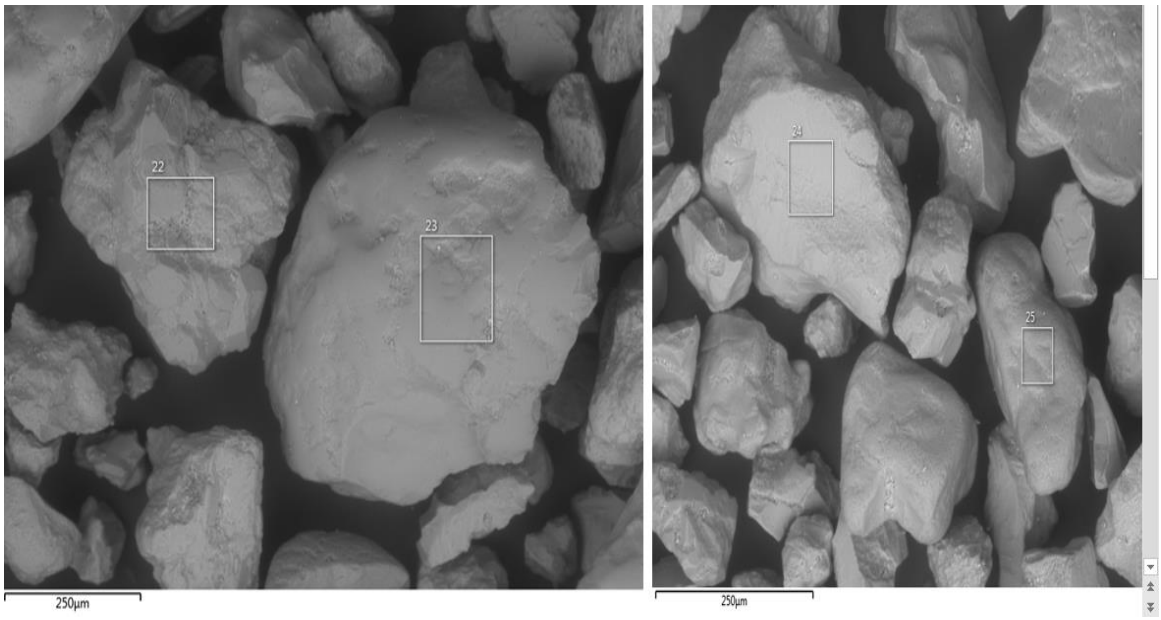

Figure 4-66: Maiduguri sand (50 cm height)

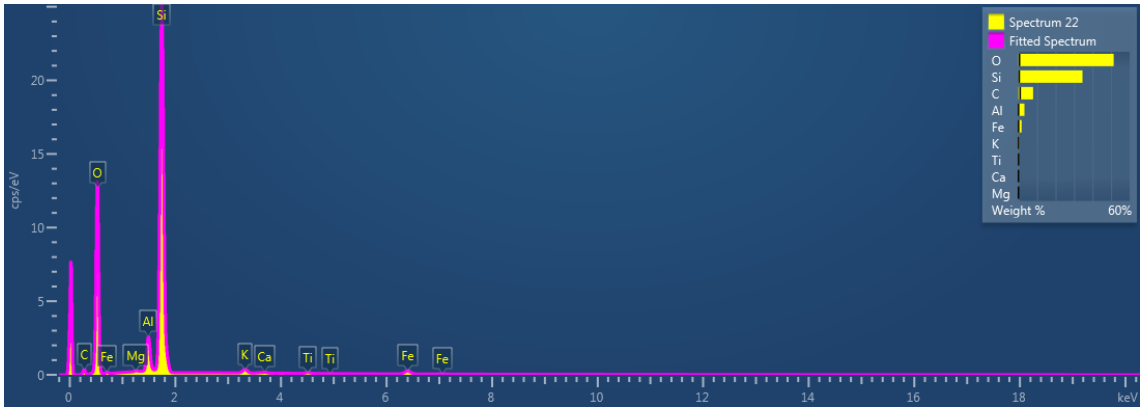

Figure 4-67: Compositional analysis (SEM and EDX) for Maiduguri sand (0.5 m height) – spectrum 22

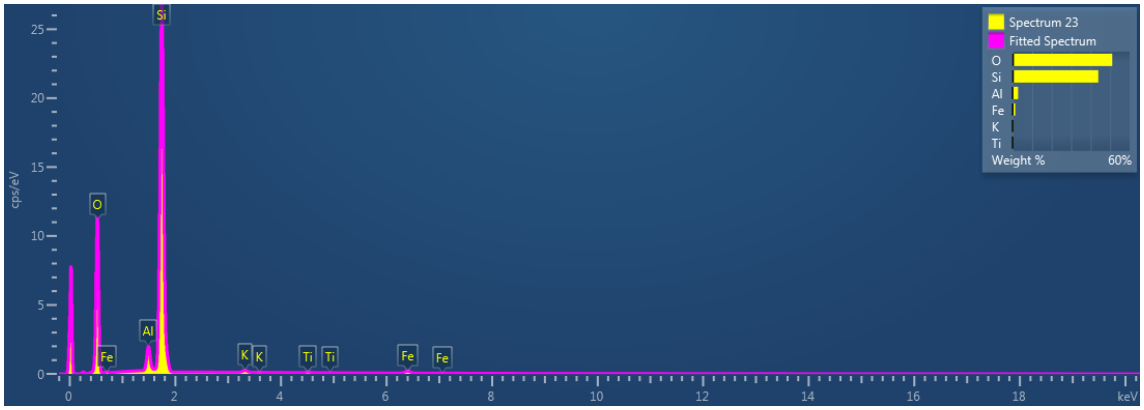

Figure 4-68: Compositional analysis (SEM and EDX) for Maiduguri sand (0.5 m height) – spectrum 23

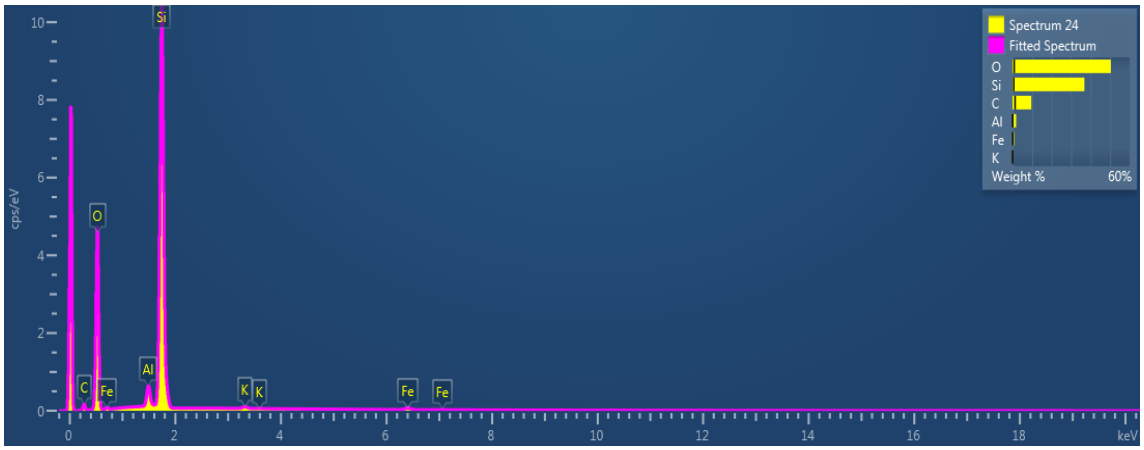

Figure 4-69: Compositional analysis (SEM and EDX) for Maiduguri sand (0.5 m height) – spectrum 24

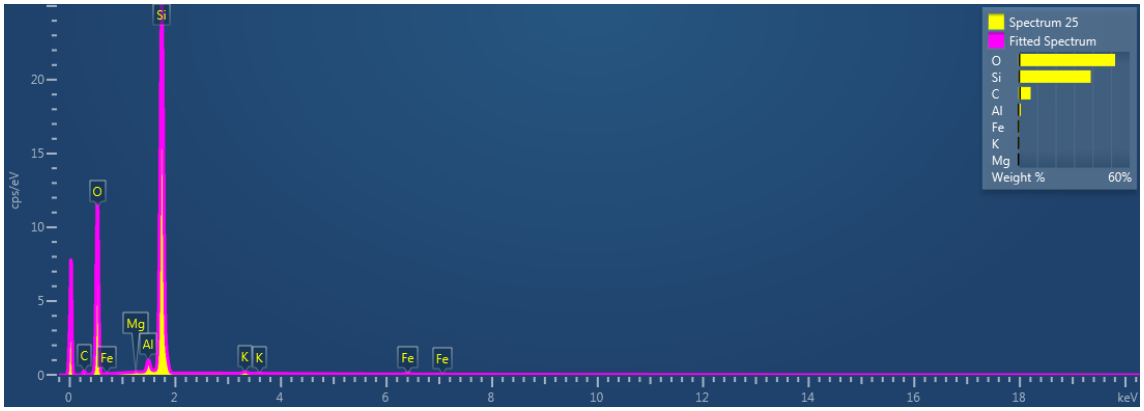

Figure 4-70: Compositional analysis (SEM and EDX) for Maiduguri sand (0.5 m height) – spectrum 25

Table 4-17: Percentage composition of individual chemicals

Spectrum Label	C	O	Mg	Al	Si	K	Ca	Ti	Fe	Total
Spectrum 22	7.92	51.41	0.1	3.21	34.55	0.66	0.19	0.3	1.67	100
Spectrum 23	4.07	50.13		2.67	41.09	0.43		0.29	1.31	100
Spectrum 24	9.64	50.38		1.88	36.83	0.34			0.93	100
Spectrum 25	6.61	52.19	0.07	1.26	38.99	0.33			0.56	100

Table 4-18: Descriptive Statistics of Chemical Composition

Variable	Mean	SE Mean	StDev	Minimum	Maximum
C	7.06	1.17	2.35	4.07	9.64
O	51.027	0.476	0.953	50.13	52.19
Mg	0.085	0.015	0.0212	0.07	0.1
Al	2.255	0.43	0.859	1.26	3.21
Si	37.87	1.41	2.81	34.55	41.09
K	0.44	0.0767	0.1534	0.33	0.66
Ca	0.19	*	*	0.19	0.19
Ti	0.295	0.005	0.00707	0.29	0.3
Fe	1.118	0.239	0.479	0.56	1.67

The mean O_2 and Si are 51.027 and 37.87 % respectively. The chemical with the lowest percentage is Mg.

Table 4-18 shows the summary of the chemical composition of the sand fraction of the samples. The percentage composition of oxygen in all the different levels are very similar ranging from 48.94 to 52.01. Figure 4-69 shows the plots of the percentage by weight of each of the chemical constituent in the sand fraction for Maiduguri.

Table 4-19: Summary of chemical composition of sand fraction

Sand	Ground	0.5 m	1.0m	1.5 m	2.0 m
Statistic	Average	Average	Average	Average	Average
C	19.53	7.06	9.47	7.01	0.44
O	48.94	51.03	51.05	52.01	51.52
Na				0.23	0.3
Mg	0.18	0.085	0.12	0.07	0.15
Al	3.1	2.25	1.88	2.94	5.07
Si	25.32	37.87	35.72	34.78	30.84
K	0.58	0.44	0.52	2.31	4.48
Ti	0.35	0.295	0.205	0.16	0.175
Fe	1.64	1.12	1.24	0.81	1.11
Ca	0.17	0.19			
Ba					0.9

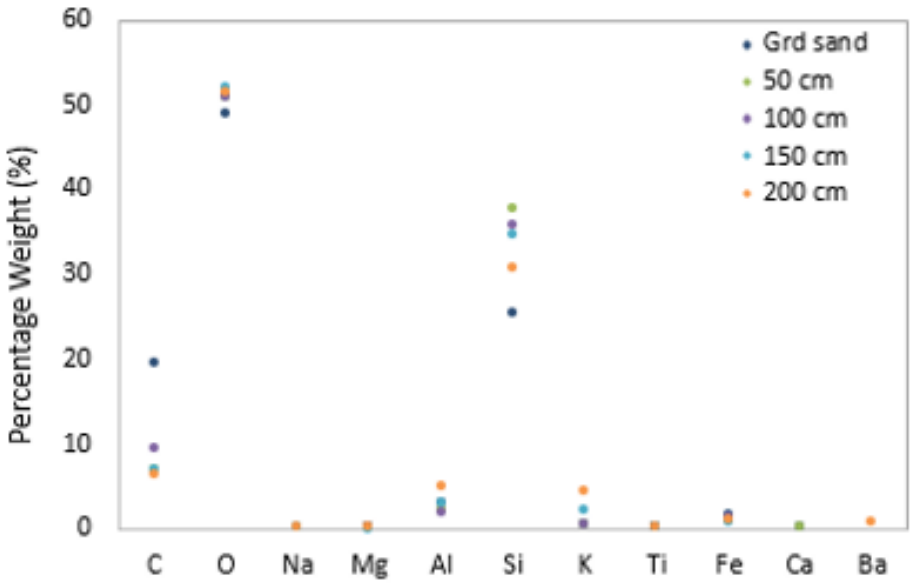

Figure 4-71: Summary of Chemical composition by percentage weight of sand fraction

Figure 4-70 shows the summary of the chemical composition of the soil fraction of the samples. The range of percentage composition of Si in the soil is less than Si range in the sand. This is logical and shows that sand contains more Si than soil.

Table 4-20: Summary of chemical composition of soil fraction

Soil	**0.5 m**	**1.0m**	**1.5 m**	**2.0 m**
Statistic	Average	Average	Average	Average
C	26.6		18.14	24.41
O	45.56	52.58	48.96	47.71
Mg	0.1			
Al	3.03	6.56	3.09	2.15
Si	21.46	33.39	26.52	23.32
K	1.95	3.99	0.83	0.5
Ti	0.24	0.32		0.25
Fe	0.98	1.46	1.8	1.46

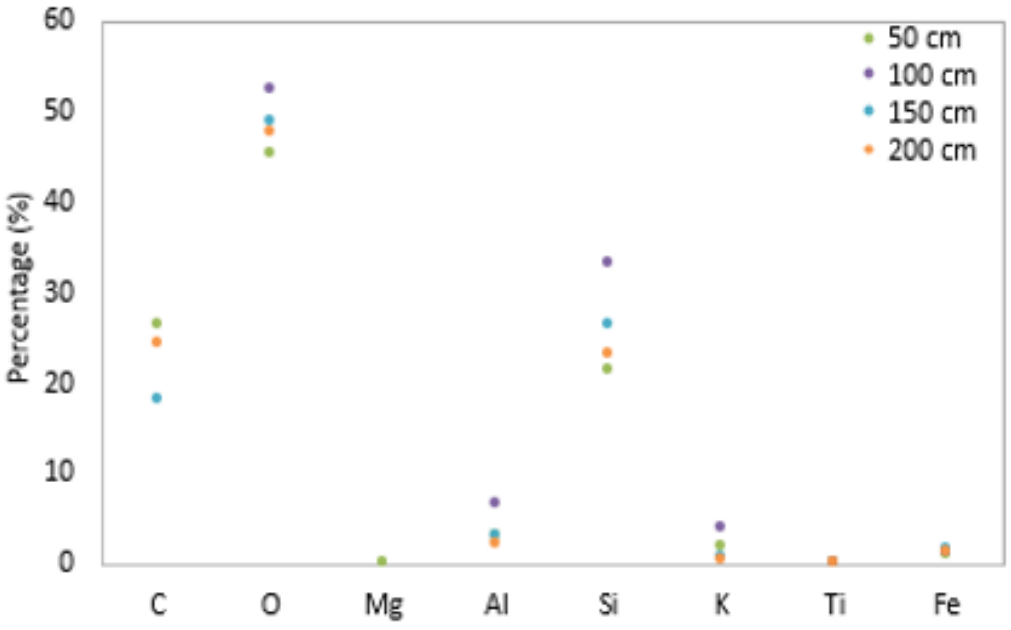

Figure 4-72: Summary of Chemical composition by percentage weight of soil fraction

Figure 4-73 shows the chart of the sand particles with transparent coloured circles overlaid used to indicate the particles collected in the experimental work here for each height. “Roundness is the measure of the sharpness of a particle's edges and corners and it is largely dependent on the sharpness of angular protrusions (convexities) and indentations (concavities) from the object” (Cruz-Matias, 2013).

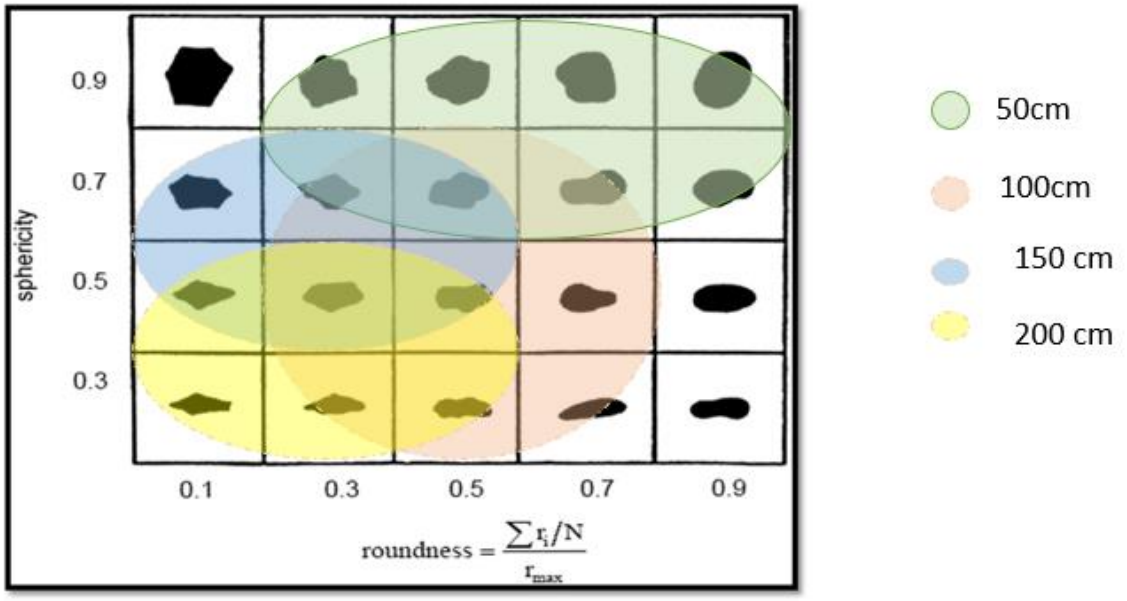

Figure 4-73: Chart of sand particle shape with results of experimental work overlaid

It can be deduced from the chart that there are different sand morphologies in the samples, but the sand particles collected at 50 cm are a little bit rounder than those present in other heights with roundness varying between 0.3 to 0.9. This is an indication that larger particle sizes are more prevalent at this height and this is in line with the conclusion of Sagga (1993) that increasing roundness is associated with increase in grain size. The sphericity is between 0.7 and 0.9, this shows that there are particles with edges which can cause degradation of the solar PV modules by creating cracks either visible or non-visible on the modules on impact. The particles at the 100 cm height mostly constitute particle sizes with roundness between 0.3 and 0.5 and sphericity of 0.3-0.7, this is the same with 150 cm height, while for 200 cm height, the roundness of the sand particle size

spanned between 0.1 - 0.5. This implies that at this height smaller particle sizes are carried (airborne) compared to the particle sizes at height 50 cm. This is associated with a decrease in roundness and reduced particle sizes.

4.9 Sand Adhesion Experiment

The result of this experiment is presented in Table 4-20 which shows the array of the experimental runs and the responses in terms of mass of sand stuck to glass (mg) for each run. Each run was performed with a new glass sample. From the results in Table 4-20, a main effects plot was calculated from the Taguchi design of experiments using Minitab 17, this is shown in Figure 4-72. Table 4-21 shows the response table for means.

Table 4-21: Array of Experimental Runs and Responses (Taguchi experimental runs)

Run #	Temp (ºC)	Particle Size (µm)	R. Humidity (%)	Sand Type	Height (cm)	Mass of sand stuck (mg)	
1	33	>212	50	Libya	100	11.4	
2	20	125-212	70	MIL	100	16.4	
3	40	75-125	70	Libya	50	5.2	
4	40	0-75	90	Egypt	100	43.3	
5	27	0-75	50	MIL	50	6	
6	40	125-212	50	Quartz	200	0.7	
7	40	>212	30	MIL	150	0.7	
8	33	0-75	70	Quartz	150	38.5	
9	33	125-212	30	Egypt	50	1.5	
10	27	75-125	30	Quartz	100	0.8	
11	20	>212	90	Quartz	50	0.2	
12	27	125-212	90	Libya	150	46.1	
13	33	75-125	90	MIL	200	0.2	
14	27	>212	70	Egypt	200	2.7	
15	20	0-75	30	Libya	200	1.3	
16	20	75-125	50	Egypt	150	9.5	

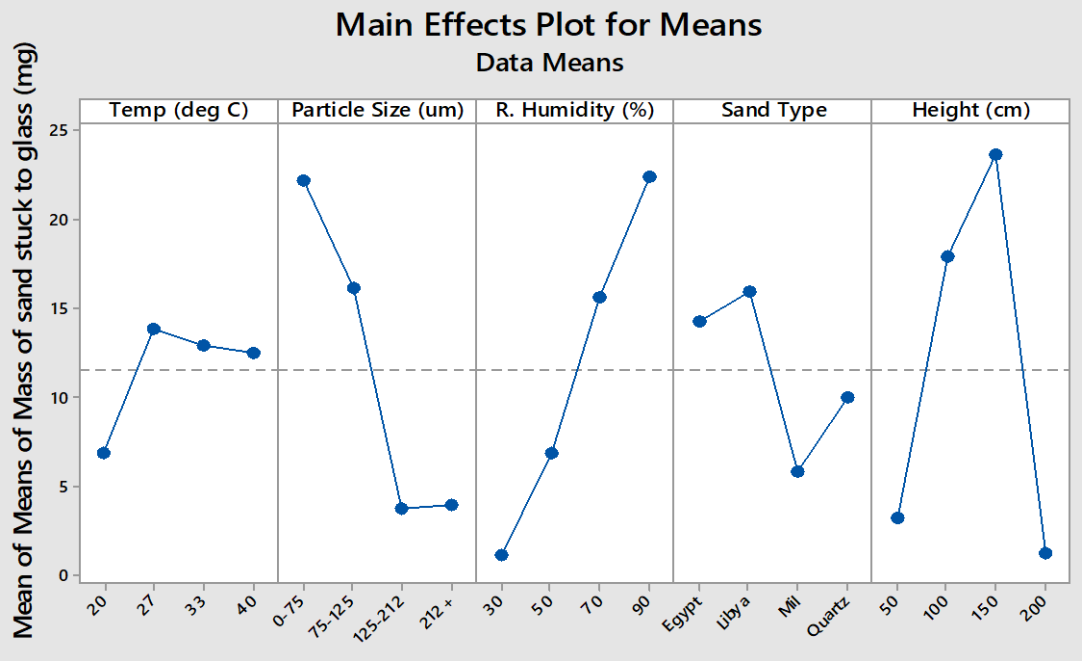

Figure 4-74: Main Effects Plot for Means

Table 4-22: Response table for Means

Mean of means					
Level	**Temp**	**Particle Size**	**R. Humidity**	**Sand type**	**Height**
1	6.85	22.275	1.075	14.25	3.225
2	13.9	16.175	6.9	16	17.975
3	12.9	3.75	15.7	5.825	23.7
4	12.475	3.925	22.45	10.05	1.225

Figure 4-72 presents the differences between level means for the five factors. It describes the effect of each factor on the response ignoring the effect of other factors. There is no Main Effect present when the line is horizontal but, in this case, there is a main effect because the line is not horizontal as different levels of a factor affect the response differently, that is different levels have different Mean of Means (response).

The temperature has little effect on the amount of sand that sticks to the glass with the highest Mean of Means of 13.9 mg occurring during 27^{o}C. It should be noted though that only the air was heated not the sand or glass

The very smallest particles stick better as they have lower mass and also the electrostatic attraction between particles of smaller size could have played a significant part while there is a general trend that larger particles do not stick as well implying that they have sufficient mass to roll down the inclined surface and fall off. The particle size of 0-75μm has the highest Mean of Means of 22.28 mg.

Relative humidity clearly has the strongest effect on how much sand is sticking. As the humidity is increased the amount of sand sticking also increases significantly. There is more moisture in the air through which the sand travels, and this is absorbed by the particles increasing their adhesion potential. Relative humidity of 90% has a Mean of Means of 22.45 mg. This finding is in agreement with the conclusion of (Cleaver and Tyrrell, 2004).

Sand type is important, there can be a significant difference in composition between two sands from different locations, as well as from artificial sand. In this experiment, the natural sands stick better which may be due to more soluble compounds being present when compared to the manufactured quart- based sands.

As the height is increased more sand sticks to the surface , except for the 200 cm height. As the height is increased, the velocity of the sand that is capable of being carried at that height is likely to be faster than at lower levels. At higher velocity, it could be argued that the sand is then more likely to break apart on impact than adhere to the surface of the glass. This could also be as a result of the fact that quartz sand is more brittle and can shatter on impact. This might explain the reduction in mass of sand that sticks to glass at 200 cm height.

4.9.1 Microscopy

Due to the non-homogenous nature of the soiling on the samples, detailed analysis using microscopy image processing is not useful due to the ranges of results across a single sample as shown in Figure 4-73.

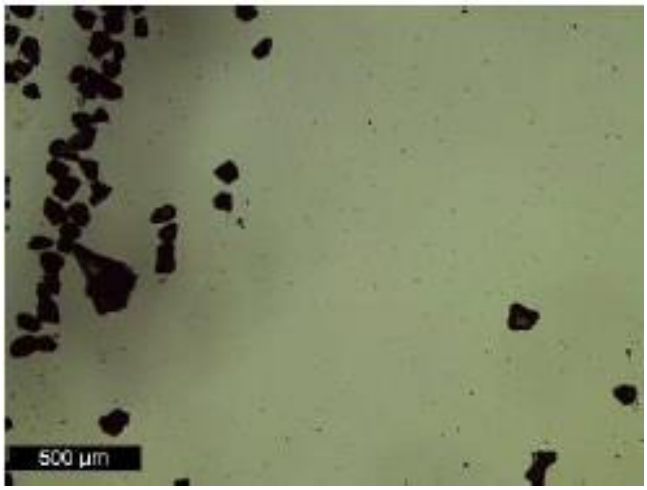

Figure 4-75: Microscope image for run 10 showing non-homogenous soiling

However, a general inspection of these images support some of the results found from weighing the samples after soiling

Figure 4-74 shows an image of run 4, done with the smallest particles at 90% humidity. It seems apparent that there was some condensation on the glass sample, which aided in causing this fine sand to stick to the glass.

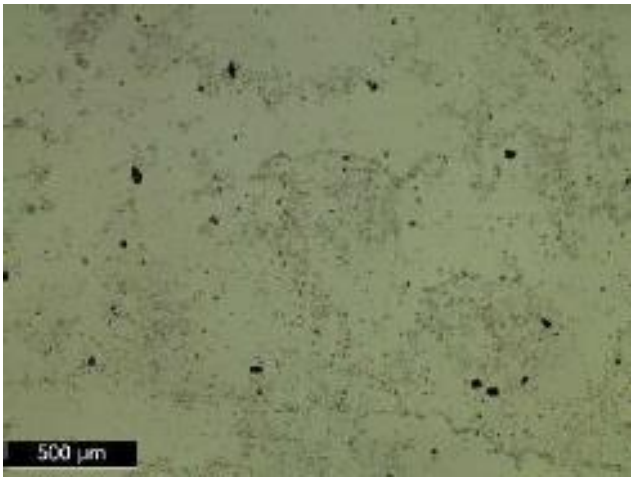

Figure 4-76: Microscope image of run 4 (0 - 75 µm, 90% humidity)

In this case, there is also a high coverage of particles across the image. Figure 4-75 shows the image of run 10, done with large particles and at low humidity.

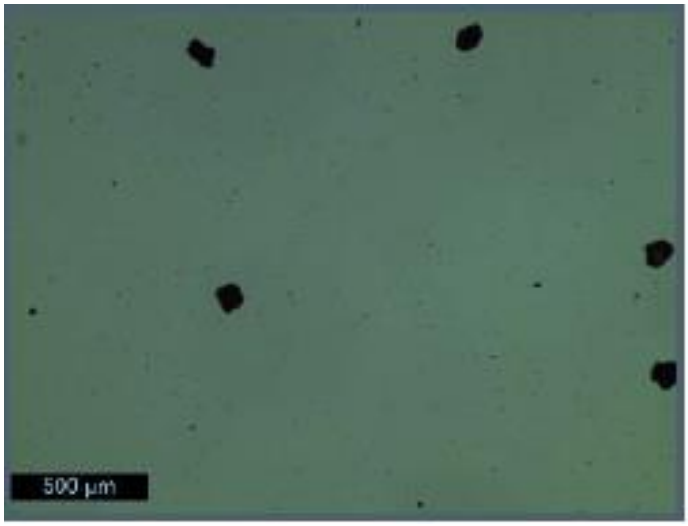

Figure 4-77: Microscope image of run 10 (75 - 125 µm), 30% humidity)

In this case there are very few particles stuck to the surface and none of the water patterning. Some background fine particles are noted, which are difficult to remove from the input sand in their entirety.

4.9.2 Reflectance

Due to the non-homogeneous nature of the soiling, shown in Figure 4-73, reliable reflectance measurements were not possible. The reflectance loss varied across the sample from no loss to total loss where there were patches of sand.

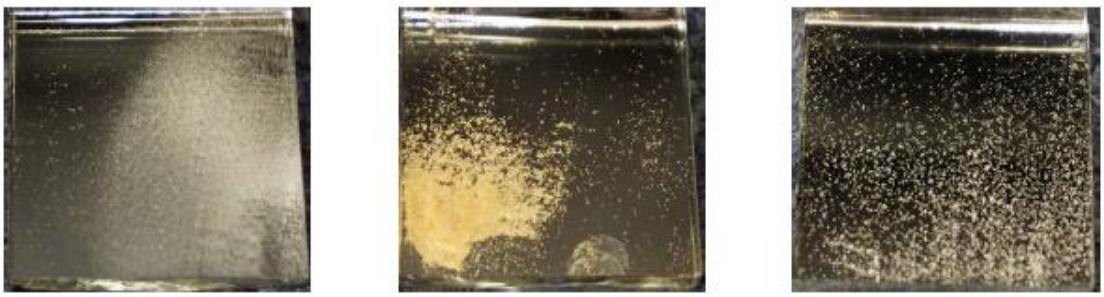

Figure 4-78: Examples of non-homogeneous soiling of samples

The results of the experiments have shown that there are a number of factors affecting the amount of sand that sticks to glass. The factor with the most influence was humidity, where a higher humidity causes more sand to adhere.

This is due to the higher moisture content of the air which aids in dissolving any soluble materials and also acts to cement or bind the particles to the surface. In addition, natural sands collected from desert environments appear to adhere more strongly than artificial quartz-based sands, this is possibly due to higher amounts of soluble materials present in natural sand.

In summary, sand adhesion to glass is an important aspect of soiling, the amount of which is affected by certain parameters studied in this research. Humidity has the highest influence on sand adhesion to glass and consequently more performance loses as expected at higher humidity. Other factors such as temperature, height, type and particle size have varying influence on the amount of sand that sticks to glass but with lower influence compared with humidity. This is one of the reasons that make Maiduguri the best of the three locations for the development of solar PV system because of its low humidity.

5 Conclusion and Future Work

5.1 Conclusion

As a recap, the aim of this research is to develop a novel and robust decision-making Solar-PV-System-Model (SPVSM) for an optimised power supply at competitive cost and to determine the impacts of dust on the performance of solar PV panel with the following objectives being the roadmap to achieving the set aim:

i. To acquire and analyse 11-year weather data from 3 radiation zones in Nigeria and to evaluate the energy demand of the village under study.
ii. To develop a robust Solar PV system Model using graphical user interface (GUI) in MATLAB with appropriate inputs and outputs and model PV module and maximum power point tracking (MPPT)
iii. To experimentally investigate the impact of dust on the performance of Solar photovoltaic module -in Nigeria and study the effect of certain pertinent parameters on sand adhesion to glass cover of PV module and to analyse the trend of impact of dust period on the performance of PV module.

All the objectives as stated above were carried out with the detailed methodology adopted presented in Chapter Three of this thesis and the results from thereof presented in the Chapter Four of this thesis.

Solar and climatic data analysis of the three locations selected for this research is certainly a contribution to the body of knowledge as the Nigerian Government Agency responsible for data collection has opined that there are inadequate data and data analysis and about 9000 weather stations are required as a result of Nigeria's huge land mass instead of the 800 that are currently on ground (Kasim Sumaina, 2018)

From the literature review, it is obvious that there are limited studies on the effect of dust and the fact that it is not quite appropriate to adopt or compare the results

from different existing studies encountered because many differences were found between them. Some of these differences include testing methodology adopted, geographical location of experiments, parameters considered for experimentation and experimental design/procedures. The study carried out in Maiduguri, a region characterized by high dust accumulation and most favourable for the development of solar PV energy conversion system in Nigeria will certainly remain an important contribution to the body of knowledge for a couple of reasons. The first being that it contributes to an emerging area of solar PV studies with renewed vigour to establish a world encyclopaedia of real dust and soiling trends and knowledge. Secondly, these data from this research will serve as a source of important information for stakeholders in solar PV system development such as the installers, system holders and practitioners. The benefits of the output of this research range from assisting in accurate location of site and also schedule of module cleaning to guarantee optimum energy output of the system. This will also guide the operation and maintenance cost for the system. Finally, this research will also gear up collaboration between researchers and developers in the field of PV system as well as soil scientist to address the mitigation of impact of soiling on PV modules.

In addition, the present drive of the Nigerian Government towards the use of solar PV energy conversion system will require a simple software which can be rapidly used for accurate sizing and conducting energy and economic analysis because many stakeholders ranging from engineers, technologist, technicians and craftsmen will be involved as this is going to be a huge investment. The development of a robust and simple solar PV system model (SPVSM) which is a decision-making toolkit for accurately sizing of the solar PV system components for optimum power supply at competitive cost and with the capability to conduct energy and economic analysis on a single graphical user interface platform is certainly novel and a contribution to the body of knowledge as this will serve as a guide to solar PV practitioners.

The solar and weather data analysis of the selected locations in the three radiation regions of Nigeria is indeed a contribution to the body of knowledge as there currently exists scant data analysis of these regions which are favourable to the development of solar PV energy conversion system in Nigeria.

Several analytical methods and the development of software were employed in the analysis of the data from the selected locations. This is imperative and an important pre-requisite to developing an efficient PV system because of the intermittent nature of the solar resource and temperature fluctuations. The descriptive statistics show that Maiduguri has higher prevalence of solar irradiance than Minna and Port Harcourt which are the other two locations that were studied.

The values presented for the standard error of means indicate that the individual sample means do not vary widely from the true population mean and this implies more than 95% confidence level at all the three locations. The Analysis of Variance (ANOVA) shows that all the fitted regression models have very high Pearson's correlation coefficients with the least and highest been 87.45% and 92.36% respectively. It can, therefore, be concluded that the fitted regression model explains about 87.45% of the total variability in the data and therefore fits the model well. The results of the descriptive statistics and Analysis of Variance implies that the data set of the locations studied are good enough for the development of solar PV systems considering the error presented and variability of data.

The analysis of interaction between the predictor variables (temperature, relative humidity and sunshine hour) which could affect the dependent variable (solar irradiance) was studied. The interaction plot shows that there exists interaction between the predictor variables but a further analysis using ANOVA shows that although there is interaction, the interaction is not statistically significant and therefore means the interaction does not affect the goodness-of-fit of the model. The result of the interaction analysis implies that the practical development of solar PV system for power supply in this locations is very viable since the

interaction between the predictor variables and the dependent variable which is the solar irradiance have no significant impact. The development of the PV system can be solely based on the available solar irradiance in these locations without any adverse effect on the design.

A unique and novel solar photovoltaic system model (SPVSM) was developed on a single graphical user interface platform. This unique tool has the capability to accurately size PV components for efficient and safe power supply, and conduct energy and economic analysis. A case study that was considered which a village in the North-eastern Nigeria with 200 houses and common facilities such as 1 primary and secondary schools, hospital, garage and police station has daily energy requirement of about 1.08 MWh. The developed model gave the following requirements to be able to meet this daily energy need based on the solar resource available in the location. A 0.67MW peak solar array which amounts to 2226 of 300 W modules and 20 of 8kW inverters are required. Considering stand-alone and 2 days of autonomy; a battery bank of 599 batteries of 6V and 1200 ah each is required. The energy analysis shows the annual energy generated as 409.2 MWh and economic analysis presents the total plant cost to be about $2.22 million and the LCOE is $0.0812kWh. Conclusively, the development of solar PV energy conversion system for power supply in Maiduguri is technically and economically viable. The results of the model were validated using existing published results.

A MATLAB/SIMULINK model of a 50 W module was developed and validated by experimental data. Single diode model of the PV cell was employed, and the controlling equations were used to develop the Simulink model which generated the I-V and P-V characteristics of the model. The I-V characteristic curve of a PV module/array is the most important characteristic of PV systems. This is because it provides important information on the performance and operating points of PV modules such as open circuit voltage, short circuit current, maximum rated power, maximum current, maximum voltage, and the module's efficiency. The simulation results gave a maximum power as 50.0 W while 48.96 W was obtained from

experiment. (This confirms the manufacturer's claim of 50 W on the nameplate of the PV module).

The impact of dust on the performance of solar PV system has not received the required global attention it deserves and only about 13% of global research reported is from Africa. This necessitated an experimental investigation into the impact of dust on solar PV modules in Maiduguri, North-eastern Nigeria. The investigation which focused on the impact of continuous dust deposition on the modules revealed that the power output of a 50 W module which was used for the experimentation dropped by more than 50% and consequently the efficiency dropped by 57.6%. This experiment was performed at the peak of a dust event in Maiduguri (known as the Harmattan season) and it can be concluded that dust deposition on solar PV modules has a tremendous effect on the overall performance of the system and cleaning of the modules at least once a week during this period will be necessary to sustain the performance of the system. Sands were collected from the site of the field experiment in Maiduguri and subjected to chemical composition analysis, morphology and size analysis. From the chemical composition and morphology of the sand collected from different heights during the field experiments, it can be concluded that the sand in the location of field experiments is quartz since the chemical analysis shows a high percentage of oxygen and silicon. Its large particles which were found in the lower collection platform has higher roundness than those found at heigher hights, therefore, deterioration or degradation rate of the PV module is expected to be low since rounder particles causes lower degradation than particles with sharp edges.

Laboratory experiments to study the effects of some parameters on sand adhesion to the glass cover of PV modules were carried out. The parameters whose effects were studied are temperature, particle size, relative humidity, sand type and height. The results of the experiments have shown that there are a number of factors affecting the amount of sand that sticks to glass. The factor with the most influence was humidity, where a higher humidity causes more sand to adhere to the surface. This is due to the higher moisture content of the air

which aids in dissolving any soluble materials and also acts to cement or bind the particles to the surface. In addition, natural sands collected from desert environments appear to adhere more strongly than artificial quartz-based sands, this is possibly due to higher amounts of soluble materials present in natural sand.

In summary, the outcome of this research has shown without a doubt that the regions where the study was conducted in Nigeria have high potential for solar PV development and its development for power supply to the rural dwellers is economically viable. The research also shows that for the same energy demand, the solar PV components required vary for the three location as a result of difference in the available solar irradiance and consequently the LCOE for each location will be different. The Nigerian Government which is showing renewed interest in renewable energy will be advised to use the novel and simple solar PV system model developed in this research for the accurate sizing of the components for optimized power supply to the rural dwellers. The research also shows the need for frequent cleaning of solar modules especially those that will be installed in the North-eastern Nigeria as a result of intense dust impact on systems performance.

5.2 Future Work

The following points are suggested for future work.

i. The development of prediction models for harmattan haze and its impact on solar photovoltaic performance should be comprehensively studied
ii. The development of autocleaning system for solar PV modules
iii. Comprehensive study and optimization of electric power network for a large standalone solar PV system
iv. A study of socio-economic implications of solar PV systems deployment on rural dwellers
v. A study of the economic implication of a grid-tied solar PV system in North-eastern Nigeria
vi. Development of highly efficient solar component system

REFERENCES

Abdulkadir, M., Samosir, A. S. and Yatim, A. H. M. (2012) 'Modeling and simulation based approach of photovoltaic system in simulink model', *ARPN J Eng Appl Sci, 7 (5) (2012)*, 7(5), pp. 616–623.

Abdullahi, M. and Singh, S. K. (2014) 'Global solar radiation evaluation for some selected stations of north Eastern', *Archives of Physics Research*, 5(2), pp. 1–8.

Abreu, E. F. M. *et al.* (2018) 'Solar resource assessment through long-term statistical analysis andtypical data generation with different time resolutions using GHI measurements', *Renewables*, 127(2018), pp. 398–411.

Adedipe, O., Abolarin, M. S. and Mamman, R. O. (2018) 'A Review of Onshore and Offshore Wind Energy Potential in Nigeria', *IOP Conference Series: Materials Science and Engineering*, 413(2018), pp. 1–8. doi: 10.1088/1757-899X/413/1/012039.

Adejumo, A. O., Suleiman, E. A. and Okagbue, H. I. (2017) 'Exploration of solar radiation data from three geo-political zones in Nigeria', *Data in Brief*, 13, pp. 60–68. doi: 10.1016/j.dib.2017.05.017.

Adinoyi, M. J. and Said, S. A. M. (2013) 'Effect of dust accumulation on the power outputs of solar photovoltaic modules', *Renewable Energy*, 60(2013), pp. 633–636.

Ahmed, M. A. M. *et al.* (2014) 'Effect of Dust Deposition on Performance of Thin Film Photovoltaic Module in Harsh Humid Climate', in *2nd International Conference on Renewable Energy Research and Applications*. Madrib, Spain.

Al-Hasan, A. Y. and Ghoeneim, A. A. (2005) 'A new

correlation between photovoltaic panel's efficiency and amount of sand dust accumulated on their surface', *International Journal of Sustainable energy*, 24(1), pp. 87–97.

Ali, A. N. A. *et al.* (2012) 'A Survey of Maximum PPT Techniques of PV Systems.', *IEEE Energytech*, pp. 1–17.

Aliyu, A. S., Dada, J. O. and Adam, brahim K. (2015) 'Current status and future prospects of renewable energy in Nigeria', *RenewableandSustainableEnergyReviews*, 48(2015), pp. 336–346.

Aliyu, A. S., Dada, J. O. and Adam, I. K. (2015) 'Current Status and Future Prospects of Renewable Energy in Nigeria', *Renewable and Sustainable Energy Reviews*, 48, pp. 336–346. doi: 10.1016/j.rser.2015.03.098.

Aliyu, A. S., Ramli, A. T. and Saleh, M. A. (2013) 'Nigeria electricity crisis : Power generation capacity expansion and environmental rami fi cations', *Energy*, 61, pp. 354–367. doi: 10.1016/j.energy.2013.09.011.

Amajama, J. and Oku, D. E. (2016) 'Effect of Relative humidity on Photovoltaic panels' output and solar illuminance/intensity', *Journal of Scientific and Engineering Research*, 3(4), pp. 126–130.

Appels, R. *et al.* (2013) 'Effect of soiling on photovoltaic modules', *Solar Energy*, 96, pp. 283–291.

Ayoola, M. A. A. *et al.* (2014) 'Measurements of net all-wave radiation at a tropical location, Ile-Ife, Nigeria', *Atmosfera*, 27(3), pp. 305–315.

Aysha, A. *et al.* (2015) 'Experimental analysis of solar PV characteristics under standard condition', *International Journal of Applied Engineering Research*, 10(20), pp.

17970–17975.

Ayvazoğluyüksel, Ö. and Filik, Ü. B. (2018) ‘Estimation methods of global solar radiation, cell temperature and solar power forecasting: A review and case study in Eskişehir’, *Renewable and Sustainable Energy Reviews*, 91(May 2017), pp. 639–653. doi: 10.1016/j.rser.2018.03.084.

Azuri to roll out PayGo Solar to 20,000 Nigerian households (2016) *PV Magazine*. Available at: https://www.pv-magazine.com/2017/02/01/azuri-to-roll-out-paygo-solar-to-20000-nigerian-households/ (Accessed: 19 February 2017).

Babaa, S. E., Matthew, A. and Pickert, V. (2014) ‘Overview of Maximum Power Point Tracking Control Methods for PV Systems’, *Journal of Power and Energy Engineering*, 02(08), pp. 59–72.

Bagher, A. mohammed, Vahid, M. M. and Mohsen, M. (2015) ‘Types of Solar Cells and Application’, *American Journal of Optics and Photonics*, 3(5), pp. 94–113. doi: 10.11648/j.ajop.20150305.17.

Bala, E. J. (2014) ‘Overview of the National Energy Policy & Energy Demand and Supply Projection Studies for Nigeria’, in *7th IAEE/NAEE Annual Conference*. Abuja, pp. 1–63.

Bamisile, O. *et al.* (2017) ‘A review of renewable energy potential in Nigeria; Solar power development over the years’, *Engineering and Applied Science Research*, 44(4), pp. 242–248.

Banu, I. V., Beniuga, R. C. and Istrate, M. (2013) ‘Study on Temperature for Modeling of Photovoltaic Solar Array using Experimental Test Data’, in *5th International Conference on Modern Power Systems*, pp. 28–31.

Barakati, M., Kazerani, M. and Aplevich, D. (2009) ‘Maximum

Power Tracking Control for a Wind Turbine System Including a Matrix Converter', *IEEE Power & Energy Society General Meeting*, 24, pp. 705–713.

BBC (2019) *The biggest energy challenges facing humanity*. London. Available at: http://www.bbc.com/future/story/20170313-the-biggest-energy-challenges-facing-humanity.

Beattie, N. S. *et al.* (2012) 'Understanding the effects of sand and dust accumulation on photovoltaic modules', *Renewable Energy*, 48(2012), pp. 448–452.

Bello, G. (2017) *Nigeria's Population now 182 million*, *National Population Commission*. Available at: http://population.gov.ng/nigerias-population-now-182-million-npc/ (Accessed: 15 July 2017).

Blair, N. *et al.* (2014) *System Advisor Model, SAM 2014.1.14: General Description*. Oak Ridge. Available at: www.nrel.gov/publications.

Boukili, Y. *et al.* (2018) 'Experimental validation of a photovoltaic panel model', in *International Conference on Renewable Energies and Energy Efficiency*, pp. 1–8.

Burns, J. E. and Kang, J. S. (2012) 'Comprehensive economic analysis for supporting policies for residential solar PV in the United States: solar renewable energy credit (SREC) potential.', *Energy Policy*, 44(2), pp. 17–25.

Chanchangi, Y. N. *et al.* (2020) 'Dust and PV Performance in Nigeria: A review', *Renewable and Sustainable Energy Reviews*, 121(2020), pp. 1–14.

Chandel, M. *et al.* (2014) 'Techno-economic analysis of solar photovoltaic power plant for garment zone of Jaipur city', *Case Studies in Thermal Engineering*, 2, pp. 1–7. doi:

10.1016/j.csite.2013.10.002.

Charfi, S., Atieh, A. and Chaabene, M. (2016) 'Modeling and cost analysis for different PV/battery/diesel operating options driving a load in Tunisia, Jordan and KSA', *Sustainable Cities and Society*. Elsevier B.V., 25, pp. 49–56. doi: 10.1016/j.scs.2016.02.006.

Chen, L. R. *et al.* (2010) 'A Biological Swarm Chasing Algorithm for Tracking the PV Maximum Power Point', *IEEE Transactions on Energy Conversion*, 25, pp. 963–973.

Chikate, B. V. and Sadawarte, Y. A. (2015) 'Factor Affecting the Performance of Solar Cells', *International Journal of Computer Applications*, pp. 1–5.

Chineke, T. C., Aina, J. I. and Jagtap, S. S. (1999) 'Solar radiation data base for Nigeria', *Discovery and Innovation*, 11(3), pp. 207–210.

Cleaver, J. A. S. and Tyrrell, J. W. G. (2004) 'The Influence of Relative Humidity on Particle Adhesion – a Review of Previous Work and the Anomalous Behaviour of Soda-lime Glass', *Powder and particle*, 22.

Coiante, D. B. (1992) 'Can photovoltaics become an effective energy option', *Solar Energy Materials and Solar Cells*, 27(1), pp. 79–89.

Costaa, S. C. S., Diniza, A. S. A. C. and Kazmerskia, L. L. (2018) 'Solar energy dust and soiling R & D progress: Literature review update for 2016', *Renewable and Sustainable Energy Reviews*, 82(2018), pp. 2504–2536.

Cruz-Matias, A. I. (2013) *Contribution to structural parameters computation: volume models and methods*. Universitat Politecnica de Catalunya, Bacelona.

Dada, B. M. and Okogbu, E. C. (2017) ‘Estimating Daily Solar Radiation from Monthly Values Over Selected Nigeria Stations for Solar Energy Utilization’, *Journal of Fundamentals of Renewable Energy J and Applications*, 7(6), pp. 1–3.

DaftLogic (2019) *List of the Power Consumption of Typical Household Appliances*, *Online web publication*. Available at: https://www.daftlogic.com/information-appliance-power-consumption.htm (Accessed: 24 April 2020).

Dorofte, C., Borup, U. and Blaabjerg, F. (2005) ‘A Combined Two-Method MPPT Control Scheme for Grid-Connected Photovoltaic Systems’, in *2005 European Conference on Power Electronics and Applications*. Dresden.

Douglah, M. (2018) ‘Oil states energy services v. Greene’s energy group: The future of Inter partes review and its impact on the energy sector’, *Oil and Gas, Natural Resources and Energy Journal*, 3(6), pp. 1343–1362.

Dudley, B. (2019) *BP Statistical Review of World Energy*. Available at: https://www.bp.com/content/dam/bp/business-sites/en/global/corporate/pdfs/energy-economics/statistical-review/bp-stats-review-2019-full-report.pdf.

Duffie, J., Beckman, W. and Worek, W. M. (2013) *Solar engineering of Thermal Processes*. 4th edn. John Wiley & Sons.

Dumont, J. *et al.* (2013) *What is a Solar Hybrid System?*, *SMA Corporate Blog*. Available at: http://www.smainverted.com/what-is-a-photovoltaic-diesel-hybrid-system/ (Accessed: 22 February 2017).

Ehsan, F. and Abbas, A.-S. (2016) ‘The Impact of the Environmental Condition on the Performance of the Photovoltaic Cell’, *American Journal of Energy Engineering*,

4(1), pp. 1–7.

EIA (2019) *Renewable Energy Explained*, *US Energy Information Administration*. Available at: https://www.eia.gov/energyexplained/?page=renewable_home (Accessed: 20 August 2019).

El-Shobokshy, M. S. and Hussein, F. M. (1993) 'Effect of dust with different physical properties on the performance of photovoltaic cells', *Solar Energy*, 51(5), pp. 5–11.

El-Shobokshy, M.S. and Hussein, F. M. (1993) 'Effect of the dust with different physical properties on the performance of photovoltaic cells', *Solar Energy*, 51(1993), pp. 505–511.

Eliminir, H. K. *et al.* (2006) 'Effect of dust on the transparent cover of solar collectors.', *Energy Conversion and Management*, 47(3), pp. 192–203.

Elminir, H. K. *et al.* (2006) 'Effect of Dust on Transparent cover of Solar Collectors', *Energy Conversion and Management*, 47(18–19), pp. 3192–3203.

Elminir, H. K. and Abdel-Moneim, K. M. (2006) 'Effect of dust on the transparent cover of solar collectors', *Energy Conversion and Management*, 47(18–19), pp. 3192–3203.

Esram, T. and Chapman, P. L. (2007) 'Comparison of Photovoltaic Array Maximum Power Point Tracking Techniques', *IEEE Transactions on Energy Conversion*, 22, pp. 439–449. Available at: http://dx.doi.org/10.1109/TEC.2006.874230.

Ettah, E. B. *et al.* (2015) 'Comparative Study of the Effects of Relative Humidity on Solar Electricity Generation in UYO and Port- Harcourt, Nigeria', *nternational Journal of Mathematics and Physical Sciences Researc*, 3(2), pp. 66–70.

Fanni, L., Virtuani, A. and Chianese, D. (2011) ‘No Title’, *Solar Energy*, 85(23), pp. 60–73.

Faranda, R. and Leva, S. (2008) ‘Energy Comparison of MPPT Techniques for PV Systems’, *WSEAS Transactions on Power Systems*, 3, pp. 447–455.

Femia, N. *et al.* (2008) ‘Distributed Maximum Power Point Tracking of Photovoltaic Arrays: Novel Approach and System Analysis’, *IEEE Transactions on Industrial Electronics*, 55, pp. 2610–2621.

Ferreira, A. *et al.* (2018) ‘Economic overview of the use and production of photovoltaic solar energy in brazil’, *Renewable and Sustainable Energy Reviews*. Elsevier Ltd, 81(April 2016), pp. 181–191. doi: 10.1016/j.rser.2017.06.102.

Friling, N. *et al.* (2009) ‘No Title’, *Energy and Buildings*, 41(105), pp. 1–7.

Garg, H. P. (1974) ‘No Title’, *Solar Energy*, 4(1974), pp. 299–302.

GENI (2014) *Global electricity grid - linking renewable energy resources around the world (how is 100% renewable energy possible for Nigeria).*

Gholami, A. *et al.* (2018) ‘Experimental investigation of dust deposition effects on photo-voltaic output performance’, *Solar Energy*, 159(2018), p. 346352.

Gholami, A., Saboonchi, A. and Alemrajabi, A. A. (2017) ‘Experimental study of factors affecting dust accumulation and their effects on the transmission coefficient of glass for solar applications’, *Renewable Energy*, 112(2017), pp. 466–473.

Giwa, A. *et al.* (2016) ‘A comprehensive review on biomass

and solar energy for sustainable energy generation in Nigeria', *Renewable and Sustainable Energy Reviews*, 69, pp. 620–641.

Goosens, D. and Kerschaever, E. V. (1999) 'Aeolian dust deposition on photovoltaic solar cells: the effects of wind velocity and airborne dust concentration on cell performance', *Solar Energy*, 66(2), pp. 77–89.

Graham-Cumming, J. (2009) *The Geek Atlas: 128 places where science & technology come alive*. First Edit. Edited by J. Steele and R. Monaghan. Sebastopol CA USA: O'Reilly Media Inc.

Guan, Y. *et al.* (2017) 'In-situ investigation of the effect of dust deposition on the performance of polycrystalline silicon photovoltaic modules', *Renewable Energy*, 101(2017), pp. 1273–1284.

Gueymard, C. A. (2004) 'The sun's total and spectral irradiance for solar energy applications and solar radiation models', *Solar Energy*, 76(4), pp. 423–453.

Hachicha, A. A., Al-Sawafta, I. and Said, Z. (2019) 'Impact of dust on the performance of solar photovoltaic (PV) systems under United Arab Emirates weather conditions', *Renewable Energy*, 141(2019), pp. 287–297.

Hahm, J. *et al.* (2015) 'Matlab-Based Modeling and Simulations to Study the Performance of Different MPPT Techniques Used for Photovoltaic Systems under Partially Shaded Conditions', *International Journal of Photoenergy*, 2015, pp. 1–10.

Hassan, A. H. *et al.* (2005) 'Effect of airborne dust concentration on the performance of PV modules', *Journal of Astronomy Society of Egypt*, 13(1), pp. 24–38.

Hayrettin, C. (2013) ‘Model of a photovoltaic panel emulator in MATLAB–Simulink’, *Turk J Electr Eng Comput Sci*, 21(2013), pp. 301–308.

Honsberg, C. and Bowden, S. (2019) *Fill Factor | PVEducation*, *PVeducation*. Available at: https://www.pveducation.org/pvcdrom/solar-cell-operation/fill-factor (Accessed: 18 April 2020).

Hunter, C. J. *et al.* (2012) ‘Absorption Characteristics of GaAs 1 − x Bi x / GaAs Diodes in the Near-Infrared’, *IEEE Photonics Technology Letters*, 24(23), pp. 2191–2194. doi: 10.1109/LPT.2012.2225420.

Ibitoye, F. I. and Adenikinju, A. (2007) ‘Future demand for electricity in Nigeria’, *Pplied Energy*, 84(5), pp. 492–504.

IEA (2017) *Key world energy statistics*.

IEA (2018) *World Energy Outlook*. Available at: https://webstore.iea.org/download/summary/190?fileName=English-WEO-2018-ES.pdf.

IEA (2019a) *Global Energy & CO2 Status Report: The latest trends in energy and emissions in 2018*. Available at: https://www.iea.org/geco/electricity/.

IEA (2019b) *What is Energy Security*, *International Energy Agency*. Available at: https://www.iea.org/topics/energysecurity/whatisenergysecurity/.

International Energy Agency (2011) *Solar Energy Perspectives: Executive Summary*.

IRENA (2019) *RENEWABLE POWER GENERATION COSTS IN 2018*. Abu Dhabi. Available at: https://www.irena.org/-

/media/Files/IRENA/Agency/Publication/2019/May/IRENA_Renewable-Power-Generations-Costs-in-2018.pdf.

Jiang, H., Lu, L. and Sun, K. (2011) 'Experimental investigation of the impact of airborne dust deposition on the performance of solar photovoltaic (PV) modules', *Atmospheric Environment Journal*, 45(4), pp. 299–304.

Jiang, Hai, Lu, L. and Sun, K. (2011) 'Experimental investigation of the impact of airborne dust deposition on the performance of solar photovoltaic (PV) modules', *Atmospheric Environment*, 45(25), pp. 4299–4304.

Jordan, D. C. and Kurtz, S. R. (2012) 'Photovoltaic Degradation Rates — An Analytical Review', *Progress in Photovoltaics*, pp. 1–32.

Ju, X. *et al.* (2017) 'A review on the development of photovoltaic/concentrated solar power (PV-CSP) hybrid systems', *Solar Energy Materials and Solar Cells*. Elsevier, 161(November 2016), pp. 305–327. doi: 10.1016/j.solmat.2016.12.004.

Kaldellis, J. K. and Kapsali, M. (2011) 'Simulating the dust effect on the energy performance of photovoltaic generators based on experimental measurements', *Energy*, 36(2011), pp. 5154–5161.

Kalogirou, Soteris A., Agathokleous, Rafaela Panayiotou, G. (2013) 'On-site PV characterization and the effect of soiling on their performance', *Energy*, 51(1), pp. 439–446.

Kane, A. and Verma, V. (2013) 'Performance enhancement of building integrated photovoltaic module using thermoelectric cooling', *International Journal of Renewable Energy Research*, 3(2), pp. 320–325.

Karafil, A., Ozbay, H. and Kesler, M. (2016) 'Temperature

and Solar Radiation Effectson Photovoltaic Panel Power', *Journal of New Results in Science*, 12(2016), pp. 48–58.

Kazem, A. A., Chainchan, M. T. and Kazem, H. A. (2014) 'Dust effect on photovoltaic utilization in Iraq: Review article', *Renewable & Sustainable Energy Reviews*, 37, pp. 734–749.

Ketlhwaafetse, R. (2016) *Comparative study of dilute nitride and bismide sub-junctions for tandem solar cells*. University of Essex.

Knier, G. (2008) *How doPhotovoltaics work?*, *NASA, USA*. Available at: https://science.nasa.gov/science-news/science-at-nasa/2002/solarcells (Accessed: 10 July 2017).

Koutroulis, E. *et al.* (2006) 'Methodology for optimal sizing of stand-alone photovoltaic/wind-generator systems using genetic algorithms', *Solar Energy*, 80(10), pp. 72–88.

Kumar, N. M. *et al.* (2019) 'Performance, energy loss, and degradation prediction of roof-integrated crystalline solar PV system installed in Northern India', *Case Studies in Thermal Engineering*, 13(2019), pp. 1–9.

Lal, S. and Raturi, A. (2012) 'Techno-economic analysis of a hybrid mini-grid system for Fiji islands', *International Journal of Energy and Environmental Engineering*, 3(10). doi: 10.1186/2251-6832-3-10.

Leonics (2017) *How to Design Solar PV System*.

LEONICS (2017) *Basics of Solar Cell*. Available at: http://www.leonics.com/support/article2_13j/articles2_13j_en.php (Accessed: 10 May 2017).

Liu, C., Wu, B. and Cheung, R. (2004) 'Advanced Algorithm for MPPT Control of Photovoltaic Systems', in *Canadian*

Solar Buildings Conference. Montreal.

Malvern-Panalytical (2020) *Mastersizer 3000*, *Mastersizer 3000 Product Overview*. Available at: https://www.malvernpanalytical.com/en/products/product-range/mastersizer-range/mastersizer-3000/?creative=317614278903&keyword=%2Bmastersizer%2B3000&matchtype=b&network=g&device=c&gclid=CjwKCAjwnIr1BRAWEiwA6GpwNXsRojTMaWvkFWaK5N_kYjjgRhYJ-tk4upjgnWYadFEO (Accessed: 23 April 2020).

Malvoni, M., De-Giorgi, G. M. and Congedo, P. M. (2017) 'Study of degradation of a grid connected photovoltaic system', *Energy Procedia*, 126(201709), pp. 644–650.

Mann, P. E. (2012) 'Africa-EU Renewable Energy Cooperation Programme (RECP) What is the RECP ?', (November). Available at: https://www.climateinvestmentfunds.org/sites/cif_enc/files/RECP - Gender SREP Feb15.pdf.

Mckinsey (2019) *Global energy perspective 2019: Reference case*. Available at: https://www.mckinsey.com/~/media/McKinsey/Industries/Oil and Gas/Our Insights/Global Energy Perspective 2019/McKinsey-Energy-Insights-Global-Energy-Perspective-2019_Reference-Case-Summary.ashx.

Mekhilef, S. *et al.* (2012) 'Solar energy in Malaysia: current state and prospects', *Renewable & Sustainable Energy Reviews*, 15(1), pp. 386–396.

Menoufi, K. *et al.* (2017) 'Dust accumulation on photovoltaic panels: A case study at the East Bank of the Nile (Beni-Suef, Egypt)', *Energy Procedia*. Elsevier B.V., 128, pp. 24–31. doi: 10.1016/j.egypro.2017.09.010.

Menoufi, K. (2017) 'Dust accumulation on the surface of

photovoltaic panels: Introducing the Photovoltaic Soiling Index (PVSI)', *Sustainability (Switzerland)*, 9(6). doi: 10.3390/su9060963.

Michael, J. J., Iniyan, S. and Goic, R. (2015) 'Flat plate solar photovoltaic-thermal (PV/T) systems: A reference guide', *Renewable and Sustainable Energy Reviews*. Elsevier, 51, pp. 62–88. doi: 10.1016/j.rser.2015.06.022.

Micheli, L. and Deceglie, M. G. (2018) 'Predicting Future Soiling Losses Using Environmental Data', in *35th European PV Solar Energy Conference & Exhibition (EU PVSEC)*. Brussels: National Renewable Energy Laboratory. NREL/CP-5K00-71127., pp. 1–4. Available at: https://www.nrel.gov/docs/fy19osti/71127.pdf.

Micheli, L. and Muller, M. (2017) 'An investigation of the key parameters for predicting PV soiling losses', *Progress in Photovoltaic Reearch and Application*, 25, pp. 291–307.

Mohammed, Y. S. and Mokhtar, A. S. (2013) 'Renewable energy resources for distributed power generation in Nigeria: A review of the potential', *Renewable and Sustainable Energy Reviews*, 22(2013), pp. 257–268.

Moreno-Tejera, S. *et al.* (2016) 'Solarresource assessment in Seville, Spain. Statistical characterisation of solar radiation at different time resolutions', *Solar Energy*, 132(2016), pp. 430–441.

Musanga, Ligavo Margdaline Barasa, W. H. and Maxwell, M. (2018) 'he Effect of Irradiance and Temperature on the Performance of Monocrystalline Silicon Solar Module in Kakamega', *Physical Science International Journal*, 19(4), pp. 1–9.

Narendiran, S. (2013) 'Grid Tie Inverter and MPPT—A Review.', in *2013 International Conference on Circuits,*

Power and Computing Technologies (ICCPCT), pp. 564–567. doi: http://dx.doi.org/10.1109/ICCPCT.2013.6529017.

NASA (2008) *Solar Irradiance*. Available at: https://www.nasa.gov/mission_pages/sdo/science/solar-irradiance.html (Accessed: 17 July 2017).

Nasiri, N. A. *et al.* (2019) 'Investigation of a single-layer EBC deposited on SiC/SiC CMCs: Processing and corrosion behaviour in high-temperature steam', *Journal of the European Ceramic Society*, 39(8), pp. 2703–2711.

Nasrin, R., Hassanuzzaman, M. and Rahim, N. A. (2017) 'Effect of high irradiation on photovoltaic power and energy', *International Journal of Energy Research*, 42(3).

Nations, U. (2015) *Transforming our world: The 2030 agenda for sustainable development.*, *UN*. Available at: https://sustainabledevelopment.un.org/content/documents/21252030 Agenda for Susta (Accessed: 6 October 2018).

NREL (2014) *Homer*, *Nationaal Renewable Energy Laboratory*. Available at: https://www.nrel.gov/docs/fy04osti/35406.pdf (Accessed: 20 September 2020).

NREL (2020a) *Country and Regional Projects in Africa*, *International Activities*. Available at: https://www.nrel.gov/international/projects-africa.html (Accessed: 27 September 2020).

NREL (2020b) *System Advisor Model (SAM) Release Notes*. Available at: https://nrel.github.io/SAM/doc/releasenotes.html (Accessed: 19 September 2020).

Ogbonnaya, C. *et al.* (2019) 'The current and emerging renewable energy technologies for power generation in

Nigeria: A Review', *Thermal Science and Engineering Progress*. doi: https://doi.org/10.1016/j.tsep.2019.100390.

Oghogho, I. *et al.* (2014) 'SOLAR ENERGY POTENTIAL AND ITS DEVELOPMENT FOR SUSTAINABLE ENERGY GENERATION IN NIGERIA: A ROAD MAP TO ACHIEVING THIS FEAT', *International Journal of Engineering and Management Sciences*, 5(2), pp. 61–67.

Ojosu, J. (1990) 'The iso-radiation map for Nigeria', *Solar & Wind Technology*, 7(5), pp. 563–575.

Onwe, C. A. (2017) *Modelling and Assessment of Renewable Energy Systems for Remote Rural Areas in Nigeria*. University of Dundee.

Osinowo, A. A. *et al.* (2015) 'Analysis of Global Solar Irradiance over Climatic Zones in Nigeria for Solar Energy Applications', *Journal of Solar Energy*, 2015, p. 9. Available at: http://downloads.hindawi.com/archive/2015/819307.pdf.

Osueke, C., Uzendu, P. and Ogbonna, I. (2013) 'Study and Evaluation of Solar Energy Variation in Nigeria', *International Journal of Emerging Technology and Advanced Engineering*, 3(6), p. 5.

Panjwani, M. K., Narejo, G. B. and Panjwani, M. K. N. (2014) 'Effect of Humidity on the Efficiency of Solar Cell (photo voltaic)', *International Journal Of Engineering Research and General Science*, 2(4).

Panwar, N. ., Kaushik, S. C. and Kothari, S. (2011) 'Role of Renewable Energy sources in Environmental Protection: A Review', *Renewable Sustainable Energy Reviews*, 15(15), pp. 13–24.

Park, N. (2017) *United Kingdom Population midyear Estimate*, *Office of Natinal Statistics*. Available at:

https://www.ons.gov.uk/peoplepopulationandcommunity/populationandmigration/populationestimates (Accessed: 15 July 2017).

Qasem, H. *et al.* (2014) 'Dust-induced shading on photovoltaic modules', *Progress in Photovoltaics*, 22(2), pp. 218–226.

Radwan, A., Ookawara, S. and Ahmed, M. (2016) 'Analysis and simulation of concentrating photovoltaic systems with a microchannel heat sink', *Solar Energy*, 136, p. 35048.

Rajesh, K., Kulkami, A. D. and Ananthapadmanabha, T. (2015) 'Modeling and Simulation of Solar PV and DFIG Based Wind Hybrid System', *Procedia Technology*, 21, pp. 667–675.

Ramli, Makbul A.M. Prasetyono, Eka Wicaksana, Ragil W. Windarko, Novie A. Sedraoui, K. and Al-Turki, Y. A. (2016) 'On the investigation of photovoltaic output power reduction due to dust accumulation and weather conditions', *Renewable Energy*, 99(2016), pp. 836–844.

Ramos-Hernanz, J. A. *et al.* (2012) 'Two photovoltaic cell simulation models in Matlab/Simulink', *International Journal on Technical and Physical problems of Engineering*, 4(10), pp. 45–51.

Reader, G. T. (2020) 'Energy, Renewables Alone?', in Stagner, J. and Ting, D. K. (eds) *Sustaining Resources for Tomorrow, Green Energy and Technology*. Windsor: Springer.

Ruuska, P., Aikala, A. and Weiss, R. (2014) 'Modelling of Photovoltaic Energy Generation Systems', in *Proceedings of 28th European Conference on Modelling and Simulation*. Brescia, Italy, p. 6.

Sagga, A. M. S. (1993) ‘Roundness of sand grains of longitudinal dunes in saudi arabia’, *Sedimentary Geology*, 87(1), pp. 63–68.

Saidan, M. *et al.* (2016) ‘Experimental study on the effect of dust deposition on solar photovoltaic panels in desert environment’, *Renewable Energy*, 92(2016), pp. 499–505.

Salari, A. and Hakkaki-Fard, A. (2019) ‘A numerical study of dust deposition effects on photovoltaic modules and photovoltaic-thermal systems’, *Renewable Energy*, 135(2019), pp. 437–449.

Salas, V. *et al.* (2006) ‘Review of the Maximum Power Point Tracking Algorithms for Stand-Alone Photovoltaic Systems’, *Solar Energy Materials and Solar Cells*, 90, pp. 555–1578.

Salehin, S., Rahman, M. and Islam, S. (2015) ‘Techno-economic Feasibility Study of a Solar PV-Diesel System for Applications in Northern Part of Bangladesh’, *International Journal of Renewable Energy*, 5(4), pp. 1220–1229.

Salim, A., Huraib, F. and Eugenio, N. (2013) ‘PV power study of system options and optimization’, in *8th european PV solar energy conference*. Florence, Italy.

Sangeetha, K. *et al.* (2015) ‘Modeling, analysis and design of efficient maximum power extraction method for solar PV system’, *Renewable and Sustainable Energy Reviews*, 15, pp. 1015–1024. doi: 10.1016/j.rser.2015.07.146.

Sansom, C. *et al.* (2017) ‘Relectometer comparison for assessment of back-silvered glass solar mirrors concentrating Solar Power’, *Solar Energy*, 155, pp. 496–505.

Sarver, T., Al-Qaraghuli, A. and Kazmersk, L. L. (2013) ‘A comprehensive review of the impact of dust on the use of solar energy: History, investigations, results, literature, and

mitigation approaches', *Renewable and Sustainable Energy Reviews*, 22, pp. 698–733.

Sayigh, A., Al-Jandal, S. and Ahmed, H. (1985) 'Dust effect on solar flat surfaces devices in Kuwait', in *Proceedings of the workshop on the physics of non-conventional energy sources and materials science for energy*. Triest, Italy, pp. 353–367.

Sera, D. *et al.* (2006a) 'Improved MPPT method for rapidly changing environmental conditions', in *Proceedings of the IEEE International Symposium on Industrial Electronics*, pp. 1420–1425.

Sera, D. *et al.* (2006b) 'Improved MPPT Method for Rapidly Changing Environmental Conditions', *IEEE International Symposium on Industrial Electronics*, 2, pp. 1420–1425. Available at: http://dx.doi.org/10.1109/ISIE.2006.295680.

Shaaban, M. and Petinrin, J. O. (2014) 'Renewable energy potentials in Nigeria: Meeting rural energy needs', *Renewable & Sustainable Energy Reviews*, 2014(29), pp. 72–84.

Silva, R. (2013) *Fourth generation solar cell technology for high efficiency, large-area, low cost photovoltaics defined by Surrey academic*, *AiOlus news*. Available at: http://en.aiolusnews.com/energy/fourth-generation-solar-cell-technology-h/ (Accessed: 17 February 2017).

Singh, G. K. (2013) 'Solar power generation by PV (photovoltaic) technology: A review', *Energy*, 53, pp. 1–13.

Smestad, G. p. *et al.* (2020) 'Modelling photovoltaic soiling losses through optical characterization', *Science Report*, 10(58), pp. 1–13. doi: https://doi.org/10.1038/s41598-019-56868-z.

Solarigis (2020) *Solar resource maps*. Available at: https://solargis.com/maps-and-gis-data/download/nigeria (Accessed: 9 September 2020).

South Africa Population Clock (Live) (2017) *South Africa Population Country meter*. Available at: http://countrymeters.info/en/South_Africa (Accessed: 19 September 2017).

Subudhi, B. and Pradhan, R. (2013) 'A comparative study on maximum power point tracking techniques for photovoltaic power systems', *IEEE Transactions on Sustainable Energy*, 4(1), pp. 89–98.

Sumaina, K. (2018) 'Nigeria Needs 9,000 Weather Stations, Says NiMet', *THIS DAY*.

Sumaina, Kasim (2018) 'Nigeria Needs 9,000 Weather Stations, Says NiMet', *THIS DAY*, 25 September. Available at: https://www.thisdaylive.com/index.php/2018/09/25/nigeria-needs-9000-weather-stations-says-nimet/.

Tanesab, J. *et al.* (2017) 'Seasonal effect of dust on the degradation of PV modules performance deployed in different climate areas', *Renewable Energy*, 111(2017), pp. 105–115.

Tanesab, J. *et al.* (2019) 'The effect of dust with different morphologies on the performancedegradation of photovoltaic modules', *Sustainable Energy Technologies and Assessments*, 31(2019), pp. 347–354.

Tanima, B., Chakraborty, A. K. and Kaushik, P. (2014) 'Effects of Ambient Temperature and Wind Speed on Performance of Monocrystalline Solar Photovoltaic Module in Tripura, India', *Journal of Solar Energy*, 2014(2014), pp. 1–5.

The largest Solar Farm in the Southern hemisphere is located in Central South Africa (2017) *Environment*. Available at: https://www.environment.co.za/renewable-energy/largest-solar-farm-southern-hemisphere.html (Accessed: 15 September 2017).

Twidell, J. and Weir, T. (2015) *Renewable Energy Resources*. 3rd edn. New York: Routledge.

USAID (2019) *Nigeria: Power Africa Fact Sheet*, *United States Agency for International Development*. Available at: https://www.usaid.gov/powerafrica/nigeria (Accessed: 19 August 2019).

Wilson, L. (2012) *Average Household Electricity Consumption around the World*, *Shrink That Footprint*.

Wu, X. D. *et al.* (2019) 'Energy use in world economy from household-consumption-based perspective', *Energy Policy*, 127(2019), pp. 287–298. Available at: https://reader.elsevier.com/reader/sd/pii/S0301421518308012?token=BCBE7F6EE848004004D9607DB1BDC31745E3A812F948D1AA81221E9288F8E3D939664700929344482E138187C7A2DF164.

You, S. *et al.* (2018) 'On the temporal modelling of solar photovoltaic soiling: Energy and economic impacts in seven cities', *Applied Energy*, 228(2018), pp. 1136–1146.

Zawilska, E. and Brooks, M. J. (2011) 'An assessment of the solar resource for Durban, SouthAfric', *Renewable Energy*, 36(2011), pp. 3433–3438.

Zweibel, K. and Herch, P. (1984) *Basic photovoltaic principles and methods.* New York: Van Nosstrand Reinhold Company Inc.

Abdulkadir, M., Samosir, A. S. and Yatim, A. H. M. (2012)

‘Modeling and simulation based approach of photovoltaic system in simulink model’, *ARPN J Eng Appl Sci, 7 (5) (2012)*, 7(5), pp. 616–623.

Abdullahi, M. and Singh, S. K. (2014) ‘Global solar radiation evaluation for some selected stations of north Eastern’, *Archives of Physics Research*, 5(2), pp. 1–8.

Abreu, E. F. M. *et al.* (2018) ‘Solar resource assessment through long-term statistical analysis andtypical data generation with different time resolutions using GHI measurements’, *Renewables*, 127(2018), pp. 398–411.

Adedipe, O., Abolarin, M. S. and Mamman, R. O. (2018) ‘A Review of Onshore and Offshore Wind Energy Potential in Nigeria’, *IOP Conference Series: Materials Science and Engineering*, 413(2018), pp. 1–8. doi: 10.1088/1757-899X/413/1/012039.

Adejumo, A. O., Suleiman, E. A. and Okagbue, H. I. (2017) ‘Exploration of solar radiation data from three geo-political zones in Nigeria’, *Data in Brief*, 13, pp. 60–68. doi: 10.1016/j.dib.2017.05.017.

Adinoyi, M. J. and Said, S. A. M. (2013) ‘Effect of dust accumulation on the power outputs of solar photovoltaic modules’, *Renewable Energy*, 60(2013), pp. 633–636.

Ahmed, M. A. M. *et al.* (2014) ‘Effect of Dust Deposition on Performance of Thin Film Photovoltaic Module in Harsh Humid Climate’, in *2nd International Conference on Renewable Energy Research and Applications*. Madrib, Spain.

Al-Hasan, A. Y. and Ghoeneim, A. A. (2005) ‘A new correlation between photovoltaic panel’s efficiency and amount of sand dust accumulated on their surface’, *International Journal of Sustainable energy*, 24(1), pp. 87–

97.

Ali, A. N. A. *et al.* (2012) ‘A Survey of Maximum PPT Techniques of PV Systems.’, *IEEE Energytech*, pp. 1–17.

Aliyu, A. S., Dada, J. O. and Adam, brahim K. (2015) ‘Current status and future prospects of renewable energy in Nigeria’, *RenewableandSustainableEnergyReviews*, 48(2015), pp. 336–346.

Aliyu, A. S., Dada, J. O. and Adam, I. K. (2015) ‘Current Status and Future Prospects of Renewable Energy in Nigeria’, *Renewable and Sustainable Energy Reviews*, 48, pp. 336–346. doi: 10.1016/j.rser.2015.03.098.

Aliyu, A. S., Ramli, A. T. and Saleh, M. A. (2013) ‘Nigeria electricity crisis : Power generation capacity expansion and environmental rami fi cations’, *Energy*, 61, pp. 354–367. doi: 10.1016/j.energy.2013.09.011.

Amajama, J. and Oku, D. E. (2016) ‘Effect of Relative humidity on Photovoltaic panels’ output and solar illuminance/intensity’, *Journal of Scientific and Engineering Research*, 3(4), pp. 126–130.

Appels, R. *et al.* (2013) ‘Effect of soiling on photovoltaic modules’, *Solar Energy*, 96, pp. 283–291.

Ayoola, M. A. A. *et al.* (2014) ‘Measurements of net all-wave radiation at a tropical location, Ile-Ife, Nigeria’, *Atmosfera*, 27(3), pp. 305–315.

Aysha, A. *et al.* (2015) ‘Experimental analysis of solar PV characteristics under standard condition’, *International Journal of Applied Engineering Research*, 10(20), pp. 17970–17975.

Ayvazoğluyüksel, Ö. and Filik, Ü. B. (2018) ‘Estimation

methods of global solar radiation, cell temperature and solar power forecasting: A review and case study in Eskişehir', *Renewable and Sustainable Energy Reviews*, 91(May 2017), pp. 639–653. doi: 10.1016/j.rser.2018.03.084.

Azuri to roll out PayGo Solar to 20,000 Nigerian households (2016) *PV Magazine*. Available at: https://www.pv-magazine.com/2017/02/01/azuri-to-roll-out-paygo-solar-to-20000-nigerian-households/ (Accessed: 19 February 2017).

Babaa, S. E., Matthew, A. and Pickert, V. (2014) 'Overview of Maximum Power Point Tracking Control Methods for PV Systems', *Journal of Power and Energy Engineering*, 02(08), pp. 59–72.

Bagher, A. mohammed, Vahid, M. M. and Mohsen, M. (2015) 'Types of Solar Cells and Application', *American Journal of Optics and Photonics*, 3(5), pp. 94–113. doi: 10.11648/j.ajop.20150305.17.

Bala, E. J. (2014) 'Overview of the National Energy Policy & Energy Demand and Supply Projection Studies for Nigeria', in *7th IAEE/NAEE Annual Conference*. Abuja, pp. 1–63.

Bamisile, O. *et al.* (2017) 'A review of renewable energy potential in Nigeria; Solar power development over the years', *Engineering and Applied Science Research*, 44(4), pp. 242–248.

Banu, I. V., Beniuga, R. C. and Istrate, M. (2013) 'Study on Temperature for Modeling of Photovoltaic Solar Array using Experimental Test Data', in *5th International Conference on Modern Power Systems*, pp. 28–31.

Barakati, M., Kazerani, M. and Aplevich, D. (2009) 'Maximum Power Tracking Control for a Wind Turbine System Including a Matrix Converter', *IEEE Power & Energy Society General Meeting*, 24, pp. 705–713.

BBC (2019) *The biggest energy challenges facing humanity*. London. Available at: http://www.bbc.com/future/story/20170313-the-biggest-energy-challenges-facing-humanity.

Beattie, N. S. *et al.* (2012) 'Understanding the effects of sand and dust accumulation on photovoltaic modules', *Renewable Energy*, 48(2012), pp. 448–452.

Bello, G. (2017) *Nigeria's Population now 182 million*, *National Population Commission*. Available at: http://population.gov.ng/nigerias-population-now-182-million-npc/ (Accessed: 15 July 2017).

Blair, N. *et al.* (2014) *System Advisor Model, SAM 2014.1.14: General Description*. Oak Ridge. Available at: www.nrel.gov/publications.

Boukili, Y. *et al.* (2018) 'Experimental validation of a photovoltaic panel model', in *International Conference on Renewable Energies and Energy Efficiency*, pp. 1–8.

Burns, J. E. and Kang, J. S. (2012) 'Comprehensive economic analysis for supporting policies for residential solar PV in the United States: solar renewable energy credit (SREC) potential.', *Energy Policy*, 44(2), pp. 17–25.

Chanchangi, Y. N. *et al.* (2020) 'Dust and PV Performance in Nigeria: A review', *Renewable and Sustainable Energy Reviews*, 121(2020), pp. 1–14.

Chandel, M. *et al.* (2014) 'Techno-economic analysis of solar photovoltaic power plant for garment zone of Jaipur city', *Case Studies in Thermal Engineering*, 2, pp. 1–7. doi: 10.1016/j.csite.2013.10.002.

Charfi, S., Atieh, A. and Chaabene, M. (2016) 'Modeling and cost analysis for different PV/battery/diesel operating options

driving a load in Tunisia, Jordan and KSA', *Sustainable Cities and Society*. Elsevier B.V., 25, pp. 49–56. doi: 10.1016/j.scs.2016.02.006.

Chen, L. R. *et al.* (2010) 'A Biological Swarm Chasing Algorithm for Tracking the PV Maximum Power Point', *IEEE Transactions on Energy Conversion*, 25, pp. 963–973.

Chikate, B. V. and Sadawarte, Y. A. (2015) 'Factor Affecting the Performance of Solar Cells', *International Journal of Computer Applications*, pp. 1–5.

Chineke, T. C., Aina, J. I. and Jagtap, S. S. (1999) 'Solar radiation data base for Nigeria', *Discovery and Innovation*, 11(3), pp. 207–210.

Cleaver, J. A. S. and Tyrrell, J. W. G. (2004) 'The Influence of Relative Humidity on Particle Adhesion – a Review of Previous Work and the Anomalous Behaviour of Soda-lime Glass', *Powder and particle*, 22.

Coiante, D. B. (1992) 'Can photovoltaics become an effective energy option', *Solar Energy Materials and Solar Cells*, 27(1), pp. 79–89.

Costaa, S. C. S., Diniza, A. S. A. C. and Kazmerskia, L. L. (2018) 'Solar energy dust and soiling R & D progress: Literature review update for 2016', *Renewable and Sustainable Energy Reviews*, 82(2018), pp. 2504–2536.

Cruz-Matias, A. I. (2013) *Contribution to structural parameters computation: volume models and methods*. Universitat Politecnica de Catalunya, Bacelona.

Dada, B. M. and Okogbu, E. C. (2017) 'Estimating Daily Solar Radiation from Monthly Values Over Selected Nigeria Stations for Solar Energy Utilization', *Journal of Fundamentals of Renewable Energy J and Applications*,

7(6), pp. 1–3.

DaftLogic (2019) *List of the Power Consumption of Typical Household Appliances*, *Online web publication*. Available at: https://www.daftlogic.com/information-appliance-power-consumption.htm (Accessed: 24 April 2020).

Dorofte, C., Borup, U. and Blaabjerg, F. (2005) 'A Combined Two-Method MPPT Control Scheme for Grid-Connected Photovoltaic Systems', in *2005 European Conference on Power Electronics and Applications*. Dresden.

Douglah, M. (2018) 'Oil states energy services v. Greene's energy group: The future of Inter partes review and its impact on the energy sector', *Oil and Gas, Natural Resources and Energy Journal*, 3(6), pp. 1343–1362.

Dudley, B. (2019) *BP Statistical Review of World Energy*. Available at: https://www.bp.com/content/dam/bp/business-sites/en/global/corporate/pdfs/energy-economics/statistical-review/bp-stats-review-2019-full-report.pdf.

Duffie, J., Beckman, W. and Worek, W. M. (2013) *Solar engineering of Thermal Processes*. 4th edn. John Wiley & Sons.

Dumont, J. *et al.* (2013) *What is a Solar Hybrid System?*, *SMA Corporate Blog*. Available at: http://www.smainverted.com/what-is-a-photovoltaic-diesel-hybrid-system/ (Accessed: 22 February 2017).

Ehsan, F. and Abbas, A.-S. (2016) 'The Impact of the Environmental Condition on the Performance of the Photovoltaic Cell', *American Journal of Energy Engineering*, 4(1), pp. 1–7.

EIA (2019) *Renewable Energy Explained*, *US Energy Information Administration*. Available at:

https://www.eia.gov/energyexplained/?page=renewable_home (Accessed: 20 August 2019).

El-Shobokshy, M. S. and Hussein, F. M. (1993) ‘Effect of dust with different physical properties on the performance of photovoltaic cells’, *Solar Energy*, 51(5), pp. 5–11.

El-Shobokshy, M.S. and Hussein, F. M. (1993) ‘Effect of the dust with different physical properties on the performance of photovoltaic cells’, *Solar Energy*, 51(1993), pp. 505–511.

Eliminir, H. K. *et al.* (2006) ‘Effect of dust on the transparent cover of solar collectors.’, *Energy Conversion and Management*, 47(3), pp. 192–203.

Elminir, H. K. *et al.* (2006) ‘Effect of Dust on Transparent cover of Solar Collectors’, *Energy Conversion and Management*, 47(18–19), pp. 3192–3203.

Elminir, H. K. and Abdel-Moneim, K. M. (2006) ‘Effect of dust on the transparent cover of solar collectors’, *Energy Conversion and Management*, 47(18–19), pp. 3192–3203.

Esram, T. and Chapman, P. L. (2007) ‘Comparison of Photovoltaic Array Maximum Power Point Tracking Techniques’, *IEEE Transactions on Energy Conversion*, 22, pp. 439–449. Available at: http://dx.doi.org/10.1109/TEC.2006.874230.

Ettah, E. B. *et al.* (2015) ‘Comparative Study of the Effects of Relative Humidity on Solar Electricity Generation in UYO and Port- Harcourt, Nigeria’, *nternational Journal of Mathematics and Physical Sciences Researc*, 3(2), pp. 66–70.

Fanni, L., Virtuani, A. and Chianese, D. (2011) ‘No Title’, *Solar Energy*, 85(23), pp. 60–73.

Faranda, R. and Leva, S. (2008) ‘Energy Comparison of

MPPT Techniques for PV Systems', *WSEAS Transactions on Power Systems*, 3, pp. 447–455.

Femia, N. *et al.* (2008) 'Distributed Maximum Power Point Tracking of Photovoltaic Arrays: Novel Approach and System Analysis', *IEEE Transactions on Industrial Electronics*, 55, pp. 2610–2621.

Ferreira, A. *et al.* (2018) 'Economic overview of the use and production of photovoltaic solar energy in brazil', *Renewable and Sustainable Energy Reviews*. Elsevier Ltd, 81(April 2016), pp. 181–191. doi: 10.1016/j.rser.2017.06.102.

Friling, N. *et al.* (2009) 'No Title', *Energy and Buildings*, 41(105), pp. 1–7.

Garg, H. P. (1974) 'No Title', *Solar Energy*, 4(1974), pp. 299–302.

GENI (2014) *Global electricity grid - linking renewable energy resources around the world (how is 100% renewable energy possible for Nigeria).*

Gholami, A. *et al.* (2018) 'Experimental investigation of dust deposition effects on photo-voltaic output performance', *Solar Energy*, 159(2018), p. 346352.

Gholami, A., Saboonchi, A. and Alemrajabi, A. A. (2017) 'Experimental study of factors affecting dust accumulation and their effects on the transmission coefficient of glass for solar applications', *Renewable Energy*, 112(2017), pp. 466–473.

Giwa, A. *et al.* (2016) 'A comprehensive review on biomass and solar energy for sustainable energy generation in Nigeria', *Renewable and Sustainable Energy Reviews*, 69, pp. 620–641.

Goosens, D. and Kerschaever, E. V. (1999) ‘Aeolian dust deposition on photovoltaic solar cells: the effects of wind velocity and airborne dust concentration on cell performance’, *Solar Energy*, 66(2), pp. 77–89.

Graham-Cumming, J. (2009) *The Geek Atlas: 128 places where science & technology come alive*. First Edit. Edited by J. Steele and R. Monaghan. Sebastopol CA USA: O’Reilly Media Inc.

Guan, Y. *et al.* (2017) ‘In-situ investigation of the effect of dust deposition on the performance of polycrystalline silicon photovoltaic modules’, *Renewable Energy*, 101(2017), pp. 1273–1284.

Gueymard, C. A. (2004) ‘The sun’s total and spectral irradiance for solar energy applications and solar radiation models’, *Solar Energy*, 76(4), pp. 423–453.

Hachicha, A. A., Al-Sawafta, I. and Said, Z. (2019) ‘Impact of dust on the performance of solar photovoltaic (PV) systems under United Arab Emirates weather conditions’, *Renewable Energy*, 141(2019), pp. 287–297.

Hahm, J. *et al.* (2015) ‘Matlab-Based Modeling and Simulations to Study the Performance of Different MPPT Techniques Used for Photovoltaic Systems under Partially Shaded Conditions’, *International Journal of Photoenergy*, 2015, pp. 1–10.

Hassan, A. H. *et al.* (2005) ‘Effect of airborne dust concentration on the performance of PV modules’, *Journal of Astronomy Society of Egypt*, 13(1), pp. 24–38.

Hayrettin, C. (2013) ‘Model of a photovoltaic panel emulator in MATLAB–Simulink’, *Turk J Electr Eng Comput Sci*, 21(2013), pp. 301–308.

Honsberg, C. and Bowden, S. (2019) *Fill Factor | PVEducation*, *PVeducation*. Available at: https://www.pveducation.org/pvcdrom/solar-cell-operation/fill-factor (Accessed: 18 April 2020).

Hunter, C. J. *et al.* (2012) 'Absorption Characteristics of GaAs 1 − x Bi x / GaAs Diodes in the Near-Infrared', *IEEE Photonics Technology Letters*, 24(23), pp. 2191–2194. doi: 10.1109/LPT.2012.2225420.

Ibitoye, F. I. and Adenikinju, A. (2007) 'Future demand for electricity in Nigeria', *Pplied Energy*, 84(5), pp. 492–504.

IEA (2017) *Key world energy statistics*.

IEA (2018) *World Energy Outlook*. Available at: https://webstore.iea.org/download/summary/190?fileName=English-WEO-2018-ES.pdf.

IEA (2019a) *Global Energy & CO2 Status Report: The latest trends in energy and emissions in 2018*. Available at: https://www.iea.org/geco/electricity/.

IEA (2019b) *What is Energy Security*, *International Energy Agency*. Available at: https://www.iea.org/topics/energysecurity/whatisenergysecurity/.

International Energy Agency (2011) *Solar Energy Perspectives: Executive Summary*.

IRENA (2019) *RENEWABLE POWER GENERATION COSTS IN 2018*. Abu Dhabi. Available at: https://www.irena.org/-/media/Files/IRENA/Agency/Publication/2019/May/IRENA_Renewable-Power-Generations-Costs-in-2018.pdf.

Jiang, H., Lu, L. and Sun, K. (2011) 'Experimental

investigation of the impact of airborne dust deposition on the performance of solar photovoltaic (PV) modules', *Atmospheric Environment Journal*, 45(4), pp. 299–304.

Jiang, Hai, Lu, L. and Sun, K. (2011) 'Experimental investigation of the impact of airborne dust deposition on the performance of solar photovoltaic (PV) modules', *Atmospheric Environment*, 45(25), pp. 4299–4304.

Jordan, D. C. and Kurtz, S. R. (2012) 'Photovoltaic Degradation Rates — An Analytical Review', *Progress in Photovoltaics*, pp. 1–32.

Ju, X. *et al.* (2017) 'A review on the development of photovoltaic/concentrated solar power (PV-CSP) hybrid systems', *Solar Energy Materials and Solar Cells*. Elsevier, 161(November 2016), pp. 305–327. doi: 10.1016/j.solmat.2016.12.004.

Kaldellis, J. K. and Kapsali, M. (2011) 'Simulating the dust effect on the energy performance of photovoltaic generators based on experimental measurements', *Energy*, 36(2011), pp. 5154–5161.

Kalogirou, Soteris A., Agathokleous, Rafaela Panayiotou, G. (2013) 'On-site PV characterization and the effect of soiling on their performance', *Energy*, 51(1), pp. 439–446.

Kane, A. and Verma, V. (2013) 'Performance enhancement of building integrated photovoltaic module using thermoelectric cooling', *International Journal of Renewable Energy Research*, 3(2), pp. 320–325.

Karafil, A., Ozbay, H. and Kesler, M. (2016) 'Temperature and Solar Radiation Effectson Photovoltaic Panel Power', *Journal of New Results in Science*, 12(2016), pp. 48–58.

Kazem, A. A., Chainchan, M. T. and Kazem, H. A. (2014)

‘Dust effect on photovoltaic utilization in Iraq: Review article’, *Renewable & Sustainable Energy Reviews*, 37, pp. 734–749.

Ketlhwaafetse, R. (2016) *Comparative study of dilute nitride and bismide sub-junctions for tandem solar cells*. University of Essex.

Knier, G. (2008) *How doPhotovoltaics work?*, *NASA, USA*. Available at: https://science.nasa.gov/science-news/science-at-nasa/2002/solarcells (Accessed: 10 July 2017).

Koutroulis, E. *et al.* (2006) ‘Methodology for optimal sizing of stand-alone photovoltaic/wind-generator systems using genetic algorithms’, *Solar Energy*, 80(10), pp. 72–88.

Kumar, N. M. *et al.* (2019) ‘Performance, energy loss, and degradation prediction of roof-integrated crystalline solar PV system installed in Northern India’, *Case Studies in Thermal Engineering*, 13(2019), pp. 1–9.

Lal, S. and Raturi, A. (2012) ‘Techno-economic analysis of a hybrid mini-grid system for Fiji islands’, *International Journal of Energy and Environmental Engineering*, 3(10). doi: 10.1186/2251-6832-3-10.

Leonics (2017) *How to Design Solar PV System*.

LEONICS (2017) *Basics of Solar Cell*. Available at: http://www.leonics.com/support/article2_13j/articles2_13j_en.php (Accessed: 10 May 2017).

Liu, C., Wu, B. and Cheung, R. (2004) ‘Advanced Algorithm for MPPT Control of Photovoltaic Systems’, in *Canadian Solar Buildings Conference*. Montreal.

Malvern-Panalytical (2020) *Mastersizer 3000*, *Mastersizer 3000 Product Overview*. Available at:

https://www.malvernpanalytical.com/en/products/product-range/mastersizer-range/mastersizer-3000/?creative=317614278903&keyword=%2Bmastersizer%2B3000&matchtype=b&network=g&device=c&gclid=CjwKCAjwnIr1BRAWEiwA6GpwNXsRojTMaWvkFWaK5N_kYjjgRhYJ-tk4upjgnWYadFEO (Accessed: 23 April 2020).

Malvoni, M., De-Giorgi, G. M. and Congedo, P. M. (2017) 'Study of degradation of a grid connected photovoltaic system', *Energy Procedia*, 126(201709), pp. 644–650.

Mann, P. E. (2012) 'Africa-EU Renewable Energy Cooperation Programme (RECP) What is the RECP ?', (November). Available at: https://www.climateinvestmentfunds.org/sites/cif_enc/files/RECP - Gender SREP Feb15.pdf.

Mckinsey (2019) *Global energy perspective 2019: Reference case*. Available at: https://www.mckinsey.com/~/media/McKinsey/Industries/Oil and Gas/Our Insights/Global Energy Perspective 2019/McKinsey-Energy-Insights-Global-Energy-Perspective-2019_Reference-Case-Summary.ashx.

Mekhilef, S. *et al.* (2012) 'Solar energy in Malaysia: current state and prospects', *Renewable & Sustainable Energy Reviews*, 15(1), pp. 386–396.

Menoufi, K. *et al.* (2017) 'Dust accumulation on photovoltaic panels: A case study at the East Bank of the Nile (Beni-Suef, Egypt)', *Energy Procedia*. Elsevier B.V., 128, pp. 24–31. doi: 10.1016/j.egypro.2017.09.010.

Menoufi, K. (2017) 'Dust accumulation on the surface of photovoltaic panels: Introducing the Photovoltaic Soiling Index (PVSI)', *Sustainability (Switzerland)*, 9(6). doi: 10.3390/su9060963.

Michael, J. J., Iniyan, S. and Goic, R. (2015) ‘Flat plate solar photovoltaic-thermal (PV/T) systems: A reference guide’, *Renewable and Sustainable Energy Reviews*. Elsevier, 51, pp. 62–88. doi: 10.1016/j.rser.2015.06.022.

Micheli, L. and Deceglie, M. G. (2018) ‘Predicting Future Soiling Losses Using Environmental Data’, in *35th European PV Solar Energy Conference & Exhibition (EU PVSEC)*. Brussels: National Renewable Energy Laboratory. NREL/CP-5K00-71127., pp. 1–4. Available at: https://www.nrel.gov/docs/fy19osti/71127.pdf.

Micheli, L. and Muller, M. (2017) ‘An investigation of the key parameters for predicting PV soiling losses’, *Progress in Photovoltaic Reearch and Application*, 25, pp. 291–307.

Mohammed, Y. S. and Mokhtar, A. S. (2013) ‘Renewable energy resources for distributed power generation in Nigeria: A review of the potential’, *Renewable and Sustainable Energy Reviews*, 22(2013), pp. 257–268.

Moreno-Tejera, S. *et al.* (2016) ‘Solarresource assessment in Seville, Spain. Statistical characterisation of solar radiation at different time resolutions’, *Solar Energy*, 132(2016), pp. 430–441.

Musanga, Ligavo Margdaline Barasa, W. H. and Maxwell, M. (2018) ‘he Effect of Irradiance and Temperature on the Performance of Monocrystalline Silicon Solar Module in Kakamega’, *Physical Science International Journal*, 19(4), pp. 1–9.

Narendiran, S. (2013) ‘Grid Tie Inverter and MPPT—A Review.’, in *2013 International Conference on Circuits, Power and Computing Technologies (ICCPCT)*, pp. 564–567. doi: http://dx.doi.org/10.1109/ICCPCT.2013.6529017.

NASA (2008) *Solar Irradiance*. Available at:

https://www.nasa.gov/mission_pages/sdo/science/solar-irradiance.html (Accessed: 17 July 2017).

Nasiri, N. A. *et al.* (2019) 'Investigation of a single-layer EBC deposited on SiC/SiC CMCs: Processing and corrosion behaviour in high-temperature steam', *Journal of the European Ceramic Society*, 39(8), pp. 2703–2711.

Nasrin, R., Hassanuzzaman, M. and Rahim, N. A. (2017) 'Effect of high irradiation on photovoltaic power and energy', *International Journal of Energy Research*, 42(3).

Nations, U. (2015) *Transforming our world: The 2030 agenda for sustainable development.*, *UN*. Available at: https://sustainabledevelopment.un.org/content/documents/21252030 Agenda for Susta (Accessed: 6 October 2018).

NREL (2014) *Homer*, *Nationaal Renewable Energy Laboratory*. Available at: https://www.nrel.gov/docs/fy04osti/35406.pdf (Accessed: 20 September 2020).

NREL (2020a) *Country and Regional Projects in Africa*, *International Activities*. Available at: https://www.nrel.gov/international/projects-africa.html (Accessed: 27 September 2020).

NREL (2020b) *System Advisor Model (SAM) Release Notes*. Available at: https://nrel.github.io/SAM/doc/releasenotes.html (Accessed: 19 September 2020).

Ogbonnaya, C. *et al.* (2019) 'The current and emerging renewable energy technologies for power generation in Nigeria: A Review', *Thermal Science and Engineering Progress*. doi: https://doi.org/10.1016/j.tsep.2019.100390.

Oghogho, I. *et al.* (2014) 'SOLAR ENERGY POTENTIAL

AND ITS DEVELOPMENT FOR SUSTAINABLE ENERGY GENERATION IN NIGERIA: A ROAD MAP TO ACHIEVING THIS FEAT', *International Journal of Engineering and Management Sciences*, 5(2), pp. 61–67.

Ojosu, J. (1990) 'The iso-radiation map for Nigeria', *Solar & Wind Technology*, 7(5), pp. 563–575.

Onwe, C. A. (2017) *Modelling and Assessment of Renewable Energy Systems for Remote Rural Areas in Nigeria*. University of Dundee.

Osinowo, A. A. *et al.* (2015) 'Analysis of Global Solar Irradiance over Climatic Zones in Nigeria for Solar Energy Applications', *Journal of Solar Energy*, 2015, p. 9. Available at: http://downloads.hindawi.com/archive/2015/819307.pdf.

Osueke, C., Uzendu, P. and Ogbonna, I. (2013) 'Study and Evaluation of Solar Energy Variation in Nigeria', *International Journal of Emerging Technology and Advanced Engineering*, 3(6), p. 5.

Panjwani, M. K., Narejo, G. B. and Panjwani, M. K. N. (2014) 'Effect of Humidity on the Efficiency of Solar Cell (photo voltaic)', *International Journal Of Engineering Research and General Science*, 2(4).

Panwar, N. ., Kaushik, S. C. and Kothari, S. (2011) 'Role of Renewable Energy sources in Environmental Protection: A Review', *Renewable Sustainable Energy Reviews*, 15(15), pp. 13–24.

Park, N. (2017) *United Kingdom Population midyear Estimate*, *Office of Natinal Statistics*. Available at: https://www.ons.gov.uk/peoplepopulationandcommunity/populationandmigration/populationestimates (Accessed: 15 July 2017).

Qasem, H. *et al.* (2014) ‘Dust-induced shading on photovoltaic modules’, *Progress in Photovoltaics*, 22(2), pp. 218–226.

Radwan, A., Ookawara, S. and Ahmed, M. (2016) ‘Analysis and simulation of concentrating photovoltaic systems with a microchannel heat sink’, *Solar Energy*, 136, p. 35048.

Rajesh, K., Kulkami, A. D. and Ananthapadmanabha, T. (2015) ‘Modeling and Simulation of Solar PV and DFIG Based Wind Hybrid System’, *Procedia Technology*, 21, pp. 667–675.

Ramli, Makbul A.M. Prasetyono, Eka Wicaksana, Ragil W. Windarko, Novie A. Sedraoui, K. and Al-Turki, Y. A. (2016) ‘On the investigation of photovoltaic output power reduction due to dust accumulation and weather conditions’, *Renewable Energy*, 99(2016), pp. 836–844.

Ramos-Hernanz, J. A. *et al.* (2012) ‘Two photovoltaic cell simulation models in Matlab/Simulink’, *International Journal on Technical and Physical problems of Engineering*, 4(10), pp. 45–51.

Reader, G. T. (2020) ‘Energy, Renewables Alone?’, in Stagner, J. and Ting, D. K. (eds) *Sustaining Resources for Tomorrow, Green Energy and Technology*. Windsor: Springer.

Ruuska, P., Aikala, A. and Weiss, R. (2014) ‘Modelling of Photovoltaic Energy Generation Systems’, in *Proceedings of 28th European Conference on Modelling and Simulation*. Brescia, Italy, p. 6.

Sagga, A. M. S. (1993) ‘Roundness of sand grains of longitudinal dunes in saudi arabia’, *Sedimentary Geology*, 87(1), pp. 63–68.

Saidan, M. *et al.* (2016) ‘Experimental study on the effect of dust deposition on solar photovoltaic panels in desert environment’, *Renewable Energy*, 92(2016), pp. 499–505.

Salari, A. and Hakkaki-Fard, A. (2019) ‘A numerical study of dust deposition effects on photovoltaic modules and photovoltaic-thermal systems’, *Renewable Energy*, 135(2019), pp. 437–449.

Salas, V. *et al.* (2006) ‘Review of the Maximum Power Point Tracking Algorithms for Stand-Alone Photovoltaic Systems’, *Solar Energy Materials and Solar Cells*, 90, pp. 555–1578.

Salehin, S., Rahman, M. and Islam, S. (2015) ‘Techno-economic Feasibility Study of a Solar PV-Diesel System for Applications in Northern Part of Bangladesh’, *International Journal of Renewable Energy*, 5(4), pp. 1220–1229.

Salim, A., Huraib, F. and Eugenio, N. (2013) ‘PV power study of system options and optimization’, in *8th european PV solar energy conference*. Florence, Italy.

Sangeetha, K. *et al.* (2015) ‘Modeling, analysis and design of efficient maximum power extraction method for solar PV system’, *Renewable and Sustainable Energy Reviews*, 15, pp. 1015–1024. doi: 10.1016/j.rser.2015.07.146.

Sansom, C. *et al.* (2017) ‘Relectometer comparison for assessment of back-silvered glass solar mirrors concentrating Solar Power’, *Solar Energy*, 155, pp. 496–505.

Sarver, T., Al-Qaraghuli, A. and Kazmersk, L. L. (2013) ‘A comprehensive review of the impact of dust on the use of solar energy: History, investigations, results, literature, and mitigation approaches’, *Renewable and Sustainable Energy Reviews*, 22, pp. 698–733.

Sayigh, A., Al-Jandal, S. and Ahmed, H. (1985) ‘Dust effect

on solar flat surfaces devices in Kuwait', in *Proceedings of the workshop on the physics of non-conventional energy sources and materials science for energy*. Triest, Italy, pp. 353–367.

Sera, D. *et al.* (2006a) 'Improved MPPT method for rapidly changing environmental conditions', in *Proceedings of the IEEE International Symposium on Industrial Electronics*, pp. 1420–1425.

Sera, D. *et al.* (2006b) 'Improved MPPT Method for Rapidly Changing Environmental Conditions', *IEEE International Symposium on Industrial Electronics*, 2, pp. 1420–1425. Available at: http://dx.doi.org/10.1109/ISIE.2006.295680.

Shaaban, M. and Petinrin, J. O. (2014) 'Renewable energy potentials in Nigeria: Meeting rural energy needs', *Renewable & Sustainable Energy Reviews*, 2014(29), pp. 72–84.

Silva, R. (2013) *Fourth generation solar cell technology for high efficiency, large-area, low cost photovoltaics defined by Surrey academic*, *AiOlus news*. Available at: http://en.aiolusnews.com/energy/fourth-generation-solar-cell-technology-h/ (Accessed: 17 February 2017).

Singh, G. K. (2013) 'Solar power generation by PV (photovoltaic) technology: A review', *Energy*, 53, pp. 1–13.

Smestad, G. p. *et al.* (2020) 'Modelling photovoltaic soiling losses through optical characterization', *Science Report*, 10(58), pp. 1–13. doi: https://doi.org/10.1038/s41598-019-56868-z.

Solarigis (2020) *Solar resource maps*. Available at: https://solargis.com/maps-and-gis-data/download/nigeria (Accessed: 9 September 2020).

South Africa Population Clock (Live) (2017) *South Africa Population Country meter*. Available at: http://countrymeters.info/en/South_Africa (Accessed: 19 September 2017).

Subudhi, B. and Pradhan, R. (2013) 'A comparative study on maximum power point tracking techniques for photovoltaic power systems', *IEEE Transactions on Sustainable Energy*, 4(1), pp. 89–98.

Sumaina, K. (2018) 'Nigeria Needs 9,000 Weather Stations, Says NiMet', *THIS DAY*.

Sumaina, Kasim (2018) 'Nigeria Needs 9,000 Weather Stations, Says NiMet', *THIS DAY*, 25 September. Available at: https://www.thisdaylive.com/index.php/2018/09/25/nigeria-needs-9000-weather-stations-says-nimet/.

Tanesab, J. *et al.* (2017) 'Seasonal effect of dust on the degradation of PV modules performance deployed in different climate areas', *Renewable Energy*, 111(2017), pp. 105–115.

Tanesab, J. *et al.* (2019) 'The effect of dust with different morphologies on the performancedegradation of photovoltaic modules', *Sustainable Energy Technologies and Assessments*, 31(2019), pp. 347–354.

Tanima, B., Chakraborty, A. K. and Kaushik, P. (2014) 'Effects of Ambient Temperature and Wind Speed on Performance of Monocrystalline Solar Photovoltaic Module in Tripura, India', *Journal of Solar Energy*, 2014(2014), pp. 1–5.

The largest Solar Farm in the Southern hemisphere is located in Central South Africa (2017) *Environment*. Available at: https://www.environment.co.za/renewable-

energy/largest-solar-farm-southern-hemisphere.html (Accessed: 15 September 2017).

Twidell, J. and Weir, T. (2015) *Renewable Energy Resources*. 3rd edn. New York: Routledge.

USAID (2019) *Nigeria: Power Africa Fact Sheet*, *United States Agency for International Development*. Available at: https://www.usaid.gov/powerafrica/nigeria (Accessed: 19 August 2019).

Wilson, L. (2012) *Average Household Electricity Consumption around the World*, *Shrink That Footprint*.

Wu, X. D. *et al.* (2019) 'Energy use in world economy from household-consumption-based perspective', *Energy Policy*, 127(2019), pp. 287–298. Available at: https://reader.elsevier.com/reader/sd/pii/S0301421518308012?token=BCBE7F6EE848004004D9607DB1BDC31745E3A812F948D1AA81221E9288F8E3D939664700929344482E138187C7A2DF164.

You, S. *et al.* (2018) 'On the temporal modelling of solar photovoltaic soiling: Energy and economic impacts in seven cities', *Applied Energy*, 228(2018), pp. 1136–1146.

Zawilska, E. and Brooks, M. J. (2011) 'An assessment of the solar resource for Durban, SouthAfric', *Renewable Energy*, 36(2011), pp. 3433–3438.

Zweibel, K. and Herch, P. (1984) *Basic photovoltaic principles and methods.* New York: Van Nosstrand Reinhold Company Inc.

Insert list of references here

APPENDICES

Appendix A MATLAB Code for SPVSM

```
function varargout = PVCsizing(varargin)
% PVCSIZING MATLAB code for PVCsizing.fig
%      PVCSIZING, by itself, creates a new PVCSIZING or raises the %existing
%      singleton*.
%
%      H = PVCSIZING returns tsimulinkhe handle to a new PVCSIZING or the handle to
%      the existing singleton*.
%
%      PVCSIZING('CALLBACK',hObject,eventData,handles,...) calls the local
%      function named CALLBACK in PVCSIZING.M with the given input arguments.
%
%      PVCSIZING('Property','Value',...) creates a new PVCSIZING or raises the
%      existing singleton*.  Starting from the left, property value pairs are
%      applied to the GUI before PVCsizing_OpeningFcn gets called.  An
%      unrecognized property name or invalid value makes property application
%      stop.  All inputs are passed to PVCsizing_OpeningFcn via varargin.
%
%      *See GUI Options on GUIDE's Tools menu.  Choose "GUI allows only one
%      instance to run (singleton)".
%
% See also: GUIDE, GUIDATA, GUIHANDLES

% Edit the above text to modify the response to help PVCsizing

% Last Modified by GUIDE v2.5 12-Dec-2019 09:45:13
% Begin initialization code - DO NOT EDIT
gui_Singleton = 1;
gui_State = struct('gui_Name',       mfilename, ...
                   'gui_Singleton',  gui_Singleton, ...
                   'gui_OpeningFcn', @PVCsizing_OpeningFcn, ...
                   'gui_OutputFcn',  @PVCsizing_OutputFcn, ...
                   'gui_LayoutFcn',  [] , ...
                   'gui_Callback',   []);
if nargin && ischar(varargin{1})
    gui_State.gui_Callback = str2func(varargin{1});
end

if nargout
    [varargout{1:nargout}] = gui_mainfcn(gui_State, varargin{:});
else
    gui_mainfcn(gui_State, varargin{:});
end
% End initialization code - DO NOT EDIT



% --- Executes just before PVCsizing is made visible.
function PVCsizing_OpeningFcn(hObject, eventdata, handles, varargin)
% This function has no output args, see OutputFcn.
% hObject    handle to figure
% eventdata  reserved - to be defined in a future version of MATLAB
% handles    structure with handles and user data (see GUIDATA)
```

```
% varargin   command line arguments to PVCsizing (see VARARGIN)

% Choose default command line output for PVCsizing
handles.output = hObject;

% Update handles structure
guidata(hObject, handles);

% UIWAIT makes PVCsizing wait for user response (see UIRESUME)
% uiwait(handles.figure1);


% --- Outputs from this function are returned to the command line.
function varargout = PVCsizing_OutputFcn(hObject, eventdata, handles)
% varargout  cell array for returning output args (see VARARGOUT);
% hObject    handle to figure
% eventdata  reserved - to be defined in a future version of MATLAB
% handles    structure with handles and user data (see GUIDATA)

% Get default command line output from handles structure
varargout{1} = handles.output;


% --- Executes during object creation, after setting all properties.
function uipanel2_CreateFcn(hObject, eventdata, handles)
% hObject    handle to uipanel2 (see GCBO)
% eventdata  reserved - to be defined in a future version of MATLAB
% handles    empty - handles not created until after all CreateFcns called


% --- Executes on button press in pushbutton4.
function pushbutton4_Callback(hObject, eventdata, handles)
% hObject    handle to pushbutton4 (see GCBO)
% eventdata  reserved - to be defined in a future version of MATLAB
% handles    structure with handles and user data (see GUIDATA)


T_power_rating=str2num(get(handles.edit_T_power_rating,'string'))% Load

invertersize=T_power_rating*1.3;

wattageinverter=str2num(get(handles.edit_wattageinverter,'string'))% Selected inverter size

Nos_inverter_rqd=invertersize/wattageinverter;

set(handles.text_invertersize,'string',invertersize)
set(handles.text_Nos_Inverter,'string',Nos_inverter_rqd)
invertersize=vpa(invertersize)
Nos_inverter_rqd=vpa(Nos_inverter_rqd)


function edit_safety_value_Callback(hObject, eventdata, handles)
% hObject    handle to edit_safety_value (see GCBO)
```

```
% eventdata  reserved - to be defined in a future version of MATLAB
% handles    structure with handles and user data (see GUIDATA)

% Hints: get(hObject,'String') returns contents of edit_safety_value as text
%        str2double(get(hObject,'String')) returns contents of edit_safety_value as a double


% --- Executes during object creation, after setting all properties.
function edit_safety_value_CreateFcn(hObject, eventdata, handles)
% hObject    handle to edit_safety_value (see GCBO)
% eventdata  reserved - to be defined in a future version of MATLAB
% handles    empty - handles not created until after all CreateFcns called

% Hint: edit controls usually have a white background on Windows.
%       See ISPC and COMPUTER.
if ispc && isequal(get(hObject,'BackgroundColor'), get(0,'defaultUicontrolBackgroundColor'))
    set(hObject,'BackgroundColor','white');
end

function edit_ND_Callback(hObject, eventdata, handles)
% hObject    handle to edit_ND (see GCBO)
% eventdata  reserved - to be defined in a future version of MATLAB
% handles    structure with handles and user data (see GUIDATA)

% Hints: get(hObject,'String') returns contents of edit_ND as text
%        str2double(get(hObject,'String')) returns contents of edit_ND as a double

 % --- Executes during object creation, after setting all properties.
function edit_ND_CreateFcn(hObject, eventdata, handles)
% hObject    handle to edit_ND (see GCBO)
% eventdata  reserved - to be defined in a future version of MATLAB
% handles    empty - handles not created until after all CreateFcns called

% Hint: edit controls usually have a white background on Windows.
%       See ISPC and COMPUTER.
if ispc && isequal(get(hObject,'BackgroundColor'), get(0,'defaultUicontrolBackgroundColor'))
    set(hObject,'BackgroundColor','white');
end


% --- Executes on button press in pushbutton3.
function pushbutton3_Callback(hObject, eventdata, handles)
% hObject    handle to pushbutton3 (see GCBO)
% eventdata  reserved - to be defined in a future version of MATLAB
% handles    structure with handles and user data (see GUIDATA)
%GTE_Demand_Villege=1122000;
GTE_Demand_Village=str2num(get(handles.edit_GTE_Demand_Village,'string'));
WP=str2num(get(handles.text_WP,'string'))

ND=str2num(get(handles.edit_ND,'string'));

Bat_P=GTE_Demand_Village*ND;

DOD=str2num(get(handles.edit_DOD,'string'));
```

```
Exp_Bat_P=Bat_P/DOD;
vpa(Bat_P)
vpa(Exp_Bat_P)
set(handles.text_Bat_P,'string',Bat_P)
set(handles.text_Expected_Bat_P,'string',Exp_Bat_P)

sV_rating_Bat=str2num(get(handles.edit_Sel_Bat_Voltage,'string'));
Bat_Cap=(Exp_Bat_P)/(sV_rating_Bat*0.85)
set(handles.text_Bat_Cap,'string',Bat_Cap)
Hour_charging=(Exp_Bat_P/WP)
set(handles.text_Hour_charging,'string',Hour_charging)
%AH=str2num(get(handles.list_AH,'string'))
AH=str2num(get(handles.edit_AH,'string'))

Nos_of_Bat_rqd=(2*Bat_P)/(AH*sV_rating_Bat)
set(handles.text_Nos_of_Bat,'string',Nos_of_Bat_rqd)

% --- Executes on button press in pushbutton2.
function pushbutton2_Callback(hObject, eventdata, handles)
% hObject    handle to pushbutton2 (see GCBO)
% eventdata  reserved - to be defined in a future version of MATLAB
% handles    structure with handles and user data (see GUIDATA)

GTE_Demand_Village=str2num(get(handles.edit_GTE_Demand_Village,'string'));

ASR=str2num(get(handles.edit_ASR,'string'));
str1 = ['Average solar irradiance (W/m', char(178),')']% To write W/sq-m correctly
sshine=str2num(get(handles.edit_sshine,'string'));
stci=str2num(get(handles.edit_stci,'string'));
str1 = ['Standard Test Condition Irradiance (W/m', char(178),')']
PVRating=str2num(get(handles.edit_PVRating,'string'));

PGF=(ASR*sshine)/(stci);
set(handles.text_PGF,'string',PGF)

EARRAY=GTE_Demand_Village*1.3;

WP=EARRAY/PGF

vpa(WP)% To write the value of wp in floting point

NOofPVC=WP/PVRating;% PVRating is the selected module rating

PV_Derate=0.66;
set(handles.text_WP,'string',WP)

Quarter_Days=str2num(get(handles.edit_Quarter_Days,'string'))

PV_Energy_Per_Quarter=WP*sshine*Quarter_Days*(ASR/stci)*PV_Derate

set(handles.text_PV_Energy_Per_Quarter,'string',PV_Energy_Per_Quarter)
%set(handles.text_PVRating,'string',PVRating)
```

```
set(handles.text_NOofPVC,'string',NOofPVC)

function edit_ASR_Callback(hObject, eventdata, handles)
% hObject    handle to edit_ASR (see GCBO)
% eventdata  reserved - to be defined in a future version of MATLAB
% handles    structure with handles and user data (see GUIDATA)

% Hints: get(hObject,'String') returns contents of edit_ASR as text
%        str2double(get(hObject,'String')) returns contents of edit_ASR as a double

% --- Executes during object creation, after setting all properties.
function edit_ASR_CreateFcn(hObject, eventdata, handles)
% hObject    handle to edit_ASR (see GCBO)
% eventdata  reserved - to be defined in a future version of MATLAB
% handles    empty - handles not created until after all CreateFcns called

% Hint: edit controls usually have a white background on Windows.
%       See ISPC and COMPUTER.
if ispc && isequal(get(hObject,'BackgroundColor'), get(0,'defaultUicontrolBackgroundColor'))
    set(hObject,'BackgroundColor','white');
end

% --- Executes on button press in pushbutton1.
function pushbutton1_Callback(hObject, eventdata, handles)
% hObject    handle to pushbutton1 (see GCBO)
% eventdata  reserved - to be defined in a future version of MATLAB
% handles    structure with handles and user data (see GUIDATA)

function edit_GTE_Demand_Village_Callback(hObject, eventdata, handles)
% hObject    handle to edit_GTE_Demand_Village (see GCBO)
% eventdata  reserved - to be defined in a future version of MATLAB
% handles    structure with handles and user data (see GUIDATA)

% Hints: get(hObject,'String') returns contents of edit_GTE_Demand_Village as text
%        str2double(get(hObject,'String')) returns contents of edit_GTE_Demand_Village as a
double

 % --- Executes during object creation, after setting all properties.
function edit_GTE_Demand_Village_CreateFcn(hObject, eventdata, handles)
% hObject    handle to edit_GTE_Demand_Village (see GCBO)
% eventdata  reserved - to be defined in a future version of MATLAB
% handles    empty - handles not created until after all CreateFcns called

% Hint: edit controls usually have a white background on Windows.
%       See ISPC and COMPUTER.
if ispc && isequal(get(hObject,'BackgroundColor'), get(0,'defaultUicontrolBackgroundColor'))
    set(hObject,'BackgroundColor','white');
end

% --- Executes on button press in pushbutton5.
function pushbutton5_Callback(hObject, eventdata, handles)
% hObject    handle to pushbutton5 (see GCBO)
% eventdata  reserved - to be defined in a future version of MATLAB
% handles    structure with handles and user data (see GUIDATA)
```

```
 function edit5_Callback(hObject, eventdata, handles)
% hObject    handle to edit5 (see GCBO)
% eventdata  reserved - to be defined in a future version of MATLAB
% handles    structure with handles and user data (see GUIDATA)

% Hints: get(hObject,'String') returns contents of edit5 as text
%        str2double(get(hObject,'String')) returns contents of edit5 as a double

% --- Executes during object creation, after setting all properties.
function edit5_CreateFcn(hObject, eventdata, handles)
% hObject    handle to edit5 (see GCBO)
% eventdata  reserved - to be defined in a future version of MATLAB
% handles    empty - handles not created until after all CreateFcns called

% Hint: edit controls usually have a white background on Windows.
%       See ISPC and COMPUTER.
if ispc && isequal(get(hObject,'BackgroundColor'), get(0,'defaultUicontrolBackgroundColor'))
    set(hObject,'BackgroundColor','white');
end

% --- Executes on button press in pushbutton6.
function pushbutton6_Callback(hObject, eventdata, handles)
% hObject    handle to pushbutton6 (see GCBO)
% eventdata  reserved - to be defined in a future version of MATLAB
% handles    structure with handles and user data (see GUIDATA)



function edit6_Callback(hObject, eventdata, handles)
% hObject    handle to edit6 (see GCBO)
% eventdata  reserved - to be defined in a future version of MATLAB
% handles    structure with handles and user data (see GUIDATA)

% Hints: get(hObject,'String') returns contents of edit6 as text
%        str2double(get(hObject,'String')) returns contents of edit6 as a double

% --- Executes during object creation, after setting all properties.
function edit6_CreateFcn(hObject, eventdata, handles)
% hObject    handle to edit6 (see GCBO)
% eventdata  reserved - to be defined in a future version of MATLAB
% handles    empty - handles not created until after all CreateFcns called

% Hint: edit controls usually have a white background on Windows.
%       See ISPC and COMPUTER.
if ispc && isequal(get(hObject,'BackgroundColor'), get(0,'defaultUicontrolBackgroundColor'))
    set(hObject,'BackgroundColor','white');
end

% --- Executes on button press in pushbutton7.
function pushbutton7_Callback(hObject, eventdata, handles)
% hObject    handle to pushbutton7 (see GCBO)
% eventdata  reserved - to be defined in a future version of MATLAB
% handles    structure with handles and user data (see GUIDATA)
```

```
NOofPVC=str2num(get(handles.text_NOofPVC,'string'))
 Area_m=2;
  Area_A=Area_m*NOofPVC
  Area_o=0.05*Area_A;
  T_area=Area_A+Area_o;
  N_Plot=T_area/464.5;
    %%
  % DIRECT CAPITAL COST
  % ALL MONIES ARE IN DOLLAR

   %% COST OF PV ARRAY
  % Cost_PkW_PV_Panel = cost per kW of PV panel ($)
  Cost_PW_Panel= 1.5;
  PVRating=str2num(get(handles.edit_PVRating,'string'))
  Total_Cost_Array=Cost_PW_Panel*PVRating*NOofPVC;

  %%
  % COST OF BATTERY
  Cost_P_kWh_Bat=400;

  Nos_of_Bat=str2num(get(handles.text_Nos_of_Bat,'string'))
  AH=str2num(get(handles.edit_AH,'string'))
  Sel_Bat_Voltage=str2num(get(handles.edit_Sel_Bat_Voltage,'string'))

  Total_Bat_cost= (Cost_P_kWh_Bat*Nos_of_Bat*(AH*Sel_Bat_Voltage))/1000;



  %%
  % COST OF INVERTERS
  % Cost_Per_W_Inv= $0.34
  Cost_PW_Inv=0.34;
  wattageinverter=str2num(get(handles.edit_wattageinverter,'string'))
  Nos_Inverter=str2num(get(handles.text_Nos_Inverter,'string'))

  Total_Inv_Cost= Cost_PW_Inv*wattageinverter*Nos_Inverter;

  %%
  % COST OF CHARGE CONTROLLERS
 % Cost_Per_Ampere_CC= $5.4
  Cost_P_Ampere_CC= 5.4;
  Amperage_CC=str2num(get(handles.edit_Amperage_CC,'string'))
  N_CC=str2num(get(handles.text_N_CC,'string'))

  Total_CC_Cost= Cost_P_Ampere_CC*Amperage_CC*N_CC;

  %%
  % COST OF CABLES
  % Panel,Battery and AC Output Cabling
  % Cost in $ and Length in meter
  length_of_Module=2;
  Length_of_Inv=0.5;
  Length_of_Bat=0.3;
  Cost_Per_meter_cable= 2.4;
  Module_cable_Cost=Cost_Per_meter_cable*NOofPVC*length_of_Module;
```

```
Inverter_cable_Cost= Cost_Per_meter_cable*Nos_Inverter*Length_of_Inv;
Bat_cable_cost=Cost_Per_meter_cable*Nos_of_Bat*Length_of_Bat;
Total_Cable_Cost=  Module_cable_Cost+Inverter_cable_Cost+Bat_cable_cost;

%%
%Total_Direct_Capital_Cost = TDCC
Sub_TDCC_1=Total_Cost_Array+Total_Bat_cost+Total_Inv_Cost;
Sub_TDCC_2=Total_CC_Cost+Total_Cable_Cost;
TDCC=Sub_TDCC_1+Sub_TDCC_2;

%%
% INDIRECT CAPITAL COST
%% Permitting and Environmental Issues
PCent_of_Direct_Cost=0.03;
%PERMITTING AND ENVIRONMENTAL ISSUES=PEI

PEI= PCent_of_Direct_Cost*TDCC;
%
%COST OF LAND REQUIRED
% Cost of plot of land= Plot_Cost (This depends on location)
% Cost of land=Land_Cost
Plot_Cost= 140;
Land_Cost=N_Plot*Plot_Cost;

%% TOTAL PROJECT COST
% Total_Project_Cost=TPC
TPC= TDCC+PEI+Land_Cost;

% set(handles.text_TPC,'string',TPC)
%FINANCIAL APPRAISAL OF THE PV SYSTEM

%% OPERATION AND MAINTENANCE COST
% O&M Cost = OM_Cost
%OM cost per MWh=OM_P_MWh (Dollar)
OM_P_MWh= 40;
WP=str2num(get(handles.text_WP,'string'))
OM_Cost=(WP*OM_P_MWh)/1000000;

%% FINANCIAL APPRAISAL
% Assumptions
% 70% of Project Cost is from Loan and 30% is equity
%Loan interest rate 5% annual
% Project Life span is 25 years
%DEG_A=0.01;
D_RATE=0.1;
TARRIF=0.12;
Loan=0.7*TPC;
Equity=0.3*TPC;
PV_Energy_PA=0;
PV_Energy_Revenue_PA=0;
PV_NET_PRESENT_VALUE=0;
CASH_IN_FLOW_T=0;
CASH_OUT_FLOW_T=0;
AA_T=0;
PV_Derate=0.66;
```

```
LOAN_P=Loan+(0.05*Loan);
sshine=str2num(get(handles.edit_sshine,'string'));
for DEG_A=0.005:0.005:0.025
for YR=1:1:28
      Year(YR)=YR+2018;

      Discount_Factor(YR)=1/((1+D_RATE)^YR);

      % plot(Year,Discount_Factor);
       stci=str2num(get(handles.edit_stci,'string'))
      ASR=str2num(get(handles.edit_ASR,'string'))

      if (YR==1)
         CASH_IN_FLOW=Loan+Equity;
      elseif (YR>=2 && YR<=3)
         CASH_IN_FLOW=0;
      elseif (YR>=4 && YR<=28)
          DEG_A_T(YR)=DEG_A*(YR-3);
          k=DEG_A*(YR-3);
      PV_Energy_PA(YR)=(WP*sshine*365*(ASR/stci)*PV_Derate*(1-k)*1.224)/1000;
      PV_Energy_Revenue_PA(YR)= PV_Energy_PA(YR)*TARRIF;
         CASH_IN_FLOW= PV_Energy_Revenue_PA(YR)*DEG_A_T(YR);
      end
      if (YR==1)
         CASH_OUT_FLOW=0.3*TPC;
         AA=0;
       elseif (YR==2)
         CASH_OUT_FLOW=0.3*TPC;
         AA=0;
       elseif (YR==3)
         CASH_OUT_FLOW=0.4*TPC;
         AA=0;
       elseif (YR>=4 && YR<=28)
         AA= OM_Cost*DEG_A;
         CASH_OUT_FLOW=AA+(0.05*LOAN_P);
      end
      PV_NET_CASH_FLOW=CASH_IN_FLOW-CASH_OUT_FLOW;
      TAX=0.3*PV_NET_CASH_FLOW;
      PV_NET_CASH_FLOW_AFTER_TAX=PV_NET_CASH_FLOW-TAX;


PV_PRESENT_VALUE_YR(YR)=PV_NET_CASH_FLOW_AFTER_TAX*Discount_Factor(YR);

PV_NET_PRESENT_VALUE=PV_NET_PRESENT_VALUE+PV_PRESENT_VALUE_YR(YR)

PV_NET_PRESENT_VALUE_T(YR)=PV_NET_PRESENT_VALUE+PV_PRESENT_VALUE_Y
R(YR);
      AA_T=AA_T+AA;

      CASH_IN_FLOW_T=CASH_IN_FLOW_T+CASH_IN_FLOW;
      CASH_OUT_FLOW_T=CASH_OUT_FLOW_T+CASH_OUT_FLOW;

%
end
hold on
```

```
figure(1)
plot(Year,PV_Energy_PA,'-*');
xlabel('Year');
ylabel('PV Energy PA (kWh)')
%title('Annual Energy Generated against Year of operation')
legend('ANNUAL DEGRADATION=0.5%','ANNUAL DEGRADATION=1%','ANNUAL
DEGRADATION=1.5%','ANNUAL DEGRADATION=2%','ANNUAL
DEGRADATION=2.5%','location','southeast')
hold on
figure (2)
plot(Year,DEG_A_T,'-*')
xlabel('Year');
ylabel('Degradation Factor')
%title('Degradation Factor against Year of operation')
legend('ANNUAL DEGRADATION=0.5%','ANNUAL DEGRADATION=1%','ANNUAL
DEGRADATION=1.5%','ANNUAL DEGRADATION=2%','ANNUAL
DEGRADATION=2.5%','location','northwest')


%legend('ANNUAL DEGRADATION=0.5%','ANNUAL DEGRADATION=1%','ANNUAL
DEGRADATION=1.5%','ANNUAL DEGRADATION=2%','ANNUAL
DEGRADATION=2.5%','location','northwest')

%PV_Energy_PA=(WP*sshine*360);
%set(handles.text_PV_Energy_PA_k,'string',PV_Energy_PA)
end

%title('PV Annual Energy Generated against Degradation Factor')
%end

%Histogram(PV_Energy_PA)
%plot(Year,PV_PRESENT_VALUE_YR)
%xlabel('Year');
%ylabel('Annual Present Value')
%title('Annual Present Value against Year of operation')
%subplot(2,2,4)
%plot(Year,PV_NET_PRESENT_VALUE_T)
%xlabel('Year');
%ylabel('Commulative NPV')
%title('Commulative NPV against Year of operation')

%place here all the codes for plotting PV annual energy generated

function edit_sshine_Callback(hObject, eventdata, handles)
% hObject    handle to edit_sshine (see GCBO)
% eventdata  reserved - to be defined in a future version of MATLAB
% handles    structure with handles and user data (see GUIDATA)

% Hints: get(hObject,'String') returns contents of edit_sshine as text
%        str2double(get(hObject,'String')) returns contents of edit_sshine as a double


% --- Executes during object creation, after setting all properties.
function edit_sshine_CreateFcn(hObject, eventdata, handles)
```

```
% hObject    handle to edit_sshine (see GCBO)
% eventdata  reserved - to be defined in a future version of MATLAB
% handles    empty - handles not created until after all CreateFcns called

% Hint: edit controls usually have a white background on Windows.
%       See ISPC and COMPUTER.
if ispc && isequal(get(hObject,'BackgroundColor'), get(0,'defaultUicontrolBackgroundColor'))
    set(hObject,'BackgroundColor','white');
end



function edit_stci_Callback(hObject, eventdata, handles)
% hObject    handle to edit_stci (see GCBO)
% eventdata  reserved - to be defined in a future version of MATLAB
% handles    structure with handles and user data (see GUIDATA)

% Hints: get(hObject,'String') returns contents of edit_stci as text
%        str2double(get(hObject,'String')) returns contents of edit_stci as a double


% --- Executes during object creation, after setting all properties.
function edit_stci_CreateFcn(hObject, eventdata, handles)
% hObject    handle to edit_stci (see GCBO)
% eventdata  reserved - to be defined in a future version of MATLAB
% handles    empty - handles not created until after all CreateFcns called

% Hint: edit controls usually have a white background on Windows.
%       See ISPC and COMPUTER.
if ispc && isequal(get(hObject,'BackgroundColor'), get(0,'defaultUicontrolBackgroundColor'))
    set(hObject,'BackgroundColor','white');
end



function edit_PVRating_Callback(hObject, eventdata, handles)
% hObject    handle to edit_PVRating (see GCBO)
% eventdata  reserved - to be defined in a future version of MATLAB
% handles    structure with handles and user data (see GUIDATA)

% Hints: get(hObject,'String') returns contents of edit_PVRating as text
%        str2double(get(hObject,'String')) returns contents of edit_PVRating as a double


% --- Executes during object creation, after setting all properties.
function edit_PVRating_CreateFcn(hObject, eventdata, handles)
% hObject    handle to edit_PVRating (see GCBO)
% eventdata  reserved - to be defined in a future version of MATLAB
% handles    empty - handles not created until after all CreateFcns called

% Hint: edit controls usually have a white background on Windows.
%       See ISPC and COMPUTER.
if ispc && isequal(get(hObject,'BackgroundColor'), get(0,'defaultUicontrolBackgroundColor'))
```

```
    set(hObject,'BackgroundColor','white');
end


% --- Executes on selection change in Sel_Bat_Voltage.
function Sel_Bat_Voltage_Callback(hObject, eventdata, handles)
% hObject    handle to Sel_Bat_Voltage (see GCBO)
% eventdata  reserved - to be defined in a future version of MATLAB
% handles    structure with handles and user data (see GUIDATA)

% Hints: contents = cellstr(get(hObject,'String')) returns Sel_Bat_Voltage contents as cell array
%        contents{get(hObject,'Value')} returns selected item from Sel_Bat_Voltage


% --- Executes during object creation, after setting all properties.
function Sel_Bat_Voltage_CreateFcn(hObject, eventdata, handles)
% hObject    handle to Sel_Bat_Voltage (see GCBO)
% eventdata  reserved - to be defined in a future version of MATLAB
% handles    empty - handles not created until after all CreateFcns called

% Hint: listbox controls usually have a white background on Windows.
%       See ISPC and COMPUTER.
if ispc && isequal(get(hObject,'BackgroundColor'), get(0,'defaultUicontrolBackgroundColor'))
    set(hObject,'BackgroundColor','white');
end

% --- Executes on selection change in list_AH.
function list_AH_Callback(hObject, eventdata, handles)
% hObject    handle to list_AH (see GCBO)
% eventdata  reserved - to be defined in a future version of MATLAB
% handles    structure with handles and user data (see GUIDATA)

% Hints: contents = cellstr(get(hObject,'String')) returns list_AH contents as cell array
%        contents{get(hObject,'Value')} returns selected item from list_AH


% --- Executes during object creation, after setting all properties.
function list_AH_CreateFcn(hObject, eventdata, handles)
% hObject    handle to list_AH (see GCBO)
% eventdata  reserved - to be defined in a future version of MATLAB
% handles    empty - handles not created until after all CreateFcns called

% Hint: listbox controls usually have a white background on Windows.
%       See ISPC and COMPUTER.
if ispc && isequal(get(hObject,'BackgroundColor'), get(0,'defaultUicontrolBackgroundColor'))
    set(hObject,'BackgroundColor','white');
end

function edit_wattageinverter_Callback(hObject, eventdata, handles)
% hObject    handle to edit_wattageinverter (see GCBO)
% eventdata  reserved - to be defined in a future version of MATLAB
% handles    structure with handles and user data (see GUIDATA)

% Hints: get(hObject,'String') returns contents of edit_wattageinverter as text
```

```
%        str2double(get(hObject,'String')) returns contents of edit_wattageinverter as a double


% --- Executes during object creation, after setting all properties.
function edit_wattageinverter_CreateFcn(hObject, eventdata, handles)
% hObject    handle to edit_wattageinverter (see GCBO)
% eventdata  reserved - to be defined in a future version of MATLAB
% handles    empty - handles not created until after all CreateFcns called

% Hint: edit controls usually have a white background on Windows.
%       See ISPC and COMPUTER.
if ispc && isequal(get(hObject,'BackgroundColor'), get(0,'defaultUicontrolBackgroundColor'))
    set(hObject,'BackgroundColor','white');
end



% --- Executes on button press in pushbutton8.
function pushbutton8_Callback(hObject, eventdata, handles)
% hObject    handle to pushbutton8 (see GCBO)
% eventdata  reserved - to be defined in a future version of MATLAB
% handles    structure with handles and user data (see GUIDATA)

NOofPVC=str2num(get(handles.text_NOofPVC,'string'))
   WP=str2num(get(handles.text_WP,'string'))
   ASR=str2num(get(handles.edit_ASR,'string'))
CONVERSION_EFF=0.18
   Area=WP/(1000*CONVERSION_EFF)
   T_area=Area%+Area_o
   N_Plot=T_area/464.5

   %%
   % DIRECT CAPITAL COST
   % ALL MONIES ARE IN DOLLAR

     %% COST OF PV ARRAY
   % Cost_PkW_PV_Panel = cost per kW of PV panel ($), cost per watt=$1.0
   Cost_PW_Panel= 1;
   PVRating=str2num(get(handles.edit_PVRating,'string'))
   Total_Cost_Array=Cost_PW_Panel*PVRating*NOofPVC;
   set(handles.text_Total_Cost_Array,'string',Total_Cost_Array)
   %%
   % COST OF BATTERY
   Cost_P_kWh_Bat=300;

   Nos_of_Bat=str2num(get(handles.text_Nos_of_Bat,'string'))
   %AH=str2num(get(handles.list_AH,'string'))
   AH=str2num(get(handles.edit_AH,'string'))
   %Sel_Bat_Voltage=str2num(get(handles.Sel_Bat_Voltage,'string'))
   Sel_Bat_Voltage=str2num(get(handles.edit_Sel_Bat_Voltage,'string'))
   Total_Bat_cost= (Cost_P_kWh_Bat*Nos_of_Bat*(AH*Sel_Bat_Voltage))/1000;
   set(handles.text_Total_Bat_cost,'string',Total_Bat_cost)



   %%
```

```
% COST OF INVERTERS
% Cost_Per_W_Inv= $0.32
Cost_PW_Inv=0.18;
wattageinverter=str2num(get(handles.edit_wattageinverter,'string'))
Nos_Inverter=str2num(get(handles.text_Nos_Inverter,'string'))

Total_Inv_Cost= Cost_PW_Inv*wattageinverter*Nos_Inverter;
set(handles.text15,'string',Total_Inv_Cost)
%%
% COST OF CHARGE CONTROLLERS
% Cost_Per_Ampere_CC= $5.0
Cost_P_Ampere_CC= 5.0;
Amperage_CC=str2num(get(handles.edit_Amperage_CC,'string'))
N_CC=str2num(get(handles.text_N_CC,'string'))

Total_CC_Cost= Cost_P_Ampere_CC*Amperage_CC*N_CC;
 set(handles.text_Total_CC_Cost,'string',Total_CC_Cost)

%%
% COST OF CABLES
% Panel,Battery and AC Output Cabling
% Cost in $ and Length in meter
length_of_Module=2;
Length_of_Inv=0.5;
Length_of_Bat=0.3;
Length_of_CC= 0.2;
Cost_Per_meter_cable= 2.4;
Module_cable_Cost=Cost_Per_meter_cable*NOofPVC*length_of_Module;
Inverter_cable_Cost= Cost_Per_meter_cable*Nos_Inverter*Length_of_Inv;
Bat_cable_cost=Cost_Per_meter_cable*Nos_of_Bat*Length_of_Bat;
CC_cable_cost=Cost_Per_meter_cable*N_CC*Length_of_CC;
Total_Cable_Cost=
Module_cable_Cost+Inverter_cable_Cost+Bat_cable_cost+CC_cable_cost;

%%
% STRUCTURL FRAME FOR PANELS
% cOST OF FRAME PER PANEL = 10
Frame_Cost=10*NOofPVC
%%

%Total_Direct_Capital_Cost = TDCC
Sub_TDCC_1=Total_Cost_Array+Total_Inv_Cost+Total_Bat_cost;
Sub_TDCC_2=Total_CC_Cost+Total_Cable_Cost+Frame_Cost;
TDCC=Sub_TDCC_1+Sub_TDCC_2;

 %%
% INSTALLATION COST
% Installation cost is 5% of total direct capital cost
Installation_cost= 0.05*TDCC;

%% Miscellaneous
% This is assumed to be 2% of TDCC
%Miscellaneous=0.02*TDCC;-------

%%
```

```
  % INDIRECT CAPITAL COST
  %% Permitting and Environmental Issues
  %PCent_of_Direct_Cost=0.01;--------
  %PERMITTING AND ENVIRONMENTAL ISSUES=PEI

  %PEI= PCent_of_Direct_Cost*TDCC;-----
 %
 %COST OF LAND REQUIRED
 % Cost of plot of land= Plot_Cost (This depends on location)
 % Cost of land=Land_Cost
% Plot_Cost= 100;----
 %Land_Cost=N_Plot*Plot_Cost;----

 %% TOTAL PROJECT COST
 % Total_Project_Cost=TPC
%  TPC= TDCC+PEI+Land_Cost+Miscellaneous+Installation_cost -------
  TPC= TDCC+Installation_cost
 %vpa(TPC)

 set(handles.text_TPC,'string',TPC)
 %FINANCIAL APPRAISAL OF THE PV SYSTEM

%% OPERATION AND MAINTENANCE COST
% O&M Cost = OM_Cost
%OM cost per MWh=OM_P_MWh (Dollar)
OM_P_MWh= 40;
WP=str2num(get(handles.text_WP,'string'));
OM_Cost=(WP*OM_P_MWh)/1000000;

LC_OM_Cost=OM_Cost*25;


%% FINANCIAL APPRAISAL
% Assumptions
% 70% of Project Cost is from Loan and 30% is equity
%Loan interest rate 5% annual
% Project Life span is 25 years
DEG_A=0.01;
%D_RATE=0.1;
TARRIF=0.16;% $0.12 = 12 cent
Loan=0.7*TPC;
Equity=0.3*TPC;
%PV_Energy_PA=0;
PV_Energy_PA_T=0;
PV_Energy_Revenue_PA=0;
PV_Energy_Revenue_PA_T=0;
PV_NET_PRESENT_VALUE=0;
CASH_IN_FLOW_T=0;
CASH_OUT_FLOW_T=0;
AA_T=0; % Operation and maintenance cost
PV_Derate=0.6;

LOAN_P=Loan+(0.05*Loan);
sshine=str2num(get(handles.edit_sshine,'string'));
for D_RATE=0.05:0.05:0.25
```

```
for YR=1:1:28
      Year(YR)=YR+2018;
      DEG_A_T(YR)=DEG_A*YR;
      Discount_Factor(YR)=1/((1+D_RATE)^YR);
      % Here Year is a scalar value and Discount_Fctor is also one single
      % value. If I understand you correct, you need to build two arrays
      % X array and Y array and then plot(X,Y)
      % Once you have build the array, you can use the plot outside the
      % loop
      % plot(Year,Discount_Factor);
      stci=str2num(get(handles.edit_stci,'string'));
      ASR=str2num(get(handles.edit_ASR,'string'));
      PV_Energy_PA=(WP*sshine*365*(ASR/stci)*PV_Derate)*(1-(DEG_A*YR)*0.20);
      PV_Energy_Revenue_PA= PV_Energy_PA*TARRIF;
      if (YR==1)
         CASH_IN_FLOW=Loan+Equity;
      elseif (YR>=2 && YR<=3)
         CASH_IN_FLOW=0;
      elseif (YR>=4 && YR<=28)
         CASH_IN_FLOW= PV_Energy_Revenue_PA %*DEG_A_T(YR);
      end
      if (YR==1)
         CASH_OUT_FLOW=0.3*TPC;
         AA=0;
       elseif (YR==2)
         CASH_OUT_FLOW=0.3*TPC;
         AA=0;
       elseif (YR==3)
         CASH_OUT_FLOW=0.4*TPC;
         AA=0;
       elseif (YR>=4 && YR<=28)
         AA= OM_Cost*(DEG_A*YR);
         CASH_OUT_FLOW=AA+(0.05*LOAN_P);
      end
      PV_NET_CASH_FLOW=CASH_IN_FLOW-CASH_OUT_FLOW;
      TAX=0.3*PV_NET_CASH_FLOW;
      PV_NET_CASH_FLOW_AFTER_TAX=PV_NET_CASH_FLOW-TAX;


PV_PRESENT_VALUE_YR(YR)=PV_NET_CASH_FLOW_AFTER_TAX*Discount_Factor(YR)

PV_NET_PRESENT_VALUE=PV_NET_PRESENT_VALUE+PV_PRESENT_VALUE_YR(YR);
      PV_NPV_T1(YR)=PV_NET_PRESENT_VALUE+PV_PRESENT_VALUE_YR(YR);
      AA_T=AA_T+AA;

      PV_Energy_PA_T= PV_Energy_PA_T+ PV_Energy_PA
      PV_Energy_Revenue_PA_T=PV_Energy_Revenue_PA_T+PV_Energy_Revenue_PA
      CASH_IN_FLOW_T=CASH_IN_FLOW_T+CASH_IN_FLOW;
      CASH_OUT_FLOW_T=CASH_OUT_FLOW_T+CASH_OUT_FLOW;
   end
%PV_Energy_PA=(WP*sshine*365)
%lcoe=
%set(handles.text_PV_Energy_PA_k,'string',PV_Energy_PA)
%hold off
%plot(Discount_Factor,Year)
%Table_a (Year,1)= Year;
```

```
%set(handles.text_PV_PRESENT_VALUE_YR,'string',PV_NPV_T1)
%set(handles.text_CASH_IN_FLOW_T,'string',CASH_IN_FLOW_T)
%set(handles.text_CASH_OUT_FLOW_T,'string',CASH_OUT_FLOW_T)
k=(TPC+AA+(0.05+LOAN_P));
LCOE=(TPC+CASH_OUT_FLOW_T)/PV_Energy_PA;
LCOE1=(CASH_OUT_FLOW_T)/PV_Energy_PA;
vpa(PV_Energy_PA);
p=PV_Energy_PA*8.3;

set(handles.text_LCOE1,'string',LCOE)
end
set(handles.text_PV_PRESENT_VALUE_YR,'string',PV_NPV_T1)
PV_Energy_PA_2=WP*sshine*365*(ASR/stci)*PV_Derate*0.20*0.05;
PV_Energy_Revenue_PA_2= PV_Energy_PA_2*TARRIF;
PV_NET_CASH_FLOW_2=CASH_IN_FLOW-CASH_OUT_FLOW;
payback_period=(TPC)/PV_Energy_Revenue_PA_2;
set(handles.text_payback_period,'string',payback_period);
PB=PV_Energy_Revenue_PA_T/PV_Energy_PA_T;
%PV_NET_PRESENT_VALUE_T
%Table_a (YR,2)= Discount_Factor;
% ... now Year and Discount_factor are arrays of equal size and you can

% THE Calculations of net present values should starts
%NPV = ?
%set(handles.text_CASH_IN_FLOW_T,'string',NPV);

function edit_Land_Cost_Callback(hObject, eventdata, handles)
% hObject    handle to text_PV_PRESENT_VALUE_YR (see GCBO)
% eventdata  reserved - to be defined in a future version of MATLAB
% handles    structure with handles and user data (see GUIDATA)

% Hints: get(hObject,'String') returns contents of text_PV_PRESENT_VALUE_YR as text
%        str2double(get(hObject,'String')) returns contents of text_PV_PRESENT_VALUE_YR as
a double



% --- Executes during object creation, after setting all properties.
function text_PV_PRESENT_VALUE_YR_CreateFcn(hObject, eventdata, handles)
% hObject    handle to text_PV_PRESENT_VALUE_YR (see GCBO)
% eventdata  reserved - to be defined in a future version of MATLAB
% handles    empty - handles not created until after all CreateFcns called

% Hint: edit controls usually have a white background on Windows.
%       See ISPC and COMPUTER.
if ispc && isequal(get(hObject,'BackgroundColor'), get(0,'defaultUicontrolBackgroundColor'))
   set(hObject,'BackgroundColor','white');
end



function edit_TDCC_Callback(hObject, eventdata, handles)
% hObject    handle to text_Total_Cost_Array (see GCBO)
% eventdata  reserved - to be defined in a future version of MATLAB
% handles    structure with handles and user data (see GUIDATA)
```

```
% Hints: get(hObject,'String') returns contents of text_Total_Cost_Array as text
%        str2double(get(hObject,'String')) returns contents of text_Total_Cost_Array as a double


% --- Executes during object creation, after setting all properties.
function text_Total_Cost_Array_CreateFcn(hObject, eventdata, handles)
% hObject    handle to text_Total_Cost_Array (see GCBO)
% eventdata  reserved - to be defined in a future version of MATLAB
% handles    empty - handles not created until after all CreateFcns called

% Hint: edit controls usually have a white background on Windows.
%       See ISPC and COMPUTER.
if ispc && isequal(get(hObject,'BackgroundColor'), get(0,'defaultUicontrolBackgroundColor'))
    set(hObject,'BackgroundColor','white');
end

 % --- Executes on button press in pushbutton10.
function pushbutton10_Callback(hObject, eventdata, handles)
% hObject    handle to pushbutton10 (see GCBO)
% eventdata  reserved - to be defined in a future version of MATLAB
% handles    structure with handles and user data (see GUIDATA)

%safety_value_CC=str2num(get(handles.edit_safety_value_CC,'string'))
S_V= str2num(get(handles.edit_S_V,'string'));
WP=str2num(get(handles.text_WP,'string'));
Amperage_CC=str2num(get(handles.edit_Amperage_CC,'string'));
CC_Cap=(WP/S_V)*1.3%safety_value_CC
N_CC=CC_Cap/Amperage_CC
set(handles.text_CC_Cap,'string',CC_Cap)
set(handles.text_N_CC,'string',N_CC)

function edit_safety_value_CC_Callback(hObject, eventdata, handles)
% hObject    handle to edit_safety_value_CC (see GCBO)
% eventdata  reserved - to be defined in a future version of MATLAB
% handles    structure with handles and user data (see GUIDATA)

% Hints: get(hObject,'String') returns contents of edit_safety_value_CC as text
%        str2double(get(hObject,'String')) returns contents of edit_safety_value_CC as a double


% --- Executes during object creation, after setting all properties.
function edit_safety_value_CC_CreateFcn(hObject, eventdata, handles)
% hObject    handle to edit_safety_value_CC (see GCBO)
% eventdata  reserved - to be defined in a future version of MATLAB
% handles    empty - handles not created until after all CreateFcns called

% Hint: edit controls usually have a white background on Windows.
%       See ISPC and COMPUTER.
if ispc && isequal(get(hObject,'BackgroundColor'), get(0,'defaultUicontrolBackgroundColor'))
    set(hObject,'BackgroundColor','white');
end

 function edit_S_V_Callback(hObject, eventdata, handles)
```

```
% hObject    handle to edit_S_V (see GCBO)
% eventdata  reserved - to be defined in a future version of MATLAB
% handles    structure with handles and user data (see GUIDATA)

% Hints: get(hObject,'String') returns contents of edit_S_V as text
%        str2double(get(hObject,'String')) returns contents of edit_S_V as a double


% --- Executes during object creation, after setting all properties.
function edit_S_V_CreateFcn(hObject, eventdata, handles)
% hObject    handle to edit_S_V (see GCBO)
% eventdata  reserved - to be defined in a future version of MATLAB
% handles    empty - handles not created until after all CreateFcns called

% Hint: edit controls usually have a white background on Windows.
%       See ISPC and COMPUTER.
if ispc && isequal(get(hObject,'BackgroundColor'), get(0,'defaultUicontrolBackgroundColor'))
    set(hObject,'BackgroundColor','white');
end

function edit_PEI_Callback(hObject, eventdata, handles)
% hObject    handle to edit_PEI (see GCBO)
% eventdata  reserved - to be defined in a future version of MATLAB
% handles    structure with handles and user data (see GUIDATA)

% Hints: get(hObject,'String') returns contents of edit_PEI as text
%        str2double(get(hObject,'String')) returns contents of edit_PEI as a double
 % --- Executes during object creation, after setting all properties.
function edit_PEI_CreateFcn(hObject, eventdata, handles)
% hObject    handle to edit_PEI (see GCBO)
% eventdata  reserved - to be defined in a future version of MATLAB
% handles    empty - handles not created until after all CreateFcns called

% Hint: edit controls usually have a white background on Windows.
%       See ISPC and COMPUTER.
if ispc && isequal(get(hObject,'BackgroundColor'), get(0,'defaultUicontrolBackgroundColor'))
    set(hObject,'BackgroundColor','white');
end
 % --- Executes on button press in pushbutton9.
function pushbutton9_Callback(hObject, eventdata, handles)
% hObject    handle to pushbutton9 (see GCBO)
% eventdata  reserved - to be defined in a future version of MATLAB
% handles    structure with handles and user data (see GUIDATA)
NOofPVC=str2num(get(handles.text_NOofPVC,'string'))
 Area_m=2;
   Area_A=Area_m*NOofPVC;
   Area_o=0.05*Area_A;
   T_area=Area_A+Area_o;
   N_Plot=T_area/464.5;

   %%
   % DIRECT CAPITAL COST
   % ALL MONIES ARE IN DOLLAR

     %% COST OF PV ARRAY
```

```
% Cost_PkW_PV_Panel = cost per kW of PV panel ($)
Cost_PW_Panel= 1.5;
PVRating=str2num(get(handles.edit_PVRating,'string'))
Total_Cost_Array=Cost_PW_Panel*PVRating*NOofPVC;

%%
% COST OF BATTERY
Cost_P_kWh_Bat=400;

Nos_of_Bat=str2num(get(handles.text_Nos_of_Bat,'string'))
AH=str2num(get(handles.edit_AH,'string'));
Sel_Bat_Voltage=str2num(get(handles.edit_Sel_Bat_Voltage,'string'))

Total_Bat_cost= (Cost_P_kWh_Bat*Nos_of_Bat*(AH*Sel_Bat_Voltage))/1000;

   %%
% COST OF INVERTERS
% Cost_Per_W_Inv= $0.32
Cost_PW_Inv=0.32;
wattageinverter=str2num(get(handles.edit_wattageinverter,'string'))
Nos_Inverter=str2num(get(handles.text_Nos_Inverter,'string'))

Total_Inv_Cost= Cost_PW_Inv*wattageinverter*Nos_Inverter;

%%
% COST OF CHARGE CONTROLLERS
% Cost_Per_Ampere_CC= $5.0
Cost_P_Ampere_CC= 5.0;
Amperage_CC=str2num(get(handles.edit_Amperage_CC,'string'))
N_CC=str2num(get(handles.text_N_CC,'string'));

Total_CC_Cost= Cost_P_Ampere_CC*Amperage_CC*N_CC;

%%
% COST OF CABLES
% Panel,Battery and AC Output Cabling
% Cost in $ and Length in meter
length_of_Module=2;
Length_of_Inv=0.5;
Length_of_Bat=0.3;
Cost_Per_meter_cable= 2.4;
Module_cable_Cost=Cost_Per_meter_cable*NOofPVC*length_of_Module;
Inverter_cable_Cost= Cost_Per_meter_cable*Nos_Inverter*Length_of_Inv;
Bat_cable_cost=Cost_Per_meter_cable*Nos_of_Bat*Length_of_Bat;
Total_Cable_Cost=  Module_cable_Cost+Inverter_cable_Cost+Bat_cable_cost;

%%
% STRUCTURAL FRAME FOR PANELS
% cOST OF FRAME PER PANEL = 10
Frame_Cost=10*NOofPVC;
%%

%Total_Direct_Capital_Cost = TDCC
Sub_TDCC_1=Total_Cost_Array+Total_Bat_cost+Total_Inv_Cost;
```

```
Sub_TDCC_2=Total_CC_Cost+Total_Cable_Cost+Frame_Cost;
TDCC=Sub_TDCC_1+Sub_TDCC_2;

 %%
% INSTALLATION COST
% Installation cost is 5% of total project cost
Installation_cost= 0.05*TDCC;

%% Miscellaneous
% This is assumed to be 2% of TDCC
Miscellaneous=0.35*TDCC;

%%
% INDIRECT CAPITAL COST
%% Permitting and Environmental Issues
PCent_of_Direct_Cost=0.02;
%PERMITTING AND ENVIRONMENTAL ISSUES=PEI

PEI= PCent_of_Direct_Cost*TDCC;
%
%COST OF LAND REQUIRED
% Cost of plot of land= Plot_Cost (This depends on location)
% Cost of land=Land_Cost
Plot_Cost= 120;
Land_Cost=N_Plot*Plot_Cost;

%% TOTAL PROJECT COST
% Total_Project_Cost=TPC
TPC= TDCC+PEI+Land_Cost+Miscellaneous+Installation_cost
%vpa(TPC)

 %set(handles.text_TPC,'string',TPC)
%FINANCIAL APPRAISAL OF THE PV SYSTEM

%% OPERATION AND MAINTENANCE COST
% O&M Cost = OM_Cost
%OM cost per MWh=OM_P_MWh (Dollar)
OM_P_MWh= 40;
WP=str2num(get(handles.text_WP,'string'));
OM_Cost=(WP*OM_P_MWh)/1000000;

%% FINANCIAL APPRAISAL
% Assumptions
% 70% of Project Cost is from Loan and 30% is equity
%Loan interest rate 5% annual
% Project Life span is 25 years
DEG_A=0.01;
%D_RATE=0.1;
TARRIF=0.12;
Loan=0.7*TPC;
Equity=0.3*TPC;
PV_Energy_PA=0;
PV_Energy_PA_T=0;
PV_Energy_Revenue_PA=0;
PV_NET_PRESENT_VALUE=0;
```

```
CASH_IN_FLOW_T=0;
CASH_OUT_FLOW_T=0;
AA_T=0;
PV_Derate=0.6;

LOAN_P=Loan+(0.05*Loan);
sshine=str2num(get(handles.edit_sshine,'string'));
for D_RATE=0.05:0.05:0.25;
for YR=1:1:28;

    Year(YR)=YR+2018
    DEG_A_T(YR)=DEG_A*YR;
    Discount_Factor(YR)=1/((1+D_RATE)^YR)
    % Here Year is a scalar value and Discount_Fctor is also one single
    % value. If I understand you correct, you need to build two arrays
    % X array and Y array and then plot(X,Y)
    % Once you have build the array, you can use the plot outside the
    % loop
    % plot(Year,Discount_Factor);
     stci=str2num(get(handles.edit_stci,'string'));
    ASR=str2num(get(handles.edit_ASR,'string'));

    if (YR==1);
       CASH_IN_FLOW=Loan+Equity;
    elseif (YR>=2 && YR<=3);
       CASH_IN_FLOW=0;
    elseif (YR>=4 && YR<=28);
        PV_Energy_PA=(WP*sshine*365*(ASR/stci)*PV_Derate)*(1-(DEG_A*YR)*0.18);
    PV_Energy_Revenue_PA= PV_Energy_PA*TARRIF;
       CASH_IN_FLOW= PV_Energy_Revenue_PA*DEG_A_T(YR);
    end
    if (YR==1);
       CASH_OUT_FLOW=0.3*TPC;
       AA=0;
     elseif (YR==2);
       CASH_OUT_FLOW=0.3*TPC;
       AA=0;
     elseif (YR==3);
       CASH_OUT_FLOW=0.4*TPC;
       AA=0;
     elseif (YR>=4 && YR<=28);
       AA= OM_Cost*DEG_A;
       CASH_OUT_FLOW=AA+(0.04*LOAN_P);
    end
    PV_NET_CASH_FLOW(YR)=CASH_IN_FLOW-CASH_OUT_FLOW;
    TAX=0.05*PV_NET_CASH_FLOW;
    PV_NET_CASH_FLOW_AFTER_TAX=PV_NET_CASH_FLOW(YR)-TAX;


PV_PRESENT_VALUE_YR(YR)=PV_NET_CASH_FLOW_AFTER_TAX(YR)*Discount_Factor(
YR)

PV_NET_PRESENT_VALUE=PV_NET_PRESENT_VALUE+PV_PRESENT_VALUE_YR(YR)

PV_NET_PRESENT_VALUE_T(YR)=PV_NET_PRESENT_VALUE+PV_PRESENT_VALUE_Y
R(YR);
```

```
    AA_T=AA_T+AA;

    CASH_IN_FLOW_T=CASH_IN_FLOW_T+CASH_IN_FLOW;
    CASH_OUT_FLOW_T=CASH_OUT_FLOW_T+CASH_OUT_FLOW;
    PV_Energy_PA_T=PV_Energy_PA_T+PV_Energy_PA;

 %figure (1)
%plot(D_RATE,PV_NET_PRESENT_VALUE_T,'-*');
%xlabel('Discount Rate');
%ylabel('PV NET PRESENT VALUE ')
%title('Net Present Value against Discount Factor')
%legend('Discount rate=5%','Discount rate=10%','Discount rate=15%','Discount
rate=20%','Discount rate=25%','location','southwest')
%hold on

end

%PV_Energy_PA=(WP*sshine*360)
set(handles.text_PV_Energy_PA_k,'string',PV_Energy_PA)
%hold on
%figure (1)
%plot(Discount_Factor,PV_NET_PRESENT_VALUE_T,'-*');
%xlabel('Discount Factor');
%ylabel('PV NET PRESENT VALUE ($) ')
%title('Net Present Value against Discount Factor')
%legend('Discount rate=5%','Discount rate=10%','Discount rate=15%','Discount
rate=20%','Discount rate=25%','location','southwest')
%hold on
figure (1)
plot(Year,PV_PRESENT_VALUE_YR,'-*')
xlabel('Year');
ylabel('Annual Net Present Value ($)')
%title('Annual Present Value against Year of operation')
legend('Discount rate=5%','Discount rate=10%','Discount rate=15%','Discount
rate=20%','Discount rate=25%','location','southeast')
hold on
figure (2)
plot(Year,Discount_Factor,'-*')
xlabel('Year');
ylabel('Discount Factor')
title('Discount Factor against Year of operation')
legend('Discount rate=5%','Discount rate=10%','Discount rate=15%','Discount
rate=20%','Discount rate=25%','location','northeast')
hold on
%figure(5)
%plot(D_RATE,PV_PRESENT_VALUE_YR,'-*')
%xlabel('Discount Rate');
%ylabel('Net Present Value')
%title('Net Present Value  against Discount Rate')
%legend('Discount rate=5%','Discount rate=10%','Discount rate=15%','Discount
rate=20%','Discount rate=25%','location','northeast')
%hold on

end
%end
```

```
vpa(PV_Energy_PA_T)

function edit_Amperage_CC_Callback(hObject, eventdata, handles)
% hObject    handle to edit_Amperage_CC (see GCBO)
% eventdata  reserved - to be defined in a future version of MATLAB
% handles    structure with handles and user data (see GUIDATA)

% Hints: get(hObject,'String') returns contents of edit_Amperage_CC as text
%        str2double(get(hObject,'String')) returns contents of edit_Amperage_CC as a double


% --- Executes during object creation, after setting all properties.
function edit_Amperage_CC_CreateFcn(hObject, eventdata, handles)
% hObject    handle to edit_Amperage_CC (see GCBO)
% eventdata  reserved - to be defined in a future version of MATLAB
% handles    empty - handles not created until after all CreateFcns called

% Hint: edit controls usually have a white background on Windows.
%       See ISPC and COMPUTER.
if ispc && isequal(get(hObject,'BackgroundColor'), get(0,'defaultUicontrolBackgroundColor'))
    set(hObject,'BackgroundColor','white');
end


% --- Executes on button press in pushbutton12.
function pushbutton12_Callback(hObject, eventdata, handles)
% hObject    handle to pushbutton12 (see GCBO)
% eventdata  reserved - to be defined in a future version of MATLAB
% handles    structure with handles and user data (see GUIDATA)
NOofPVC=str2num(get(handles.text_NOofPVC,'string'))
ASR=str2num(get(handles.edit_ASR,'string'))
stci=str2num(get(handles.edit_stci,'string'))
 Area_m=2;
   Area_A=Area_m*NOofPVC;
   Area_o=0.05*Area_A;
   T_area=Area_A+Area_o;
   N_Plot=T_area/464.5;

   %%
   % DIRECT CAPITAL COST
   % ALL MONIES ARE IN DOLLAR

     %% COST OF PV ARRAY
   % Cost_PkW_PV_Panel = cost per kW of PV panel ($)
   Cost_PW_Panel= 1.5;
   PVRating=str2num(get(handles.edit_PVRating,'string'))
   Total_Cost_Array=Cost_PW_Panel*PVRating*NOofPVC;

   %%
   % COST OF BATTERY
   Cost_P_kWh_Bat=400;

   Nos_of_Bat=str2num(get(handles.text_Nos_of_Bat,'string'))
   %AH=str2num(get(handles.list_AH,'string'))
```

```
AH=str2num(get(handles.edit_AH,'string'))
Sel_Bat_Voltage=str2num(get(handles.edit_Sel_Bat_Voltage,'string'))

Total_Bat_cost= (Cost_P_kWh_Bat*Nos_of_Bat*(AH*Sel_Bat_Voltage))/1000;


%%
% COST OF INVERTERS
% Cost_Per_W_Inv= $0.34
Cost_PW_Inv=0.34;
wattageinverter=str2num(get(handles.edit_wattageinverter,'string'))
Nos_Inverter=str2num(get(handles.text_Nos_Inverter,'string'))

Total_Inv_Cost= Cost_PW_Inv*wattageinverter*Nos_Inverter;

%%
% COST OF CHARGE CONTROLLERS
% Cost_Per_Ampere_CC= $5.4
Cost_P_Ampere_CC= 5.4;
Amperage_CC=str2num(get(handles.edit_Amperage_CC,'string'))
N_CC=str2num(get(handles.text_N_CC,'string'))

Total_CC_Cost= Cost_P_Ampere_CC*Amperage_CC*N_CC;

%%
% COST OF CABLES
% Panel,Battery and AC Output Cabling
% Cost in $ and Length in meter
length_of_Module=2;
Length_of_Inv=0.5;
Length_of_Bat=0.3;
Cost_Per_meter_cable= 2.4;
Module_cable_Cost=Cost_Per_meter_cable*NOofPVC*length_of_Module;
Inverter_cable_Cost= Cost_Per_meter_cable*Nos_Inverter*Length_of_Inv;
Bat_cable_cost=Cost_Per_meter_cable*Nos_of_Bat*Length_of_Bat;
Total_Cable_Cost=  Module_cable_Cost+Inverter_cable_Cost+Bat_cable_cost;

%%
%Total_Direct_Capital_Cost = TDCC
Sub_TDCC_1=Total_Cost_Array+Total_Bat_cost+Total_Inv_Cost;
Sub_TDCC_2=Total_CC_Cost+Total_Cable_Cost;
TDCC=Sub_TDCC_1+Sub_TDCC_2;

%%
% INDIRECT CAPITAL COST
%% Permitting and Environmental Issues
PCent_of_Direct_Cost=0.03;
%PERMITTING AND ENVIRONMENTAL ISSUES=PEI

PEI= PCent_of_Direct_Cost*TDCC;
%
%COST OF LAND REQUIRED
% Cost of plot of land= Plot_Cost (This depends on location)
% Cost of land=Land_Cost
```

```
 Plot_Cost= 140;
 Land_Cost=N_Plot*Plot_Cost;

 %% TOTAL PROJECT COST
 % Total_Project_Cost=TPC
 TPC= TDCC+PEI+Land_Cost;

 % set(handles.text_TPC,'string',TPC)
%FINANCIAL APPRAISAL OF THE PV SYSTEM

%% OPERATION AND MAINTENANCE COST
% O&M Cost = OM_Cost
%OM cost per MWh=OM_P_MWh (Dollar)
OM_P_MWh= 40;
WP=str2num(get(handles.text_WP,'string'))
OM_Cost=(WP*OM_P_MWh)/1000000;

 %% FINANCIAL APPRAISAL
% Assumptions
% 70% of Project Cost is from Loan and 30% is equity
%Loan interest rate 5% annual
% Project Life span is 25 years
DEG_A=0.01;
D_RATE=0.1;
TARRIF=0.12;
Loan=0.7*TPC;
Equity=0.3*TPC;
PV_Energy_PA=0;
PV_Energy_Revenue_PA=0;
PV_NET_PRESENT_VALUE=0;
CASH_IN_FLOW_T=0;
CASH_OUT_FLOW_T=0;
AA_T=0;
PV_Derate=0.8;


LOAN_P=Loan+(0.05*Loan);
sshine=str2num(get(handles.edit_sshine,'string'))
for YR=1:1:28
      Year=YR+2018;
      DEG_A_T=DEG_A*YR;
      Discount_Factor=1/((1+D_RATE)^YR);
      % Here Year is a scalar value and Discount_Fctor is also one single
      % value. If I understand you correct, you need to build two arrays
      % X array and Y array and then plot(X,Y)
      % Once you have build the array, you can use the plot outside the
      % loop
      % plot(Year,Discount_Factor);
      PV_Energy_PA=WP*sshine*365*(ASR/stci)*PV_Derate
      %PV_Energy_PA=(WP*sshine*365*(ASR/stci)*PV_Derate)*(1-(DEG_A*YR))%*0.20)
      PV_Energy_Revenue_PA= PV_Energy_PA*TARRIF;
      if (YR==1)
         CASH_IN_FLOW=Loan+Equity;
      elseif (YR>=2 && YR<=3)
         CASH_IN_FLOW=0;
```

```
    elseif (YR>=4 && YR<=28)
       CASH_IN_FLOW= PV_Energy_Revenue_PA*DEG_A_T;
    end
    if (YR==1)
       CASH_OUT_FLOW=0.3*TPC;
       AA=0;
     elseif (YR==2)
       CASH_OUT_FLOW=0.3*TPC;
       AA=0;
     elseif (YR==3)
       CASH_OUT_FLOW=0.4*TPC;
       AA=0;
     elseif (YR>=4 && YR<=28)
       AA= OM_Cost*DEG_A;
       CASH_OUT_FLOW=AA+(0.05*LOAN_P);
    end
    PV_NET_CASH_FLOW=CASH_IN_FLOW-CASH_OUT_FLOW;
    TAX=0.3*PV_NET_CASH_FLOW;
    PV_NET_CASH_FLOW_AFTER_TAX=PV_NET_CASH_FLOW-TAX;

    PV_PRESENT_VALUE_YR=PV_NET_CASH_FLOW_AFTER_TAX*Discount_Factor;
    PV_NET_PRESENT_VALUE=PV_NET_PRESENT_VALUE+PV_PRESENT_VALUE_YR

PV_NET_PRESENT_VALUE_T=PV_NET_PRESENT_VALUE+PV_PRESENT_VALUE_YR;
    AA_T=AA_T+AA;

    CASH_IN_FLOW_T=CASH_IN_FLOW_T+CASH_IN_FLOW;
    CASH_OUT_FLOW_T=CASH_OUT_FLOW_T+CASH_OUT_FLOW;



end
%PV_Energy_PA=(WP*sshine*360)
Quarter_Days=str2num(get(handles.edit_Quarter_Days,'string'))
PV_Energy_Per_Quarter=(WP*sshine*Quarter_Days*(ASR/stci)*PV_Derate)/1000
set(handles.text_PV_Energy_Per_Quarter,'string',PV_Energy_Per_Quarter)
PV_Energy_PA_k=PV_Energy_PA/1000
set(handles.text_PV_Energy_PA_k,'string',PV_Energy_PA_k)
PV_Energy_Per_Day=PV_Energy_PA_k/365
set(handles.text_PV_Energy_Per_Day,'string',PV_Energy_Per_Day)
%hold off
%plot(Discount_Factor,Year)
%Table_a (Year,1)= Year;
%Table_a (YR,2)= Discount_Factor;
% ... now Year and Discount_factor are arrays of equal size and you can



function edit19_Callback(hObject, eventdata, handles)
% hObject    handle to edit19 (see GCBO)
% eventdata  reserved - to be defined in a future version of MATLAB
% handles    structure with handles and user data (see GUIDATA)

% Hints: get(hObject,'String') returns contents of edit19 as text
%        str2double(get(hObject,'String')) returns contents of edit19 as a double

% --- Executes during object creation, after setting all properties.
```

```
function edit19_CreateFcn(hObject, eventdata, handles)
% hObject    handle to edit19 (see GCBO)
% eventdata  reserved - to be defined in a future version of MATLAB
% handles    empty - handles not created until after all CreateFcns called

% Hint: edit controls usually have a white background on Windows.
%       See ISPC and COMPUTER.
if ispc && isequal(get(hObject,'BackgroundColor'), get(0,'defaultUicontrolBackgroundColor'))
    set(hObject,'BackgroundColor','white');
end

function edit_DOD_Callback(hObject, eventdata, handles)
% hObject    handle to edit_DOD (see GCBO)
% eventdata  reserved - to be defined in a future version of MATLAB
% handles    structure with handles and user data (see GUIDATA)

% Hints: get(hObject,'String') returns contents of edit_DOD as text
%        str2double(get(hObject,'String')) returns contents of edit_DOD as a double


% --- Executes during object creation, after setting all properties.
function edit_DOD_CreateFcn(hObject, eventdata, handles)
% hObject    handle to edit_DOD (see GCBO)
% eventdata  reserved - to be defined in a future version of MATLAB
% handles    empty - handles not created until after all CreateFcns called

% Hint: edit controls usually have a white background on Windows.
%       See ISPC and COMPUTER.
if ispc && isequal(get(hObject,'BackgroundColor'), get(0,'defaultUicontrolBackgroundColor'))
    set(hObject,'BackgroundColor','white');
end

function edit21_Callback(hObject, eventdata, handles)
% hObject    handle to edit_PVRating (see GCBO)
% eventdata  reserved - to be defined in a future version of MATLAB
% handles    structure with handles and user data (see GUIDATA)

% Hints: get(hObject,'String') returns contents of edit_PVRating as text
%        str2double(get(hObject,'String')) returns contents of edit_PVRating as a double

 % --- Executes during object creation, after setting all properties.
function edit21_CreateFcn(hObject, eventdata, handles)
% hObject    handle to edit_PVRating (see GCBO)
% eventdata  reserved - to be defined in a future version of MATLAB
% handles    empty - handles not created until after all CreateFcns called

% Hint: edit controls usually have a white background on Windows.
%       See ISPC and COMPUTER.
if ispc && isequal(get(hObject,'BackgroundColor'), get(0,'defaultUicontrolBackgroundColor'))
    set(hObject,'BackgroundColor','white');
end

function edit_AH_Callback(hObject, eventdata, handles)
% hObject    handle to edit_AH (see GCBO)
```

```
% eventdata  reserved - to be defined in a future version of MATLAB
% handles    structure with handles and user data (see GUIDATA)

% Hints: get(hObject,'String') returns contents of edit_AH as text
%        str2double(get(hObject,'String')) returns contents of edit_AH as a double

 % --- Executes during object creation, after setting all properties.
function edit_AH_CreateFcn(hObject, eventdata, handles)
% hObject    handle to edit_AH (see GCBO)
% eventdata  reserved - to be defined in a future version of MATLAB
% handles    empty - handles not created until after all CreateFcns called

% Hint: edit controls usually have a white background on Windows.
%       See ISPC and COMPUTER.
if ispc && isequal(get(hObject,'BackgroundColor'), get(0,'defaultUicontrolBackgroundColor'))
    set(hObject,'BackgroundColor','white');
end

function edit_Sel_Bat_Voltage_Callback(hObject, eventdata, handles)
% hObject    handle to edit_Sel_Bat_Voltage (see GCBO)
% eventdata  reserved - to be defined in a future version of MATLAB
% handles    structure with handles and user data (see GUIDATA)

% Hints: get(hObject,'String') returns contents of edit_Sel_Bat_Voltage as text
%        str2double(get(hObject,'String')) returns contents of edit_Sel_Bat_Voltage as a double



% --- Executes during object creation, after setting all properties.
function edit_Sel_Bat_Voltage_CreateFcn(hObject, eventdata, handles)
% hObject    handle to edit_Sel_Bat_Voltage (see GCBO)
% eventdata  reserved - to be defined in a future version of MATLAB
% handles    empty - handles not created until after all CreateFcns called

% Hint: edit controls usually have a white background on Windows.
%       See ISPC and COMPUTER.
if ispc && isequal(get(hObject,'BackgroundColor'), get(0,'defaultUicontrolBackgroundColor'))
    set(hObject,'BackgroundColor','white');
end

% --- Executes on button press in pushbutton14.
function pushbutton14_Callback(hObject, eventdata, handles)
% hObject    handle to pushbutton14 (see GCBO)
% eventdata  reserved - to be defined in a future version of MATLAB
% handles    structure with handles and user data (see GUIDATA)
NOofPVC=str2num(get(handles.text_NOofPVC,'string'))
 Area_m=2;
   Area_A=Area_m*NOofPVC;
   Area_o=0.05*Area_A;
   T_area=Area_A+Area_o;
   N_Plot=T_area/464.5;

   %%
   % DIRECT CAPITAL COST
   % ALL MONIES ARE IN DOLLAR
```

```
  %% COST OF PV ARRAY
% Cost_PkW_PV_Panel = cost per kW of PV panel ($)
Cost_PW_Panel= 1.5;
PVRating=str2num(get(handles.edit_PVRating,'string'))
Total_Cost_Array=Cost_PW_Panel*PVRating*NOofPVC;

%%
% COST OF BATTERY
Cost_P_kWh_Bat=400;

Nos_of_Bat=str2num(get(handles.text_Nos_of_Bat,'string'))
AH=str2num(get(handles.edit_AH,'string'))
Sel_Bat_Voltage=str2num(get(handles.edit_Sel_Bat_Voltage,'string'))

Total_Bat_cost= (Cost_P_kWh_Bat*Nos_of_Bat*(AH*Sel_Bat_Voltage))/1000;


%%
% COST OF INVERTERS
% Cost_Per_W_Inv= $0.34
Cost_PW_Inv=0.34;
wattageinverter=str2num(get(handles.edit_wattageinverter,'string'))
Nos_Inverter=str2num(get(handles.text_Nos_Inverter,'string'))

Total_Inv_Cost= Cost_PW_Inv*wattageinverter*Nos_Inverter;

%%
 % COST OF CHARGE CONTROLLERS
% Cost_Per_Ampere_CC= $5.4
Cost_P_Ampere_CC= 5.4;
Amperage_CC=str2num(get(handles.edit_Amperage_CC,'string'))
N_CC=str2num(get(handles.text_N_CC,'string'))

Total_CC_Cost= Cost_P_Ampere_CC*Amperage_CC*N_CC;

%%
% COST OF CABLES
% Panel,Battery and AC Output Cabling
% Cost in $ and Length in meter
length_of_Module=2;
Length_of_Inv=0.5;
Length_of_Bat=0.3;
Cost_Per_meter_cable= 2.4;
Module_cable_Cost=Cost_Per_meter_cable*NOofPVC*length_of_Module;
Inverter_cable_Cost= Cost_Per_meter_cable*Nos_Inverter*Length_of_Inv;
Bat_cable_cost=Cost_Per_meter_cable*Nos_of_Bat*Length_of_Bat;
Total_Cable_Cost=  Module_cable_Cost+Inverter_cable_Cost+Bat_cable_cost;

%%
%Total_Direct_Capital_Cost = TDCC
Sub_TDCC_1=Total_Cost_Array+Total_Bat_cost+Total_Inv_Cost;
Sub_TDCC_2=Total_CC_Cost+Total_Cable_Cost;
TDCC=Sub_TDCC_1+Sub_TDCC_2;
```

```
 %%
 % INDIRECT CAPITAL COST
 %% Permitting and Environmental Issues
 PCent_of_Direct_Cost=0.03;
 %PERMITTING AND ENVIRONMENTAL ISSUES=PEI

 PEI= PCent_of_Direct_Cost*TDCC;
%
%COST OF LAND REQUIRED
% Cost of plot of land= Plot_Cost (This depends on location)
% Cost of land=Land_Cost
Plot_Cost= 140;
Land_Cost=N_Plot*Plot_Cost;

%% TOTAL PROJECT COST
% Total_Project_Cost=TPC
TPC= TDCC+PEI+Land_Cost;

% set(handles.text_TPC,'string',TPC)
%FINANCIAL APPRAISAL OF THE PV SYSTEM

%% OPERATION AND MAINTENANCE COST
% O&M Cost = OM_Cost
%OM cost per MWh=OM_P_MWh (Dollar)
OM_P_MWh= 40;
WP=str2num(get(handles.text_WP,'string'))
OM_Cost=(WP*OM_P_MWh)/1000000;


%% FINANCIAL APPRAISAL
% Assumptions
% 70% of Project Cost is from Loan and 30% is equity
%Loan interest rate 5% annual
% Project Life span is 25 years
DEG_A=0.01;
D_RATE=0.1;
TARRIF=0.12;
Loan=0.7*TPC;
Equity=0.3*TPC;
PV_Energy_PA=0;
PV_Energy_Revenue_PA=0;
PV_NET_PRESENT_VALUE=0;
CASH_IN_FLOW_T=0;
CASH_OUT_FLOW_T=0;
AA_T=0;
PV_Derate=0.66;
LOAN_P=Loan+(0.05*Loan);
sshine=str2num(get(handles.edit_sshine,'string'));
%for DEG_A=0.005:0.005:0.025
for YR=1:1:28
      Year(YR)=YR+2018;

      Discount_Factor(YR)=1/((1+D_RATE)^YR);
```

```
      % plot(Year,Discount_Factor);
       stci=str2num(get(handles.edit_stci,'string'))
      ASR=str2num(get(handles.edit_ASR,'string'))

      if (YR==1)
         CASH_IN_FLOW=Loan+Equity;
      elseif (YR>=2 && YR<=3)
         CASH_IN_FLOW=0;
      elseif (YR>=4 && YR<=28)
          DEG_A_T(YR)=DEG_A*(YR-3);
          k=DEG_A*(YR-3);
      PV_Energy_PA(YR)=WP*sshine*365*(ASR/stci)*PV_Derate*(1-k)*1.224;
      PV_Energy_Revenue_PA(YR)= PV_Energy_PA(YR)*TARRIF;
         CASH_IN_FLOW= PV_Energy_Revenue_PA(YR)*DEG_A_T(YR);
      end
      if (YR==1)
         CASH_OUT_FLOW=0.3*TPC;
         AA=0;
       elseif (YR==2)
         CASH_OUT_FLOW=0.3*TPC;
         AA=0;
       elseif (YR==3)
         CASH_OUT_FLOW=0.4*TPC;
         AA=0;
       elseif (YR>=4 && YR<=28)
         AA= OM_Cost*DEG_A;
         CASH_OUT_FLOW=AA+(0.05*LOAN_P);
      end
      PV_NET_CASH_FLOW=CASH_IN_FLOW-CASH_OUT_FLOW;
      TAX=0.3*PV_NET_CASH_FLOW;
      PV_NET_CASH_FLOW_AFTER_TAX=PV_NET_CASH_FLOW-TAX;


PV_PRESENT_VALUE_YR(YR)=PV_NET_CASH_FLOW_AFTER_TAX*Discount_Factor(YR);

PV_NET_PRESENT_VALUE=PV_NET_PRESENT_VALUE+PV_PRESENT_VALUE_YR(YR)

PV_NET_PRESENT_VALUE_T(YR)=PV_NET_PRESENT_VALUE+PV_PRESENT_VALUE_Y
R(YR);
      AA_T=AA_T+AA;

      CASH_IN_FLOW_T=CASH_IN_FLOW_T+CASH_IN_FLOW;
      CASH_OUT_FLOW_T=CASH_OUT_FLOW_T+CASH_OUT_FLOW;
     %
end
hold on
%figure(1)
plot(Year,PV_Energy_PA,'-*');
xlabel('Year of Operation');
ylabel('PV ENRGY PA ANNUM')
%title('Annual Energy Generated against Year of operation')
legend('ANNUAL DEGRADATION=0.5%','ANNUAL DEGRADATION=1%','ANNUAL
DEGRADATION=1.5%','ANNUAL DEGRADATION=2%','ANNUAL
DEGRADATION=2.5%','location','southeast')
hold on
%figure (2)
```

```
plot(Year,DEG_A_T,'-*')
xlabel('Year');
ylabel('Degradation Factor')
%title('Degradation Factor against Year of operation')
legend('ANNUAL DEGRADATION=0.5%','ANNUAL DEGRADATION=1%','ANNUAL
DEGRADATION=1.5%','ANNUAL DEGRADATION=2%','ANNUAL
DEGRADATION=2.5%','location','northwest')


%legend('ANNUAL DEGRADATION=0.5%','ANNUAL DEGRADATION=1%','ANNUAL
DEGRADATION=1.5%','ANNUAL DEGRADATION=2%','ANNUAL
DEGRADATION=2.5%','location','northwest')

%PV_Energy_PA=(WP*sshine*360);
%set(handles.text_PV_Energy_PA_k,'string',PV_Energy_PA)
%end
figure (1)
plot(DEG_A_T,PV_Energy_PA,'-*')
xlabel('Degradation Factor');
ylabel('PV Annual Energy Generated')
%title('PV Annual Energy Generated against Degradation Factor')
%end

% --- Executes on button press in pushbutton15.
function pushbutton15_Callback(hObject, eventdata, handles)
% hObject    handle to pushbutton15 (see GCBO)
% eventdata  reserved - to be defined in a future version of MATLAB
% handles    structure with handles and user data (see GUIDATA)

 % --- Executes on button press in pushbutton16.
function pushbutton16_Callback(hObject, eventdata, handles)
% hObject    handle to pushbutton16 (see GCBO)
% eventdata  reserved - to be defined in a future version of MATLAB
% handles    structure with handles and user data (see GUIDATA)

 % --- Executes on button press in pushbutton17.
function pushbutton17_Callback(hObject, eventdata, handles)
% hObject    handle to pushbutton17 (see GCBO)
% eventdata  reserved - to be defined in a future version of MATLAB
% handles    structure with handles and user data (see GUIDATA)

% --- Executes on selection change in listbox5.
function listbox5_Callback(hObject, eventdata, handles)
% hObject    handle to listbox5 (see GCBO)
% eventdata  reserved - to be defined in a future version of MATLAB
% handles    structure with handles and user data (see GUIDATA)

% Hints: contents = cellstr(get(hObject,'String')) returns listbox5 contents as cell array
%        contents{get(hObject,'Value')} returns selected item from listbox5

% --- Executes during object creation, after setting all properties.
function listbox5_CreateFcn(hObject, eventdata, handles)
% hObject    handle to listbox5 (see GCBO)
% eventdata  reserved - to be defined in a future version of MATLAB
% handles    empty - handles not created until after all CreateFcns called
```

```
% Hint: listbox controls usually have a white background on Windows.
%       See ISPC and COMPUTER.
if ispc && isequal(get(hObject,'BackgroundColor'), get(0,'defaultUicontrolBackgroundColor'))
    set(hObject,'BackgroundColor','white');
end

function edit_Quarter_Days_Callback(hObject, eventdata, handles)
% hObject    handle to edit_Quarter_Days (see GCBO)
% eventdata  reserved - to be defined in a future version of MATLAB
% handles    structure with handles and user data (see GUIDATA)

% Hints: get(hObject,'String') returns contents of edit_Quarter_Days as text
%        str2double(get(hObject,'String')) returns contents of edit_Quarter_Days as a double

% --- Executes during object creation, after setting all properties.
function edit_Quarter_Days_CreateFcn(hObject, eventdata, handles)
% hObject    handle to edit_Quarter_Days (see GCBO)
% eventdata  reserved - to be defined in a future version of MATLAB
% handles    empty - handles not created until after all CreateFcns called

% Hint: edit controls usually have a white background on Windows.
%       See ISPC and COMPUTER.
if ispc && isequal(get(hObject,'BackgroundColor'), get(0,'defaultUicontrolBackgroundColor'))
    set(hObject,'BackgroundColor','white');
end

function edit_T_power_rating_Callback(hObject, eventdata, handles)
% hObject    handle to edit_T_power_rating (see GCBO)
% eventdata  reserved - to be defined in a future version of MATLAB
% handles    structure with handles and user data (see GUIDATA)

% Hints: get(hObject,'String') returns contents of edit_T_power_rating as text
%        str2double(get(hObject,'String')) returns contents of edit_T_power_rating as a double

% --- Executes during object creation, after setting all properties.
function edit_T_power_rating_CreateFcn(hObject, eventdata, handles)
% hObject    handle to edit_T_power_rating (see GCBO)
% eventdata  reserved - to be defined in a future version of MATLAB
% handles    empty - handles not created until after all CreateFcns called

% Hint: edit controls usually have a white background on Windows.
%       See ISPC and COMPUTER.
if ispc && isequal(get(hObject,'BackgroundColor'), get(0,'defaultUicontrolBackgroundColor'))
    set(hObject,'BackgroundColor','white');
end

% --- Executes on button press in pushbutton19.
function pushbutton19_Callback(hObject, eventdata, handles)
% hObject    handle to pushbutton19 (see GCBO)
% eventdata  reserved - to be defined in a future version of MATLAB
% handles    structure with handles and user data (see GUIDATA)
NOofPVC=str2num(get(handles.text_NOofPVC,'string'))
  WP=str2num(get(handles.text_WP,'string'))
```

```
  ASR=str2num(get(handles.edit_ASR,'string'))
CONVERSION_EFF=0.18
  Area=WP/(ASR*CONVERSION_EFF)
  %Area_m=2;
  %Area_A=Area_m*NOofPVC;
  %Area_o=0.05*Area_A;
  T_area=Area%+Area_o;
  N_Plot=T_area/464.5

  %%
  % DIRECT CAPITAL COST
  % ALL MONIES ARE IN DOLLAR

    %% COST OF PV ARRAY
  % Cost_PkW_PV_Panel = cost per kW of PV panel ($)
  Cost_PW_Panel= 1;
  PVRating=str2num(get(handles.edit_PVRating,'string'))
  Total_Cost_Array=Cost_PW_Panel*PVRating*NOofPVC;
  set(handles.text_Total_Cost_Array,'string',Total_Cost_Array)
  %%
  % COST OF BATTERY
  Cost_P_kWh_Bat=300;

  Nos_of_Bat=str2num(get(handles.text_Nos_of_Bat,'string'))
  %AH=str2num(get(handles.list_AH,'string'))
  AH=str2num(get(handles.edit_AH,'string'))
  %Sel_Bat_Voltage=str2num(get(handles.Sel_Bat_Voltage,'string'))
  Sel_Bat_Voltage=str2num(get(handles.edit_Sel_Bat_Voltage,'string'))
  Total_Bat_cost= (Cost_P_kWh_Bat*Nos_of_Bat*(AH*Sel_Bat_Voltage))/1000;
  set(handles.text_Total_Bat_cost,'string',Total_Bat_cost)

  %%
  % COST OF INVERTERS
  % Cost_Per_W_Inv= $0.32
  Cost_PW_Inv=0.18;
  wattageinverter=str2num(get(handles.edit_wattageinverter,'string'))
  Nos_Inverter=str2num(get(handles.text_Nos_Inverter,'string'))

  Total_Inv_Cost= Cost_PW_Inv*wattageinverter*Nos_Inverter;
  set(handles.text15,'string',Total_Inv_Cost)
  %%
  % COST OF CHARGE CONTROLLERS
 % Cost_Per_Ampere_CC= $5.0
  Cost_P_Ampere_CC= 5.0;
  Amperage_CC=str2num(get(handles.edit_Amperage_CC,'string'))
  N_CC=str2num(get(handles.text_N_CC,'string'))

  Total_CC_Cost= Cost_P_Ampere_CC*Amperage_CC*N_CC;
   set(handles.text_Total_CC_Cost,'string',Total_CC_Cost)

  %%
  % COST OF CABLES
  % Panel,Battery and AC Output Cabling
  % Cost in $ and Length in meter
  length_of_Module=2;
```

```
  Length_of_Inv=0.5;
  Length_of_Bat=0.3;
  Length_of_CC= 0.2;
  Cost_Per_meter_cable= 2.4;
  Module_cable_Cost=Cost_Per_meter_cable*NOofPVC*length_of_Module;
  Inverter_cable_Cost= Cost_Per_meter_cable*Nos_Inverter*Length_of_Inv;
  Bat_cable_cost=Cost_Per_meter_cable*Nos_of_Bat*Length_of_Bat;
  CC_cable_cost=Cost_Per_meter_cable*N_CC*Length_of_CC;
  Total_Cable_Cost=
Module_cable_Cost+Inverter_cable_Cost+Bat_cable_cost+CC_cable_cost;

  %%
  % STRUCTURL FRAME FOR PANELS
  % cOST OF FRAME PER PANEL = 10
  Frame_Cost=10*NOofPVC
  %%

  %Total_Direct_Capital_Cost = TDCC
  Sub_TDCC_1=Total_Cost_Array+Total_Bat_cost+Total_Inv_Cost;
  Sub_TDCC_2=Total_CC_Cost+Total_Cable_Cost+Frame_Cost;
  TDCC=Sub_TDCC_1+Sub_TDCC_2;

   %%
  % INSTALLATION COST
  % Installation cost is 5% of total project cost
  Installation_cost= 0.05*TDCC;

  %% Miscellaneous
  % This is assumed to be 2% of TDCC
  Miscellaneous=0.035*TDCC;

  %%
  % INDIRECT CAPITAL COST
  %% Permitting and Environmental Issues
  PCent_of_Direct_Cost=0.02;
  %PERMITTING AND ENVIRONMENTAL ISSUES=PEI

  PEI= PCent_of_Direct_Cost*TDCC;
 %
 %COST OF LAND REQUIRED
 % Cost of plot of land= Plot_Cost (This depends on location)
 % Cost of land=Land_Cost
 Plot_Cost= 120;
 Land_Cost=N_Plot*Plot_Cost;

 %% TOTAL PROJECT COST
 % Total_Project_Cost=TPC
 TPC= TDCC+PEI+Land_Cost+Miscellaneous+Installation_cost
%vpa(TPC)

 set(handles.text_TPC,'string',TPC)
 %FINANCIAL APPRAISAL OF THE PV SYSTEM
 %% OPERATION AND MAINTENANCE COST
% O&M Cost = OM_Cost
%OM cost per MWh=OM_P_MWh (Dollar)
```

```
OM_P_MWh= 40;
WP=str2num(get(handles.text_WP,'string'));
OM_Cost=(WP*OM_P_MWh)/1000000;

 %% FINANCIAL APPRAISAL
% Assumptions
% 70% of Project Cost is from Loan and 30% is equity
%Loan interest rate 5% annual
% Project Life span is 25 years
DEG_A=0.01;
%D_RATE=0.1;
TARRIF=0.12;
Loan=0.7*TPC;
Equity=0.3*TPC;
%PV_Energy_PA=0;
PV_Energy_PA_T=0
PV_Energy_Revenue_PA=0;
PV_NET_PRESENT_VALUE=0;
CASH_IN_FLOW_T=0;
CASH_OUT_FLOW_T=0;
AA_T=0;
PV_Derate=0.66;

LOAN_P=Loan+(0.05*Loan);
sshine=str2num(get(handles.edit_sshine,'string'))
for D_RATE=0.05:0.05:0.25
for YR=1:1:28
      Year(YR)=YR+2018;
      DEG_A_T(YR)=DEG_A*YR;
      Discount_Factor(YR)=1/((1+D_RATE)^YR);
      % Here Year is a scalar value and Discount_Fctor is also one single
      % value. If I understand you correct, you need to build two arrays
      % X array and Y array and then plot(X,Y)
      % Once you have build the array, you can use the plot outside the
      % loop
      % plot(Year,Discount_Factor);
      stci=str2num(get(handles.edit_stci,'string'))
      ASR=str2num(get(handles.edit_ASR,'string'))
      PV_Energy_PA=(WP*sshine*365*(ASR/stci)*PV_Derate)*(1-(DEG_A*YR)*0.20)
      PV_Energy_Revenue_PA= PV_Energy_PA*TARRIF;
      if (YR==1)
         CASH_IN_FLOW=Loan+Equity;
      elseif (YR>=2 && YR<=3)
         CASH_IN_FLOW=0;
      elseif (YR>=4 && YR<=28)
         CASH_IN_FLOW= PV_Energy_Revenue_PA*DEG_A_T(YR);
      end
      if (YR==1)
         CASH_OUT_FLOW=0.3*TPC;
         AA=0;
       elseif (YR==2)
         CASH_OUT_FLOW=0.3*TPC;
         AA=0;
       elseif (YR==3)
         CASH_OUT_FLOW=0.4*TPC;
         AA=0;
```

```
       elseif (YR>=4 && YR<=28)
          AA= OM_Cost*(1-(DEG_A*YR));
          CASH_OUT_FLOW=AA+(0.05*LOAN_P)
       end
       PV_NET_CASH_FLOW=CASH_IN_FLOW-CASH_OUT_FLOW;
       TAX=0.3*PV_NET_CASH_FLOW;
       PV_NET_CASH_FLOW_AFTER_TAX=PV_NET_CASH_FLOW-TAX;


PV_PRESENT_VALUE_YR(YR)=PV_NET_CASH_FLOW_AFTER_TAX*Discount_Factor(YR);

PV_NET_PRESENT_VALUE=PV_NET_PRESENT_VALUE+PV_PRESENT_VALUE_YR(YR);
       PV_NPV_T1(YR)=PV_NET_PRESENT_VALUE+PV_PRESENT_VALUE_YR(YR);
       AA_T=AA_T+AA;

       PV_Energy_PA_T= PV_Energy_PA_T+ PV_Energy_PA

       CASH_IN_FLOW_T=CASH_IN_FLOW_T+CASH_IN_FLOW;
       CASH_OUT_FLOW_T=CASH_OUT_FLOW_T+CASH_OUT_FLOW;

end
%PV_Energy_PA=(WP*sshine*365)
%lcoe=
%set(handles.text_PV_Energy_PA_k,'string',PV_Energy_PA)
%hold off
%plot(Discount_Factor,Year)
%Table_a (Year,1)= Year;
set(handles.text_PV_PRESENT_VALUE_YR,'string',PV_NET_PRESENT_VALUE)
%set(handles.text_CASH_IN_FLOW_T,'string',CASH_IN_FLOW_T)
%set(handles.text_CASH_OUT_FLOW_T,'string',CASH_OUT_FLOW_T)
k=(TPC+AA+(0.05+LOAN_P))
LCOE=(TPC+CASH_OUT_FLOW_T)/PV_Energy_PA
LCOE1=(CASH_OUT_FLOW_T)/PV_Energy_PA
vpa(PV_Energy_PA)
p=PV_Energy_PA*8.3

set(handles.text_LCOE1,'string',LCOE1)
end
PV_Energy_PA_2=(WP*sshine*365*(ASR/stci)*PV_Derate)*0.06*0.20
PV_Energy_Revenue_PA_2= PV_Energy_PA_2*TARRIF
payback_period=TPC/PV_Energy_Revenue_PA_2
set(handles.text_payback_period,'string',payback_period)

PV_NET_PRESENT_VALUE_1=TPC;


%PV_NET_PRESENT_VALUE_T
%Table_a (YR,2)= Discount_Factor;
% ... now Year and Discount_factor are arrays of equal size and you can

% THE Calculations of net present values should starts
%NPV = ?
%set(handles.text_CASH_IN_FLOW_T,'string',NPV);
```

```
 % --- Executes on button press in pushbutton20.
function pushbutton20_Callback(hObject, eventdata, handles)
% hObject    handle to pushbutton20 (see GCBO)
% eventdata  reserved - to be defined in a future version of MATLAB
% handles    structure with handles and user data (see GUIDATA)


% --- Executes on button press in pushbutton21.
function pushbutton21_Callback(hObject, eventdata, handles)
% hObject    handle to pushbutton21 (see GCBO)
% eventdata  reserved - to be defined in a future version of MATLAB
% handles    structure with handles and user data (see GUIDATA)
```

A.1 Flowchart and Equations for Maximum Power Point Tracking (MPPT) system

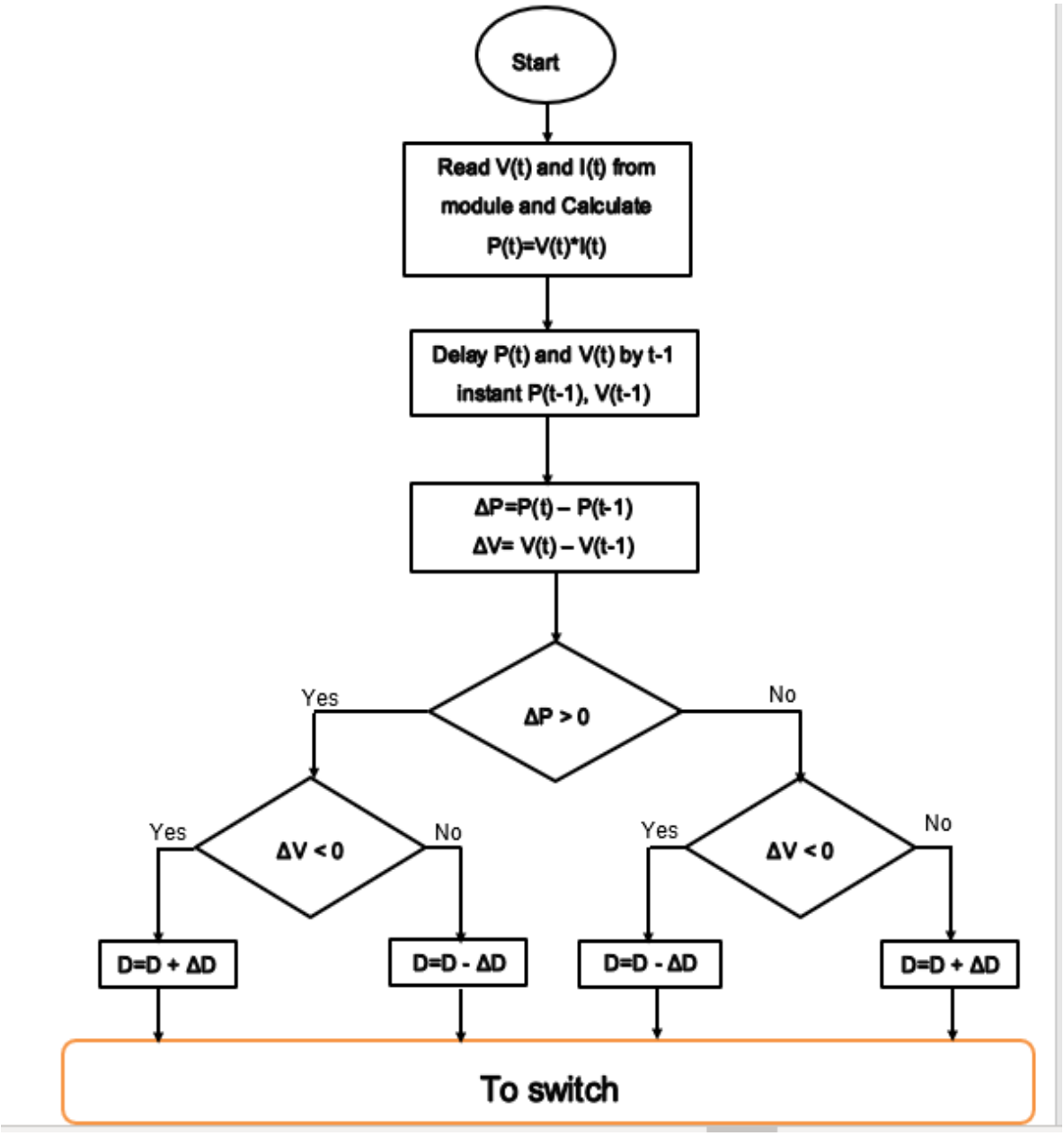

A.1.1 MPPT ALGORITHM BASED ON PERTURB AND OBSERVE

MPPT ALGORITHM BASED ON SIMULINK DIAGRAM

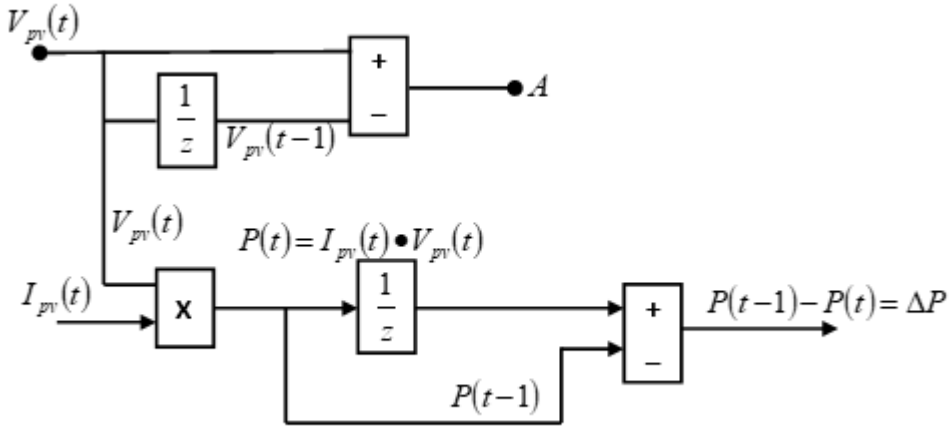

V_{pv} is from solar PV model

I_{pv} is from solar pv model

$P(t)$ is instantaneous measured power from solar PV

$V_{pv}(t)$ is an instantaneous measured voltage from solar PV

$I_{pv}(t)$ is instantaneous measured current from solar PV

$V_{pv}(t-1)$ is previously measured value before $V_{pv}(t)$ The Simulink block $\frac{1}{z}$ is used to realize it

$I_{pv}(t-1)$ is previously measured the value

ΔP_{pv} is a change in power used to set a condition for MPPT algorithm

ΔV_{pv} is a change in voltage used to set a condition for MPPT algorithm

SIMULINK BLOCKS FOR ADJUSTING DESIRED VOLTAGE Vref THROUGH MPPT ALGORITHM

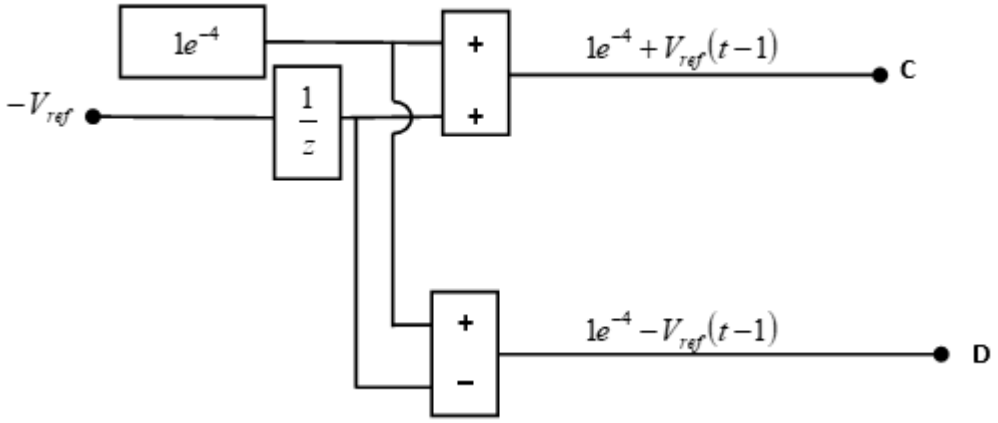

SIMULINK BLOCKS FOR REALIZING MPPT ALGORITHMS

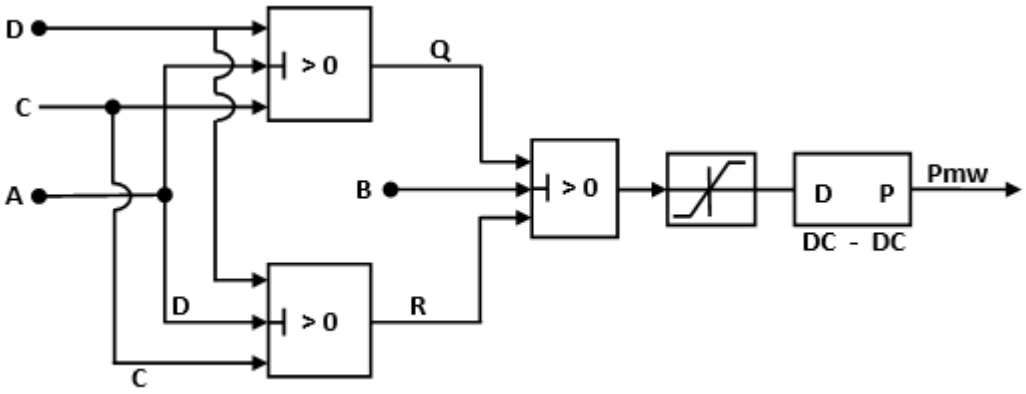

$A:\ \Delta V_{pv} = V_{pv}(t) - V_{pv}(t-1);$

$B:\ \Delta P_{pv} = P_{pv}(t-1) - P(t);$

$C:\ 1e^{-4} + V_{ref}(t-1)$

$C:\ 1e^{-4} - V_{ref}(t-1)$

EQUATIONS THAT GENERATE SIGNALS FROM SOLAR ARRAY

$\Delta V_{pv} = V_{pv}(t) - V_{pv}(t-1)$

$$\Delta I_{pv} = I_{pv}(t) - I_{pv}(t-1)$$

$$\Delta P_{pv} = V_{pv}(t) \bullet I_{pv}(t) - \Delta V_{pv} \bullet \Delta I_{pv}$$

MPPT ALGORITHM

$\Delta V_{pv} > 0$ and $\Delta P_{pv} > 0$

$\Delta V_{pv} < 0$ and $\Delta P_{pv} < 0$

$\Delta V_{pv} < 0$ and $\Delta P_{pv} > 0$

$\Delta V_{pv} > 0$ and $\Delta P_{pv} < 0$